

Role of matriptase in the regulation of epithelial barrier permeability studied using MDCK cells

Salma Elghadban

Thesis submitted for the degree of Doctor of Philosophy

University of East Anglia
School of Biological Sciences

September 2014

© This copy of the thesis has been supplied on condition that anyone who consults it is understood to recognise that its copyright rests with the author and that use of any information derived there from must be in accordance with current UK Copyright Law. In addition, any quotation or extract must include full attribution.

***I would like to dedicate this thesis to my wonderful
parents Wael and Wafa, for their never-ending love
and support.***

Abbreviations

AJ	Adherens junction
ARIH	Autosomal recessive ichthyosis with hypertrichosis
ARIH	Autosomal Recessive Ichthyosis with Hypotrichosis
BBB	Blood-brain barrier
CAP1	Channel Activating Protease-1
CF	Cystic fibrosis
CUB	Complement C1r/C1s, Uegf, Bmp1
DAPI	4',6-diamidino-2-phenylindole
DMEM	Dulbecco's Modified Eagles Medium
DOX	Doxycycline
DSS	Dextran sulfate sodium
ECM	Extracellular matrix
EDTA	Ethylenediaminetetraacetic acid
EGF	Epidermal growth factor
EGFR	Epidermal growth factor receptor
EGTA	Ethyleneglycoltetraacetic acid
EL1	Extracellular loop1
EL2	Extracellular loop2
ENaC	Epithelial sodium channel
ER	Endoplasmic reticulum
ERK	Extracellular signal-regulated kinase
FCS	Fetal Calf Serum
FITC	Fluorescein isothiocyanate
GFP	Green fluorescence protein
GPI	Glycosylphosphatidylinositol
HAI-1	Hepatocyte activator inhibitor-1
HAI-2	Hepatocyte activator inhibitor-2
HBSS	Hank's balanced salt solution
HGF	Hepatocyte Growth Factor
HGFA	Hepatocyte growth factor activator
HRP	Horseshoe peroxidase
HSC	Heat Shock Protein 70
IBD	Inflammatory bowel disease
IFN	Interferon
IL	Interleukin
JAMs	Junction Adhesion Complexes
LDLRa	Low density lipoprotein receptor-like protein type a
mCAP	Mouse channel activating proteases
MDCK	Madin Darby Canine Kidney
MMP	Matrix Metalloproteinase
MOI	Multiplicity Of Infection

mRNA	Messenger RNA
MSCV	Murine Stem Cell Virus
NTC	Non Target control
PAR-2	Protease activated receptor-2
PBS	Phosphate Buffered Saline
PC3	Human prostate cancer cell line
PCR	Polymerase chain reaction
PKC	Protein kinase C
PMSF	phenylmethanesulfonylfluoride
PN1	Protease nexin-1
PVDF	polyvinylidene fluoride
qRT-PCR	Quantitative Real Time-PCR
RTKs	Receptor tyrosine kinases
SCL	Scanning-Substrate Combinatorial Library
SDS	Sodium Dodecyl Sulphate
SEA	Sperm protein, enteropeptidase, agrin
SFM	Serum free media
shRNA	Short-hairpin RNA
siRNA	Small-interfering RNA
SSC	Squamous single cell carcinoma
ST14	Suppressor of tumorigenesis 14
TEER	Transepithelial electrical resistance
TTSP	Type II transmembrane bound serine proteases
uPA	Urokinase Plasminogen Activator
uPAR	Urokinase Plasminogen Activator receptor
VEGF	Vascular endothelial growth factor
ZO	Zonula Occludin

Abstract

The type-II transmembrane serine protease matriptase plays an important role in the integrity of epithelial barriers. However, the molecular mechanisms underlying the role of matriptase are unknown.

To study these mechanisms, two variants of Madin-Darby canine kidney (MDCK) cells were used, together with the “calcium-switch” model of epithelial function with measurements of transepithelial electrical resistance (TEER).

Inhibitors of matriptase proteolytic activity delayed the restoration of TEER after calcium-switch in MDCK-I, which develop high TEER and lack the “leaky” tight junction protein claudin-2, but not MDCK-II. This effect was confirmed in MDCK-I, established to stably express matriptase targeted shRNA.

The influence of matriptase inhibition on MDCK-I was shown not to involve altered expression or assembly of relevant components of paracellular junctions or cytoskeleton. This excluded a role for claudin-2 in the function of matriptase, which had previously been shown in human Caco-2 cells, and this was confirmed using MDCK-I cells stably overexpressing claudin-2.

To investigate the claudin-2-independent function of matriptase, a candidate substrate approach was used. Proteolytic activation of pro-HGF/c-Met, PAR-2, ENaC, EGFR and prostasin by matriptase has effects on epithelial cell function, but none were found to have a role in matriptase restoration of TEER after calcium-switch in MDCK-I cells. As the direct proteolytic target of matriptase could not be identified, potential mediators were studied using arrays for phosphorylated signalling proteins and inflammatory cytokines. IL-1 β and complement component C5 were identified as genes downregulated by matriptase inhibition, while IL-13 showed upregulation.

This work has confirmed the key role of matriptase activity in regulating epithelial barrier integrity. The differential properties of MDCK-I and MDCK-II cells excluded a role for claudin-2. None of the known proteolytic targets of matriptase were involved, however, changes in cytokine gene expression may be a potential route for matriptase effects on epithelial barrier maintenance

List of publications

Gray K, **Elghadban S**, Thongyoo P, Owen KA, Szabo R, Bugge TH, Tate EW, Leatherbarrow RJ, Ellis V. Potent and specific inhibition of the biological activity of the type-II transmembrane serine protease matriptase by the cyclic microprotein MCoTI-II. *Thromb Haemost.* 2014;112(2):402-11.

Table of Contents

Abbreviations	3
Abstract	5
List of publications	6
List of figures	10
List of tables	12
Chapter 1. Literature review	14
1.1 Functions of proteases and their implication in different diseases	14
1.2 Structural features and biochemistry of serine proteases	15
1.2.1 Trypsin-like serine proteases	15
1.2.2 Type II transmembrane bound serine proteases (TTSP).....	16
1.1.2.1 Matriptase	18
1.2.2.1 Matriptase activation mechanism	20
1.2.2.2 Regulation of matriptase activity: Hepatocyte growth factor activator inhibitor-1 and 2 (HAI-1 and HAI-2).....	22
1.2.2.3 Matriptase epithelial expression.....	24
1.3 Epithelial tissue structure and barrier functions	24
1.3.1 The development and function of the “stratified” epidermal barrier	25
1.3.2 The development and function of the “simple” and polarized epithelial barriers	25
1.3.3 Simple epithelial apical-basolateral polarity	26
1.3.4 Epithelial tight junctions have important roles in determining barrier polarisation, permeability and function.....	26
1.3.4.1 Junction structure	28
1.3.4.2 The Claudins and occludin:.....	29
1.3.4.3 The zonula occludens proteins (ZO)	30
1.3.5 Claudin regulation of paracellular permeability in different epithelia.....	32
1.3.5.1 Role in ion transport.....	32
1.3.5.2 Claudins regulation of paracellular integrity.....	32
1.3.5.3 Biophysical methods to study tight junction permeability	33
1.4 The role of matriptase in barrier epithelia	35
1.4.1 Matriptase regulation of stratified epidermal barrier differentiation and integrity	35
1.4.2 Matriptase regulation of simple intestinal barrier function and integrity	36
1.4.2.1 HAI-1 and HAI-2 regulation of epithelial barrier integrity	38

1.5 Putative substrates of matriptase in the epithelia	40
1.5.1 Proastasin or channel activating protease-1 (CAP1).....	40
1.5.2 Hepatocyte Growth Factor (HGF).....	41
1.5.3 Urokinase Plasminogen Activator (uPA).....	42
1.5.4 Protease activated receptor-2 (PAR-2).....	43
1.6 MDCK cells as a model of matriptase function in epithelial biology.....	45
Hypothesis and objectives	47
Chapter 2. Materials and Methods	49
2.1 General Reagents and Cell Culture.....	49
2.1.1 General Chemicals	49
2.1.2 Antibodies	52
2.1.3 Buffers and solutions.....	53
2.1.4 Chemical inhibitors, antagonist, agonists and recombinant growth factors	54
2.2 Cell culture	55
2.2.1 MDCK-I, MDCK-I-CLD2 Tet-off and MDCK-II Cell Culture	55
2.2.2 MDCK-I mission shRNA stable cells	55
2.2.3 A549 Tet-off cells	56
2.2.4 Routine Mycoplasma testing.....	56
2.3 DNA propagation.....	57
2.3.1 Transformation and colony expansion.....	57
2.3.2 DNA purification.....	58
2.3.2.1 Plasmid Miniprep.....	58
2.3.2.2 PCR purification.....	58
2.3.2.3 DNA gel extraction.....	58
2.3.2.4 DNA precipitation	59
2.4 Protein extraction and analysis	59
2.4.1 Cell lysate preparation.....	59
2.4.2 Pierce Bicinchoninic acid (BCA) assay for protein quantification.....	60
2.4.3 Western blotting.....	60
2.4.4 Pathscan® RTK signaling antibody array (Chemiluminescent Readout).....	61
2.5 Gene expression analysis (RT-PCR).....	62
2.5.1 RNA extraction and reverse transcription (Two methods – superscript or mmlv)	62
2.6 Regular PCR.....	63
2.6.1 Quantitative Real Time-PCR (qRT-PCR)	64
2.6.1.1 SYBR® Green qRT-PCR assay	64
2.6.1.2 TaqMan® qRT-PCR assay	64
2.7 siRNA design and transfection.....	66
2.7.1 Design of siRNA targeting the human and dog st14 mRNA.....	66
2.7.2 siRNA knockdown of matriptase in MDCK cells	66
2.8 Developing miR30-based shRNA expression for inducible knockdown of matriptase (see Appendix 2).....	67
2.8.1.1 Design 96mer miR30 based shRNA	67
2.8.2 Digestion of insert and ligation with pBluescript	67
2.8.3 Sanger DNA sequencing	68
2.9 Matriptase knockdown using Mission™ shRNA lentivirus system	69
2.9.1.1 Mission Lentivirus Packaging.....	69
2.9.2 Generating stable MDCK cells expressing matriptase targeting shRNAs and NTC using Mission lentivirus system.....	70
2.10 Assays for studying epithelial barrier function	70
2.10.1 Measurements of barrier integrity: Transepithelial Electrical Resistance (TEER) assay	70

2.10.1.1 Seeding of cells on permeable support for measuring barrier function	71
2.10.1.2 Measurement of TEER.....	71
2.10.2 Calcium switch.....	72
2.10.2.1 TEER recovery assay: Addition of various inhibitors and growth factors	74
2.10.2.2 siRNA TEER experiments	74
2.10.2.3 Mission shRNA transduction and TEER analysis	74
2.10.2.4 Stable mission MDCK-I TEER assay	74
2.10.2.5 MDCK-I claudin-2 Tet-off TEER recovery with IN-1	75
2.10.3 Measurements of barrier integrity: Paracellular flux of 4kDa FITC-dextran	75
2.10.3.1 Fluorescence standard curve for 4 kDa FITC dextran.....	75
2.10.3.2 Measuring diffusion of FITC-dextran across MDCK monolayer under different conditions.....	75
2.11 Video timelapse microscopy: Hepatocyte growth factor (HGF)-induced cell migration assay.....	76
2.12 Immunofluorescence labelling	77
2.13 RT² Profiler™ array: Dog inflammatory cytokines and receptors	78
2.14 Statistical analysis.....	79
Chapter 3. Validating MDCK-I and MDCK-II as model epithelial cells for investigating the role of matriptase on epithelial barrier function.....	80
3.1 Introduction.....	80
3.1.1 MDCK-I and MDCK-II cells: an important culture model of barrier epithelium .	82
3.1.2 Aims and objectives	84
3.2 Results	84
3.2.1 MDCK-I and MDCK-II cell line behavior and morphology	84
3.2.2 MDCK-I and MDCK-II cells form barriers with differential transepithelial electrical resistance (TEER)	86
3.2.2.1 TEER development assay: MDCK-I cell culture and seeding density	88
3.2.2.2 TEER development assay: MDCK-I and MDCK-II cell culture and seeding density ..	89
3.2.2.3 MDCK-I and MDCK-II overall barrier paracellular physiology: 4 kDa FITC-dextran flux assay	91
3.2.2.4 Expression of tight junction and adhesion junction complexes by MDCK-I and MDCK-II cells	94
3.2.2.5 Formation of apical-basolateral microtubule array and apical tight junctions.....	96
3.2.3 Calcium switch effect on MDCK barrier functional integrity.	98
3.2.4 Expression of matriptase in MDCK cells	103
3.2.4.1 Analysing matriptase protein expression in MDCK-I and MDCK-II cells.....	103
3.2.4.2 Analysing matriptase gene expression in MDCK-I and MDCK-II cells	106
3.2.5 Matriptase knockdown by siRNA in MDCK cells	109
3.2.5.1 Efficiency of siRNA knockdown of matriptase in MDCK-I and MDCK-II cells	109
3.2.6 Matriptase knockdown using Mission lentivirus transduction system	112
3.2.6.1 Generating stable MDCK-I cells with mission PLKO.1 shRNA lentivirus system	112
3.2.6.2 Matriptase gene expression in stable pLKO.1-shRNA expressing MDCK-I cells	114
3.3 Discussion.....	116
3.4 Conclusion	119
Chapter 4. Matriptase role in regulating MDCK barrier integrity and repair function.....	120
4.1 Introduction.....	120
4.1.1 Matriptase inhibitor binding and function ablation	122
4.1.2 Matriptase approach to study its role in MDCK model of epithelial barrier	126
4.1.3 Aims and objectives	127
4.2 Results	128

4.2.1 Effect of matriptase inhibition on MDCK-I and MDCK-II pro-HGF activation induced cell migration	128
4.2.2 Effect of matriptase inhibition on MDCK-I and MDCK-II barrier integrity and TEER	131
4.2.3 Influence of matriptase inhibition on recovery of barrier paracellular integrity and restricted permeability to macromolecules: 4 kDa FITC-dextran flux assay.....	136
4.2.4 Matriptase expression in MDCK-I and MDCK-II cells before, during and after calcium switch	139
4.2.5 Effect of matriptase inhibition on the expression of the major components of tight junctions and adhesion junctions in recovering MDCK-I cells monolayers.....	141
4.2.6 Role of claudin-2 in the matriptase-dependent regulation of MDCK-I barrier integrity	143
4.2.7 Effect of matriptase inhibition on tight junction and adhesion junction protein expression	145
4.2.8 Effect of matriptase inhibition on the re-establishment of intracellular junctions in MDCK-I cells	146
4.2.9 Specific depletion of matriptase by siRNA in MDCK cells: Effect on barrier formation and TEER re-establishment in MDCK-I cells.	150
4.2.9.1 Transient knockdown affect on TEER in MDCK-I cells.....	151
4.2.9.2 Effect of matriptase stable knockdown on the establishment and re-establishment of MDCK-I barrier integrity	154
4.3 Discussion.....	156
4.4 Conclusion	160

Chapter 5. Investigation into the mechanism of matriptase in epithelial barrier function and restitution in MDCK cells using a candidate substrate approach

5.1 Introduction.....	161
5.1.1 Matriptase substrates and role in epithelial tissue function.....	162
5.1.2 Prostasin	163
5.1.3 The HGF/SF-c-Met signaling axis	167
5.1.4 Protease activated receptor-2 activation and physiological function	168
5.2 Results	170
5.2.1 Expression of prostasin, hepsin and PAR-2 in MDCK-I and MDCK-II cells	170
5.2.2 Prostasin expression and function in MDCK-I barrier epithelia	173
5.2.2.1 Relative quantification of prostasin mRNA expression in MDCK-I barrier: influence of calcium switch.....	173
5.2.2.2 Effect of matriptase inhibition on prostasin mRNA levels in MDCK-I monolayers.	175
5.2.2.3 Attempt to analyse prostasin activity and complex binding in MDCK-I cells.....	177
5.2.3 Influence of amiloride, an inhibitor of uPA and ENaC, on MDCK-I barrier function.....	179
5.2.4 EGFR function during recovery of MDCK-I monolayer	180
5.2.5 PAR-2 effect on TEER recovery in MDCK-I cells.....	182
5.2.5.1 Relative expression of PAR-2 (F2RL1) during matriptase inhibition with IN-1	182
5.2.5.2 Influence of PAR-2 antagonists and agonists on TEER restoration in MDCK-I cells	183
5.2.6 HGF/c-Met signaling function in MDCK barrier epithelia	185
5.2.6.1 Function of intrinsic pERK 1/2 activity on TEER and claudin-2 expression	185
5.2.6.2 Pro-HGF activation, stimulation and regulation of claudin-2 expression in MDCK-I and MDCK-II cells.....	188
5.2.7 c-Met activity and function in MDCK-I and MDCK-II cells.....	188
5.2.7.1 Function of intrinsically active pERK in MDCK-I barrier TEER development and recovery	191

5.2.7.2 c-Met role in MDCK-I and II barrier recovery following calcium switch.....	193
5.2.8 HGF stimulation effect on MDCK barrier recovery and role during matriptase inhibition.....	195
5.2.9 Effect of matriptase inhibition on receptor tyrosine kinase phosphorylation in MDCK-I cells during recovery from calcium switch.....	197
5.2.10 Cytokine and inflammatory receptor 384 Gene analysis array	199
5.3 Discussion.....	203
5.4 Conclusion	211
Chapter 6. General discussion and future direction.....	212
6.1 Conclusion and future work.....	219
References	221
Appendices.....	239

List of figures

Figure 1.1 Schematic showing the different sub-families of TTSPs and the domain structures of all 17 protease members.....	17
Figure 1.2 A schematic demonstrating the complex structure of the TTSP member matriptase (Bugge et al., 2007)	21
Figure 1.3 Process of activation of matriptase zymogen at the cell surface.....	21
Figure 1.4 Simple and polarised epithelial cells form tight cell-cell associations that assembly to separate between the apical and basolateral tissue domains.	27
Figure 1.5 An illustration of the structure and assembly of the tight junction strands as cell-cells interphase.....	29
Figure 1.6 This diagram illustrates the major tight junction and adherens junctions formed in simple epithelial barriers.....	31
Figure 1.7 Methods for measurement of epithelial paracellular permeability.	34
Figure 1.8 Summery of the effect of genetic ablation of matriptase or HAI-1 in both knockout and conditional knockout mice on epithelial barrier integrity.....	39
Figure 1.9 <i>In vivo and in vitro</i> substrates of matriptase proteolysis.....	45
Figure 3.1 Characterization of MDCK-I and MDCK-II cells in culture.....	86
.....	88
Figure 3.4 Characterization of MDCK-I and MDCK-II barrier transepithelial paracellular resistance (TEER).....	90
Figure 3.6 Expression of different components of the tight junctions and adhesion junctions between MDCK-I and MDCK-II cells.....	95
Figure 3.7 Determining tight junction and microtubule polarization in MDCK-I and MDCK-II cells grown on permeable support.....	98
Figure 3.8 Diagram illustrated sequence of barrier establishment and stages of TEER acquisition, before and after calcium “switch”.....	99
Figure 3.9 Effect of calcium-switch on MDCK-I monolayer TEER.....	101
Figure 3.10 Effect of calcium depletion/repletion on MDCK-I and MDCK-II monolayer TEER and tight junction physiology.....	102

Figure 3.11 Matriptase protein expression in MDCK-II cells. Total cell lysates were collected from confluent MDCK-II cell from plastic culture plates.....	104
Figure 3.12 Cell surface detection of human Matriptase by immunofluorescence using M32 mAb in tet-off A549 cells.	106
Figure 3.13 Quantification of matriptase gene expression in MDCK-I and MDCK-II cells.	108
Figure 3.14 Matriptase cDNA sequence in dog.....	110
Figure 3.15 Matriptase knockdown by siRNA in MDCK-I and MDCK-II cells.....	111
Figure 3.16 Puromycin kill curve on MDCK-I cells.	113
Figure 3.17 Determining packaged Mission PLKO.1 lentivirus titer using GFP signal.	114
Figure 3.18 Effect of stable PLKO.1 shRNA expression on levels of endogenous matriptase expressed by MDCK-I cells.....	115
Figure 4.1 MCoTI-II structure and inhibition properties.....	124
Figure 4.2 Chemical structures and inhibition properties of CJ-730 and CJ-1737.	125
Figure 4.3 Chemical structure and inhibition properties of IN-1.....	126
Figure 4.4 Examination of different sample preparations of recombinant proHGF.	129
Figure 4.5 Effect of CJ-1737 on proHGF induced cell migration in MDCK-I cells. .	130
Figure 4.6 MDCK-II HGF cell scatter assay with MCoTI-II inhibitor.....	131
Figure 4.7 Matriptase MCoTI-II inhibitor affect on TEER establishment and re-establishment in MDCK-I and MDCK-II cells.....	132
Figure 4.8 Effect of matriptase inhibitors CJ-730 and CJ-1737 and general inhibitor Aprotinin on TEER re-establishment in MDCK-I and MDCK-II monolayer. ...	133
Figure 4.9 Matriptase inhibitor IN-1 effect on TEER re-establishment in MDCK-I and MDCK-II cells.....	135
Figure 4.10 Matriptase inhibition effect on recovery of restricted paracellular integrity toward 4kDa FITC-dextran in MDCK-I and MDCK-II cells.	138
Figure 4.11 Matriptase expression in MDCK-I cells before and after calcium switch.	140
Figure 4.12 Tight junctions protein expression in MDCK-I monolayers, following calcium switch and during matriptase inhibition.....	142
Figure 4.13 Effect of matriptase inhibition on claudin-2 expressing MDCK-I cells.	144
Figure 4.14 Effect of matriptase inhibition on adhesion junction protein expression in MDCK-I monolayers, during recovery from calcium switch.....	146
Figure 4.15 Immunofluorescence analysis of paracellular junctions and cytoskeletal structures in MDCK-I cells during TEER recovery assay.	150
Figure 4.16 Effect of transient knockdown of matriptase in MDCK-I epithelial monolayers during TEER development and reestablishment.	154
Figure 4.17 Effect of stable knockdown of endogenous matriptase expression on MDCK-I TEER recovery.	155
Figure 5.1 Schematic representation of mechanism of Na ⁺ reabsorption and fluid balance mediated by the amiloride-sensitive ENaC at the surface of epithelial cells.	166
Figure 5.3 Quantitative mRNA expression of hepsin, PAR-2 and prostasin in MDCK-I and MDCK-II cells.....	172

Figure 5.4 Expression of prostasin mRNA and protein in MDCK-I and MDCK-II during and after calcium switch in MDCK-I cells.	174
Figure 5.4 Effect of matriptase inhibition on prostasin expression in MDCK-I during monolayer recovery from calcium switch.	176
Figure 5.5 Effect of matriptase inhibition on prostasin activation and endogenous inhibitor complex formation during MDCK-I barrier restitution.	179
Figure 5.6 Effect of amiloride and EGFR inhibitor on TEER recovery of MDCK-I monolayer.	182
Figure 5.7 PAR-2 function and role in matriptase mediated MDCK-I barrier reestablishment.	185
Figure 5.8 Intrinsic pERK activity and effect on claudin-2 expression in MDCK-I and MDCK-II cells.	187
Figure 5.9 Intrinsic c-Met and p-ERK activity and regulation of claudin-2 expression in MDCK-I and MDCK-II cells.	190
Figure 5.10 Intrinsic p-ERK inhibition during MDCK-I barrier development and repair in MDCK-I and MDCK-II cells.	192
Figure 5.11 Intrinsic c-Met activity and p-ERK levels control over claudin-2 expression in MDCK-I and MDCK-II cells.	195
Figure 5.12 Role of HGF signaling in recovery of TEER in MDCK-I monolayers....	196
Figure 5.13 Effect of matriptase inhibition with CJ-1737 on protein kinase phosphorylation (Pathscan array).	198
Figure 5.14 Effect of matriptase inhibition with IN-1 on protein kinase phosphorylation (Pathscan array).	199
Figure 5.15 Effect of matriptase inhibition on the expression of inflammatory cytokines during MDCK-I barrier recovery assay.	202

List of tables

Table 2.1 The list of reagents and buffers used for the assays	49
Table 2.2 list of the reagents used for bacterial culture and Plasmid propagation.	51
Table 2.3 the list of primary and secondary antibodies used to tag proteins of interest.	52
Table 2.4 Details the various buffer solutions used for different experiments.	53
Table 2.5 Detail of inhibitors, antagonists and agonists used in this study:	54
Table 2.6 Details the reagents and concentrations used for the two reverse transcription reaction methods.	63
Table 2.7 A summary of primers used for analysis and detection of genes using RNA from human and dog cells, as well as sequences of primers used for the development of the inducible shRNA system.	65
Table 2.8 Details the vectors used for the Mission™ shRNA Lentivirus system.	69

Acknowledgments

I would like to start by thanking the Big C for funding my studies. Research is not possible without funding and the generous fundraising of the Big C supporters made this work possible.

There are so many people who I would like to thank for their continuing support and encouragement throughout my PhD. Without them, I would not be here to write this and so I would like to express my gratitude to:

My project supervisor, Professor Vince Ellis, for hiring me in the first place and encouraging and directing me through the tough times of this project.

Many thanks must go to Dr Stephen Robinson for encouraging me and supporting me on a daily basis in the lab. You always believed in me and made me feel better for which I thank you.

To Dr Helen James thank you for your constant words of encouragement and support. Your belief helped me to get to where I am today.

A huge thank you goes to Professor Dylan Edwards and his group. To the person who became my go-to person for much-needed confidence boosts during my three years in the lab; Dr Lin Cooley, you believed in me and were awesome.

Richard, you also became a go-to support and you still are. Thank you for always being there.

Julie, Sally and Wout; you have always been great friends, thank you.

Christian, I have so much admiration for you. You are such a hard working person and I will always aspire to be as focused, driven and determined as you.

Thank you to my bully partner, Tim, my wonderful friend, Veronica and my Boo person, Sandy, for always being so amazing. I am forever grateful to have you as friends.

To the Clark and Riley lab groups, thank you for letting me borrow stuff and generally helping me out. Also, I'd like Dr Darren Sexton for his help and support.

I cannot describe how thankful I am to Liz Shedden for your great support during the writing of this thesis. Thank you for listening and understanding and providing healing hugs when I needed them most. Also, thank you for enabling my fledgling addiction by always ensuring that I never run out of KitKats!

I always wished that I had a sister so I was blessed when I met you, Sara Hazim. I cannot even begin to describe how much you mean to me and how thankful I am that you are in my life.

Omar, Khalid, Tariq and Tuti; you are my constant source of joy. Thank you must also go to my grandmother, Sara, my auntie Hana, my cousin Hadeel, and all my UK friends for always phoning to check up on me and for truly believing in me.

Finally, my biggest thanks has got to go to my wonderful parents, to whom I dedicate this thesis. My love and appreciation to you both goes beyond any description.

Chapter 1. Literature review

1.1 Functions of proteases and their implication in different diseases

Proteolytic enzymes comprise 2% of the known proteome and display a variety of important biological functions (Puente et al., 2003). Protease-dependent peptide bond hydrolysis is a highly classified system of posttranslational modification and is fundamental in biological processes including development, tissue homeostasis, turnover and remodelling, healing and immune response. Their central role in these processes is often distinguished through association with a range of human diseases. Thus, imbalances in the activity and function of various proteases has been linked to acquired and inherited human conditions (Netzel-Arnett et al., 2006). Often dysregulation of protease expression and activity are associated with progression of tumours, predominantly partaking in promoting cancer cell metastasis and invasion. Other pathological diseases linked with protease function also exist and, often, the identified mutations instigating such diseases provide breakthroughs in understanding their proteolytic function. For example, a mutation in corin, and loss of activation leads to hypertension and heart disease (Dong et al., 2013, Wang et al., 2008).

According to Carlos Lopez-Otin 584 protease enzymes have been identified in humans, which were further classified by the type of catalytic residues found in their active site, as these are essentially responsible for the catalytic function and specificity of their reaction (see review Puente et al., 2003) . As such, there are five different classes of proteases; metalloproteinases which contain a metal ion in their active site, cysteine proteases, aspartyl proteases, threonine proteases and finally serine proteases on which this study is focused.

1.2 Structural features and biochemistry of serine proteases

Serine proteases, which belong to two distinct classes, the trypsin-like and subtilisin-like proteases, are among the first enzymes to be extensively studied due to their involvement in multiple physiological processes such as blood coagulation, digestion and tissue differentiation (Carter and Wells, 1988, Neurath, 1985, Neurath, 1994, Siezen and Leunissen, 1997). At the highpoint of discovery of proteolytic enzymes, came the identification of the primary sequences and 3D structures for the serine proteases trypsin and chymotrypsin (Walsh and Neurath, 1964). Later, studies established the functionally significant residues in these sequences, contributing to the understanding of their catalytic mechanism and defining substrate specificity. Therefore, by the early 1990s, the catalytic mechanism of serine proteases was recognised as one of the best-studied mechanisms in biochemistry (Perutz, 1992).

Serine proteases display similarities in their structures and share a common catalytic mechanism for selective cleavage of substrates, involving a catalytic triad in their active site with Ser-195, His-57 and Asp-102 amino acids (positions of triad residues in reference to chymotrypsin), the S1 specificity pocket, the oxyanion hole and the substrate main chain binding site. These features are known to contribute to the stabilization of intermediates formed by catalysis and substrate binding specificity (Carter and Wells, 1988). The enzymatic activity of serine proteases also functions in complex regulatory mechanisms such as fertilisation and embryogenesis (List et al., 2006a, Netzel-Arnett et al., 2006, Netzel-Arnett et al., 2009).

1.2.1 Trypsin-like serine proteases

The trypsin family encompasses a vast range of enzymes found ubiquitously in prokaryotes and eukaryotes, and there are ~240 expressed in humans (Bachovchin and Cravatt, 2012). Although a large number of the trypsin-like enzymes are soluble proteins, including chymotrypsin and trypsin, one subclass consists of membrane-associated enzymes. Amongst these enzymes are those that

are classified as the type II transmembrane bound serine proteases (Bugge et al., 2009).

1.2.2 Type II transmembrane bound serine proteases (TTSP)

Analysis of genome and expressed sequence tag databases revealed this new family of serine proteases, which are unique due to their associations with the plasma membrane, known as the type-II transmembrane serine proteases (Hooper et al., 2001). They provide focal proteolysis for many biologically active proteins in various cellular and developmental processes and are frequently involved in consecutive protease cascades. The human TTSP family consists of 17 members while 19 members (Figure 1.1) are found in rodents, which are further divided into four different sub-families (Bugge et al., 2009).

Matriptase is a transmembrane bound serine protease belonging to the matriptase sub-family of TTSPs along with matriptase-2, matriptase-3 and polyserase-I (Figure 1.1) and is the most studied protease in this group (Bugge et al., 2009). Matriptase was identified in 1993 as a secreted gelatinase expressed by human breast cancer cells and proposed to play a role in promoting invasion and metastasis (Shi et al., 1993). First structural analysis based on isolated cDNA sequence for matriptase revealed a soluble enzyme, however shortly after this cDNA was reported to be missing the 5' end sequence (Lin et al., 1999b). Therefore, a later study revealed that this sequence codes for an N-terminal anchor domain (54 residues), which is a transmembrane domain that localised matriptase to the membrane surface (Takeuchi et al., 2000). The matriptase cDNA was cloned by several independent groups, who gave it different names in the literature, including, matriptase, MT-SP1, TADG-15, epithin and SNC19 (Cao et al., 1997, Zhang et al., 1998, Kim et al., 1999, Takeuchi et al., 1999, Lin et al., 1999b, Tanimoto et al., 2001, Cereijido et al., 1978, Szabo et al., 2008).

Matriptase-2 and matriptase-3 were discovered shortly after Matriptase, showing significant structural similarities, mainly consisting of a large stem region made up of multiple domains (Velasco et al., 2002, Szabo et al., 2005). So far only the physiological function of matriptase and matriptase-2 have been characterized, and linked with functional mutations in humans.

Matriptase has multiple roles in epithelial development and homeostasis:

Matriptase is the most studied member of the matriptase subfamily up to date, and displays diverse physiological functions by acting thorough multiple signalling routes. Studies of individuals with homozygosity for null and hypomorphic mutations in the ST14 gene (coding for matriptase) and development of knockout and hypomorphic mice (<1% st14 mRNA), revealed a critical function in epidermal barrier development, thymic homeostasis and hair follicle development which are important for postnatal survival (List et al., 2002). Furthermore matriptase has been found to play a key role in epithelial cancer progression, as found elevated in a variety of late stage human carcinomas, and is suggested to play a role in cancer cell invasion (List et al., 2005, Riddick et al., 2005, Uhland, 2006). Therefore, matriptase activity must be tightly regulated in epithelial tissue, as dysregulation in either direction (reduced or increased activity) can result in epithelial tissue dysfunctions and lead to diseases such as cancer.

Matriptase-2 and iron homeostasis:

The proteolytic activity of matriptase and matriptase-2 have been intensely studied and shown to be vital for the regulation of various mechanisms and imperative for normal physiological function. Unlike matriptase, matriptase-2 expression is restricted to the liver of foetal and adult humans where it conveys its predominant role in regulating iron homeostasis (Velasco et al., 2002). Generation of knockout mice for matriptase-2 showed that they developed an iron-deficiency anaemia phenotype due to elevated levels of hepcidin, a peptide hormone produced by the liver (Park et al., 2001). This effect is mediated through the loss of the proteolytic processing and inactivation of hemojuvelin, a regulator of hepcidin, by matriptase-2 (Silvestri et al., 2008, Ramsay et al., 2009). Matriptase-2 deficiency, or loss of function mutations in TMPRSS6 discovered in humans, lead to iron-refractory iron-deficiency anaemia, which is hereditary condition marked by severe microcytic anaemia, low transferrin saturation and high blood/serum hepcidin levels (De Falco et al., 2013).

Matriptase-3:

Matriptase-3 is expressed by the TMPRSS7 gene and has high homology to matriptase as revealed through bioinformatics and molecular cloning techniques in 2005 (Szabo et al., 2005). The expression pattern of matriptase-3 is similar in both humans and mice where mRNA expression is abundant in various tissues, including the brain, skin salivary gland, reproductive and oropharyngeal tissues (Blikslager et al., 1999). Similarly to matriptase and matriptase-2, matriptase-3, once activated shows proteolytic activity toward macromolecules such as gelatin, casein and albumin and is able to form inhibitor complexes with many serpins including PAI-1, α 2-antiplasmin and antithrombin (Blikslager et al., 1999). Not much is known regarding the physiological function of matriptase-3 as no knockout or human mutations have been identified yet. In fact, in the past decade, most studies have focused heavily on matriptase for unveiling its physiological influence and functional mechanisms both in humans and mice, which led to some significant discoveries in wide areas of development and health.

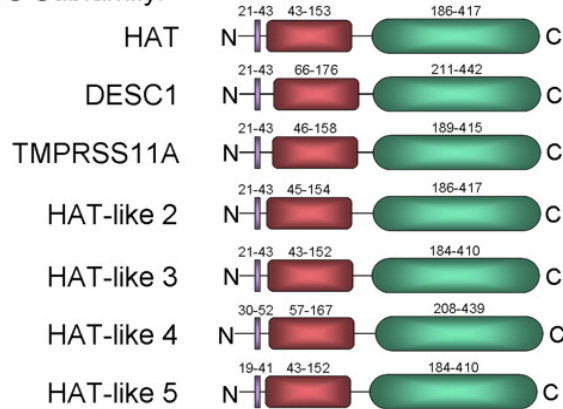
1.1.2.1 Matriptase

Structure

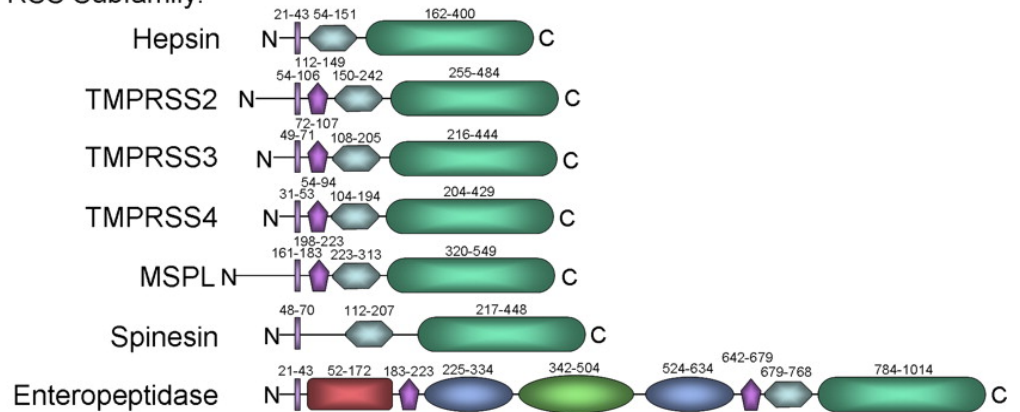
The overall structural organisation of matriptase was determined through analysis of the cDNA sequence, which revealed a complex multi-domain protease. This structure comprises a short N-terminal signal anchor domain that facilitates matriptase localisation at the epithelial cell membrane and is predicted to associate with filamin (a large dimeric protein that cross links actin filaments) and link matriptase to the actin cytoskeleton (Kim et al., 2005). There is also the transmembrane domain which links with the extracellular region, which contains the SEA domain, two CUB domains followed by the four LDLRa domains and finally the serine protease domain (Figure 1.1). The extracellular non-catalytic domains are thought to contribute to substrate specificity and binding, autocatalytic

activation of matriptase, along with localisation and inhibition (Oberst et al., 2003b).

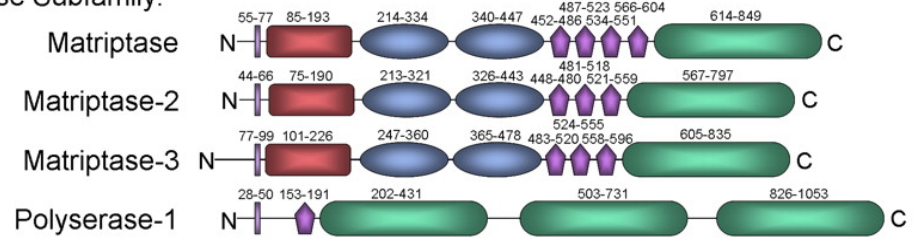
HAT/DESC Subfamily:



Hepsin/TMPRSS Subfamily:



Matriptase Subfamily:



Corin Subfamily:

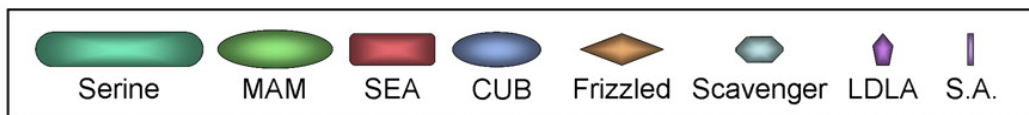


Figure 1.1 Schematic showing the different sub-families of TTSPs and the domain structures of all 17 protease members (Bugge et al., 2009).

1.2.2.1 Matriptase activation mechanism

Matriptase is initially synthesised as a proteolytically inactive single-chain zymogen consisting of 855 amino acids with a molecular weight of approximately 95kDa. The activation of the matriptase zymogen requires two sequential cleavage events. First occurs a N-terminal non-enzymatic cleavage after Arg-149 in the Gly-Ser-Val-Ile-Ala motif present in the SEA domain, which remains tightly attached via a strong covalent bond (Macao et al., 2006, Cho et al., 2001). It has been proposed that pre-activation cleavage within the SEA domain is required to generate a low intrinsic catalytic activity in the zymogen form of matriptase to aid an autocatalytic activation mechanism between matriptase zymogens on the cells surface (Oberst et al., 2003b, Miyake et al., 2010). Full catalytic activation of matriptase only occurs following a second proteolytic cleavage, after Arg-614, in the Arg-Val-Val-Gly-Gly motif present in the C-terminal serine protease domain (Oberst et al., 2003b). Once activated matriptase zymogen is converted to a disulphide-linked-two-chain active enzyme (figure 1.3), which is suggested to activate other matriptase molecules at the cell surface. This autocatalytic activation mechanism was proposed based on the observation that the canonical activation cannot happen if any of the catalytic site residues are mutated (List et al., 2006a, Oberst et al., 2003b).

The suggested autoactivation mechanism of matriptase is rare among the serine proteases as the most common activation mechanism is mediated by another upstream protease. Not much is therefore known about what triggers this autoactivation, yet some studies have shown that this is rapidly induced upon exposure to mildly acidic pH (Lee et al., 2007, Oberst et al., 2003b). This feature though suggests that matriptase acts at the pinnacle of proteolytic activation cascades.

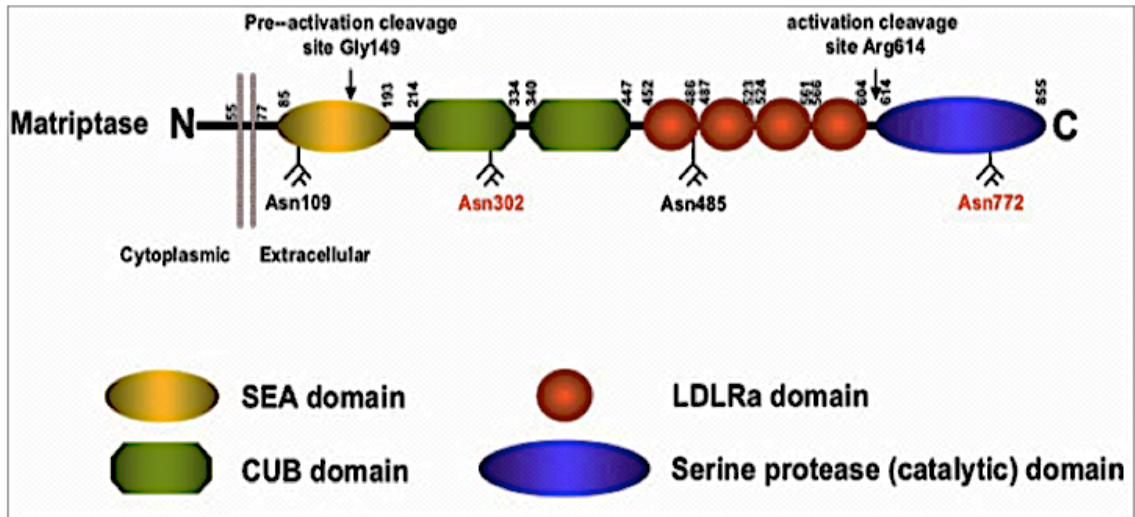


Figure 1.2 A schematic demonstrating the complex structure of the TTSP member **matriptase** (Bugge et al., 2007).

This diagram shows the intracellular and extracellular domains of matriptase, and illustrates some of the important protein residues including those targeted for posttranslational modification and sequentially cleaved, to give rise to the active form of matriptase. The structure of matriptase includes the intracellular N-terminal domain, linked to the extracellular domains via a short transmembrane domain. The extracellular part of the protease consists of the non-catalytic Sea urchin sperm protein, enteropeptidase, agrin (SEA) domain, the two C1s/C1r, urchin embryonic growth factor, bone morphogenesis protein-1 (CUB) domains followed by the four low density lipoprotein receptor-like protein type-a repeat (LDLRa) domains (Bugge et al. 2007).

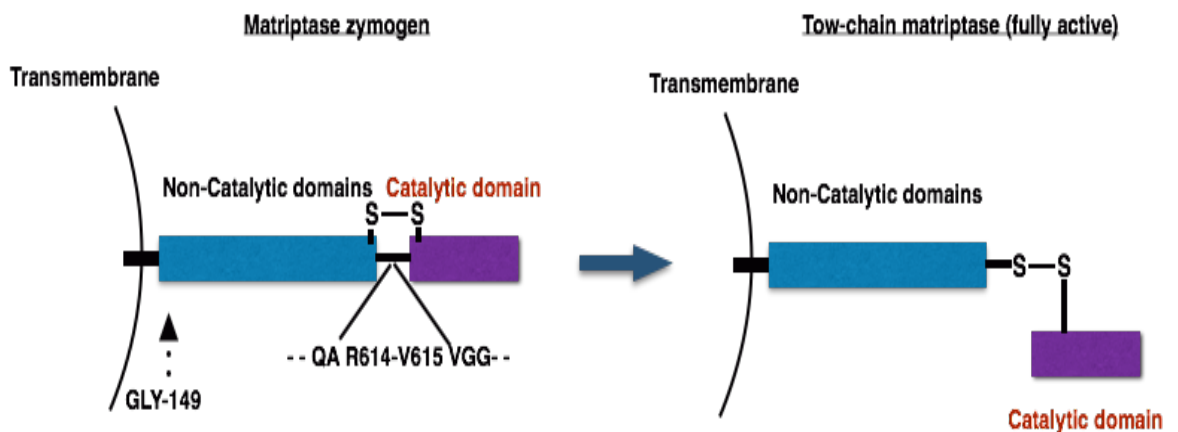


Figure 1.3 Process of activation of matriptase zymogen at the cell surface. Proteolytic conversion of matriptase from a single-chain inactive protease to a two-chain fully activated enzyme at the cell surface. During synthesis and maturation, matriptase is cleaved at Gly-149, and this cleavage is necessary for subsequent autoactivation carried by proteolytic cleavage after Arg-614, at the cell surface.

1.2.2.2 Regulation of matriptase activity: Hepatocyte growth factor activator inhibitor-1 and 2 (HAI-1 and HAI-2)

Matriptase activity is tightly regulated *in vivo* by the cognate inhibitors known as the hepatocyte growth factor (HGF) activator inhibitors, HAI-1 and HAI-2, which were initially identified as inhibitors of the Hepatocyte growth factor activator, a serine protease derived from the liver (Shimomura et al., 1997). These inhibitors are type-I transmembrane proteins, their structure consisting of two extracellular Kunitz-type serine protease inhibitor domains (Velasco et al., 2002, Szabo et al., 2005). HAI-1 is a more efficient inhibitor of matriptase, while HAI-2 conveys a wider inhibitory spectrum against other serine proteases and it is a much more efficient inhibitor of hepsin (a TTSP closely related to matriptase) (Oberst et al., 2003b). A similar expression distribution between HAI-I and matriptase was shown at both the pre and post-natal stages of development. Both proteins coincide at the cell surface on the epithelial component of epithelium-containing tissues, suggesting matriptase is a physiological target of HAI-1 (Kataoka et al., 1999, Oberst et al., 2003a, Oberst et al., 2005).

This mechanism of regulation of matriptase activity is strictly fundamental for development and maintenance of tissue functions, as dysregulation underlies a number of pathological events observed in both humans and mice with severe and fatal consequences (Riddick et al., 2005, List et al., 2007b, List et al., 2002). A post-development study of matriptase regulation by HAI-1, using transgenic mice, has illustrated that overexpression or hyperactivation of matriptase enhanced oncogenesis and promoted tumour progression (List et al., 2005). Here, they showed that simple ectopic overexpression of matriptase in the basal keratinocyte compartment of the skin where matriptase, HAI-1 or HAI-2 are not abundant, significantly enhanced the development of carcinogen-induced Squamous Cell Carcinoma (SCC). This effect was shown completely negated by the co-expression of matriptase with HAI-1 or HAI-2, suggesting that SCC induction occurred through matriptase hyperactivity (List et al., 2005).

Altered balance between matriptase and the cognate inhibitors has been shown in many human carcinomas including prostate and ovarian cancers. This change in expression and balance was particularly prominent in the late stage tumours, signifying a role in progression of the disease (Bergum and List, 2010, Riddick et al., 2005, Oberst et al., 2002). Another clinical study conducted in a cohort of node negative breast carcinomas also showed a tight correlation between matriptase and HAI-1, with poor patient outcome (Kang et al., 2003). Therefore control of matriptase activity, by HAI-1 and HAI-2 is essential in preventing matriptase-enhanced tumourigenesis and now matriptase is widely viewed as a strong potential target for cancer therapy.

Although the process by which HAI-1 and HAI-2 regulate matriptase activity is as yet unclear, biological studies of the function of HAI-1 showed a role in promoting the trafficking of matriptase to the epithelial cell surface. Some have even argued a role in mediating matriptase transactivation as well as inhibition. HAI-1 activation of matriptase requires the intact LDLRa domain of HAI-1, which interacts with matriptase and other proteins (Oberst et al., 2003b). This function of HAI-1 compares to a situation shown for matrix metalloproteinase-2 (MMP-2), when the tissue inhibitor of metalloproteinases, TIMP-2, adapts a complex to bring MMP-2 together with other proteins such as membrane type-1 MMP (MT1-MMP), to mediate its canonical activation subsequent to its inhibition (Kinoshita et al., 1998, Hernandez-Barrantes et al., 2000). Therefore, HAI-1 may be able to establish multi-complexes via the LDLRa protein-binding domain, facilitating binding between two matriptase molecules for auto-activation or matriptase and other activating enzymes. Although HAI-1 may facilitate the activation of matriptase, its main and critical function is to regulate this activity for tissue homeostasis. To expand, the functional significance of HAI-1/matriptase liaison was strongly demonstrated *in vitro*, when often the expression of full-length matriptase cDNA requires co-transfection with HAI-1 to ensure stable expression and proper localisation of the matriptase enzyme (Oberst et al., 2003b, Oberst et al., 2005).

1.2.2.3 Matriptase epithelial expression

During embryogenesis, matriptase expression occurs in the embryo proper, as detection was shown in the epithelial lining of different developing tissue and becomes increasingly distinct with stage progression, and the extra embryonic tissue (Frizelle, 2006). This pattern is highly conserved across mammalian species and implies a role for matriptase in these tissues (List et al., 2006b).

Post-developmental expression of matriptase in human and mouse tissue has been studied using various techniques such as *in situ* hybridization, immunohistochemistry, and enzymatic gene trapping with the beta-galactosidase gene trapping system. These techniques showed that matriptase expression is predominantly seen in epithelial rich tissue and therefore found in multiple organs, including the skin, ductal epithelium of the breast, kidney, pancreas, the lung epithelium, small and large intestine, stomach, oesophagus, bladder, reproductive epithelia including epididymis, ovary, cervix and glandular epithelium (Oberst et al., 2003a, List et al., 2006b). The function of these organs is profoundly reliant on their epithelial structure and integrity, which are features know to be regulated by matriptase in the skin and intestine. However, the specific function of matriptase in many of these tissues has not yet been fully determined.

1.3 Epithelial tissue structure and barrier functions

In simple multicellular organisms, the strict passage of liquids, ions and solutes is very important for their development as this feature allows individual cell types to interface with the external environment. In more complex organisms, the diversity of cell types that form barriers is considerably higher. The epithelia of multicellular organisms are a specialized and highly robust tissue that forms the lining of external and internal body surfaces. The difference in the association and organization of individual epithelial cells in these tissues is largely dependent on the external environment and the overall function of this tissue. The stratified epithelia, such as the skin epidermal tissue, and the simple epithelia, such as that forming the lining of the intestine, are the two major structures found in vertebrate species. These tissues consist of tightly packed cells that reside on a

basement membrane and are linked via a well-differentiated network of intercellular junctions. These junctions are important as they allow for tight interaction between adjacent cells and regulate transport of material across the tissue while preventing ingress of macromolecules and pathogens (Presland and Jurevic, 2002).

1.3.1 The development and function of the “stratified” epidermal barrier

The stratified epidermis is a multilayer tissue originating from keratinocytes, which arises from proliferating basal cells. These keratinocytes are directed outwards to undergo a series of distinct differentiation events to form the stratum corneum, which consists of a lipid rich extracellular matrix in which the corneocytes (dead keratinocytes) are embedded. Both the stratum corneum along with the underlying differentiating keratinocytes that are closely interlinked via tight junctions constitute the epidermal barrier (Fuchs and Raghavan, 2002, Segre, 2003). This tissue fully develops prior to birth and functions as an external permeability barrier that prevents excessive water loss and entry of toxic chemicals and microbes (Presland and Jurevic, 2002). This tissue is organised to withstand great pressures presented by the direct exposure to the external environment.

1.3.2 The development and function of the “simple” and polarized epithelial barriers

Unlike the stratified epithelia, the simple epithelium develops from a single layer of tightly packed and well-polarised cells that coat the inner body cavities such as the kidney tubules, lung and intestinal tract. This tissue carries important roles in the diffusion and absorption of molecules, but is also a protective and separation barrier for inner organs. Here, epithelial cells undergo a set of complex structural and biochemical changes during differentiation to achieve a polarity that is characterized by a differential positioning of plasma membrane domains and specific organelles, to the apical and basolateral axis, known as apical-basolateral polarity (Shin et al., 2006). This aids in structural definition of the simple epithelial

tissues, where the apical membrane faces the luminal space and takes on specialized tissue functions, while the basolateral membrane carries more general functions such as the uptake of nutrients from the blood (Martin-Belmonte and Perez-Moreno, 2012).

1.3.3 Simple epithelial apical-basolateral polarity

High interest in the subject of epithelial polarity and tissue permeability, particularly in the field of drug delivery, has yielded much research aiming to clarify the mechanisms that takes part in regulating the establishment and maintenance of epithelial cell polarity among different organisms and cell types. The organised sequence of events that lead to apical-basolateral polarity are guided by multiple mechanisms that partly partake in what is described as the epithelial polarity program (EPP) (see review (Tanos and Rodriguez-Boulan, 2008). This EPP is executed upon the establishment of separate apical-basolateral domains, redistribution of the cytoskeletal network, apical assembly of the lateral tight junction proteins and polarised trafficking, when mechanisms of basal and apical sorting of protein take place. Here the organisation of the cytoskeleton is accomplished in preparation for the polarised trafficking, whereby drastic changes in the microtubule cytoskeleton occur. These changes involve the repositioning of the microtubule filament along the apical-basolateral membrane axis, where they associate with the lateral adhesion junctions (Bacallao et al., 1989, Musch, 2004).

1.3.4 Epithelial tight junctions have important roles in determining barrier polarisation, permeability and function

Substance transport is an important aspect of epithelial physiology, and this is directed through two routes, the paracellular route where substances pass through the intercellular space between cells and the transcellular route (Figure 1.4) where substances pass through the cell across the apical and basolateral membrane (Zeuthen, 2002). Both pathways are important for absorption, particularly in tissues such as the gastrointestinal tract (GIT) and kidney. The physiology of the

paracellular pathway in epithelial tissue defines tissue permeability by a specialised network of cell-cell junctions that seal the paracellular space. These junctions also help define the overall structure and function of different epithelial tissues. The paracellular epithelial route consists of many families of intercellular junctions, including the tight junctions, adhesion junction proteins, the gap junctions and desmosomes, which either provide mechanical attachments between cells (e.g. adhesion junctions, desmosomes and tight junctions) or provide channels for selective diffusion of ions and small molecules (e.g. gap junctions and tight junctions) (Anderson and Van Itallie, 1995). The tight junctions are the most important for determining barrier selective permeability and tightness.

Tight junctions form the most apical adhesion strands between epithelial cells, which function as selective gates for restricting the paracellular flow of ions and solutes from the apical to the basolateral surface and *vice versa*, required for defining the paracellular permeability of many different epithelial tissues (Mandel et al., 1993).

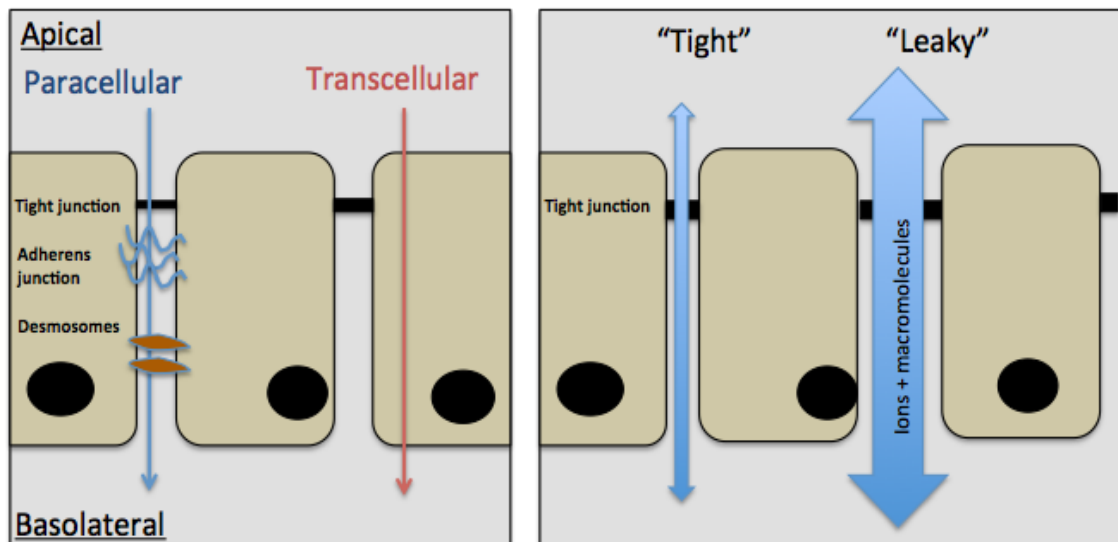


Figure 1.4 Simple and polarised epithelial cells form tight cell-cell associations that assemble to separate between the apical and basolateral tissue domains. The left schematic describes the two major routes of transport across epithelial layers, the “Paracellular” and the “Transcellular” pathways. The tight junctions determine a “tight” or “leaky” paracellular permeability property of the epithelial layers (right diagram).

1.3.4.1 Junction structure

The tight junction (also termed *zonula occludens*) were first observed by electron microscopy in the 1960s, as an apparent fusion of adjacent cell membranes (Farquhar and Palade, 1963). It was subsequently shown that these were intramembranous-particle chains made by the crosslinking between multiple integral proteins (Staehelin, 1973, van Deurs and Koehler, 1979). These chains were later described as lateral strands, which formed at the apical domain between epithelial cells after the basolateral adherens junctions are formed (Denker and Nigam, 1998, Staehelin, 1973, van Deurs and Koehler, 1979). Later studies identified many types of proteins that are part of the tight junction family, which includes transmembrane and intracellular non-membrane bound components. The membrane-associated proteins are the claudins, occludin and Junctional Adhesion Complexes (JAMs), while the zonula occludens (ZO) proteins (Figure 1.6) are part of the non-membrane associated but still peripheral tight junction proteins (Anderson and Van Itallie, 1995).

The establishment and stability of tight junctions involves complex interactions between claudins, occludin, JAMs and ZO proteins with the cytoskeletal actin network (Minond et al., 2006). These membrane proteins can join and form linear aggregates to create continuous homotypic or heterotypic network strands at the most-apical domain of the lateral plasma membrane (Denker and Nigam, 1998). The membrane strands form tight or weak hydrophobic associations with other strands on opposing membranes of neighbouring cells, determined by the ratio of the different claudin isoforms expressed (Figure 1.5). These direct interactions between intracellular tight junctions, mainly determined by the ratio between the different claudin members expressed, determines the permeability and physiological function of different epithelial tissues. For example, high expression of claudin-2 isoform in the tight junctions is typical of water-transporting epithelia, such as the proximal tubule of the kidney. While much tighter epithelia such as that of the distal kidney tubules, where the reabsorption of water molecules takes

place, express much lower levels of claudin-2 (Lee et al., 2006, Heitz et al., 2008, Enck et al., 2001).

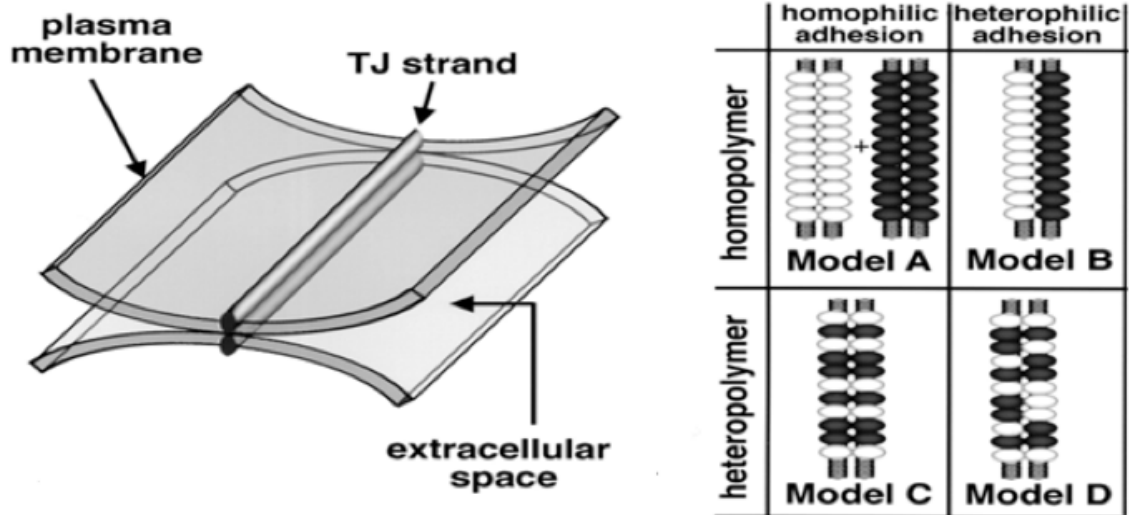


Figure 1.5 An illustration of the structure and assembly of the tight junction strands at the cell-cell association sites. Membrane integrated tight junction strands join with other strands on opposing lateral membranes and this restricts the intercellular space to almost zero. The composition and ratio of the different claudins embedded within these strands is what determines the permeability of such barrier systems. Homotypic and heterotypic associations can be formed between different claudins on opposing plasma membranes to reflect the function of the tissue in which they become expressed (Denker and Nigam, 1998).

1.3.4.2 The Claudins and occludin:

There are 24 identified mammalian claudins; 23 in humans, which have been shown to exhibit a tissue specific expression pattern. They are coded by a multi-gene family, which is thought to arise from a single gene, through evolutionary duplication. Claudins are small multi-domain proteins (approximately 21 kDa), with a similar structure to occludin (63 kDa), which is another type of membrane associated tight junction protein (Van Itallie and Anderson, 2006). The structure of claudins consists of a short intracellular amino-terminal sequence, a first extracellular loop (EL1) consisting of approximately 60 amino acid residues, an

intracellular loop that is followed by another extracellular loop (EL2), which consists of only 24 residues and finally an intracellular C-terminal sequence that varies in the number of residues between the different claudins, ranging between 21 and 63 residues (Krause et al., 2008).

Various studies have shown that the two extracellular loops of these claudins have different functions. The EL1 domain of some claudin isoforms, for example, contains charged amino acids that are responsible for mediating ion selectivity and aid the formation of aqueous pores within the apical tight junction adhesion strands (Van Itallie and Anderson, 2006). The EL2 is responsible for claudin dimerisation at opposing strands via hydrophobic interactions between aromatic side-chains of the amino acid residues (Krause et al., 2008). However, the recruitment and stability of claudins in the tight junctions is mostly due to the C-terminal domain binding with specific intracellular/ peripheral components such as the ZO proteins (Denker and Nigam, 1998).

1.3.4.3 The zonula occludens proteins (ZOs)

The zonula occludens proteins, ZO-1, ZO-2 and ZO-3, are intracellular scaffolding protein members of the membrane-associated guanylate kinase (MAGUK) family, which can associate with each other (Haskins et al., 1998, Gumbiner et al., 1991). These proteins are large (approximately 225 kDa), and made up of multi-domains including the Src Homology 3 (SH3) domain, a guanylate kinase homologous domain and a proline-rich C-terminal domain, involved in the direct or indirect associations with the cytoskeletal actin filaments and the PDZ domains that binds a diverse set of junction proteins (Hartsock and Nelson, 2008). As major components of the tight junction they have been shown to have a critical role in the recruitment, localisation and stabilization of the transmembrane tight junction proteins as well as adhesion proteins (Hartsock and Nelson, 2008). Studies have shown that they can facilitate tight junction formation independent of the preceding formation of adhesion junction belts in fibroblasts, and the silencing of ZO-1 in polarised epithelial cells was shown to delay the development of tight junction strands and overall epithelial polarisation (McNeil et al., 2006).

Overall the claudins, occludin and ZOs, are major structural and functional component of the tight junctions in epithelial and endothelial systems. The claudins however represent the most important components of the tight junctions, known to establish the paracellular barrier and control the flow of molecules across the intracellular space between epithelial cells. Regulation of these proteins is very important for epithelial tissue homeostasis as dysregulation is found in many epithelial carcinomas and independently some claudins were shown to play a role in EMT (Ikenouchi et al., 2003).

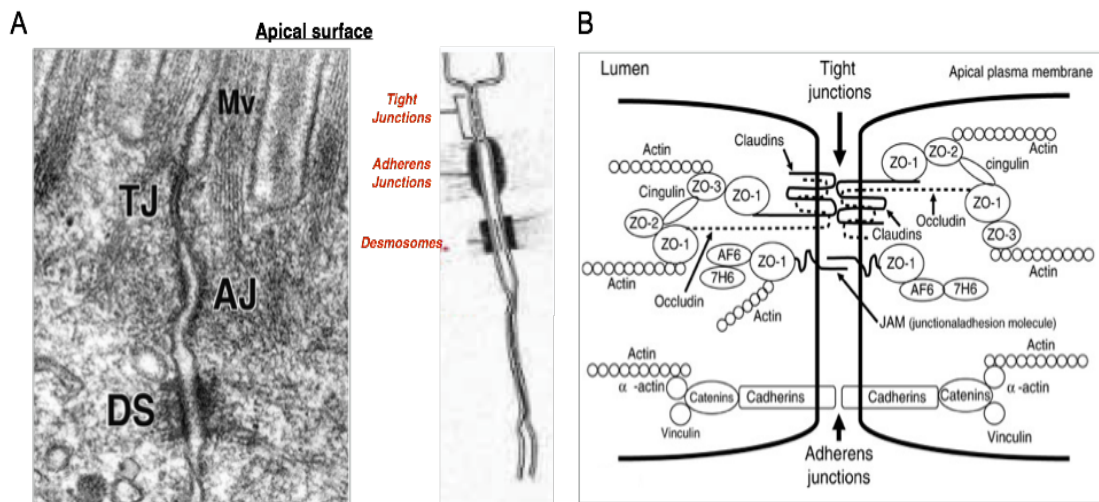


Figure 1.6 This diagram illustrates the major tight junction and adherens junctions formed in simple epithelial barriers. A) Electron microscopy demonstrated the abundance of sequential dense paracellular junction strands, representing the most apical tight junctions, followed by the adherens junctions, desmosomes and gap junctions. B) Complex interactions between membrane tight junctions with the intercellular peripheral components (e.g. ZOs) which provide a link to the actin cytoskeleton (Shalom Avraham, 2008, Van Itallie et al., 2008).

1.3.5 Claudin regulation of paracellular permeability in different epithelia

1.3.5.1 Role in ion transport

Many claudins are differentially expressed in various epithelia. Specific isoforms have been shown to display a critical role in specific tissues. Hence, much of our knowledge about the physiological functions of the individual claudins was discovered through human hereditary conditions or *in vivo* knockout models. For example, two recessive frame-shift mutations altering the second extracellular loop of claudin-16, was associated with primary hypomagnesaemia, as a result of high renal magnesium wasting, with hypercalciuria and nephrocalcinosis in humans (Muller et al., 2003). Other claudin isoforms such as claudin-11 and claudin-14 are particularly important for ear function and hearing. Here, knockout mice illustrated their importance in mediating cochlear compartmentalization and hair cell function (Ben-Yosef et al., 2003).

1.3.5.2 Claudins regulation of paracellular integrity

The different members of the claudin family express different permeability properties. Claudin-1 is one component defined as a sealing tight junction protein with a specific role in the stratified epithelia of the epidermis. Here, deficiency in claudin-1 as achieved in knockout mice, results in the loss of continuous tight junction structures in the stratum granulosum compartment, leading to a leaky epidermal barrier and fatal dehydration (Furuse et al., 2002). However, claudin-1 is expressed in most epithelial tissues including those defined as leaky, such as the proximal tubules of the kidney, where its sealing property is compromised due to weakened interactions forced by the high abundance of claudin-2, defined as a “leaky” tight junction protein (Furuse et al., 2001). In knockout mice with claudin-2 deficiency, the leaky property of the renal proximal tubules was lost and over-expression of claudin-2 in non-leaky tissue or cell lines results in a gain in permeability without loss of any tight junction components (Buzza et al., 2010, Muto et al., 2010, Furuse et al., 2001). This clearly showed that the heterogeneity

of claudins is a major influence in diversified barrier properties of the different types of epithelium.

The regulation of claudin expression is key also for the maintenance of simple and stratified epithelial barrier permeability and function. These proteins and their assembly can be regulated consequent to signalling or can be altered by pathogenic bacteria, which increase barrier permeability to permit invasion (Guttman and Finlay, 2009). Some of the signalling pathways involved in the assembly, disassembly, and maintenance of tight junctions are controlled by various signaling molecules, such as protein kinase C (PKC), mitogen-activated protein kinases (MAPK), and Rho GTPases (Ulluwishewa et al., 2011). These molecules can be activated downstream of numerous cascades, some of which are initiated by enzymatic function, including enzymes such as the trypsin like serine proteases. Changes in these pathways are often associated with compromised barrier epithelial function, and onset of diseases such as inflammatory bowel disease and epithelial cancers (Li et al., 2005).

Tight junctions are highly specialized and dynamic structures, responsive to a range of pathological and physiological stimuli. Tight junction disruption and an associated decrease in epithelial barrier permeability can be documented by changes in the transepithelial electrical resistance (TEER) measure, once cells are grown on permeable transwell filters with a porous membrane.

1.3.5.3 Biophysical methods to study tight junction permeability

Transepithelial electrical resistance (TEER)

TEER is a robust measure of epithelial tight junction permeability, which is used to study properties of the tight junctions expressed by different epithelia and endothelia. TEER measurements are highly sensitive to the expression of individual claudins, which carry different permeability properties. Many claudins such as claudin-1 and claudin-5 function and abundance increase TEER (Low permeability), while the high expression of other molecules such as claudin-2 is

associated with high permeability epithelia and low TEER (Furuse et al., 2001). TEER can be used as a tool to measure barrier integrity continuously during experiments (Douville et al., 2010).

TEER development of barrier forming cells grown on porous membranes can be precisely and repetitively measured using chopstick electrodes (Figure 1.7). In general, resistance is measured by applying a current pulse across the epithelial monolayer and measuring the voltage change, which is calculated using Ohms' law after subtracting the resistance of the bathing medium without the epithelial monolayer (Blank resistance). This measure of conductance is proportional to the area of the epithelial monolayer and the larger the area the lower the resistance, therefore TEER is calculated as Ohms multiplied by area to give $\Omega \cdot \text{cm}^2$.

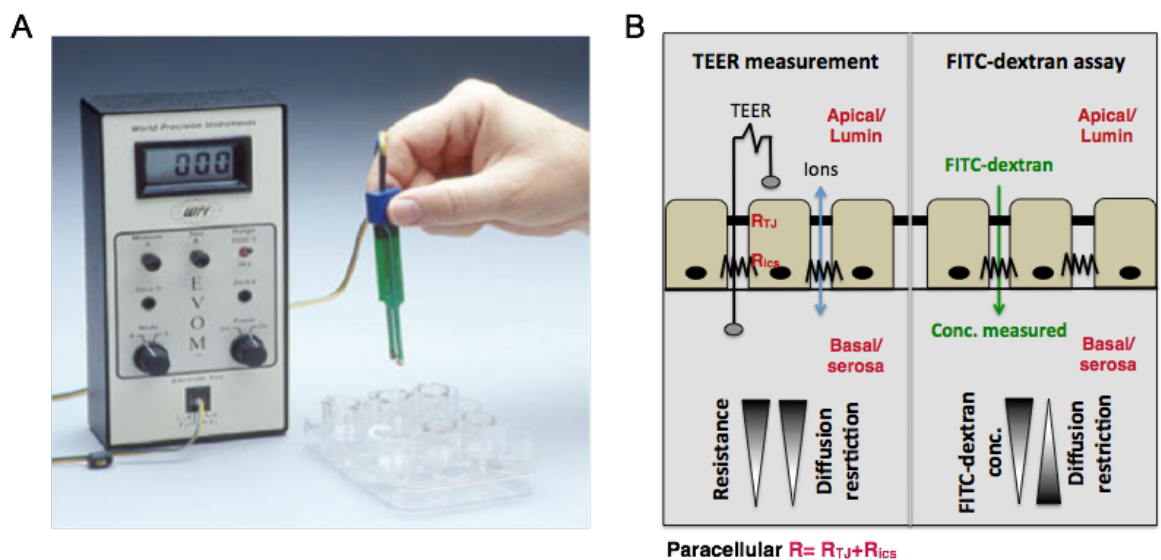


Figure 1.7 Methods for measurement of epithelial paracellular permeability.

A) Epithelial Volt-ohmmeter and chopstick electrodes used to measure the transepithelial electrical resistance (TEER) of epithelial monolayer once cultured on polycarbonate or polyester transwell filters (World Precision Instruments, 2006). B) Different methods used for evaluating epithelial paracellular permeability, include measuring the TEER, which is developed for studying paracellular tight junction integrity and macromolecular flux assays, which can be used to examine physiological permeability of all barrier tissue.

1.4 The role of matriptase in barrier epithelia

1.4.1 Matriptase regulation of stratified epidermal barrier differentiation and integrity

Initially the essential role of matriptase in the epithelia was discovered through gene targeting studies, which revealed aberrant skin development in matriptase knockout mice (List et al., 2002). These showed that matriptase expression is essential for the proper and complete cornification and formation of the stratum corneum epidermal layer, as deficiency led to epidermal aberration, which was associated with loss of pro-filaggrin processing and loss of tight junction function (List et al., 2009, List et al., 2003). The deficiency of matriptase therefore triggered the loss of inward and outward surface barrier function, resulting in the excessive loss of water from the body surface (List et al., 2002). And, although these mice developed to term, they died 48hrs following birth from severe dehydration. The role of matriptase in regulating epidermal barrier function in mice was also confirmed by conditional knockout mice, which also showed increased epidermal permeability and loss of tight junction function and generalised epithelial demise (List et al., 2009).

The discovery of the skin phenotype in the matriptase knockout mice, led to the mutational analysis of human individuals with marked skin hyperkeratosis. Using classical mapping, which was followed by mutational analysis of the ST14 gene, a substitution missense mutation of the Gly-827 catalytic domain residue of matriptase to Arg was identified (List et al., 2007a, Basel-Vanagaite et al., 2007). Individuals with this mutation who were all siblings from one consanguineous marriage, were diagnosed with a newly defined syndrome, Autosomal Recessive Ichthyosis with Hypotrichosis (ARIH) which is characterized by thickened, scaly and shiny skin with follicular hypoplasia (Alef et al., 2009, Basel-Vanagaite et al., 2007). These individuals expressed similar skin and follicular abnormalities as the matriptase knockout mice but without the accompanying fatality.

Subsequent analysis of the G827R human mutation by expression of recombinant protein showed that this induced a large reduction in matriptase catalytic function (List et al., 2007a). And later, this was supported by the survival phenotype of the hypomorphic mice, which expressed significantly lower amount of matriptase mRNA (<1% mRNA). Surprisingly, these mice were virtual phenocopies of the epidermal phenotype in human patients with ARIH, displaying similar epidermal and follicular abnormalities but showing normal survival (List et al., 2007a).

The main mechanism linked with matriptase's role in regulating epidermal barrier homeostasis involves the processing of pro-filaggrin, a filament associated protein essentially responsible for barrier structure and integrity (List et al., 2003). Further studies have shown that this process required the activation of the serine protease prostaticin downstream of matriptase (Steven and Steinert, 1994, Pearton et al., 2002). This is a GPI anchored serine protease, which serves as an essential activating partner as will be explained later in this chapter (List et al., 2007b). Studies of this pathway were directed by the similarity in skin phenotype seen in mice with complete deficiency of prostaticin, compared to the matriptase knockout mice (Netzel-Arnett et al., 2006). Although matriptase and prostaticin are widely co-expressed in almost all epithelia, the mechanism of pro-filaggrin processing is unique to the epidermis. Therefore, matriptase has different functions and possibly different substrates in separate epithelial tissues.

1.4.2 Matriptase regulation of simple intestinal barrier function and integrity

The "global" role of matriptase in the maintenance of homeostasis of multiple and diverse epithelia was revealed using mice developed with a conditional *ST14* allele to perform tissue-specific, embryonic or postnatal matriptase gene ablation (List et al., 2009). These mice were initially developed to overcome the lethal knockout phenotype, and allow for the study of matriptase's role in postnatal development and function of various epithelia. In these studies the effect of conditional embryonic ablation of matriptase on the development and function of the simple epithelia of the GIT was investigated. For intestinal specific ablation of matriptase,

a Cre-LoxP mediated recombination system was generated by interbreeding mice carrying the *ST14^{LoxP}* allele, with mice carrying the Cre transgene under the control of the intestine specific villin-promoter to generate *villin-Cre^{+ / 0};St14^{LoxP} / -*. Littermates of these mice developed severe colonic epithelial abnormalities and suffered from persistent diarrhoea, inflammation, oedema and loss of mucosal epithelial barrier function resulting in death shortly after weaning (Netzel-Arnett et al., 2012, List et al., 2009). Therefore matriptase has been shown to have an essential role in the intestine, which was further highlighted in the hypomorphic model (List et al., 2007a).

Analysis of intestinal epithelial function and integrity in the hypomorphic mice under normal conditions presented striking evidence of abnormal gut epithelial barrier. These mice developed leaky gut epithelia, explained by a 35% decrease in intestinal TEER (Buzza et al., 2010). This phenotype was mimicked *in vitro* with well-known barrier forming human intestinal cell lines (Caco-2 and T84) either with specific ablation of matriptase expression using siRNAs or treatment of cells with a matriptase inhibitor (Buzza et al., 2010, Netzel-Arnett et al., 2012). This increased permeability was largely associated with loss of tight junction function, which in cell culture correlated with an increased expression and incorporation of the leaky tight junction protein claudin-2 (Buzza et al., 2010). Increased levels of this protein were also observed in intestinal epithelia of patients diagnosed with inflammatory bowel disease (IBD). In these patients, examination of matriptase expression showed a decline in colonic mucosa (Netzel-Arnett et al., 2012).

Although mice hypomorphic for matriptase developed a leaky and weak intestinal barrier, they were free of intestinal disease (List et al., 2007a, Buzza et al., 2010). However in an experimental colitis model, these mice showed higher sensitivity to stress, and imposed injury to the intestine became severe, persistent and irreversible. They were incapable of recovering their intestinal barrier once DSS induced colitis was discontinued unlike their littermate controls. These findings suggest that normal matriptase activity and expression is required for barrier maintenance and repair following injury and that this could be dependent on the regulation of claudin-2 (Netzel-Arnett et al., 2012).

1.4.2.1 HAI-1 and HAI-2 regulation of epithelial barrier integrity

Although loss of matriptase does not affect embryonic development, uncontrolled matriptase activity appears to result in embryonic lethality. This was shown by combined deficiency of HAI-1 and HAI-2 (Szabo et al., 2007). To elucidate whether HAI-1 plays a role in epithelial barrier development, mice with homozygous HAI-1 depletion (but expressed in the placenta) were generated. Surprisingly these mice developed an ichthyosis-like condition with altered pro-filaggrin processing and abnormal hair development (Nagaike et al., 2008). However even more surprising, the conditional knockdown of HAI-1 in the intestinal cells increased intestinal permeability and susceptibility to damage similar to the matriptase hypomorphic mice (Kawaguchi et al., 2011). These studies demonstrate that the loss of HAI-1, has equally detrimental effects to loss of matriptase expression and activity, but it is still yet unknown whether matriptase plays a role in this process (summary in Figure 1.8). Despite this, a study showed that matriptase hyperactivity is the main effector of embryonic lethality conveyed by depleted HAI-1 and HAI-2 in knockout mice (Oberst et al., 2005, Friis et al., 2014).

It is important to mention that HAI-1/HAI-2 function as cognate inhibitors of other epithelial components, some of these have been linked with matriptase, such as prostasin (Kataoka et al., 2003).

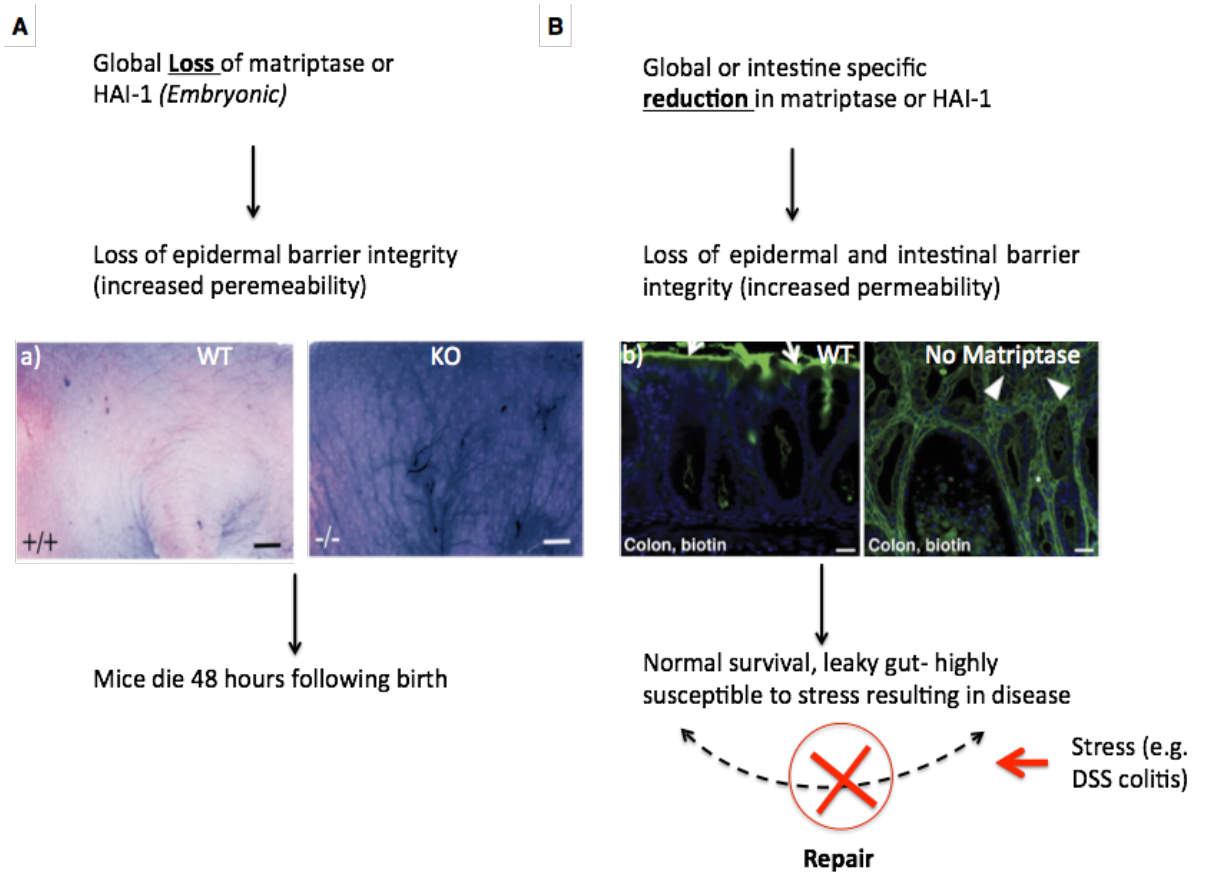


Figure 1.8 Summary of the effect of genetic ablation of matriptase or HAI-1 in both knockout and conditional knockout mice on epithelial barrier integrity.

A) Matriptase knockout mice display aberrant epidermal barrier formation similar to the chimeric HAI-1 knockouts with normal placenta, shown by the aberrant processing of pro-filaggrin. The inserted image shows higher penetration of Toluidine Blue in the skin of matriptase knockout mice (Bottom image) compared to wild-type mice (Top image) (List et al., 2002). B) Low matriptase expression but not complete loss, as well as intestinal specific deficiency resulted in a leaky gut epithelia that is more permeable to macromolecules such as biotin (higher FITC-biotin penetration seen in *inset b* compared to control mice in *inset a*). Similarly mice with intestine specific ablation of HAI-1 displayed leaky intestinal epithelia. This tissue from both matriptase and HAI-1 mice expressed increased sensitivity to stress, demonstrated by their incapacity to recover from damage caused by short-term treatment with the colitis-inducing agent, DSS (Kawaguchi et al., 2011, Kosa et al., 2012, Nagaike et al., 2008, List et al., 2002).

1.5 Putative substrates of matriptase in the epithelia

Despite all of the physiological *in vivo* studies that have analysed and confirmed the role of matriptase in simple epithelial barrier function, the relevant substrates involved remain unclear. Many putative substrates of matriptase have been identified biochemically and some confirmed *in vivo*, when revealing their biological role. Overall, some of the direct substrates include hepatocyte growth factor (HGF) (Owen et al., 2010), protease-activated receptor 2 (PAR-2), urokinase-type plasminogen activator (uPA)(Takeuchi et al., 2000, Lee et al., 2000), and Channel activating protease-1 (CAP-1) also known as prostasin (Netzel-Arnett et al., 2006).

Independently, these proteins play an important role in mediating epithelial function and epithelial integrity as shown *in vivo* and *in vitro*, but whether their roles are mediated by matriptase activity and are distinctive between different tissues is yet to be determined.

1.5.1 Prostasin or channel activating protease-1 (CAP1)

Serine proteases, including matriptase, take part in several proteolytic cascades, in which one active serine protease facilitates the proteolytic activation of another downstream zymogen serine protease. This mechanism is crucial in many physiological and pathological processes, such as in blood coagulation. At the cell surface, matriptase can mediate the activation of other serine proteases, including some surface bound serine proteases such as prostasin (Friis et al., 2013, Netzel-Arnett et al., 2006). Prostasin is a type-I GPI-anchored trypsin-like serine protease expressed by epithelial cells, including those forming the digestive tract, pseudostratified epithelium of the integumentary tracts as well as the urogenital and respiratory tracts where it supports barrier integrity (Verghese et al., 2006, List et al., 2007b). Similarly to other serine proteases, prostasin is synthesized as an inactive zymogen that requires proteolytic processing. This occurs after Arg⁴⁴ in the amino acid sequence QPR⁴⁴ITG (Chen et al., 2010a). Matriptase is a key

upstream activator of zymogen proastatin and both activities are tightly regulated by HAI-1 and HAI-2 (Netzel-Arnett et al., 2006).

As previously mentioned, proastatin activation by matriptase is required for the processing of pro-filaggrin in the maintenance of the epidermal tissue (List et al., 2007b). However, proastatin is also a key regulator of sodium and fluid homeostasis. It was discovered an activator of the epithelial sodium channel ENaC, which is also a substrate of matriptase (Clark et al., 2010, Vuagniaux et al., 2002, Andreasen et al., 2006, Bruns et al., 2007) through cleavage of its gamma-subunit (Vuagniaux et al., 2002, Andreasen et al., 2006, Bruns et al., 2007). Over-activated ENaC has been associated with dehydration in cystic fibrosis (CF) making proastatin and matriptase potential targets for therapeutic inhibition for treatment of the disease (Tong et al., 2004, Rickert et al., 2008, Rotin and Schild, 2008).

Studies have been combined to show that matriptase and proastatin associate and form part of a single proteolytic cascade in epithelia. Both enzymes have been shown to function as part of a reciprocal zymogen activation complex (Friis et al., 2013), with a mutual role in development and regulation of epithelial barrier integrity, particularly the epidermis (Netzel-Arnett et al., 2006).

1.5.2 Hepatocyte Growth Factor (HGF)

HGF is a paracrine growth factor containing 728 residues, which is secreted as an inactive single chain precursor by mesenchymal cells, to signal through cognate receptor, c-Met, on the cell surface of epithelial and endothelial cells (Bottaro et al., 1991). HGF is closely related to the serine protease zymogen plasminogen, comprising a protease domain with mutations in two of the three catalytic triad residues, resulting in an enzymatically inactive protein (Donate et al., 1994). For biological activity the HGF zymogen needs to be converted to the active form by hydrolysis of the canonical Arg⁴⁹⁴-Val⁴⁹⁵ bond (Naldini et al., 1992). Single chain pro-HGF is therefore converted to the double chain form consisting of an α - and β -chain heterodimer interlinked via a single disulphide bridge, between Cys⁴⁸⁷ and

Cys⁶⁰⁴ (Donate et al., 1994). The α -chain consists of an N-terminal PAN/apple domain, which is followed by four kringle domains, while the β -chain consists of the C-terminal protease domain, and both are required for the agonistic function of HGF (Stamos et al., 2004).

Although the critical role of HGF/c-Met signalling in development, tissue repair and carcinogenesis is well founded, the identity of the proteolytic enzymes required for their activation in such contexts is still unclear. Activation site cleavage of pro-HGF can be undertaken by many trypsin-like serine proteases, including membrane bound and soluble proteases. Previously, it was thought that the serine protease uPA is the principle proteolytic activator of HGF, but recent biochemical studies have found no evidence of this activation (Owen et al., 2010). However this and other studies showed highly favourable activation kinetics against pro-HGF in purified systems, by related proteases, matriptase and hepsin (Owen et al., 2010, Herter et al., 2005, Lee et al., 2000). A recent study by Szabo et al showed direct genetic evidence that matriptase can activate pro-HGF *in vivo* as well as identified matriptase as the sole mediator of c-Met initiated oncogenesis (Szabo et al., 2011).

HGF activity is key in many cellular response pathways, taking part in the initiation of multiple cellular processes such as proliferation, migration and even structure and adhesions. One well-known function of HGF is for loosening cell-cell contacts to promote cell migration (*i.e.* scatter factor), a process also promoted by matriptase activation (Lee et al., 2000). However the regulation of HGF by matriptase and role in various aspects of normal epithelial function, in particular regulation of barrier integrity remains unclear.

1.5.3 Urokinase Plasminogen Activator (uPA)

The urokinase plasminogen activator (uPA) is a serine protease and primary activator of plasminogen, which is enhanced by its association with the GPI-anchored, cell surface uPA receptor (uPAR) (Ellis et al., 1989). The product of this

reaction, plasmin, is a potent activator of pro-uPA leading to a “reciprocal zymogen activation” system and an exponential phase of plasmin generation. Previous studies have shown uPA to hold a small intrinsic activity (Ellis et al., 1987, Ellis et al., 1991)), which constitutes the initial proteolytic event leading to the activation of plasminogen to plasmin (Ellis and Dano, 1993). However, more recently our lab studied the effect of matriptase proteolytic activity on the initiation of plasminogen activation in matriptase expressing and non-expressing monocytic cell-lines in culture. THP-1 cells expressing matriptase displayed a rapid linear generation of plasmin without a lag phase, demonstrating that matriptase activates pro-uPA, and that this can occur independently of plasmin. However matriptase is a 100 fold less efficient activator of uPA in purified systems (Kilpatrick et al., 2006).

uPA consists of three domains; the epidermal growth factor (EGF)-like domain required for association with uPAR, a kringle domain, and a 15-residue connecting peptide which links to the serine protease domain (Vincenza Carriero et al., 2009). uPA is synthesised as an inactive zymogen and becomes proteolytically cleaved near the N-terminus of the catalytic domain between Lys 158/15 and Ile 159/16. Once bound to uPAR, uPA mediated activation can initiate a number of biological events (Behrens et al., 2011). This pathway leading to plasminogen activation is implicated in the event of ECM degradation and remodelling, partly through the activation of several matrix-degrading proteases such as the matrix metalloproteases, MMPs. This is important for events such as cell migration, adhesion, invasion as well as proliferation. Often the uPA/plasminogen activation system is dysregulated in a number of human diseases, including cancer.

1.5.4 Protease activated receptor-2 (PAR-2)

PAR-2 is a type of G-protein coupled receptor with seven transmembrane domains and an extracellular N-terminal domain, which becomes proteolytically cleaved to unmask the tethered ligand for receptor activation (Bohm et al., 1996). PAR-2 is found in many tissues, most notable in epithelial tissues including the intestinal epithelium (Bohm et al., 1996) and the skin (Santulli et al., 1995), in which it has

been shown to influence epithelial permeability (Bueno and Fioramonti, 2008). PAR-2 is putatively activated by trypsin-like serine proteases including matriptase, and plays an important role in development and body postnatal homeostasis. PAR-2 dysregulation often contributes to a number of diseases mostly associated with inflammation, triggered by receptor signalling (Bocheva et al., 2009, Sales et al., 2014, Takeuchi et al., 2000, Sales et al., 2014(Sales et al., 2014). One study showed matriptase-mediated activation of PAR-2 is important for regulating the expression of inflammatory cytokines such as IL-6 and IL-8, which become induced and are implicated in conditions such as atherosclerosis (Seitz et al., 2007).

Recently, a study revealed the specific contribution of PAR-2 activity in matriptase mediated oncogenesis, highlighting an essential role in driving the pre-malignant progression of Ras-mediated SCC downstream of matriptase, particularly through proinflammatory cytokine signalling (Sales et al., 2014, Bocheva et al., 2009). As PAR-2 is found co-expressed with matriptase in the epidermis and most other epithelia tissues, such findings proposed an important role for the matriptase/PAR-2 pathway in regular tissue function and homeostasis.

Despite the revelation of the diverse potential substrates of matriptase that have roles in epithelial tissue development, maintenance and function, not much is known as to whether any are key components of the regulatory pathway of matriptase in the simple intestinal epithelia. The previously described role of matriptase in the maintenance of the epidermis is mediated through a tissue-specific mechanism unique to only the epidermis. This mechanism does not take place in other matriptase-expressing epithelia such as the intestine but tight junction establishment in the presence of matriptase and the effects of loss of matriptase have been shown to be important there. Whether these or other identified substrates (Figure 1.9) are key downstream targets of matriptase in the simple polarised epithelia and regulation of barrier integrity needs to be further elucidated. Hence further studies can be carried, *in vitro*, by utilizing some well-understood epithelial cell lines, such as MDCK cells in an attempt to add to the understanding of matriptase's role in the regulation of epithelia.

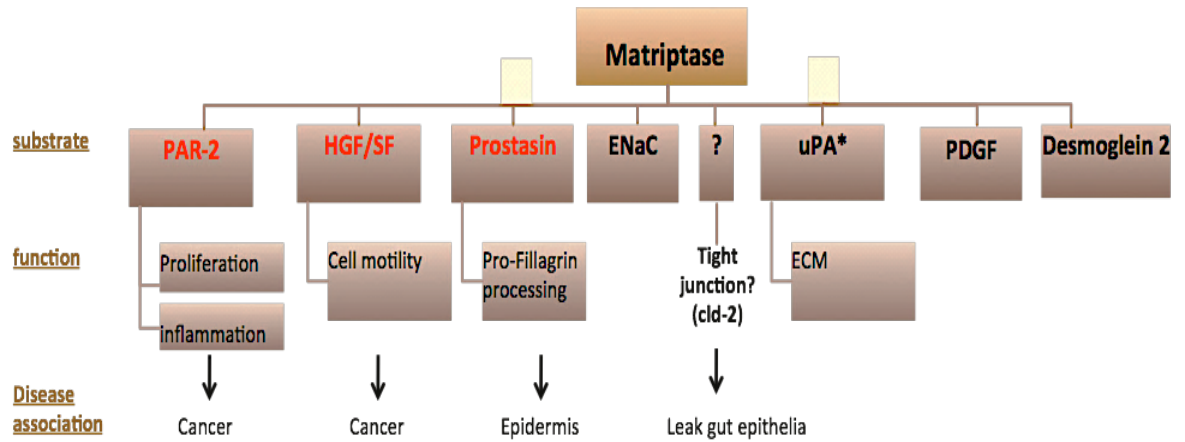


Figure 1.9 *In vivo* and *in vitro* substrates of matriptase proteolysis.

The chart displays the *in vivo* substrates of matriptase proteolysis (red) and substrates shown in other *in vitro* studies (black), along with some of the regulatory downstream functions citing their association with diseases. Evidence for the activation of PDGF-D, Desmoglein-2, and uPA from recombinant or cell culture assays predict directed cleavage (Ustach et al., 2010, Wadhawan et al., 2012, Lee et al., 2000), while ENaC activation was determined in a *Xenopus* model, by monitoring effects on sodium transport (Vuagniaux et al., 2002).

1.6 MDCK cells as a model of matriptase function in epithelial biology

Madin-Darby canine kidney (MDCK) cells are widely used as an epithelial cell model for studying various aspects of epithelial biology. We have recently used MDCK cells to study the effects of matriptase inhibition by the plant-derived protease inhibitor MCoTI-II (*Momordica cochinchinensis* trypsin inhibitor II) (Gray et al). MCoTI-II was found to inhibit cell scattering induced by pro-HGF, but not active HGF, by inhibition of matriptase activation of the pro-HGF.

Therefore MDCK cells may represent an appropriate model system to study the role of matriptase despite the disadvantages brought by species origin, as very limited biological and molecular research tools can be available (Gray et al., 2014).

As strong evidence demonstrated a role of matriptase in the maintenance of intestinal epithelial integrity *in vivo* and *in vitro*, we aim to use the MDCK model, to gain further evidence for this role and begin to elucidate the mechanism involved. For this study the aim is to use two cell strains of MDCK cells that have different barrier characteristics as will be further described in chapter 3. Furthermore, various cell culture techniques will be utilized to study the effect of matriptase on barrier integrity of MDCK cells using two approaches – inhibitors and si/shRNA.

Hypothesis and objectives

Main Hypotheses:

- 1) Matriptase mediates barrier development and recovery in MDCK-I and MDCK-II model cell line is dependent on the tight junction protein claudin-2.
- 2) Matriptase role in regulation MDCK barrier function and the tight junctions is mediated through known substrates.

This research was designed to investigate mainly:

- A. matriptase proteolytic activation is required for the function and maintenance of paracellular integrity in two strains of MDCK cells, as a model for simple barrier epithelia.
- B. Matriptase is essential for tight junction function, and mediates barrier development and recovery of MDCK-I and MDCK-II cells through inhibiting claudin-2 expression.
- C. Matriptase's role in the regulation of MDCK barrier function and the tight junctions is mediated through known substrates.

To summarise research objectives and approaches in this thesis, the following were conducted:

Establishment and classification of model MDCK-I and MDCK-II cells, for the retrospective analysis of matriptase function on ability to maintain paracellular integrity. Includes; characterisation of MDCK-I and MDCK-II structural phenotype in culture, identifying the type of paracellular junctions expressed, define their barrier structure, polarisation and diffusion properties, validation of a calcium switch technique and characterising responses by both strains of MDCK cells, defining matriptase expression and developing a stable model for it knockdown in MDCK-I cells (Chapter 3).

Investigation into the role of matriptase on MDCK-I and MDCK-II barrier using inhibitor and knockdown systems. Outcomes included transepithelial response of MDCK-I and MDCK-II cells to loss of matriptase function and barrier disruption via calcium switch, tight junction expression and reassembly following barrier disruption and with matriptase inhibition, the role of claudin-2 in matriptase mediated effect on barrier function (Chapter 4).

Carrying out a candidate substrate approach for an initial attempt to elucidate the mechanism through which matriptase regulates barrier function in MDCK cells. Includes; analysing the role of prostatic (Including ENaC, EGFR and uPA), HGF/c-met, and PAR-2, and additional analysis of RTK activity and cytokine response (chapter 5).

Chapter 2. Materials and Methods

2.1 General Reagents and Cell Culture

2.1.1 General Chemicals

Table 2.1 The list of reagents and buffers used for the assays

	<u>Reagent/ Chemicals</u>	<u>Source</u>	<u>Property/ function</u>
Transduction: Mission Lenti- virus	1,5-dimethyl-1,5-diazaundecamethylene polymethobromide	Sigma-Aldrich (H9268)	Cationic Polymer: neutralizes the charge between Virions and Sialic acids on the surface of the mammalian cells
General reagents	Phosphate Buffered Saline (PBS) Dulbecco A tablets- without Calcium or Magnesium	Oxoid (BR0014)	Sodium Chloride (0.16 mol), Potassium Chloride (0.003 mol), disodium hydrogen phosphate (0.008 mol), potassium dihydrogen phosphate (0.001 mol), pH 7.3
	tris(hydroxymethyl)aminomethane (TRIS-Base)	Fisher Scientific (BP152)	Primary amide (Organic compound) pH 8.07
	Polyethylene glycol (Triton X-100)	Sigma (100-155)	Non ionic surfactant (micellar average molecular weight, 80,000)
	Polysorbate 20 (Tween 20)	Sigma (93443)	Polysorbate surfactant, Detergent and emulsifier
	Hydrochloric acid (HCL)	Fisher Scientific (S/3160/60)	Inorganic acid, Monoprotonic (Regulate acidity (pH) of solutions)
	Sodium Hydroxide (NaOH)	Fisher Scientific (S302)	Inorganic compound, alkali salt (Regulates alkalinity (pH) of solutions)
	Ethylenediaminetetracetic acid (EDTA)	Fisher Scientific (D/0700/53)	Aminopolycarboxylic acid- Ion chelating agent
	Ethyleneglycoltetraacetic acid (EGTA)	Merck Millipore (324625)	Aminopolycarboxylic acid- Ion chelating agent more selective for calcium compared to EDTA.

	Reagent/ Chemicals	Source	Property/ function
General reagents	Glycerol	Fisher (G/0650/17)	Polyolol.
	Phenol-chloroform	Thermo-Scientific (17908)	DNA extraction
	Agarose	Fisher (BP1360-100)	DNA and RNA gel electrophoresis
Western Blotting: SDS gel electrophoresis	ProtoGel 30% (w/v) Acrylamide: 0.8% Bis-acrylamide.	National Diagnostics (EC-890)	Cross linking agent
	Tetramethylethylenediamine (TEMED)	Invitrogen (15524-010)	Catalyses the polymerization of acrylamide
	Ammonium persulfate (10% APS)	Sigma-Aldrich (A3678)	Catalyses the polymerization of acrylamide
	Sodium Dodecyl Sulphate (10% SDS)	Sigma-Aldrich (L3771)	An anionic surfactant: disrupts non-covalent bonds causing protein denature
	5%(w/v) Bovine serum Albumin (BSA)	Fisher Scientific (BPE9701)	Blocking agent
	Skimmed milk powder	Oxoid (LP0031)	Blocking agent
	Bromophenol blue	Sigma-Aldrich (B0126)	Acid-Base indicator dye
	Coomassie blue	Sigma-Aldrich (M9140)	Staining of proteins separated on polyacrylamide gels
	PonceauS	Electran (44083)	Diazo Dye
	Glacial Acetic acid	Fisher Scientific (A-0400-BP17)	Fixative agent used within gel dye solutions (e.g. Ponceau S and Coomassie blue stains)

Reagents purchased exclusively are discussed in the relevant method.

Table 2.2 list of the reagents used for bacterial culture and Plasmid propagation.

	BioReagent	Source	Properties and roles
Plasmid propagation	Yeast Extract	Fisher Scientific (BP1422)	Source of Vitamins and Growth Factors
	Tryptone	Oxoid (LP0042)	Pancreatic digest of casein (rich source of amino acid nitrogen)
	Sodium Chloride (NaCl)	Fisher Scientific (BP3581)	Sodium Source
	Ampicillin	Formedium (AMP25)	Antibiotic: used in selection for cells that contain the puromycin N-acetyl transferase (PAC) resistance gene
	Agar	Oxoid (LP013T)	Solidifying agent for microbial culture media

2.1.2 Antibodies

Table 2.3 the list of primary and secondary antibodies used to tag proteins of interest.

	Targeting	Antibody	W/B	IF	Species	Source	Block for W/B
Primary Antibodies	Tight and Adhesion Junctions	<i>Claudin-1 (2H10D10)</i>	1/1000	1/50	Rabbit	Invitrogen (374900)	Milk
		<i>Claudin-2 (12H12)</i>	1/500	1/250	Mouse	Invitrogen (32-5600)	Milk
		<i>Claudin-3</i>	1/1000	1/500	Rabbit	Millipore (ABT43)	Milk
		<i>Claudin-7</i>	1/1000	1/500	Rabbit	Millipore (ABT 47)	Milk
		<i>Claudin-9</i>	1/1000	1/500	Rabbit	Santa Cruz (sc-17672)	Milk
		<i>Occludin (N-Term) Polyclonal Antibody</i>	1/1000	1/1000	Rabbit	Invitrogen (406100)	BSA
		<i>ZO-1 alexa fluor 488 conjugate (ZO-1-1A12)</i>	1/250	1/50	Mouse	Invitrogen (339188)	BSA
		<i>E-cadherin (24E10)</i>	1/1000	1/1000	Mouse	Cell Signaling (3195)	Milk
Primary Antibodies	Signalling molecules	<i>p-Erk 22/24 (Thr 202/ Tyr 204)</i>	1/1000	---	Rabbit	Cell Signaling (#9216)	BSA
		<i>Total Erk</i>	1/1000	---	Rabbit	Cell Signaling (#9216)	BSA
		<i>V5 tag</i>	1/1000	---	Mouse	Invitrogen (46-0705)	BSA
		<i>p-Met (tyr 1234/1235)</i>	1/500	---	Rabbit	Cell Signaling (#3126)	BSA
		<i>Total Met</i>	1/500	---	Rabbit	Cell Signaling (#4560)	BSA
		<i>p-EGFR (Tyr 1068)</i>	1/500	---	Rabbit	Cell Signaling (#2234)	BSA
		<i>pAKT (Ser 473)</i>	1/250	---	Rabbit	Cell Signaling (#9271)	BSA
		<i>Stat 1 (tyr 701)</i>	1/1000	---	Rabbit	Cell Signaling (#9271)	BSA
		<i>Rac 1/ 2/ 3</i>	1/1000	---	Rabbit	Cell Signaling (#2465)	BSA
		<i>P-src (Y527)</i>	1/1000	---	Rabbit	Cell Signaling (#2105)	BSA
	<i>p-FAK (Y397)</i>	1/1000	---	Rabbit	Cell Signaling (#3283)	BSA	
		<i>p-PKC ζ/λ (Thr 410/403)</i>	1/1000	---	Rabbit	Cell Signaling (#9378)	BSA
	Matriptase	<i>M32</i>	1/1000	1/100	Mouse	---	Milk
IF secondary antibodies		Alexa Fluor® 647 Goat Anti-Rabbit IgG (H+L)	---	1/1000	Rabbit	Life Technologies (A-11001)	NA
		Alexa Fluor® 488 Goat Anti-Mouse IgG (H+L)	---	1/1000	Mouse	Life Technologies	NA
		Alexa Fluor® 488 Goat Anti-Mouse IgG (H+L)	---	1/1000	Mouse	Life Technologies	NA
WB secondary antibodies		2° anti-Mouse HRP	1/1000	---	Rabbit	DAKO	NA
		2° anti-Rabbit HRP	1/1000	---	Goat	DAKO	NA

* Normal Goat Serum (NGS) was used to block for immunofluorescence

2.1.3 Buffers and solutions

Table 2.4 Details the various buffer solutions used for different experiments.

Buffer	Formula	Method
LB Broth	10g NaCl, 10g Tryptone, 5g yeast dissolved in 1L ddH ₂ O and sterilised by autoclave	Bacterial inoculation
LB Agar	10g NaCl, 10g Tryptone, 5g yeast, 15g Agar dissolved in 1L ddH ₂ O. Sterilised by autoclave	Producing bacterial colonies.
2yt	5g NaCl, 16g Tryptone, 10g yeast dissolved in 1L ddH ₂ O and sterilized by autoclave.	Bacterial transformation.
TAE	2M Tris-HCl and 1M glacial acetic acid with 100ml 0.5M EDTA made up to 1L with ddH ₂ O	Preparing agarose DNA gels.
Ponceau S stain	5% acetic acid, 2% Ponceau S in 30%	Staining and testing protein transfer on western blot membranes
Methylene Blue	2g Methylene Blue, 500ml ddH ₂ O and 500ml methanol	Fixed cell staining
Coomassie Blue	1g of Coomassie Blue added to solution made at 45% Methanol, 10% Glacial acetic acid and 45% ddH ₂ O.	staining protein separated on acrylamide gels
Destain	45% Methanol with 10% Glacial acetic acid and 45% ddH ₂ O.	Removal of non-specific stain acrylamide gels
PBS	1x tablet of PBS dissolved in 100ml of ddH ₂ O.	Multiple purpose
TBS	Dissolved 6.05g of Tris, 8.7g of NaCl in 1L of ddH ₂ O. pH7.5	Western Blot.
SDS sample buffer	10mM Tris, 20% Glycerol, 4% SDS and trace of Bromophenol blue. pH 6.8	Western blots
Western transfer buffer	10X: Dissolved 30.3g Tris and 144g glycine into 800ml of ddH ₂ O and 200ml (20%) Methanol.	Western blots
Western gel running buffer	Dissolved 0.2M Tris, 0.2M glycine and 10% SDS into 1L of ddH ₂ O.	Western blots
Lower gel buffer	1.5 M Tris-Cl, pH 8.8	Western blots
Resolving (Upper) gel buffer	0.5 M Tris-Cl, pH 6.8	Western blots
Sodium Acetate	Added 40.8g NaAc.3H ₂ O to 100mL ddH ₂ O. The pH was adjusted by glacial acetic acid to pH5.2.	DNA precipitations.

2.1.4 Chemical inhibitors, antagonist, agonists and recombinant growth factors

Table 2.5 Detail of inhibitors, antagonists and agonists used in this study:

Type	Inhibitor	Target	Specificity	Source	Applied Concentration
Matriptase Inhibitors	CJ-730 (Inhibitor 8*)	Matriptase S1 specificity pocket (Active site)	Ki 40nM	Gift from Prof Torsten Steinmetzer, Institute of Pharmaceutical Chemistry, Germany.	100 μ M
	CJ-1737 (Inhibitor 59*)	Matriptase S1 specificity pocket (Active site)	Ki 0.4 μ M	Gift from Prof Torsten Steinmetzer, Institute of Pharmaceutical Chemistry, Germany.	100 μ M
	MCoTI-II	Protease domain	Ki 9 nM	Gift from Prof Robin Leatherbarrow, Imperial College London. UK.	100 nM to 1 μ M
	IN-1	Protease domain and catalytic triad Serine residue	Ki 11 nM	Gift from Prof Eric Marsault, University of Sherbrooke. Quebec, Canada.	50 μ M
Signalling pathways	U0126	ERK (antagonize AP-1 transcriptional activity)	IC50 >58nM	Cayman Chemicals (CAS109511-5-82)	1 μ M-10 μ M
	PHA-665752	C-Met (HGFR)	IC50>200 nM	Sigma-Aldrich (PZ0147)	1 μ M-20 μ M
	Tyrphostin-AG 1478	(EGFR)	IC50 3 nM (Reversible)	Sigma-Aldrich (T4182)	0.1 μ M-10 μ M
	Amiloride	(ENaC and uPA)	--	Sigma-Aldrich (A7410)	1 μ M-50 μ M
	ENMD-1068	PAR-2	--	Sigma-Aldrich	1-1.5 mM
General protease inhibitors i.e. PMSF, halt and aprotinin	Aprotinin	Serine Proteases	up to 30 μ M	--	1 μ M
	pmsf	Serine Proteases	--	Sigma-Adrich (p7626)	1X
	Halt's protease and phosphatase inhibitors	Protease and phosphatase inhibitors	--	Fisher	1X
Agonists	PAR-2-AP (2-Furoyl-LIGRLO-amide)	PAR-2	--	R and D systems	5 μ M

2.2 Cell culture

2.2.1 MDCK-I, MDCK-I-CLD2 Tet-off and MDCK-II Cell Culture

MDCK-I cells were a kind gift from Dr Roman Szabo at the national institutes of Health (Bethesda, MD). MDCK-II cells were a gift from Mette Mogensen's group at the University of East Anglia (Norwich, UK). Both MDCK-I and MDCK-II cells were grown in T75 cm² plastic culture flasks (Nunclon, Denmark) with High Glucose Dulbecco's Modified Eagles Medium DMEM (Gibco®, Invitrogen) supplemented with 2mM L-Glutamine (Gibco®, 25030-081) and 10% (v/v) heat inactivated Fetal Calf Serum (FCS) (HyClone, SV30160.03) and maintained at 37°C in a humidified atmosphere with 5% (v/v) CO₂.

MDCK-I-CLD2 cells were a kind gift from Professor Alan Yu at the University of Kansas Medical Center (Kansas City). These cells were maintained using DMEM supplemented with 10% (v/v) FCS at 37°C and 5% (v/v) CO₂ and kept under selection using 100 µg/ml Geneticin® G418 and 150 µg/ml hygromycin (Sigma-Aldrich®). To induce claudin-2 expression cells were maintained in 10% tetracycline free FCS (Gibco®, 26140-087) in DMEM in the absence of doxycycline. To switch off claudin-2 expression 20 ng/ml doxycycline (Sigma-Aldrich®, D9891) was added to the culture media. All MDCK cells were passaged twice a week once they reached 80 to 90% confluence in 75cm² tissue culture flasks using 0.25% (w/v) trypsin with 1mM EDTA (GIBCO, 25200-072).

2.2.2 MDCK-I mission shRNA stable cells

MDCK-I cell lines transfected with the Sigma Mission® PLKO.1-Puro-CMV-GFP for stable expression of two matriptase targeting shRNAs (see method 2.8.2) and the Non Target control (NTC) construct, were cultured in DMEM supplemented with 10% FCS and 2mM L-Glutamine at 37°C and 5% (v/v) CO₂. These cells were kept under selection with 2.2 µg/ml Puromycin (Gibco®, A11138-03). The stably transfected cells were passaged twice a week once they reached 80 to 90%

confluence in 75 cm² tissue culture flasks using 0.25% (w/v) Trypsin with 1mM EDTA (GIBCO, 25200-072).

2.2.3 A549 Tet-off cells

The A549 lung epithelial cancer cell line was originally obtained from ATCC (ATCC®-CCL185™). These cells were maintained using DMEM supplemented with 10% FCS at 37°C and 5% (v/v) CO₂. An inducible (Tet-off) matriptase expression system in A549 cells has been established in the lab (Kelly Gray at the University of East Anglia, UK). To induce matriptase expression by the A549-mat cells, 10% tetracycline-free FCS in DMEM was used. To suppress matriptase expression in this system the cells were also incubated with 1 µg/ml of doxycycline. To maintain selection cells were cultured with 200 µg/ml G418, 0.25 µg/ml puromycin and 1 µg/ml doxycyclin. A549 cells were passaged twice a week once they reach 80 to 90% confluence using 0.25% (w/v) trypsin with 1mM EDTA (GIBCO, 25200-072).

2.2.4 Routine Mycoplasma testing

Cells were tested regularly to ensure they were mycoplasma negative by conducting a regular PCR on culture supernatant collected two days following seeding of the cells. The culture supernatant was boiled for 5 minutes and centrifuged for 60 seconds at high speed. The PCR reaction was prepared using 2.0 µl of the boiled culture supernatant added to this were 5 µl of 5xPhusion Buffer, 0.25 µl Phusion high fidelity Taq Polymerase, 2.5 µl 2mM dNTPs, 2.5 µl 10 µM Myco1 primer and Myco2 primer (see table 2.7) and 10.25 µl Water (Finzymes). The PCR was set to heat the samples for 30 seconds at 98°C, then run 40 cycles of: 10 seconds at 98°C, 20 seconds at 52°C, 30 seconds at 72°C finished with 2 minutes at 72°C. The end products were run on a 2% agarose gel and a band is observed at 270 base pairs in positive samples.

2.3 DNA propagation

2.3.1 Transformation and colony expansion

DH5 α

Most transformations were carried out using DH5 α - T1® and according to manufacturer's instructions. In brief 1 μ l of 1 μ g/ml plasmid DNA (pBluescript) was added to 50 μ l of competent bacteria and incubated on ice for 30 minutes. Cells were subject to heat-shock at 42°C in a water bath for 45 seconds. Cells were incubated on ice for 2 minutes prior to the addition of 900 μ l of room temperature super optimal broth with catabolic repressor (SOC) (Invitrogen. UK. 15544-034). Samples were shaken horizontally at 225 rpm in a 37°C incubator for 1 hour before centrifugation at 5000 rpm for 5 minutes. Approximately 850 μ l of supernatant was gently removed and the palette of cell resuspended in the remaining 100 μ l of medium supernatant before spreading onto agar plate (10 g NaCl, 10 g tryptone, 5 g yeast and 20 g agar added to 1000 ml of sterile water) containing 50 μ g/ml Ampicillin. The plates were cultured at 37°C for 12 hours and single transformed colonies were chosen and expanded by transferring them into 5 ml of LB containing 50 μ g/ml Ampicillin. LB media plus the cell were shaken horizontally at 180 rpm in a 37°C incubator for 12 hours before conducting a miniprep for DNA isolation (see method 2.3.2.1).

STBL-3

The One Shot® Stbl-3™ Chemically Competent *Escherichia coli* (Invitrogen, UK. C7373-03) were used for transformation with the mission PLKO.1 shRNA vectors, the viral packaging vectors and the pInducer 10 (See appendix 1). The transformation was conducted according to the manufacturer's instructions. In brief, 1 to 5 μ l of DNA (10 pg to 100 ng) was added 50 μ l of Stbl3 cells and incubated on ice for 30 minutes. The bacteria was subject to heat shock at 42° C for 45 seconds in a water bath and then placed on ice for 2 minutes before incubating with 250 μ l of SOC at 37°C for 1 hour in an orbital shaker. Cells were centrifuged at 5000 rpm for 5 minutes to generate a bacterial pellet and a

supernatant of which 200 µl was removed. The bacterial pelett was resuspended in the remaining 100 µl of medium supernatant before spreading onto agar plate containing 50 µg/ml Ampicillin. The plates were cultured at 37°C for 12 hours and chosen colonies were expanded by transferring them into 5 ml of LB containing 50 µg/ml Ampicillin and incubating in an orbital shaker at 180 rpm at 37°C for 12 hours before conducting a miniprep for DNA extraction.

2.3.2 DNA purification

2.3.2.1 Plasmid Miniprep

Bacterial culture minipreps were performed using the Plasmid Mini kit II according to manufacturer's instructions (Omega. D6945-01). For the final step the DNA was eluted in 50 µl of nuclease-free water at room temperature and quantified using a Nanodrop™ 2000 (ThermoScientific).

2.3.2.2 PCR purification

For purifying small PCR products as small as 100 bp, the QIAquick® PCR purification kit (Qiagen. 28104) was used as suggested by manufacturers. For the final step the DNA was eluted in 30 µl of nuclease free water. DNA quantification and purity was measured with the Nanodrop™ 2000 instrument.

2.3.2.3 DNA gel extraction

For purifying plasmid DNA, DNA fragments or PCR products directly from an agarose gel, the QIAquick® Gel extraction kit (Qiagen. 28704) was used as suggested by manufacturers. For the final step the DNA was eluted in 30 µl of nuclease free water. DNA quantification and purity was measured with the Nanodrop™ 2000 instrument.

2.3.2.4 DNA precipitation

PCR amplified 96-mer DNA inserts of approximately 100 bps were difficult to extract using the QIAquick® PCR purification kit. Therefore the DNA was precipitated out using ethanol as follows. To the measured volume of the DNA sample 1/10 3M sodium acetate at pH 5.2 was added with 3 volumes of 100% ethanol. The sample mix was vortexed for 30 seconds before incubating on dry ice or at -80°C for two hours. The sample was centrifuged at full speed at 4°C for 30 minutes, placing the tube in a specific orientation to be able to predict the position of the pellet if not completely visible. The pellet was washed with 70% ethanol and centrifuged at full speed for 5 minutes. The 70% ethanol was carefully removed and the pellet was left to air dry at room temperature. The pellet was resuspended in 20 µl-40 µl of nuclease free water. DNA concentration was measured with the Nanodrop™ 2000 instrument before incubating with digestive enzymes and running onto agarose DNA gel.

2.4 Protein extraction and analysis

2.4.1 Cell lysate preparation

Media was removed from cells either in inserts or petri dish. The cells were washed three times with cold sterile PBS to ensure complete removal of media. Cells were directly scraped into 1 x Pathscan® lysis buffer (Cell Signaling, 9803S) with added protease and phosphatase inhibitors (Halt™ Protease and phosphatase inhibitor cocktail with added PMSF (Table 2.5) and left to incubate on ice for 15 minutes. The samples were then harvested into 1.5ml Eppendorf tubes and cellular debris was removed by centrifugation at 12000 rpm for 10 minutes at 4°C. Samples were stored at -80°C for long-term storage or -20°C for short term ready for protein quantification (BCA) and analysis.

2.4.2 Pierce Bicinchoninic acid (BCA) assay for protein quantification

Sample protein was quantified against a standard dilution range (concentration range from 2, 1.5, 1, 0.75, 0.5, 0.25, 0.125, and 0 mg/ml) generated with Bovine Serum Albumin (BSA) protein of a known concentration (2 mg/ml) diluted in the same lysis buffer used for the samples, using the Pierce kit (Pierce Biotechnologies). The kit provided solutions A and B which were mixed at a ratio of 50:1 and of which 200 μ l was required for each 10 μ l of protein standard added to wells of a 96 well plate (usually a triplicate of standard is made). Also 10 μ l of the protein test sample diluted (1:10 or 1:5) was added to a separate well and mixed with 200 μ l of solutions A and B. the plate was covered to prevent the evaporation of samples and incubated at 37°C for 30 minutes. A purple colour standard is observed (due to the chemical reactivity between the peptide bonds and the copper ions which become reduce) and intensity measured at 550 nm using the MRX Spec machine (Dynatech Laboratories). The test sample protein concentration was calculated using the line equation for the BSA standard using excel.

2.4.3 Western blotting

Equal amounts of proteins from cell lysates (30 μ g total amount of protein unless stated otherwise) were mixed with sample buffer (100mM TRIS, 20% Glycerol, 4% SDS with added trace of Bromophenol Blue; pH6.8). Where stated, reducing agent was added (4% β -mecaptoethanol) to sample. Samples reduced and non-reduced were boiled for 3 minutes, unless stated otherwise. Samples were separated by gel electrophoresis with 4% stacking gel and 10% or 8% resolving polyacrylamide gel and run along with Dual colour protein molecular weight (mw) marker from BioRad. The gels containing the samples were run at 200 volts for approx. 45 minutes. The gels were rested in transfer buffer 20% methanol for a period of 30 minutes alongside blotting paper and Immuno-Blot® polyvinylidene fluoride (PVDF) (BIO-RAD, 1620177) membrane or nitrocellulose (GE Healthcare, RPN 203D).

The transfer of proteins from gel to the blotting membrane was conducted using the Bio-Rad semi-dry blotting device at 15V for one gel and 25V for two for approx. 1 hour. Membranes were always stained for 10 minutes with ponceau S red dye (Table 2.4) to ensure a clean (e.g. no bubbles) and efficient transfer with similar loading. After washing away the ponceau S red dye, the membranes were blocked with 5% (w/v) nonfat milk powder or 5% (w/v) Bovine Serum Albumin (BSA) made in TBS 0.1 or 0.05% Tween 20 solution for one hour at room temperature on orbital shaker. Primary antibodies were diluted in 5% non-fat milk or BSA (Table 2.1) mixed in TBS with added 0.1% Tween 20. The primary antibody solution was added onto the membrane and incubated at 4°C overnight on an orbital shaker. The membranes were washed in 0.1% (v/v) Tween 20 TBS every 10 minutes for 30 minutes, and incubated with Horseradish peroxidase (HRP) anti-Mouse or anti-Rabbit IgG (dilutions in table 2.3) at room temperature for 1 hour. The blots were washed again for 30 minutes and chemiluminescence detected following 5 minute treatment with enhanced chemiluminescence (ECL) substrate (Thermo Scientific, 32106). Images of the blots were developed using UV Fujifilm Darkbox imager (LAS-3000). Gel band pixel intensity was measured using image J software (<http://rsweb.nih.gov/ij/>).

2.4.4 Pathscan® RTK signaling antibody array (Chemiluminescent Readout)

The Pathscan® RTK signaling antibody array kit with chemiluminescent readout used target specific capture antibodies spotted in duplicates onto nitrocellulose coated glass slides. This allowed for the detection of 28 different receptor tyrosine kinases (RTKs) as well as 11 important signaling nodes once phosphorylated at a tyrosine or other residues (see Appendix 3). According to the manufacturer, lysates were collected from MDCK-I cells grown in 12 mm transwell inserts at 1, 2, 5 and 10 hours post TEER recovery following calcium switch, in the presence and absence of 50 µM IN-1 inhibitor of matriptase in 75 µl 1x Pathscan lysis buffer. Protein concentration was determined using the BCA assay (see method 2.4.2). Each lysate was diluted to 100 µg in array diluent buffer to a final volume of 150 µl. Samples were added to the eight separated pads on one array slide after blocking.

The array slide was incubated at 4°C overnight on an orbital shaker before the addition of Detection Antibody Cocktail, for 1 hour, followed by HRP-linked streptavidin secondary antibody cocktail also for 1 hr, on orbital shaker at room temperature. The resulting array was treated with a solution mix, combining LumiGLO® and peroxide reagent and imaged immediately with UV Fujifilm imager (LAS-3000) at high exposure. Dot pixel intensity was quantified using Image J software.

2.5 Gene expression analysis (RT-PCR)

2.5.1 RNA extraction and reverse transcription (Two methods – superscript or mmlv)

RNA collection and extraction:

RNA-Bee total RNA extraction reagent was added to live cells in inserts or plastic culture wells after washing twice with sterile PBS (AMS biotechnology). Samples were immediately placed at -80°C for long-term storage. For RNA Isolation samples were defrosted on ice before adding 100µl of chloroform. Samples were incubated on ice for 5 minutes before centrifuging at 15000 rpm for 15 minutes at 4°C. The clear uppermost layer was transferred to a fresh eppendorf tube ensuring nothing from the lower layers has been transferred with. RNA isolation from the upper layer was completed by ethanol precipitation with spin columns provided with the SV RNA isolation kit from Promega (done according to the manufacturer's instruction). Sample RNA quantification and purity were determined using the Nanodrop™ 2000.

Reverse transcription:

For conversion to cDNA, up to 1 µg in of RNA (determined by the smallest amount available in each sample) was mixed with 1 µl of random hexamers and incubated at 70°C for 10 minutes. Samples were allowed to cool at room temperature and centrifuged before the addition of 9 µl mastermix (2 µl DTT, 4 µl first strand buffer, 1 µl dNTPs, 1 µl superscript reverse transcriptase, 1 µl RNasin). Samples were

incubated at 70°C for 10 minutes, lightly centrifuged and stored at -20°C ready for PCR reaction.

Table 2.6 Details the reagents and concentrations used for the two reverse transcription reaction methods.

A)

10X MMLV buffer 2 µl	2 µl
MMLV	1 µl
RNaseOut (40 units/µl)	0.5 µl
Nuclease free water	6.5 µl

B)

Superscript reverse transcriptase	1 µl
DTT (Invitrogen)	2 µl
10X first strand buffer	4 µl
dNTPs	1 µl
RNaseOut (40 units/µl)	1 µl

2.6 Regular PCR

Polymerase chain reactions (PCR) were carried out in 25 µl with the following constituent; 100 ng template DNA, 10x PCR buffer (200 mM Tris pH 8.4, 500 mM KCl), 1.5 mM MgCl₂, 1.5U/µl Taq polymerase and 400 µM of each of the forward and the reverse primers (table 2.7) and 200 µM dNTPs made up to 25 µl with DNase free H₂O. PCR reactions were run on the ABI Prisma 7700 Sequence Detection system (Applied Biosystems). The reaction conditions were as follows: 2 min at 94°C, 35 cycles of 10 seconds at 94°C, 30 seconds at 61°C (T_m of primers) and 15 sec at 72°C which was followed by 10 min incubation at 72°C outside of the PCR cycles. To determine the relative size of the amplicons, 5 µl of DNA from each PCR sample was mixed with 5 µl DNase free water and 2 µl of DNA loading solution. Later 12 µl of each sample, including the negative control (containing no

DNA) and the DNA loading ladder (Sigma) was loaded into 1.5% agarose gel containing 9 µl ethidium bromide and run for 1 hour at 60 mV. The gel was imaged using a BIO RAD UV trans-illuminator 2000®.

2.6.1 Quantitative Real Time-PCR (qRT-PCR)

2.6.1.1 SYBR® Green qRT-PCR assay

Syber green TaqMan PCR reactions were run to allow for quantification of the dog matriptase cDNA from MDCK-I and MDCK-II cells. Specific forward 5'-ACAGAACCAGCAGTGTGACG and reverse 3'CACAGTCGCAATCCTTCTCA primers were designed and obtained from Sigma. SYBR green cyanine dye was used instead of a fluorogenic probe for quantification. PCR was performed using ABI 7700 sequence detection system from Applied Biosystems. Each PCR reaction consisted of a 25 µl mix of 5ng cDNA (1 µl of 0.5ng/µl dilution), 12.5 µl 2x Master SYBR green mix (Applied Biosystems), 200 nM of each of the forward and reverse primers and the total volume was made using TaqMan nuclease free water. The PCR was performed using the following cycles: 2 mins at 50°C, 10 mins at 95°C, 40 cycles of 15 seconds at 90°C, 1 min at 60°C followed by a melt curve step to check for the efficiency of the custom designed primers. The data was analysed using the $2^{-\Delta C_t}$ for comparing the quantitative C_t value for the gene of interest to that of the 18S rRNA housekeeping gene from the same samples.

2.6.1.2 TaqMan® qRT-PCR assay

For quantifying expression of a gene of interest (see table 2.6) in RNA extracted from MDCK cells in culture using the TaqMan quantification system the samples were prepared as follows. A total of 5 ng cDNA (10 µl of 0.5 µg/µl dilution) was loaded per well with 8.33 µl of mastermix (KAPA Biosystems), the appropriate primers-probe (Table 2.6) and nuclease free water to total up the reaction to 25 µl for each well. For the 18S housekeeping gene only 1 ng cDNA (10 µl of 1:10 dilution of 0.5 ng/µl sample dilution) was inserted into the appropriate well in the TaqMan PCR plate. PCR was performed using ABI 7700 sequence detection system

from Applied Biosystems. The PCR was performed using the following cycles: 2 mins at 50°C, 10 mins at 95°C, 40 cycles of 15 secs at 90°C followed by 1 min at 60°C. The data was analysed using the $2^{-\Delta C_t}$ for comparing the quantitative Ct value for the gene of interest to that of the 18S housekeeping gene from the same samples.

Table 2.7 A summary of primers used for analysis and detection of genes using RNA from dog cells, as well as sequences of primers used for the development of the inducible shRNA system.

	Target	Sequence
qRT-PCR Sybr green	Matriptase (human)	Fp: 5' GACAATGCCCTCAAGTGT-3' Rp: 5' CCATTAAGCCGAGTGATGGT-3'
	Matriptase (Dog)	Fp: 5'ACAGAACCAGCAGTGTGACG-3' Rp: 5' CCATTAAGCCGAGTGATGGT-3'
	IL-6 (Dog)	Fp: 5'-GGCTACTGCTTTCCTACCC-3' Rp: 5'-TTTTCTGCCAGTGCCTCTTT-3'
	IL-6R (Dog)	Fp: 5'-AGAAGACGTGGAAGCTGCAT-3' Rp: 5'-AGGTGTTGTGACACCAAGG-3'
	Claudin-2 (Human/ Dog)	Fp: 5'-TTGGCTCGGGAGTCTGGCA-3' Rp: 5'-TGGAGTGCGCCACACACAGC-3'
	Prostasin (Dog)	Fp: 5'-TGTGCTGGCTATGTGAGAGG-3' Rp: 5'-GGCATAGCTGGAGGTCAGAG-3'
	HAI-1/spint1 (Dog)	Fp: 5'-TTCGAGGAGCTCCAGAACAT-3' Rp: 5'-AGGCCGAAAACATCCTTCTT-3'
qRT-PCR TaqMan	Hepsin (HPN- Dog)	Applied Biosystem Cf01056333_m1 FAM
	PAR-2 (F2RL1- Dog)	Applied Biosystem Cf03811559_m1 FAM
	Claudin-2 (CLD2- Dog)	Applied Biosystem Cf02624295_g1 FAM
	Prostasin (PRSS8- Dog)	Applied Biosystem Cf02700856_g1 FAM
For mer96 PCR amplification	pSMC-2	Fp 5'-GATGGCTGCTCGAGAAGGTATATTGCTGTTGACAGTGAGCG-3' Rp 5'-GTCTAGAGGAATTCCGAGGCAGTAGGCA-3'.
Detection of Mycoplasma	Myco1 primer	Fp 5'GGGAGCAAACAGGATTAGATACCCT-3'
	Myco2 primer	Rp 5'-TGCACCATCTGTCACTCTGTTACCCTC-3'

2.7 siRNA design and transfection

2.7.1 Design of siRNA targeting the human and dog st14 mRNA

Invitrogen BLOCK-IT RNAi Designer with guaranteed 70% knockdown was used for the design of siRNA using the provided cDNA sequence (<http://rnaidesigner.lifetechnologies.com/rnaiexpress/>). The program blasts sequence databases of different organisms to allocate unique regions on the provided cDNA sequence as targets. An siRNA sequence was generated against matriptase dog cDNA. siRNA-1403 (5'-GCAAGAACAAGUUCUGCAA-3') targeted nucleotides 1403 to 1424. Matriptase scrambled siRNA duplex (5'-GCAACAAUUGAGUCGACAA-3') was designed as a non-target control for the knockdown experiments.

2.7.2 siRNA knockdown of matriptase in MDCK cells

siRNAs were designed by Invitrogen as duplexes and transfection was conducted using lipofectamine™2000 (Invitrogen) transfection reagent in 24 well plate according to the manufacturer's instructions. In summary, transfection was carried out 6hrs subsequent to cell seeding at low density (7000 cells per well) in 500 µl of DMEM with 10% FCS without antibiotics. Lipofectamine (1 µl) was diluted in 50 µl of OptiMEM serum free medium (Invitrogen). The lipofectamine OptiMEM was added to 50 µl of 33 nM siRNA oligomer (diluted in OptiMEM) or 50 µl of OptiMEM medium only for the transfection reagent control. This mix was incubated at room temperature for 20 minutes and added to 500 µl of cells in full DMEM.

Quantitative real time PCR (TaqMan) was performed 48 hrs (single knockdown) or 96 hrs double knockdown) following transfection.

2.8 Developing miR30-based shRNA expression for inducible knockdown of matriptase (see Appendix 2)

2.8.1.1 Design 96mer miR30 based shRNA

Using the Cold Spring Harbor Laboratory (NY, USA) website: <http://katahdin.cshl.edu/homepage/siRNA/RNAi.cgi?type=shRNA> the single strand 96mer sequence holding the siRNA sequence “TGCTGTTGACAGTGAGCGC**TGCAAGAACAAGTTCTGCAAG**TAGTGAAGCCACAGATGT**ACTTGCAGAACTTGTTCCTTGCAT**TGCCTACTGCCTCGGA” designed for targeting the dog ST14 mRNA was selected and ordered from Sigma. The ordered oligos are then diluted to 10 nM of which 1 µl was added to a PCR reaction mix containing 1 µl of PSMC2 forward and reverse primers (pSMC2 primers span approximately 18 bases 3' and 16 bases 5' of the 96mer sequence) made to 0.3 µM final concentration (See table 2.7), 5 µl 10X Pfu buffer, 1µl PFX Polymerase (Invitrogen) and nuclease free water to make a total reaction volume of 50 µl. The PCR was performed as follows; 94°C for 5 minutes, 23 cycles of 94°C for 30 seconds, 54°C for 30 seconds, 68°C for 3 seconds, followed by a single step of 68°C for 2 minutes. To test for successful amplification 4 µl of PCR samples mixed with 2X DNA sample buffer were electrophoresed on a 1.5% Agarose-TAE gel along with a negative control sample (without amplification by PCR) at 100 V. A band approx. 100 bp was visualized under UV using ethidium bromide and imaged using the UVP's BIO-DOC it™ system.

2.8.2 Digestion of insert and ligation with pBluescript

Digestion of 96mer amplified DNA

The amplified DNA fragment should hold the two restriction sites for Xho-I and EcoR-I restriction enzymes. Following the amplification 8 µl of the product was digested with 0.5 µl of each digestion enzyme with the addition of 1 µl of SuRE/Cut Buffer H (10X) in which both are 100% compatible. Digestion was conducted at 37°C for three hours before precipitating the DNA using phenol/chloroform (see method 2.3.2.4).

Digestion of pBluescript plasmid

pBluescript plasmid was cut with both Xho-I and EcoRI restriction enzyme and the cut plasmid was electrophoresed along side uncut pBluescript (without addition of restriction enzymes) and digested product was purified from 1% agarose-TAE gel using the QIAquick® Gel extraction kit as described in methods section 2.3.2.3. For positive identification of the restricted pBluescript a negative control without the addition of any restriction enzymes was loaded onto the agarose gel.

Ligation with pBluescript

Once both vector and insert were digested and purified a 10 µl ligation reaction was set up by adding 2 µl of T4 5x DNA ligase buffer and 1 µl T4 ligase (Invitrogen) to varying insert to vector ratios using the equation $((\text{ng of vector} \times \text{kb size of insert}) / \text{kb size of vector}) \times \text{molar ratio of insert/ vector}$ (used 20 ng for pBluescript at 1:3 and 1:6 ratio). Samples were incubated overnight at 16°C. Transformations were carried out using stbl-3™ cells according to manufacturer instructions (also see method sections 2.3.1). Transformed cells were selected for using ampicillin and recombinant clones were identified by restriction mapping and sequencing of the product within the vector (see methods 2.6.3).

2.8.3 Sanger DNA sequencing

For sequencing plasmid DNA was diluted to 100 ng/µl of which 5 µl was prepared and sent for sequencing (Applied Biosystems™). Along with the plasmid DNA a 5 µl volume of primers at a concentration of 3.2 pmol/µl were sent. Primers chosen for each sequencing product sent is below:

1. Sequencing of pINDUCER 10 and 11 vectors.

Primer custom sequence: 5'GCGGCCGCAAGCCTTGTTAAGT'3

2. Primer name: T7-20-mer

Primer sequence: 5'TAATACGACTCACTATAGGG'3

2.9 Matriptase knockdown using Mission™ shRNA lentivirus system

2.9.1.1 Mission Lentivirus Packaging

HEK293T cells were seeded at 7×10^5 per well in 4.5 mL 10% FCS DMEM in a 6 well plate and incubated at 37°C and 5% (v/v) CO₂ for 24 hours. To 200 µL of serum free OPTI-MEM 1 µg of pLKO.1, (See table 2.8) 750 ng psPAX2 p and 250 ng pMD2.G vectors were added and left to incubate at RT for 30 minutes along with a separate mix of serum free OPTI-MEM with added 20 µl Lipofectamine 2000 reagent. The two solutions were combined and gently mixed by inverting action before addition to the wells containing the HEK293T cells. The cells were incubated at 37°C and 5% (v/v) CO₂ for 12- 15 hours. Following on the medium was then removed and replaced with 4.5 ml 10% FCS DMEM containing pen/strep. The next day the medium containing the first batch of the virus particles was collected and stored at 4°C before replacing it again with 4.5 ml 10% FCS DMEM containing pen/strep. On day 5 the second batch of medium was collected and mixed with the first batch. This medium was passed through 0.45 µm sterile filter before dividing into aliquots and stored at -80°C.

Table 2.8 Details the vectors used for the Mission™ shRNA Lentivirus system.

	Plasmid/vector	CLONE ID	selection antibiotic	shRNA insert sequence (5'-3')
Mission shRNA vectors	PLKO.1-puro-CMV-tGFP	ST14 1	Puromycin	GTGGGCTTCAGTGTGTGTATT
	PLKO.1-puro-CMV-tGFP	ST14 2	Puromycin	CATGCGGGTTCAGAAGATCTT
	PLKO.1-puro-CMV-tGFP	ST14 3	Puromycin	TGCAAGAACAAGTTCTGCAAG
	PLKO.1-puro-CMV-tGFP	NTC	Puromycin	PASS

2.9.2 Generating stable MDCK cells expressing matriptase targeting shRNAs and NTC using Mission lentivirus system

MDCK-I cells were seeded at 2×10^4 cells per well in a 6 well plate using three separate plates for each lentivirus including: the shRNA sequence 1 GTGGGCTTCAGTGTGTGTATT, shRNA sequence 3 TGCAAGAACAAGTTCTGCAAG and shRNA non target control (NTC). Cells were allowed to adhere overnight at 37°C and 5% (v/v) left to grow overnight before the addition of 2.2 µg/ml Puromycin for initiating the selection. Cells were trypsinized and seeded again at 2×10^4 cells per well in the presence of Puromycin insuring media change every 2 days until no cell death occurred and all cells are expressing GFP. Cells were then carried onto a larger T75 cm² cell culture flask and allowed to grow under the selection of Puromycin. A fraction of the cells were maintained in cell culture for experimentation and a larger fraction was frozen down in vials and stored at -210°C. mRNA knockdown was investigated by qRT-PCR using the custom dog matriptase primers with SYBR green (Table 2.7). TEER assays were conducted as described in method 2.10.2.1.

2.10 Assays for studying epithelial barrier function

2.10.1 Measurements of barrier integrity: Transepithelial Electrical Resistance (TEER) assay

In culture MDCK cells grown onto a porous polyester membrane in transwell inserts are able to differentiate with apical-basal polarization and develop TEER. These inserts have a membrane diameter of 6.5 mm, 12 mm and 24 mm and pore size of 0.4 micron that permits cells to take up and secrete molecules on both their apical and basal surfaces. This system allows the cells to carry out natural metabolic activities. Transwell inserts were purchased from Corning™ Costar, MA.

2.10.1.1 Seeding of cells on permeable support for measuring barrier function

The inserts were incubated, prior to cell seeding, with 5% (w/v) FCS DMEM in the well chamber (600 µl DMEM added to the bottom well chamber and 100 µl on top of the insert) at 37°C for 1 hr to hydrate the membrane. The blank TEER was measured and apical media was removed before addition of cells.

Cell culture for TEER experiments in which MDCK cells were cultured on the semi-permeable inserts were prepared as follows. MDCK cells were trypsinised and pelleted by centrifugation (Room temperature, at 1000rpm for 5 minutes). The pellet was suspended in 6ml of DMEM with 5% (w/v) FCS before the cells were counted. The ideal cell density worked out for each insert was 5×10^4 . The total number of cells required per experiment was calculated and this volume of cells was added to a fresh 15 ml cell culture sterile falcon tube. Each 5×10^4 cells were required in a 150 µl of 5% (w/v) FCS containing DMEM final seeding volume, therefore the remaining media was added to the cells to give a density of 5×10^4 cells per 150 µl volume. This was carefully suspended with a pipette to mix and a 150 µl was added slowly to each insert. Cells were allowed to attach on inserts at 37°C and 5% (v/v) CO₂.

2.10.1.2 Measurement of TEER

TEER developed across MDCK monolayers was measured using a Volt-Ohm meter (World Precision Instruments, Sarasota, FL) with a chopstick electrode (World Precision Instruments, Sarasota, FL). Before applying the electrodes these were made sterile with 70% ethanol and neutralized with regular DMEM (or Epilife® for the calcium free conditions) to give an “r” test value of 1000. TEER formation was measured every time before replacement of the cell medium (apical and basal DMEM), which was done every 48 hours before conducting a “calcium switch” (method 2.9.1.2).

Separate triplicate clones were run for each cell line and for each experimental condition (Unless stated otherwise in results). TEER values obtained for each insert were subtracted from the blank value (resistance measure from empty wells

containing only the media used for the experiment) and multiplied by surface area of the filter (0.33 cm²) to give the resistance of the cell layer [$\Omega \cdot \text{m}^2$].

2.10.2 Calcium switch

TEER is a convenient and robust measure of epithelial tight junction permeability. The integrity of tight junctions, and therefore TEER, can be rapidly disrupted by removal of extracellular Ca²⁺ and re-established on its replacement: the so-called “calcium-switch” method. This method has been previously used as a valid approach for studying variables that contribute to the dynamic modulation of tight junctions and therefore TEER (Cereijido et al., 1978).

There are a number of techniques to applying a calcium switch on cells grown in culture. Three different methods of calcium depletion were initially tested by measuring changes in TEER of MDCK cell monolayer. All three methods are described below in this section. In the end the Epilife® calcium free method was adopted for further TEER experiments.

The calcium switch was always applied once the cells had reached optimum TEER value and introduced back once this value had dropped nearer the blank value.

1. Calcium depletion: HBSS/ dialyzed serum

Dialysis tube (MEDICELL international, UK, mw cutoff; 6000-8000) was boiled in ddH₂O for 30 minutes. Later 25 ml of FCS was placed into the tube that was sealed at both ends and placed into 2 litres of 1X PBS solution. This was allowed to stir at room temperature for 2 hours before replacing the 2 litres with a fresh 1 litre of PBS. This was also left to stir at room temperature for 1 hour. This PBS was replaced with a fresh solution every 1 hour as this was repeated 3 times. The dialysis tube containing the serum was then re-incubated in 2 litres of PBS at 4°C and left to stir overnight. The serum was divided into smaller aliquots and stored at -20°C.

The dialyzed serum was added to Hank’s balanced salt solution (HBSS); calcium and magnesium free at 5% before each experiment. During calcium depletion the

MDCK containing inserts were washed twice and then incubated for 1 hour or overnight with the final solution of HBSS with 5% (w/v) dialysed FCS at 37°C and 5% (v/v) CO₂. The re-establishment of extracellular calcium required the replacement of calcium free HBSS media/serum with regular 5% serum/DMEM or DMEM serum free media (SFM).

2. Calcium depletion: chelation with EGTA

For “calcium chelation”, confluent MDCK cells grown on cell culture filter inserts for 4 days were treated with EGTA as follows (Cereijido et al., 1978). A stock solution of 25 mM EGTA was prepared (pH 8) and sterilized by passing through a 0.2 µm syringe filter. EGTA was added to 5% FCS DMEM at 2 mM concentration. Concisely, the regular 5% DMEM with the cells was carefully replaced with the EGTA DMEM before the inserts were incubated at 37°C 5% CO₂. TEER was measured at several short time points between 30 to 120 minutes. For calcium repletion the DMEM with EGTA was removed gently before washing inserts and wells once with sterile PBS. Regular calcium containing 5% DMEM was added and cells were left to incubate at 37°C 5% CO₂ for 12 hours before measuring TEER reestablishment.

3 Calcium depletion: calcium free EpiLife® Medium

The calcium-free and serum-free EpiLife® Medium which was developed to expand the life-span of epithelial cells under serum-free conditions contained essential and non-essential amino acids, vitamins, other organic compounds, trace minerals, and inorganic salts (Invitrogen). EpiLife® was added to the developed MDCK monolayer (100 µl to the top of the insert and 600 µl to the bottom) after washing the inserts three times with sterile PBS. The inserts were left at 37°C 5% CO₂ for 12 hours before measuring TEER. For calcium repletion the EpiLife® media was simply replaced with serum free regular DMEM with added 2mM L-glutamine. This method of ‘calcium switch’ was adopted for all TEER experiments unless stated otherwise in the specific results section.

2.10.2.1 TEER recovery assay: Addition of various inhibitors and growth factors

MDCK cells were seeded on inserts and left to develop and establish TEER. At high resistance the cell monolayer was subject to calcium depletion followed by calcium repletion (see method 2.9.1.2) in the presence of subset of chemical inhibitors including the matriptase inhibitors (Table 2.5), growth factors or both combined. TEER measures were obtained at different time points following calcium switch and continued for up to 32 hours or longer as described in specific results sections.

2.10.2.2 siRNA TEER experiments

MDCK-I cells were seeded and transfected with siRNA (details method section 2.6). Media containing transfection reagent and siRNA was removed 48 hours post transfection. The cells were detached with trypsin-EDTA and pools from the same conditions (siRNA) were made (triplicate wells). Cells were counted and seeded at 1×10^5 per insert. TEER was measured at 24 and 48 hours before calcium switch was performed using EpiLife® calcium free media.

2.10.2.3 Mission shRNA transduction and TEER analysis

The Mission® Lentivirus (using the particles provided from Sigma) was added to MDCK-I cells day 2 post seeding at Multiplicity of Infection (MOI) unit of 4 with 8 µg/ml hexadimethrine bromide (Sigma). The media was replaced after 24 hours after measuring TEER. TEER was measured at days 2, 3 and 4 before conducting a calcium switch using EpiLife® calcium-free media.

2.10.2.4 Stable mission MDCK-I TEER assay

MDCK-I cells stably transfected with custom Mission shRNA lentivirus PLKO.1-GFP vectors and kept under selection with puromycin were seeded onto transwell inserts at density of 5×10^4 cells per insert without puromycin. TEER was measured for each cell line including the non-target control for up to 4 days before conducting a calcium switch (see method 2.9.1.2) to investigate the recovery of TEER. Experiments were done in triplicate repeats.

2.10.2.5 MDCK-I claudin-2 Tet-off TEER recovery with IN-1

MDCK-I cells made to express claudin-2 in an inducible system were detached with Trypsin-EDTA solution and centrifuged. The pellet of cells was suspended in 6 ml of 5% FCS (Tet-free) DMEM before counting. As described in method 2.9.1.1 cells were seeded at a density of 5×10^4 cells per insert either with or without 20 ng/ml DOX. Media was changed every 48 hours ensuring the addition of fresh DOX where claudin-2 expression by these cells is required. TEER was measured for up to 4 days before conducting a calcium switch using EpiLife® calcium free media (See method 2.9.1.2) to investigate the recovery of TEER. Experiments were done in triplicate repeats.

2.10.3 Measurements of barrier integrity: Paracellular flux of 4kDa FITC-dextran

2.10.3.1 Fluorescence standard curve for 4 kDa FITC dextran

For measuring 4 kDa FITC dextran (Sigma- Aldrich, Gillingham, UK) concentration in regular serum free DMEM with L-glutamine a standard serial dilution, factor 1.5, was prepared with a starting concentration of 50 µg/ml. Initially two standard curves were generated in DMEM with or without phenol red (Gibco, 31053-028). Absorbance of the samples was measured at 530 nm following excitation at 492 nm using the BMG Labtech® Flustar plate reader.

2.10.3.2 Measuring diffusion of FITC-dextran across MDCK monolayer under different conditions.

MDCK cells were seeded on cell culture filter inserts as instructed in method 2.9.1.1 for measuring diffusion of 4 kDa FITC-dextran across MDCK cell barriers, before calcium switch, the inserts were washed twice with sterile PBS kept at 37°C and the regular 5% DMEM media was replaced with phenol red-free serum-free DMEM. FITC-dextran assay was performed by addition of FITC-dextran at 0.5 mg/ml (1 µl of 50mg/ml stock) to the apical media on top of the cells and incubating for 1 hour at 37°C and 5% (v/v) CO₂. Media samples from the apical and the basolateral medium were collected separately for each insert and

experiment condition. The apical medium was always diluted 1:100 before measuring FITC dextran levels in the BMG Labtech® Flustar plate reader. For obtaining fluorescence value for each sample duplicates of 100 µl were pipetted into a clear 96 well plate. Absorbance of the samples was measured at 530 nm following excitation at 492 nm. For measuring FITC-dextran diffusion after calcium switch usually the calcium repletion media used is DMEM phenol red-free. Inserts without any cells seeded served as positive control.

FITC-dextran or phenol red-free DMEM has no disruptive effect on TEER therefore following the 1 hr incubation period and sample collection the cells can still be maintained for longer periods in culture by simply reincubating in regular media (5% FCS DMEM). This was only applied to experiments conducted without calcium switch.

2.11 Video timelapse microscopy: Hepatocyte growth factor (HGF)-induced cell migration assay

Cells were seeded at 8000 cells per well in a 12 well plate in 10%FCS DMEM and left to adhere overnight at 37°C and 5% CO₂. The cells were washed twice with serum-free media and incubated under serum-free conditions for 4 hours before treatment with pro-HGF (Kelly Gray. University of East Anglia), active HGF (R & D Systems, 294-HGN-005) and matriptase inhibitor. The plate was directly inserted into the Zeiss CCD inverted upright microscope under 37°C and 5% CO₂ and positions adjusted for automated imaging. Microscopic images of the same group of cells in each well were taken every 10 minutes for 16 hours at x10 magnification using the Zeiss Axiovision software. Video sets produced were analysed using the 'Manual tracking' tool and the 'Chemotaxis' application in the added plugins settings in Image J.

2.12 Immunofluorescence labelling

Methanol fixation

Cells grown on glass coverslips or inserts were washed three times with 1% goat serum/PBS (Fisher, UK) and fixed with methanol for (kept at -20°C) for 7 minutes. For some experiments cells were permeabilized with 1% NP40 (depending of the protein of interest and the antibody binding region) for 2 minutes. The cells were washed again 3x 1% goat serum/PBS and incubated with 10% goat serum/PBS at room temperature for 30 minutes.

Paraformaldehyde (PFA) fixation

For specific staining of the actin and microtubules cytoskeleton network, cells were fixed for 25 minutes at RT with 4% Paraformaldehyde (PFA) after washing twice with PBS. The PFA was removed before washing once with PBS and incubating with 500ul of PBS containing 4 drops of 1M glycine for 5 minutes. Cells were washed again once with PBS before permeabilizing with PBS containing 1% Triton x100 for 4 minutes at RT. The cells were washed twice with PBS and stained with anti- α tubulin (table 2.3) for the primary antibody step (as mentioned previously in this section) and secondary combined both secondary Alexa-647 antibody was with Phalloidin-488 for 30minutes.

Immunolabelling with primary and secondary antibodies

Cells were incubated with primary antibodies (dilutions in table 2.3) for 1 hr in humidified atmosphere. Samples were then removed and washed x6 for 30 minutes with 1% GS PBS. Samples were incubated with species complementary secondary antibodies (table 2.3) for 30 minutes under dark and humidified conditions, then washed 3x with 1%GS PBS. DAPI staining (1:2000) was applied to all the coverslips for 5 minutes before applying 3 quick washes with 1%GS PBS and fixing onto glass microscope slides with hydromount (with 2.5 g DAPCO). ProlongGold® with DAPI (Invitrogen) was used for fixing coverslips and inserts

onto microscope slides before incubating at 4°C for two days before imaging. Images were obtained using Zeiss Axiovert 200M equipped with a Zeiss AxioCam Camera, using x63 objective (Carl Zeiss, Thornwood, NY). Confocal images were taken with the Zeiss LSM 510-META laser-scanning microscope, using x63 objective (Carl Zeiss, Thornwood, NY). Images were analysed through software such as Image J and Volocity 3D images analysis software (PerkinElmer)

2.13 RT² Profiler™ array: Dog inflammatory cytokines and receptors

MDCK cell monolayers grown on culture inserts were treated with 500ul of RNAbee (TEL TEST, NC9850755). Pools from three separate inserts of the same condition were made. RNA was gathered from MDCK-I cells at 1, 2, 5 and 10 hours post recovery following calcium switch in the presence and absence of 50 µM IN-1 inhibitor of matriptase (see table 2.5). The RNA was purified with the Promega® SV RNA purification kit and a reverse transcription reaction was done on 500ng of this to cDNA using the MMLV method described in Materials and Methods section 2.5.1 (See table 2.6).

The quality and accuracy of the RT was determined by investigating variation in the 18S cycle threshold (C_t) making sure that this value for all sample reside within 1.5 C_t range.

For the kit, samples were diluted in nuclease free water to 420ng total cDNA per sample and prepared with 2x RT² SYBR green masermix (Qiagen, 330500) as instructed by manufacturer shortly before loading the plates. Equal loading of 10 µl were added to the appropriate wells (96 wells per sample) fitting 4 different samples into each of the two 384 well plates. The PCR was run on AB7900 Machine as follows: 1 cycle for 10 minutes at 95°C, 40 cycles of 15 seconds at 95°C, 30 seconds at 55°C and 30 seconds at 72°C. A melt curve step was added at the end of the reaction as instructed by manufacturer (Qiagen, PABT-011Z). Analysis was carried using the SDSv2.4 software for Applied Biosystems 7900HT Fast Real-Time PCR system. Data were analysed using Microsoft® Excel.

2.14 Statistical analysis

Unless stated otherwise, data were tested using two-tailed Student's *t* tests and are presented as mean \pm S.E.

Chapter 3. Validating MDCK-I and MDCK-II as model epithelial cells for investigating the role of matriptase on epithelial barrier function.

3.1 Introduction

A key feature of epithelial tissues is the polarised structure that enables them to function not just as barriers for separating two compartments but also to regulate transport of water, ions and solutes. Therefore, they hold a key function in tissue maintenance and body homeostasis. Epithelial cells feature different roles, to give rise to tissue barriers with different structures and functions, determined by their location and surrounding environment. Simple and polarised epithelial barriers form with tight cell-cell adhesions, mediated by a complex network of interactions between the individual apical junction proteins and the tight junction proteins (see review Rodriguez-Boulan and Macara, 2014). The expression and functional features of the junction structures are dynamic and are therefore well regulated either directly or indirectly by various effector molecules including some serine proteases. Continual matriptase expression is found to be essential for maintenance of such epithelial tissues and regulation of tight junction function and cell polarity. Particularly, the loss of matriptase has been widely associated with defects in the function of these tight junctions and enhanced epithelial tissue permeability in humans and mice (Netzel-Arnett et al., 2012, Buzza et al., 2010, Basel-Vanagaite et al., 2007).

As mentioned in the introduction chapter 1, the specific ablation of matriptase expression in the intestinal tissue of the conditional knockout mice, altered the architectural organization and compromised barrier integrity, articulated by excessive diarrhea, edema and premature death (List et al., 2009, Buzza et al., 2010). This requirement of matriptase activity in the formation and maintenance of the inward and outward barrier is not restricted to only the simple epithelial

tissue of the intestine, but also to the epidermis (List et al., 2002). Loss of matriptase expression also caused trans-epidermal water loss that led to severe dehydration as a cause of death in knockout mice (List et al., 2002). Much more is known about the mechanism of matriptase in the epidermis but yet its mechanism of regulation in the intestinal epithelia and whether matriptase function is required in other types of simple epithelial tissues is yet not understood.

As tight junctions are an essential part of simple epithelial barrier systems, one study by Buzza et al, had analysed and linked these structures with matriptase function, highlighting its role in the development of tight junctions and regulation of paracellular permeability (Buzza et al., 2010). This function was also illustrated *in vitro* in Caco-2 intestinal epithelial cells derived from human colon carcinoma (Buzza et al., 2013). It is important to mention that although matriptase may be involved in the same development and maintenance of different types of epithelial barrier tissues, the mechanisms are likely distinct, as shown in the epidermis. Here, matriptase regulates epidermal barrier function via a mechanism that is unique to that tissue, via the processing of the epidermal-specific pro-filaggrin (List et al., 2002). Therefore, this supports the idea that matriptase possibly plays a wider role in regulating epithelial barrier function in different tissues.

Unlike the stratified epithelia, in the polarised epithelia matriptase function may trigger the activation of different substrates and this may be due to spatial and temporal restrictions including localization, which represent part of the key defining parameters for such epithelia. Specifically, in the simple polarised epithelial cells, matriptase has been shown to be mostly abundant nearer the lateral intercellular adherens junctions and at the basolateral cell surface, away from known substrates such as prostasin, and therefore this can play a part in restricting its mechanistic involvements, which could be altered depending on the physiological environment (Friis et al., 2011).

To be able to provide a further understanding of matriptase function, it is therefore important to study its role in different systems, and this study focuses on its function in the simple and polarised epithelia, utilizing a model approach for

the study of simple epithelial barriers. As matriptase has been shown to regulate the tight junctions, we aimed to use the model Madin-Darby Canine Kidney (MDCK) epithelial cell line.

3.1.1 MDCK-I and MDCK-II cells: an important culture model of barrier epithelium

For a long time researchers have been using various models to study epithelial biology and barrier formation and function in normal and stress induced states. MDCK cells derived from the kidney tubules of a Cocker Spaniel in 1958 have contributed greatly to the current understanding of epithelial behavior and barrier function (Madin et al., 1957, Leighton et al., 1970). These cells provide a tractable model for studying biological processes such as trafficking, polarity, and cell junctions. MDCK cells can form a well-polarised and differentiated simple columnar epithelial monolayer once cultured under optimal conditions, and establish apical tight junctions, which provide the barrier with selective permeability. These polarised epithelial cells develop well-defined apical and basal surface domains, with specific chemical composition. This polarization is key for tissue function such as establishing a polarity for nutrient uptake from the lumen to the inner basal tissue. Many studies have used MDCK cells to investigate the transport of different nutrients and drug delivery across a tight epithelia as they exhibit extremely low permeability to water and small non-electrolytes compared to other cells in culture, and therefore resembling more that of intact epithelia (Lavelle et al., 1997).

Based on our previous analysis of matriptase function in MDCK-II cells, which serve as a standard model for HGF scattering, we showed these cells require matriptase activity for conversion of extracellular pro-HGF and activation of the subsequent pathway (Gray et al., 2014). Therefore we aimed to validate and use MDCK-II cells, along with another strain known as MDCK-I, in a culture model to study barrier responses to altered matriptase function. Under the right conditions, MDCK-I and MDCK-II cells should model the barrier epithelia of *in vivo*. These

strains of MDCK cells are derived from the same parental NBL-2 line but obtained at different passages (Dukes et al., 2011). The dog origin of these cells represents limitations in terms of available research tools for the target species. Therefore, for the study of matriptase function in this chapter, our aim was also to develop custom tools for expression and function analysis in MDCK-I and MDCK-II cells.

Under specific culture conditions MDCK-I cells derived from low passage parental cells form “Tight” monolayers with high TEER while MDCK-II cells monolayers are “Leaky” with low TEER (Suzuki et al., 2011, Gaush et al., 1966, List et al., 2007a). Although they bear similar number of tight junction strands, the difference in TEER between MDCK-I and MDCK-II is caused by changes in their functional permeability. The leaky phenotype in MDCK-II cells is largely triggered by a high expression of claudin-2 protein at the tight junctions (Amasheh et al., 2002, Furuse et al., 2001). In MDCK-II cells, claudin-2 expression, despite having a large effect on TEER, does not influence the overall barrier structure or function. Indeed in previous studies demonstrating matriptase’s role in the intestinal epithelium, matriptase deficiency was linked with increased claudin-2 protein abundance at the tight junctions and hence increased tissue leakiness. In part most of the intestinal studies support that matriptase activity is important for barrier integrity. Therefore the two cell lines can be used to further validate this role in a different model. However it is also worth mentioning that a study by Szabo et al, aimed at investigating the effect of HAI-2, the cognate inhibitor of matriptase, in MDCK-I barrier development and TEER establishment, were able to show that HAI-2 overexpression in fact promotes these processes and mediates barrier integrity in MDCK-I by promoting the rapid acquisition of tight junctions (Szabo et al., 2009). Therefore it is important to thoroughly investigate the role of matriptase in these MDCK-I and MDCK-II cells as they can be used to provide proper insight into its function in development of well structure and tight epithelial system.

3.1.2 Aims and objectives

Our aim was to evaluate the use of MDCK-I and MDCK-II cells in parallel as a model for investigating the influence of matriptase activity and overall expression on the development and the structure of the apical membrane barrier, and regulation of the tight junction. To approach this, a model system, providing an important tool to trace the development and dynamic behavior of both MDCK-I and MDCK-II barriers must be validated. Here, the key differences between the two strains will be further highlighted with relevance to this study of matriptase function. Subsequently, this model will be used throughout the study to identify and characterize the effect of matriptase and relevant *in vivo* substrates on barrier behaviour and characterisation of the relevant response pathways.

3.2 Results

3.2.1 MDCK-I and MDCK-II cell line behavior and morphology

MDCK-I and MDCK-II cells grow efficiently under the same conditions and same saline culture medium. Under normal growth environment the pattern and cell morphology during low and high stages of confluence for both cell types were examined.

Although derived from the same parental cell line, MDCK-I and MDCK-II cells were found to exhibit distinct growth and structural morphologies from one another. Grown under the same conditions in culture as MDCK-II cells, MDCK-I cells possessed a highly distinct scattered phenotype at growth days 2 to 3 (Figure 3.1A). These cells exhibited many protrusions and grew as single cells, while MDCK-II cells derived from the high passage NBL-2 cells came together almost immediately after seeding to form islets with a defined all-round membrane edge, showing few protrusions (Figure 3.1A). Once both cell types grew to a high confluence (approx. 100%) after 4-5 days in culture, with a high splitting dilution

factor of 1/18, the morphology of the confluent sheet they form was strikingly similar. The cells in both strains had an indistinguishable tight morphology and appeared to form similar tight lateral adhesions with the neighboring cells (Figure 3.1 A). To examine this further, immunofluorescence imaging of the adhesion structures representing the underlying molecules for mediating cell-cell linkage which include E-cadherin and β -catenin molecules between MDCK-I and MDCK-II seeded at a high density and grown for 2 days were obtained. Between the two strains of MDCK cells, E-cadherin and β -catenin showed similar structural co-localization and level of intensity at the cell periphery (Figure 3.1B).

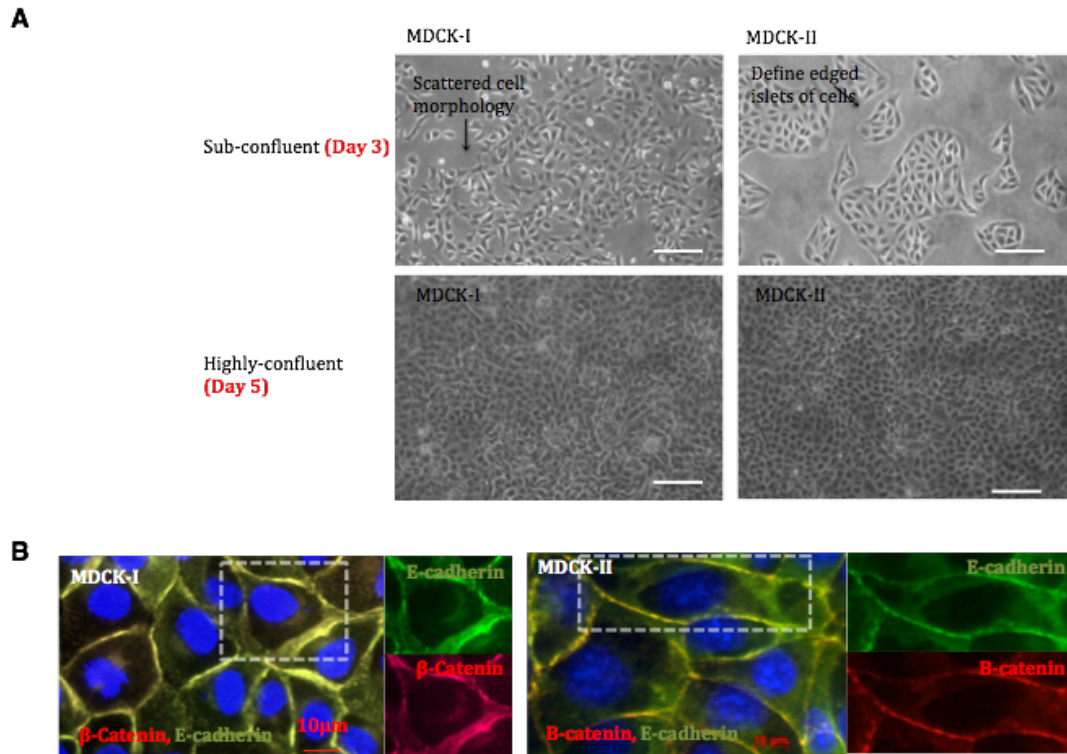


Figure 3.1 Characterization of MDCK-I and MDCK-II cells in culture.

A) Bright field images were taken of MDCK-I and MDCK-II cells grown in culture flasks, for 3 (low confluence) and 5 days (high confluence). B) MDCK-I and MDCK-II cells were seeded at high density (2×10^5) and allowed to grow for 2 days on 1.3 cm glass culture coverslips. Cells were fixed with cold methanol and stained for E-cadherin (green) and β -catenin (red), nuclei were stained with DAPI (blue). The white dashed box in the immunofluorescence images represents a zoomed in single cell chosen to display staining from individual protein channels separately, as can be seen by the insets on the right of the merged images. Images were taken of live cells with an x10 objective. Images for immune-stained cells were taken at an x63 objective. Images were taken from three separate coverslips per individual cell line.

3.2.2 MDCK-I and MDCK-II cells form barriers with differential transepithelial electrical resistance (TEER)

In vitro, optimal expression of epithelial phenotype requires the primary consideration of the polarity of nutrient uptake. Cells grown on plastic or glass coverslips still form tight junctions that seal the passage of important components in the growth medium to the basolateral side. Therefore the basal surface becomes

isolated from growth medium and for these cells to be able to form properly differentiated epithelia the basolateral surface need to be exposed to this medium. This is achieved by growing the cells on permeable support such as polycarbonate or polyester (transparent) filters. These supports are built with multiple small sized pores that allow the exchange of nutrients and ions between the apical and basolateral surface of the cell monolayer creating a diffusion system similar to tissue *in vivo* (Figure 3.2).

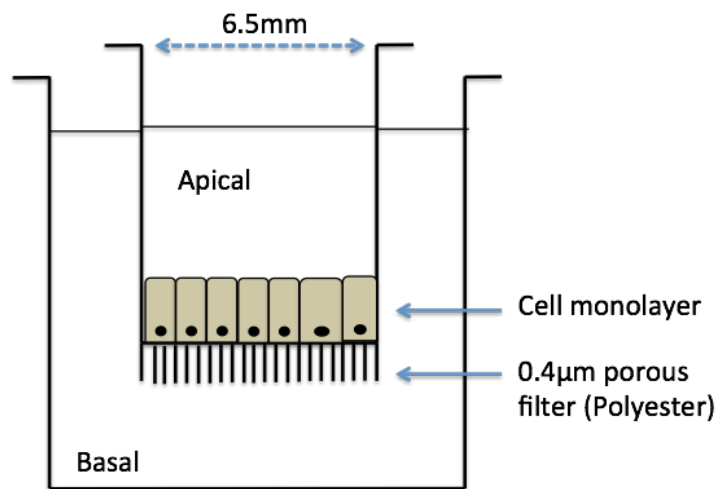


Figure 3.2 Transwell permeable support growth filters. These filters possess small size pores that provide independent access to both sides of epithelial cell monolayer. They also provide a versatile tool to study transport and permeability of anchorage dependent cell monolayer structures *in vitro*.

When MDCK-I and MDCK-II cells are plated on a permeable support, they are joined at their apices by the tight junctions that act as seals to separate the apical face of the epithelium from the basolateral (Collares-Buzato et al., 1998). The properties of these tight junctions widely differ among simple epithelial tissues that vary in their passive transepithelial permeability. In culture studies, the tight junction physiology can be assessed, in part, by measuring TEER of epithelial monolayer (Benson et al., 2013). Initial correlation between tight junction morphology and TEER measure was observed through freeze fracture electron microscopy of different simple epithelia and epithelial subject to different physiological states (Erlj and Martinez-Palomo, 1972, DiBona and Civan, 1973,

Humbert et al., 1976). Therefore the tight junctions in the simple epithelia determine the characteristics of the permeability across the paracellular route.

3.2.2.1 TEER development assay: MDCK-I cell culture and seeding density

Although MDCK-I and MDCK-II cells form similar cell-cell adhesions, they develop differential barriers once cultured on porous membranes in Transwell inserts. TEER measurements were conducted initially to determine a cell seeding density for the establishment of TEER. MDCK-I cells seeded at higher density of 5×10^4 cells per insert developed TEER at an earlier time post seeding compared to a density of 1×10^4 cells per insert. TEER values with barrier development continued to increase up to days 8 and 9 following seeding while this increase was considerably poorer at the lower density, in which monolayers expressed a significantly lower optimal TEER measure (figure 3.3).

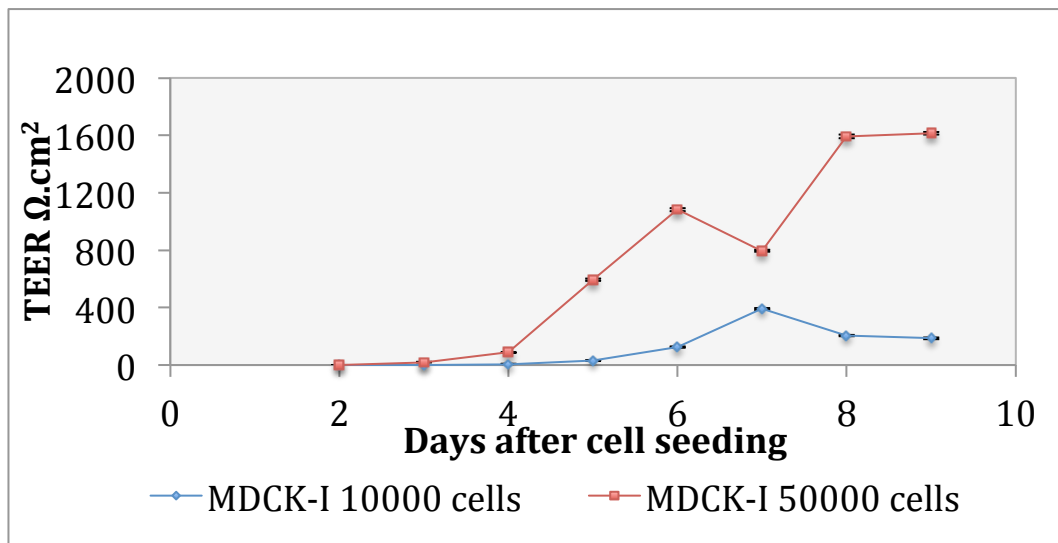


Figure 3.3 MDCK-I TEER establishment.

MDCK-I cells were seeded at low (1×10^4) and high density (5×10^4) in 6.5mm polyester Transwell™ inserts in 5%FCS MEM. Inserts with cells were incubated at 37°C 5% CO_2 and TEER measurement were taken ever 24 hours. Medium was replenished every 48 hours. $n=3$, Mean \pm SEM.

3.2.2.2 TEER development assay: MDCK-I and MDCK-II cell culture and seeding density

Following the seeding of MDCK-I and MDCK-II cells at a density of 5×10^4 under the same conditions TEER measurements were taken every 24 hours. The TEER was calculated per insert area and plotted in graph, which showed MDCK-I cells are able to develop very high TEER reaching up to $6000 \Omega \cdot \text{cm}^2$ after only 6 days of growth on inserts (Figure 3.4 A and C). In contrast MDCK-II cells developed much lower TEER of $<200 \Omega \cdot \text{cm}^2$ compared to MDCK-I cells seeded under the same conditions, but they achieved maximum resistance much quicker, only 4-5 days after seeding. MDCK-I TEER therefore illustrated a strict paracellular system of diffusion while in MDCK-II cells, displaying low TEER, this system is more permeable with “leakier” paracellular properties (Figure 3.4 B and C).

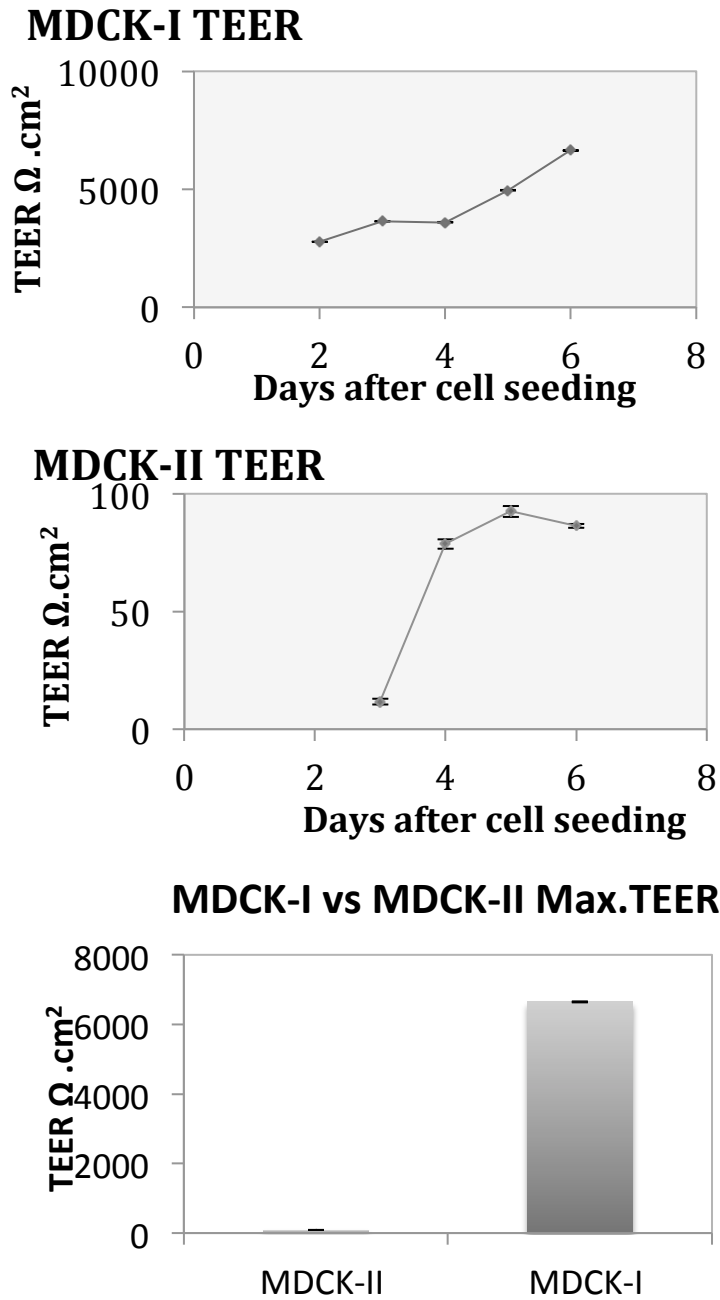


Figure 3.4 Characterization of MDCK-I and MDCK-II barrier TEER.

A) MDCK-I cells seeded at 5×10^4 on permeable membrane support system in 6.5mm Transwell™ inserts., with 5%FCS DMEM and TEER measurement taken every 24 hours up to day 6. B) MDCK-I cells seeded at 5×10^4 on permeable membrane support system in 6.5 mm Transwell™ inserts. with 5% FCS DMEM and TEER measurements taken every 24 hours up to day 6. C) Bar graph to display the difference in maximum TEER between MDCK-I and MDCK-II cells, at 6 days post cell seeding. N=3, Mean \pm SEM.

3.2.2.3 MDCK-I and MDCK-II overall barrier paracellular physiology: 4 kDa FITC-dextran flux assay

Studies of physiological permeability of epithelial barriers to investigate the paracellular space *in vivo* and *in vitro*, often refer to the use of macromolecular tracers that define the state of junctional sealing. Dextran is a complex polysaccharide, made of many glucose molecules and used in many studies to characterize permeability and obtain information about epithelial barrier integrity (Godiksen et al., 2008, Momose et al., 2012). FITC-labeled dextran of various molecular weights, ranging between 4 and 2000 kDa, provides a high sensitivity of detection down to 1 ng/ml using a regular fluorescence plate reader, where excitation is best performed at 490 nm and fluorescence emission measured at 520 nm (Momose et al., 2012). Fluorescence measurements from FITC-labeled dextran provide quantitative real-time data on permeability of barriers under different treatments and conditions.

Often, low molecular weight 4 kDa FITC-dextran is used to study paracellular permeability to ions and solutes while the high molecular weight >4 kDa FITC-dextran is used to test protein permeability (Hoffmann et al., 2011). To determine whether the paracellular permeability toward macromolecules differs between MDCK-I and MDCK-II epithelial monolayers, 4 kDa FITC-dextran was used. For this 50 µg/ml 4 kDa FITC-dextran was administered at the apical side of the epithelial layer formed by MDCK-I and MDCK-II cells seeded on Transwell supports. Following 1 hour of incubation, the quantification of FITC-dextran either concentration or percentage diffusion across to the basolateral side of each monolayer was determined.

Initially to be able to determine the concentration of FITC-dextran that diffuses across the cell monolayer a fluorescence standard curve was established for fixed concentrations of 4 kDa FITC-dextran (0-50 µg/ml). Initially samples for standard curve were diluted in either phenol red containing DMEM or phenol red-free DMEM to determine whether the presence of phenol red influenced the absorbance measurements for FTIC (Figure 3.5 A). Absorbance measure at 530 nm

from FITC-dextran diluted in phenol red DMEM was approximately 50% lower than non phenol-red samples. Therefore dextran experiments on MDCK cells were carried out using phenol red-free DMEM to ensure detection of even smaller changes in FITC-dextran.

In determining the physiological permeability of MDCK-I and MDCK-II monolayers 1 day and 4 days after cell seeding, the concentration of FITC-dextran diffusing into the basolateral medium after 1 hour of incubation was measured. After 1 day in culture approximately 53% more FITC-Dextran diffused across MDCK-II monolayer cells compared to MDCK-I cells (Figure 3.5B). Once maximum TEER was established at day 4 MDCK-I monolayer showed highly restrictive paracellular properties toward the passage of 4 kDa FITC-dextran, with only $\sim 0.04 \mu\text{g/ml}$ diffusing across after 1 hour. Although MDCK-II cells also showed increased paracellular integrity, more dextran diffused across to the basolateral medium $\sim 0.2 \mu\text{g/ml}$, compared to MDCK-I cells. This difference in paracellular permeability reflected that of TEER measurements for the two cell lines.

The measuring of dextran concentration was compared to relative diffusion of dextran across MDCK-I and MDCK-II monolayer from the apical to the basolateral medium, using cells at day 4. Here fluorescence was measured both in the apical and basolateral medium and relative diffusion amount was calculated. This showed a similar difference between MDCK-I and MDCK-II cells, as demonstrated by the concentration method. Therefore both methods present a reliable measure of paracellular diffusion.

The higher concentration of diffused dextran and the higher relative diffusion, measuring around 95% and 93%, in MDCK-II cells compared to MDCK-I cells at day 4 confirm that MDCK-I cells express much tighter paracellular barriers, toward both ions and macromolecules in culture compared to MDCK-II cells (Figure 3.5 Ci).

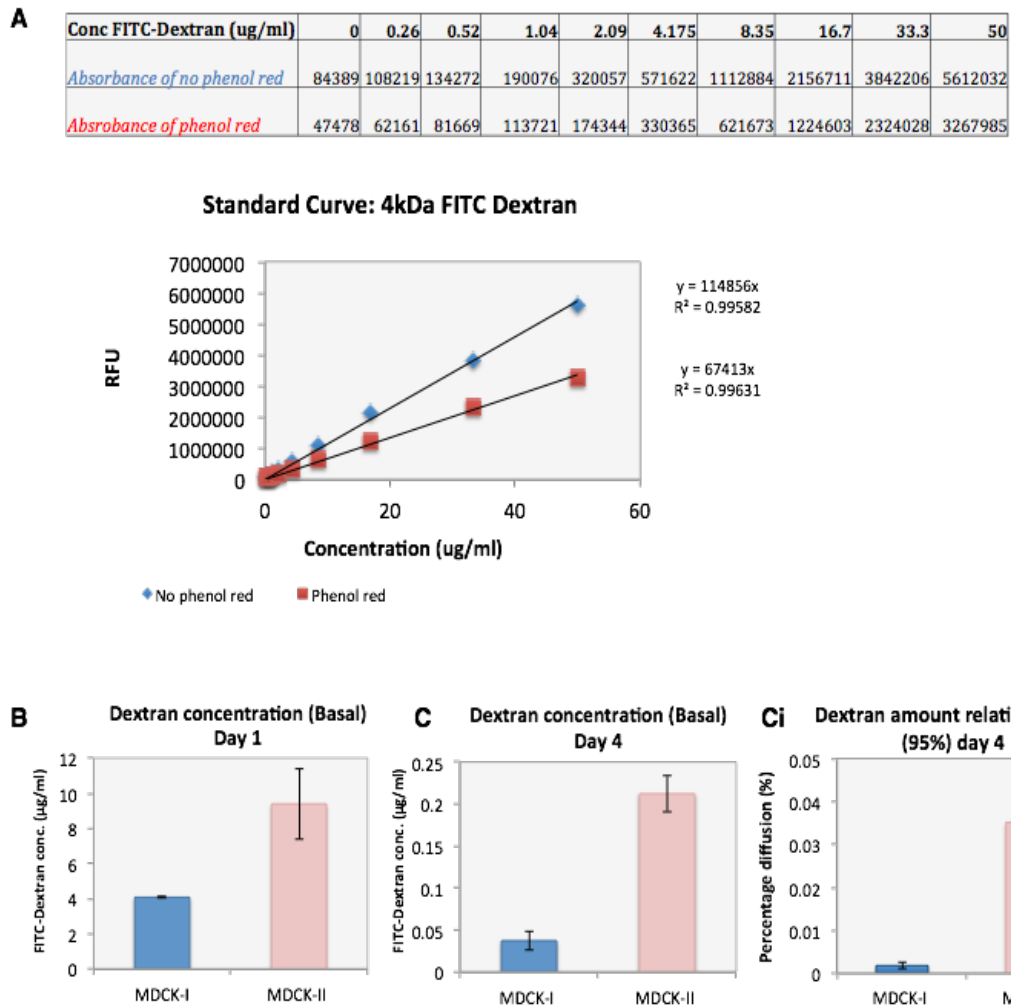


Figure 3.5 Characterization of MDCK-I and MDCK-II barrier paracellular permeability using macromolecular 4 kDa FITC-dextran flux assay.

A) A fluorescence standard curve for calculated concentrations of dextran from 0-50 $\mu\text{g/ml}$ diluted in culture medium with and without phenol red. Absorbance for each sample was measured at 530 nm following excitation at 492 nm. Standard curves are generated after subtracting the blank absorbance of MEM without FITC-dextran. B) MDCK-I and MDCK-II cells were seeded into 6.5mm inserts with 5% FCS MEM at a density of 5×10^4 . After 24 hours medium was changed to phenol red free without serum and incubated for 1 hr with 50 $\mu\text{g/ml}$ FITC-dextran added in the apical chamber medium. After 1 hr basolateral medium was collected and absorbance measures at 530 nm. Graph represents FITC-dextran concentration as calculated using the standard curve presented in A. C) similar to B but applied at day 4 following seeding. Ci). Graph represents the percentage of relative diffusion of dextran basolateral/apical after day 4. Dextran assays were conducted at 37°C and 5% CO_2 . $N=3$, mean \pm SEM. ***= $p < 0.05$

3.2.2.4 Expression of tight junction and adhesion junction complexes by MDCK-I and MDCK-II cells

To analyse the structural paracellular properties of MDCK-I and MDCK-II epithelial monolayers, cells were seeded at high density of 5×10^4 in 6-well plates. Once fully confluent cell lysates were collected from each cell line. Western blot analysis was carried out to determine and compare the level of expression of various components of the tight and adhesion junctions between MDCK-I and MDCK-II cells. Protein bands visualized with chemiluminescence for occludin, ZO-1, claudin-3 and claudin-7 showed similar expression between MDCK-I and MDCK-II cells, while claudin-1 was more highly expressed in MDCK-II cells as compared to MDCK-I cells (Figure 3.6 A).

The largest difference in the tight junction between the two strains of MDCK cells was in the expression of claudin-2. Here, a high expression of claudin-2 was detected in MDCK-II cells, while in MDCK-I cells claudin-2 was completely undetectable (Figure 3.6 A). Analysis of claudin-2 gene expression by qRT-PCR using canine specific TaqMan primers and probe revealed a relatively low cycle-threshold (C_t) value (average 25.7) for MDCK-II cells implying high levels of mRNA, while MDCK-I cells show no claudin-2, as high C_t value of 37.7 suggested deficient levels of claudin-2 mRNA. This therefore illustrated that the difference in protein level of claudin-2 is based on the level of gene activation between MDCK-I and MDCK-II cells, and not due to differences in protein-turnover (Figure 3.6 B).

Although the tight junction proteins establish their individual apical sealing strands, these cannot develop or mature without the prior and proper establishment of the adhesion junctions of which E-cadherin and β -catenin are key components. Therefore the levels of these proteins were examined in MDCK-I and MDCK-II and western blotting of E-cadherin and β -catenin in confluent MDCK-I and MDCK-II cells identified equal expression by both cell lines (Figure 3.6 A). Level of proteins expressed was confirmed against a loading control.

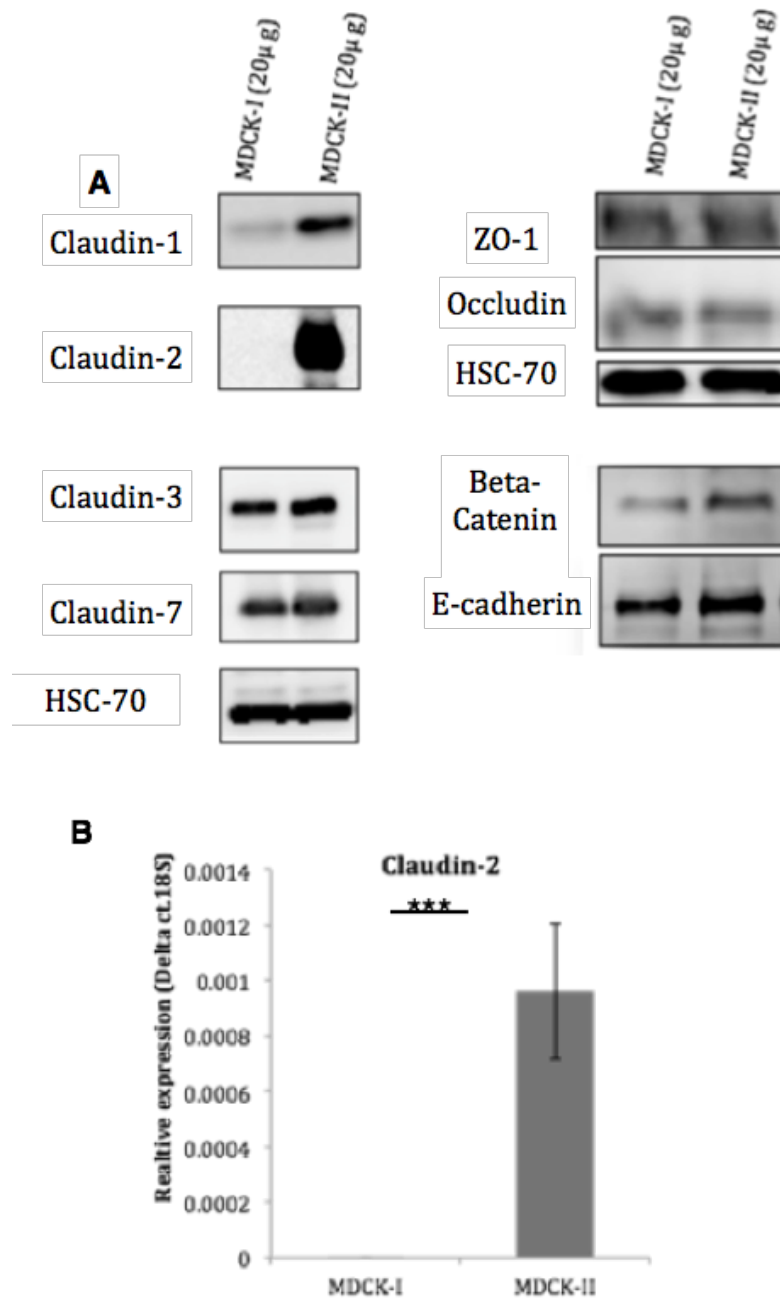


Figure 3.6 Expression of different components of the tight junctions and adhesion junctions between MDCK-I and MDCK-II cells.

A) Western blot analysis of protein lysate obtained from confluent MDCK-I and MDCK-II cells grown for 4 days in sterile culture 6 well plate. HSC-70 mouse antibody was used for loading control. B) Quantitative TaqMan RT-PCR was conducted using AB primers and probe mix (see table 2.7) to quantify levels of claudin-2 gene expression in MDCK-I and MDCK-II cells. Quantitative expression was calculated relative to the expression of the stable levels of the 18S house keeping gene, using the $2^{-\Delta C_t}$ method for determining the relative quantification ratio. For TaqMan qRT-PCR data N=6, mean \pm SEM. Statistical significance analysed using excel and annotated as ***: p<0.05

3.2.2.5 Formation of apical-basolateral microtubule array and apical tight junctions

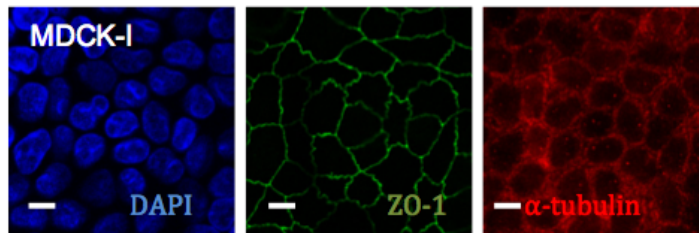
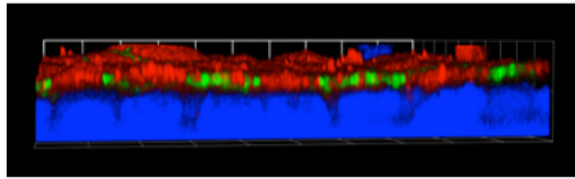
In polarised epithelia, apical tight junctions physically separate the plasma membrane generating distinct apical and basolateral cell surfaces. This type of epithelial differentiation is extremely significant in barrier formation and barrier function. To characterize the development and type of structural polarisation in both MDCK-I and MDCK-II barrier cells once it becomes established on permeable support, indirect immunofluorescence staining of tight junction and cytoskeletal proteins in combination with confocal microscopy and digital image processing were used. To determine whether MDCK-I and MDCK-II expressed different structural polarities as established monolayers, the organisation of the cytoskeleton and organization of the tight junction were studied using immunofluorescence in combination with confocal microscopy and digital image processing.

Confocal sections taken of MDCK-I and MDCK-II monolayers grown on permeable supports for 5 days following staining with microtubules showed peripheral distribution of microtubules, which occurs after they are released from the nucleation site (Mogensen, 1999). These were observed in ring structures that form at the cell periphery indicating non-radial apico-basolateral organization (Figure 3.7 A). A dense horizontal network of microtubule filaments could also be observed at the most apical cell surface in both MDCK-I and MDCK-II (Figure 3.7 A). This non-radial microtubule organization is explained in a brief schematic in Figure 3.7 B. During epithelial polarization microtubules form a non-radial apico-basal array as they are released from the centrosome and translocate to new sites. Here microtubules bind via their minus ends to junction proteins including components present at apical sites such as the tight junctions. This is known as the release and capture model, and has been shown to be important for tight junction-related epithelial morphogenesis (Yano et al., 2013) (Figure 3.7A).

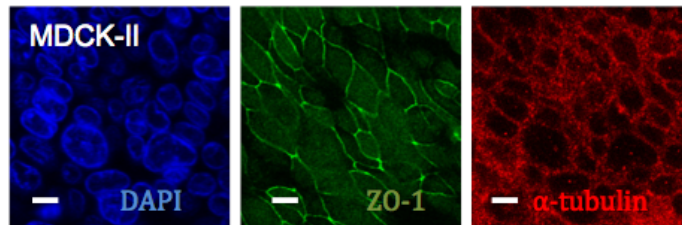
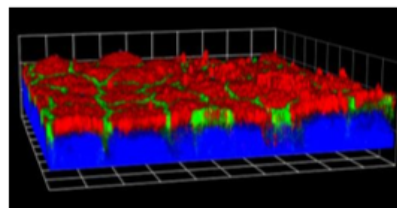
Confocal analysis of ZO-1 confirmed the distinct localisation to the apical surface, of the epithelial monolayer in both MDCK-I and MDCK-II, as shown through the green fluorescence staining in the 3D images in Figure 3.7 A. As ZO-1 associated directly with the tight junction strands this confirms similar apical polarity of the tight junctions in the two strains of MDCK cells.

A

MDCK-I:
DAPI, ZO-1, Microtubules



MDCK-II:
DAPI, ZO-1, Microtubules



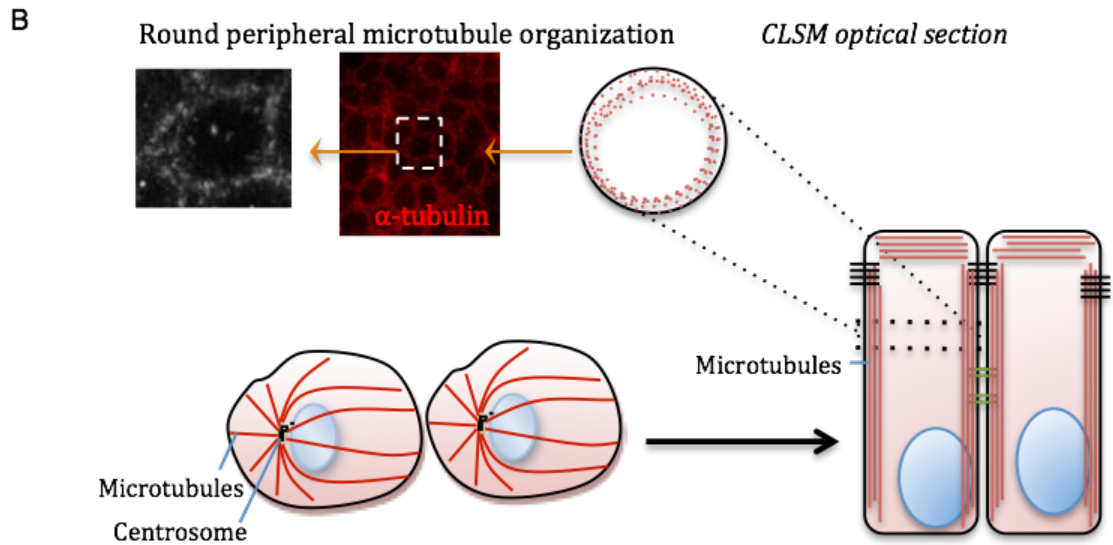


Figure 3.7 Determining tight junction and microtubule polarization in MDCK-I and MDCK-II cells grown on permeable support.

A) Following 5 days growth on permeable Transwell support, confluent MDCK-I and MDCK-II cells were stained for proteins ZO-1 (Alexa-488 Green), α -tubulin (Cy647 Far Red) and nuclei with DAPI (Blue). Confocal 3D stacks and 2D sections combining all staining were obtained. DAPI staining of the nuclei was used to determine the base of the cells in the images slice section. B) Diagrammatic representation of loss of radial microtubule array and development of non-radial microtubule polarization further illustrated via the vertical sections displaying strong red staining for α -tubulin focused at the cell periphery. Immunofluorescence images were observed with x63 objective.

3.2.3 Calcium switch effect on MDCK barrier functional integrity.

During barrier formation calcium ions are critical for assembly of adherens junction and tight junctions between neighbouring cells. Calcium has been shown to regulate junction integrity through direct association with junction proteins, such as E-cadherin (Wodarz, 2002, Ozawa et al., 1990, Colombo et al., 2012, Cereijido et al., 1978). In the TEER assay cells are seeded down in growth medium containing calcium. In the presence of extracellular calcium, MDCK cells formed fully functional barriers with normal adhesions and TEER. At this stage, extracellular calcium is essential for the maintenance of the established cell-cell junction integrity, therefore depletion of calcium in the extracellular medium denatured the cell-cell junctions causing cells to separate from each other. The

effect of short-term depletion of calcium on barrier junction integrity can be easily reversed upon calcium repletion (Figure 3.8).

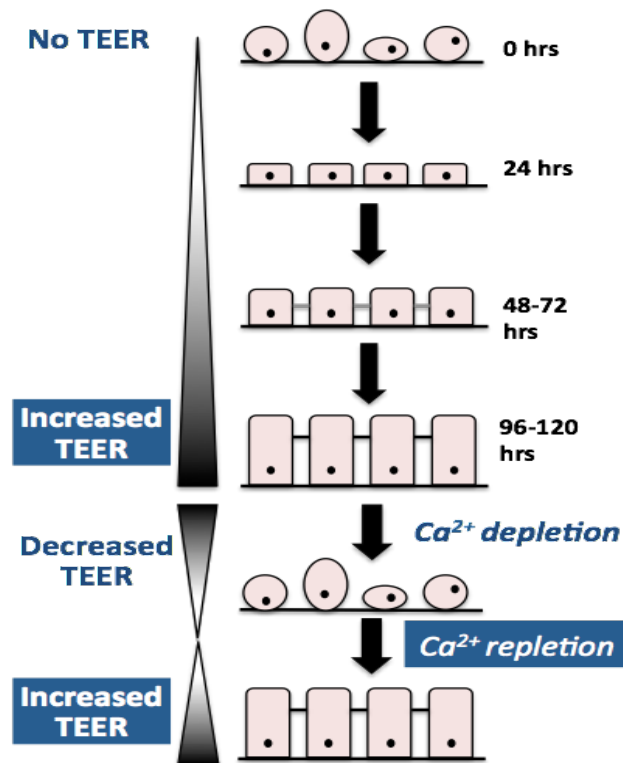


Figure 3.8 Diagram illustrated sequence of barrier establishment and stages of TEER acquisition, before and after calcium “switch”.

Calcium switch can be achieved using different approaches. Methods used for depletion of calcium ions from the extracellular medium include the use of chelating agents such as EGTA, use of calcium-free cell culture medium supplemented with FCS dialyzed in calcium-free buffer or the use of serum-free and calcium-free modified Epilife medium for prolonged serum-free cell culture (Figure 3.9 A). The effect of these approaches on the loss of TEER of MDCK-I cells was examined and the ability of the barrier to regain TEER following the different calcium treatments was also investigated to determine the best method to use later in the TEER assays on MDCK-I and MDCK-II cells.

When MDCK-I and MDCK-II monolayers were exposed to Epilife calcium-free medium conditions, the cells become detached from adjacent cells (Figure 3.9 B).

Figure 3.9 A illustrates the effect on TEER of treating cells with regular 5% FCS DMEM with added EGTA chelating agent at 2 mM, on both sides of the MDCK-I monolayer. Following treatment, TEER dropped sharply by a maximum of 91% after 30 minutes and stayed consistent up to 2 hours before treating the cells with 4 mM EGTA. Increasing the EGTA almost completely abolished the resistance (>99%) after 1 hour. This effect was promptly reversed upon replacement of the medium without EGTA and TEER fully re-established after 2 days.

Other calcium switch methods were conducted using dialysed serum added to HBSS culture medium, calcium-free or using Epilife calcium-free medium. Both methods resulted in almost a complete loss in TEER after 8 hours, which was reversed upon the repletion of extracellular calcium achieved simply through replacement of the calcium-free extracellular medium with regular medium supplemented with calcium. Therefore, following calcium repletion, TEER was fully recovered within approximately 1 day in both MDCK-I and MDCK-II cells (Figure 3.10 A). Both MDCK-I and MDCK-II display this ability to re-establish their monolayer and therefore TEER upon stress induced by manipulating extracellular calcium (Figure 3.10). As the Epilife calcium-free method gave a highly consistent effect on TEER loss and a full TEER recovery within 24 hours; this therefore was adopted for the calcium-switch techniques applied to MDCK-I and MDCK-II cells (Figure 3.10A).

To study the effects of calcium switch using the Epilife calcium free method on barrier integrity and tight cell-cell attachments, MDCK-I monolayers were subject to immunolabelling of the tight junction. Before calcium switch MDCK-I cells form tight apical connecting junction strands, around the cell periphery as seen by claudin-1 (red) and ZO-1 (green) staining. During calcium depletion this staining is almost completely abolished despite cells remaining in close proximity. After 24 hours following calcium repletion these junctions are fully recovered at the cell periphery (Figure 3.10B). No change in total expression of the ZO-1 tight junctions was observed during the calcium switch, suggesting that calcium depletion affects tight junction location and binding but not expression (Figure 3.10 C).

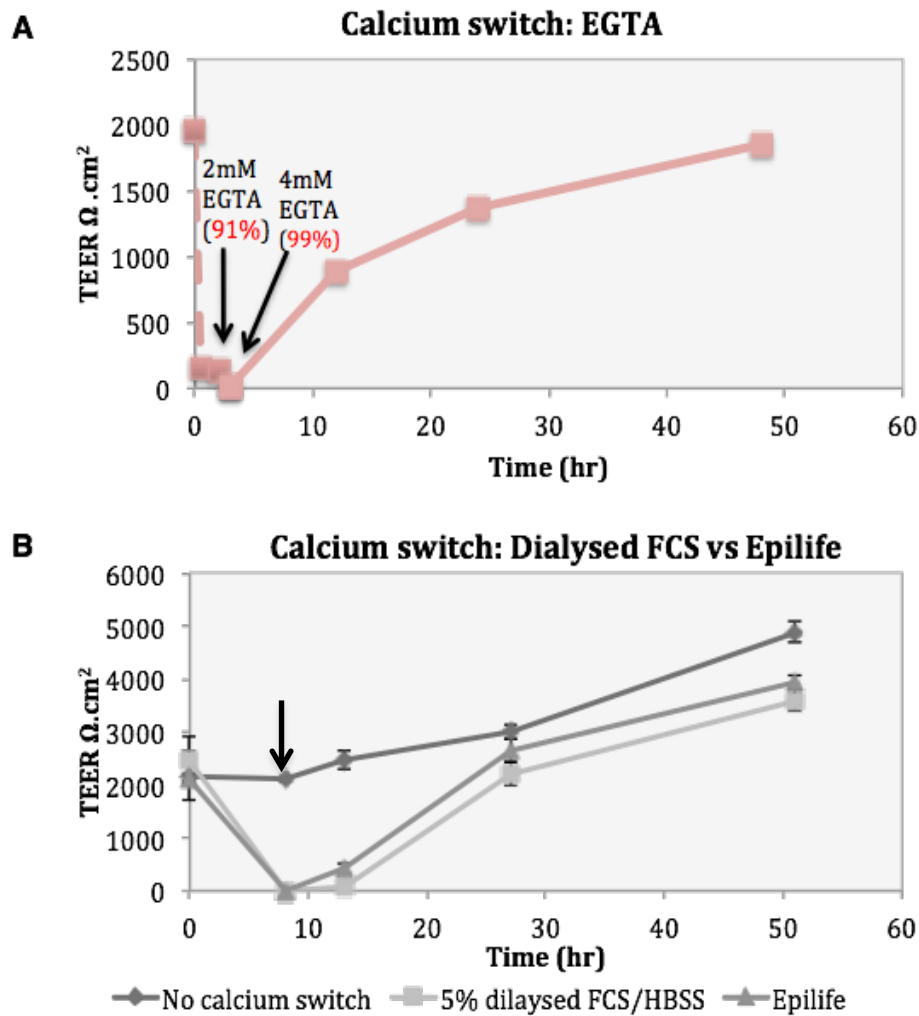


Figure 3.9 Effect of calcium-switch on MDCK-I monolayer TEER.

Calcium removal and addition of EGTA effect on the TEER of a monolayer of MDCK-I cells was studied A) Confluent MDCK-I monolayer (high TEER) established on permeable Transwell supports were treated with 2 mM EGTA calcium chelating agent on the apical and basolateral side. TEER was measure every 30minutes up to 2 hours before EGTA concentration was increased to 4 mM and measured up to 1 added hour. Complete removal of EGTA was carried out following the 3 hours of EGTA treatment by replacement of the medium to regular serum-free MEM and continual measurements of TEER were taken up to 2 days. B) MDCK-I monolayers were also subject to calcium depletion by simply incubating them with calcium-free medium. Confluent MDCK monolayer were incubated with calcium-free HBSS supplemented with 5% dialysed FCS or serum-free/calcium-free Epilife medium for 8 hours before TEER was measured. Calcium repletion was carried by replacement of calcium-free solutions with serum-free DMEM supplemented with calcium. Data points in n=2, mean± SEM.

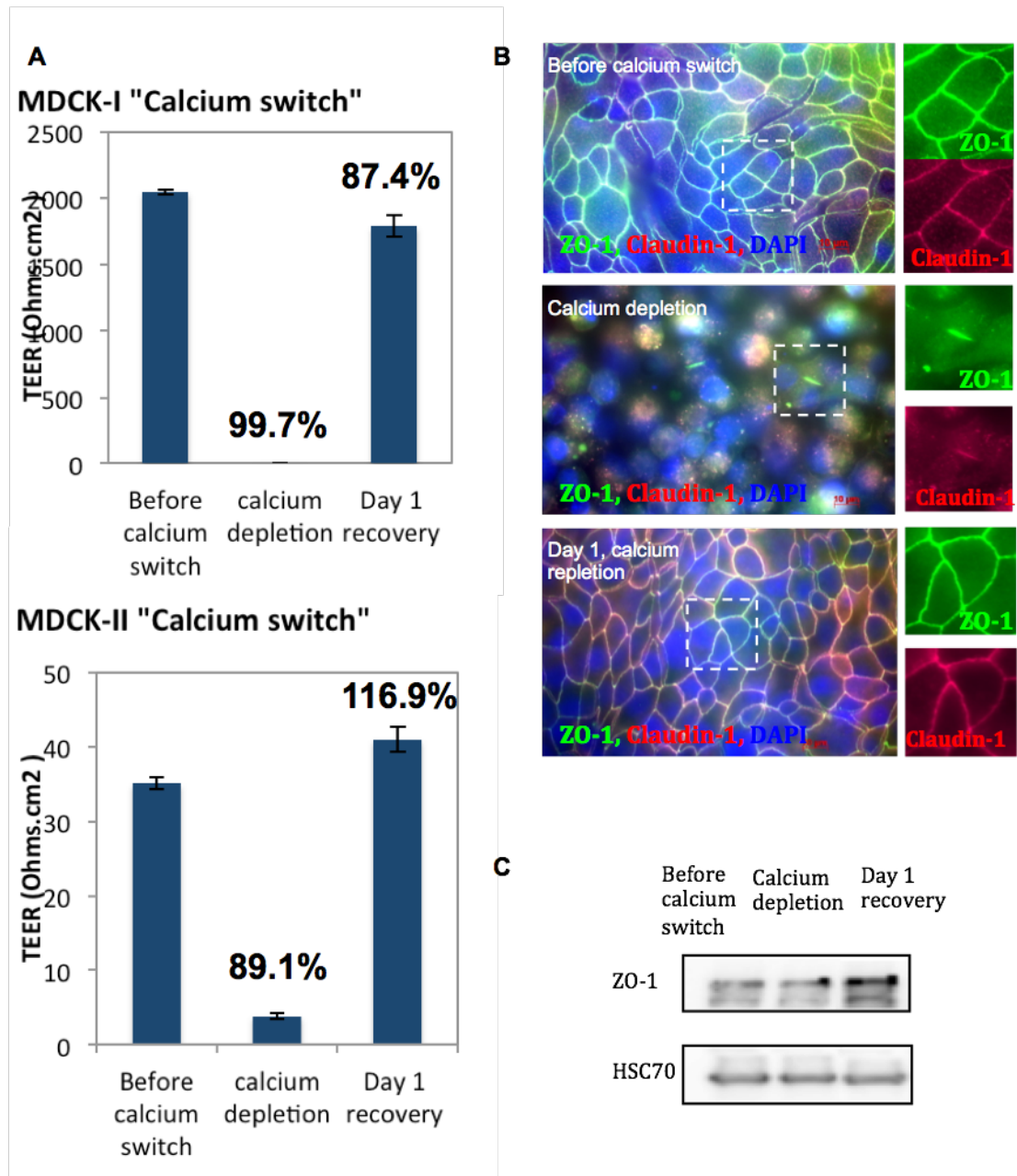


Figure 3.10 Effect of calcium depletion/repletion on MDCK-I and MDCK-II monolayer TEER and tight junction physiology.

A) MDCK-I and MDCK-II cells seeded on permeable support at 5×10^4 were and grown for 5 days in 5% FCS DMEM, were fully incubated with fresh Epilife calcium-free medium, for 12 hours. TEER was measure for each cell line before, during and after calcium depletion. B) The influence of calcium switch on barrier cell-cell junction physiology was demonstrated through immunofluorescence labeling of tight junction proteins ZO-1 (FITC-green) and claudin-1 (Alexa 647-red) in MDCK-I cells. Immunofluorescence was conducted on established epithelial monolayers (after 5 days on inserts), in the presence of calcium, during calcium depletion and 24 hours following calcium repletion. C) Total protein expression of tight junction protein ZO-1 was analysed during calcium switch, with HSC 70 protein loading control. Data points in A $n=3$, mean \pm SEM.

3.2.4 Expression of matriptase in MDCK cells

Orthologs of matriptase have been found in all vertebrate species but matriptase has only previously been directly studied in human and mouse (see review List et al., 2006). The predominant form of matriptase is as a monomeric protein, measuring around 70 kDa. A 120 kDa band is also observed referring to matriptase in a complex with HAI-1, a cognate inhibitor that forms strong direct associations with matriptase and tightly regulates its cellular activity in epithelial cells (Benaud et al., 2001, Lee et al., 2007). Several effective antibodies for detection of human matriptase protein have been generated. One of the most useful is the M32 mouse-derived monoclonal antibody (IgG₁), which detects both latent single-chain and active two-chain forms of the enzyme and works in immunofluorescence (Lin et al., 1999a). The same antibody is known to be inefficient at associating with the mouse protein being raised in a mouse (Oberst et al., 2003b). Based on the database the mouse matriptase shares 79% amino acid sequence identity with the human protein, while the dog shares 82% identity (dog matriptase sequence in Appendix 1).

3.2.4.1 Analysing matriptase protein expression in MDCK-I and MDCK-II cells

As an epithelial kidney cell line, we expect MDCK cells to express matriptase. So far no antibody against the dog matriptase protein has been reported. However an attempt was made to check if the M32 anti-human matriptase antibody could detect the protease from the MDCK lysate. Protein lysate collected from confluent MDCK-I and MDCK-II cells was loaded into SDS-page along with positive control lysate from the matriptase human prostate carcinoma cell line PC3. The western blots probed with M32 antibody showed positive bands around 70 kDa for the PC3 positive control in both reduced and non-reduced conditions. M32 antibody however did not detect matriptase expressed by MDCK-I and MDCK-II cells (Figure 3.11). Further antibodies against matriptase were also tested against the MDCK lysates giving a negative outcome. These include IM1014 recognising amino acids

near the C-terminus, GTX108375 recognising a region within amino acids 269-362, and GTX113557 recognising a region within amino acids 37-296 (data not shown).

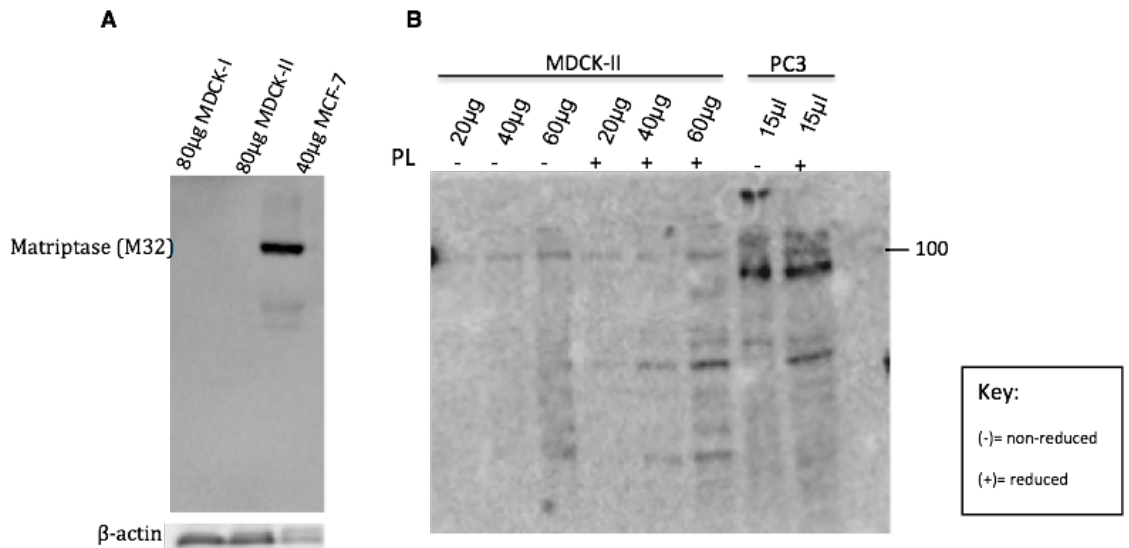


Figure 3.11 Matriptase protein expression in MDCK-I and MDCK-II cells. Total cell lysates were collected from confluent MDCK-II cells and protein content analysed western blots. Matriptase expression was analysed using the mouse M32 anti-matriptase monoclonal antibody was carried. Different amounts of lysates were loaded A) for MDCK-I, and MDCK-II cells using MCF-7 cells for positive control for their high intrinsic expression of human matriptase. Lystes were loading without reducing agent and protein loading was confirmed with the labelling of β -actin. B) Different amounts of lysates were loaded for MDCK-II cells with (+) and without (-) reducing agent β -mecaptoethanol. PC3 lysate was added for human positive control.

Although the M32 antibody failed to detect the dog protein, this batch was used to determine ability to recognize exogenous human matriptase in overexpressing A549 cells and to test the efficiency of using it in an immunofluorescence detection assay.

In previous studies matriptase has been shown to localize at the plasma membrane of epithelial cells and specifically at the basal membrane domain along with its cognate inhibitor HAI-I in polarized epithelia (Quimbar et al., 2013). Although M32 failed to bind the third extracellular LDLR domain in cell lysate, it might be able to associate with the dog protein while it is still at the cell surface. Initially we

investigated this in A549 cells over-expressing the human sequence in a Tet-promoter system (figure 3.12 A). Immunofluorescence labeling of PFA-fixed cells with M32, once expression of matriptase was determined in A549 cells not treated with doxycycline, showed positive localization at the cell periphery. This was not detected in A549 cells treated with doxycycline to suppress matriptase expression (figure 3.12 B). Therefore this immuno-labeling method was used for MDCK-I cells using the same M32 antibody, in an attempt to detect matriptase on the cell surface. However this failed to reveal any protein fluorescence, even when the cell layer was treated with SDS to unfold the protein and expose epitopes (Data not shown).

To ensure that matriptase is expressed in MDCK cells we investigated endogenous mRNA measurements.

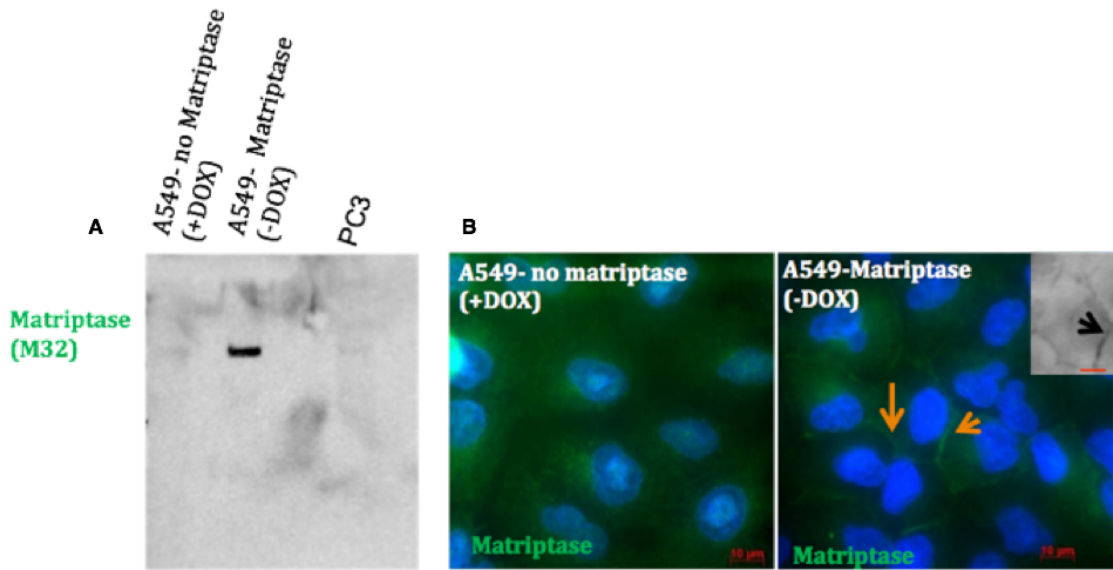


Figure 3.12: Immunofluorescence labelling of human Matriptase over-expressed in tet-off A549 cells using M32 mAb.

A) Western blot labelled with M32 mAb for the detection of matriptase in A549 cells presented with a Tet-off expression system for human matriptase (developed by Dr Kelly Gray). A549 cell were seeded in 6 well plates at 5×10^4 and left to grow in the absence or presence of doxycycline (+Dox or -DOX). PC3 cell lysate loaded for a positive control. B) Confluent A549 cells with and without doxycycline were fixed with 4% PFA and immune-labelled for matriptase using M32 mAb and secondary anti-mouse Alexa™ 488 antibody (green) or DAPI (blue) for staining of nuclei. Inverted insert displayed with arrows pointing to peripheral positive protein detection. Objective used x63. Size bars: 10 µm.

3.2.4.2 Analysing matriptase gene expression in MDCK-I and MDCK-II cells

The intrinsic level of expression of matriptase between MDCK-I and MDCK-II cells was determined through quantitative measurement of mRNA expression using qRT-PCR. Primers designed from the cDNA sequence of the dog matriptase (Table 2.7 Materials and Methods), provided successful evidence for the expression of matriptase in both MDCK-I and MDCK-II. The quantitative analysis revealed similar expression in both strains of MDCK cells, whereby the average C_t value for each cell line ranged between 25 and 26 indicated intrinsically high levels of mRNA (Figure 3.13 A). Melt curve analysis was used to determine that the amplification resulted in a single and specific PCR product sharing the same melting point between each

sample given. Also this was used to check for primer dimers, which could affect the quality of the amplification. The melt curve from the matriptase amplification gave a single peak at melting temperature of 85.67°C. This indicated a specific amplification of a single product. For further confirmation, Dog matriptase cDNA samples were run on an ethidium bromide 2% agarose gel to check for the size of the amplicon (169bp), to confirm the primers were specifically amplifying matriptase. The gel revealed two bands at the 200bp DNA marker in both MDCK-I and MDCK-II (Figure 3.13 B). The negative control (cDNA and primers with just water) showed no bands (Figure 3.13 B). Blast analysis of the sequence of the custom designed primers, confirmed gene specificity, as both forward and reverse primer sequences (highlighted in the cDNA sequence Appendix 1) match 100% with only the ST14 transcript in the dog. These primers had <93% identity with the human ST14 sequence but haven't been tested on human cDNA samples.

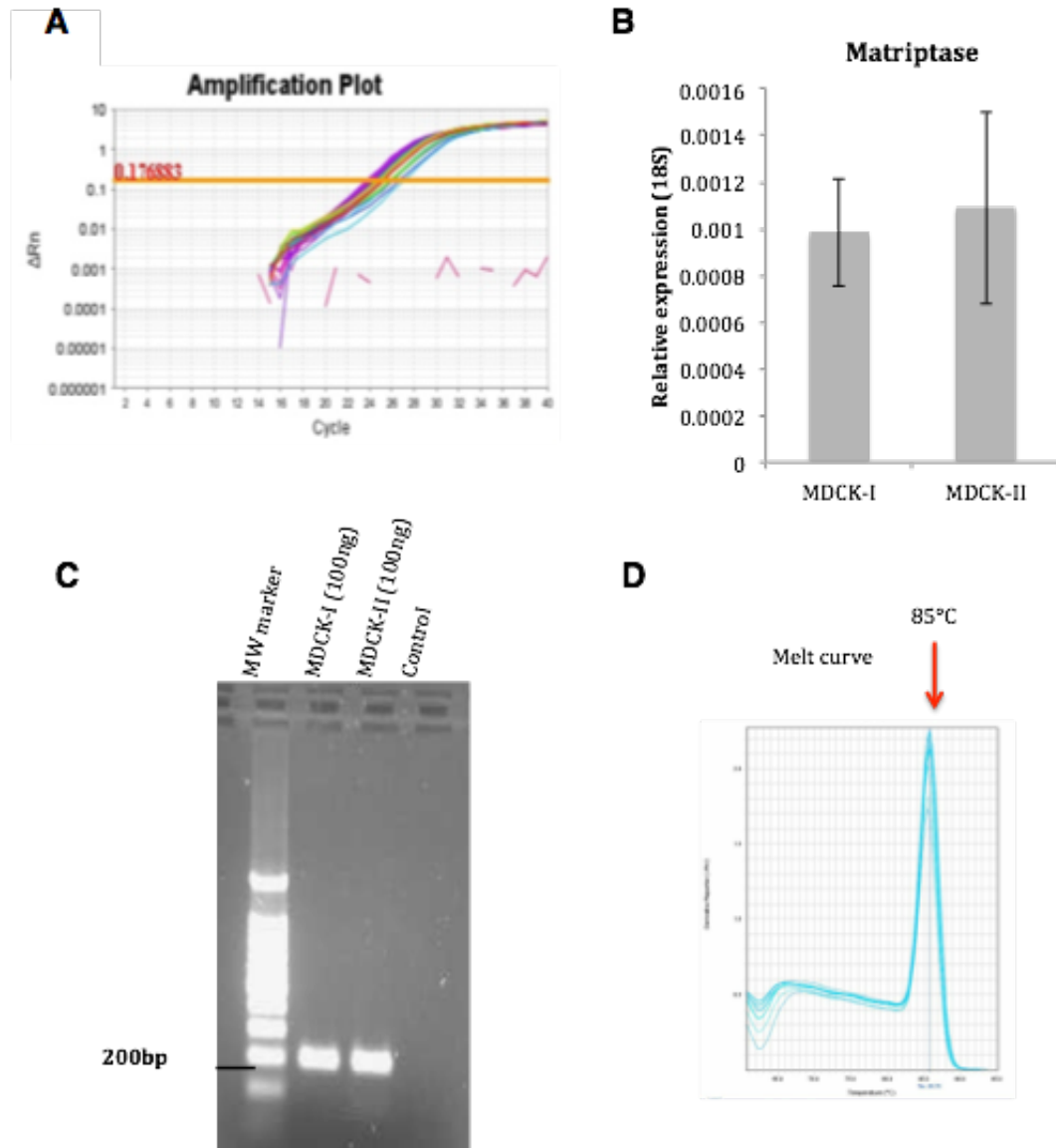


Figure 3.13 Quantification of matriptase gene expression in MDCK-I and MDCK-II cells.

A) Amplification curve for matriptase (st14) mRNA in MDCK cells displaying relatively low C_t ranging between 25 and 26 cycles. B) Quantitative RT-PCR technique with SYBR Green was used to confirm the expression of the matriptase gene in both MDCK-I and MDCK-II cells using custom designed primer for specific detection of the dog sequence. Relative to the level of expression of the 18S ribosomal RNA housekeeping gene a quantitative measure of the level of matriptase expression was analysed and compared between MDCK-I and MDCK-II cells. C) The specificity of the custom-made dog matriptase primers designed for the amplification of the 169bp amplicon was tested once the cDNA was subject to amplification by standard PCR. MDCK-I and MDCK-II c-DNA at 100ng each, alongside a non-primer control was loaded on to ethidium bromide agarose (2%) gel electrophoresis revealed. Gels were run at 140mV for 1 hour and imaged under UV light. D) The reaction melt curve from qRT-PCR analysis.. Data points in A, n=3, mean \pm SEM.

3.2.5 Matriptase knockdown by siRNA in MDCK cells

Because siRNA oligos specifically targeting the dog matriptase were not commercially obtainable, a custom siRNA sequence was designed and tested for knockdown of matriptase gene expression in MDCK cells. This sequence was designed using the Invitrogen BLOCKiT RNAi designer and chosen due to possible capacity to knockdown matriptase expression in both human and dog cells and potentially could be converted to an shRNA for cloning to generate a stable knockdown system for further studies of matriptase function (Figure 3.15).

3.2.5.1 Efficiency of siRNA knockdown of matriptase in MDCK-I and MDCK-II cells

Knockdown efficiency of matriptase following transfection of the custom siRNA into MDCK cells was determined by quantification of mRNA levels using qRT-PCR technique. MDCK-I and MDCK-II cells were subject to single and double transfection with targeting st14 siRNA, scrambled siRNA and no siRNA control including the transfection reagent alone. At 48 hours following single transfection, greater than 84% of mRNA expression was lost in MDCK-I cells and greater than 45% in MDCK-II cells (Figure 3.15). Furthermore a second transfection at 96 hours increased the knockdown to approximately 90% of mRNA was observed in MDCK-I and 99% in MDCK-II cells, compared to controls (Figure 3.15).

- Dog Matriptase cDNA

- >ENSCAFT00000015905 cdna:KNOWN_protein_coding

```
G TTCAGAGCATGAGTGGCGTCGAGGAGGGCGTGGAGTTCCTGCCGGTCAACAACACCAGGAAGGTGGAGAA
G CGGGGGCCCAAGCGCTGGGTGCTGCTGGTGACCGGGCTGGCCGGCCTGGTCTGCTTCCCTCGTGGCTTG
C CTCTGATGTGGCATTTCAGTACCAGAACATGCGGGTTCAGAAGATCTTCAATGGCTACCTGAGGATCA
C CAAACGAGAACTTCGTGGATGCCTATGAGAACTCCAACCTCACGGAGTTTGCAAACCTGGCCAACAGGGTG
A AAGGAAGCGCTCAAGCTGTTGTACAGTGGGGTGGCTCCCTGGGCCCTACCACAAGAAGTCGATGGTGAC
C GCCTTCAGCGAGGGCAGCGTCATCGCCTACTACTGGTCCGAGTTCAGCATCCCCAGTACCTGGTGGAGGA
T TGCCGAGCGGTCATGGCCCAGGAGCGGGCGGCGTGTGCCGCCCGAGCCCCGCGCCCTCAACTCCTTCGT
G GCTCACCTCGTGGTGGCCTTCCCCTGACCCCAGAACAGTACAGACCGCCAGGACAACAGTGCAGCTT
C GCCCTGCACGCCCCGAGCGGGGAGCTGATGCGCTTACCACGCCCCGCTTCCCCGACAGCCGTACCCGGC
C CGGGCCCCGCTGCCAGTGGACCCTGCGTGGGGATGCCGACTTCGTGCTGAGCCTCACCTCCGAGCTTTGA
C GTCGCGACCTGTGACGACCGGGCAGCGACCTGGTTCATGGTGTATGACACCTGAGCCCCGTGGAACCCCG
G GGCCGTGGTGCAGCTGTGTGGCACCTACCCTCCCTCCTACAACCTGACCTTCTCTCCTCCAGAACGTCTCTG
C TCGTCACGCTGATACCAACACGGAGCGGGCAGACCCTGGCTTTGAGGCCAGTTCCTCCAGTGCCTAAG
C TGAGCAGCTGTGGCGGCTCCTTACGCGGACGCCAGGGGACCTTTAGCAGCCCTACTATCCTGGCCACTAC
C CGCCCAACATGAACTGCACCTGGGACATTGAGGTGCCAGCCACCAGAACGTGAAGGTGCTCTTCAAGGCC
T TTCTACATGCTGGAGCCCAACCCCCCTGGGCACCTGCTCCAAGGACTACGTGGAGGTCAACGGGGAGAAG
T ACTGCGGAGAGAGGCCCCAGTTTGTGGTCACCAGCAGGAGCAACAAGATCACCGTTCGCTTCCACTCCGAC
C AGTCTACACCGACACGGGGTCTTGGCCGAGTACCTGTACATCGATTCCAGTGACCCGTGCCGGGGAAG
T TCCATGTGTCACACGGGGAGATGCATCCGGAATGAGCTGCGCTGTGACGGCTGGGCTGACTGCACGGACTA
C CAGCGACGAGCTCAACTGCCAATGCAACGCCACCTACCAGTTCACA TGCAAGAACAAGTTCTGCAAGCCCC
T TTTCTGGGTGTGCGACAGCGTGAACGACTGCGGAGACAACAGCGATGAGCAGGAGTGCAGCTGCCCGGCT
C CAGACCTTCAGGTGTGGCAACGGGAAGTGCCTCCACAGAACCAGCAGTGTGACGGGACGGACAACCTGCCG
G GACGGATCCGATGAGGCCACGTGTGACCTGGTGAGAACTGTGGCCTGCACCAAACACACCTATCGCTGCCA
C AACGGGCTCTGTTTGAGCAAGAGCAACCCGAGTGTGATGGGAAGAAGGACTGTAGCGACGGCTCGGATG
A GAAGGATTGCGACTGTGGCAGTCCCGGTGCTCGGGGGCACGAATGCGGACGAAGCGGAGTGGCCCTGGC
A AGGTGAGCCTCCACGTGCTGGGCCAGGGCCAGTGTGCGGGGCTTCCATCATCTCTCCAACCTGGCTGGTGT
C CGGCGCTCAGTCTTATCGACGACCGAGGATTGAGTACTCGGACCACATGGTGTGGACCCGCTTCTTGG
G CCTGCATGACCAGCAAGCGCAGCGCCACTGGGTGCAGGAGCTCGGCCCTAAGCGCATCATCTCCACC
C TTACTTCAACGACTTACCTTCGACTATGACATTGCGCTGCTGGAGCTGGAGCAGGCGGCGGAGTACAGCA
G CACCGTCCGGCCCATCTGCCTGCCGAGACCTCGCACAGCTTCCCCGCCGGAAGGCCATCTGGGTACCG
G GCTGGGGTACACCGCAGGAAGGAGGCTCCGGCGCGCTGGTCTGCAGAAGGGCGGAGATCCGCGTCATCAAC
C CAGACCACCGGAGAACGGCTCCCGCAGCAGATCACGCCGCGCATGATGTTTCGTGGGCTACCTCAGCGGGC
G GTGGACGCTGCCATGGCGACTCCGGGGGCCCTGTCCAGCGTGGAGGCCGACGGGCGGATCTTCCAGGCC
G GCGTGGTGTGCTGGGGCGACGGCTGCGCTCAGAGGGACAAGCCGGCGTGTACACGAGGCTCGCTGTATT
T CCGGACTGGATCAGAGAGGAGACGGGGGTGTAG
```

siRNA sequence used for transient kd of dog matriptase gene (Highlighted in RED)

Dog	GCAACGCCACCTACCAGTTCACA TGCAAGAACAAGTTCTGCAAG CCCCCTCTTCTGGGTGTGC
Human	GCGACGCCGGCCACCAGTTCACG TGCAAGAACAAGTTCTGCAAG CCCCCTCTTCTGGGTCTGC
Mouse	GCAATGCCACCCACCAGTTCACG TGCAAA AACC AGTTCTGCAAG CCCCCTCTTCTGGGTCTGT

Figure 3.14 Matriptase cDNA sequence in dog.

Highlighted in red is the chosen siRNA sequence for targeted knockdown in dog. This sequence is fully compatible with human cDNA for matriptase but not 100% compatible with mouse.

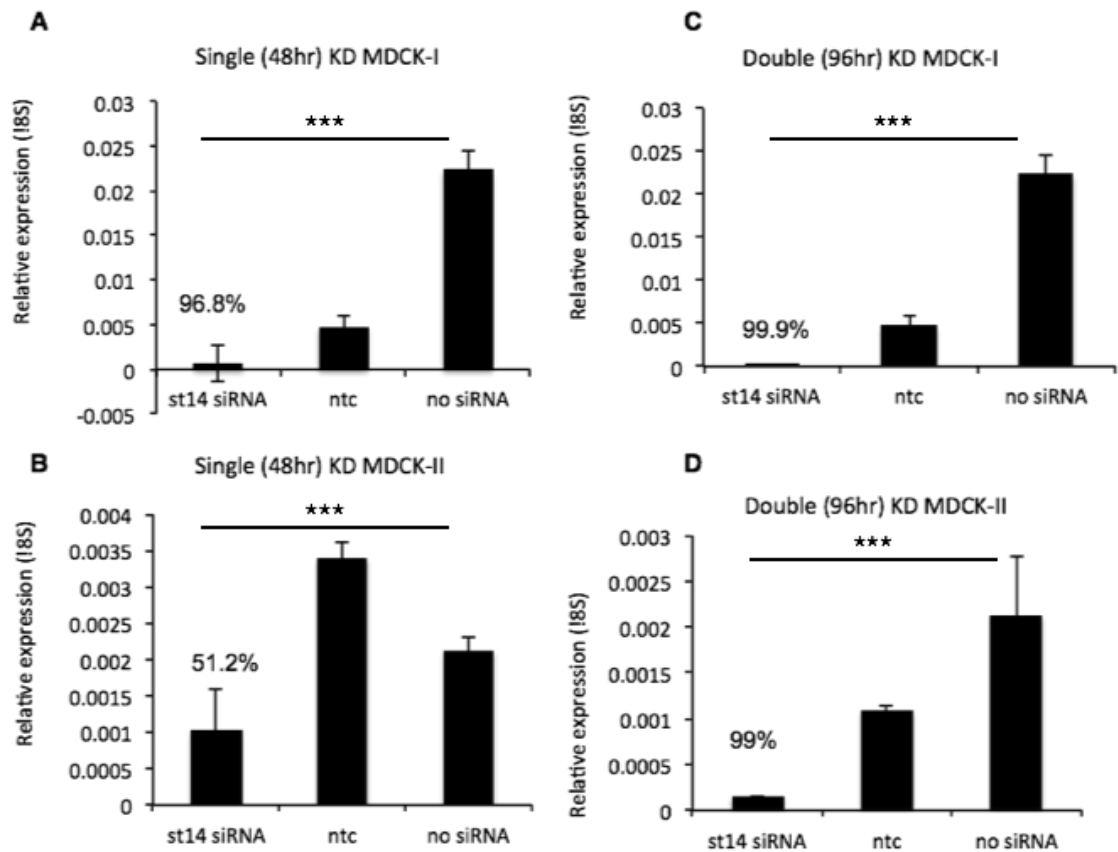


Figure 3.15 Matriptase knockdown by siRNA in MDCK-I and MDCK-II cells.

A) MDCK-I cells were seeded at 8×10^3 cells per well (24 well plate) and treated with 33nM dog matriptase siRNA, 33nM NTC (scrambled) control and no siRNA/lipofectamine only control for 48hr. qRT-PCR carried for quantitative analysis of dog matriptase expression. B) MDCK-II cells were seeded at 8×10^3 cells per well (24 well plate) and treated with 33nM dog matriptase siRNA, 33nM NTC (scrambled) control and no siRNA/lipofectamine only control for 48hr. qRT-PCR carried for quantitative analysis of dog matriptase expression. C) MDCK-I or D) MDCK-II cells were subject to a double transfection, with 33nM dog matriptase siRNA, 33nM NTC (scrambled) control and no siRNA/lipofectamine only control. Gene knockdown was also analysed via qRT-PCR using dog specific matriptase primers. Data points in A, $n=3$, mean \pm SEM.

3.2.6 Matriptase knockdown using Mission lentivirus transduction system

Attempt to generate inducible matriptase-targeting shRNA system

Initially, we attempted to generate an inducible system for the knockdown of matriptase using shRNA designed for dog. Here the same st14 siRNA sequence used in the transient knockdown study was converted to shRNA designed in a mir96 construct to be cloned into a Tet-off pINDUCER vector. The 96-mer-shRNA sequence was amplified by PCR using specific forward and reverse primer set containing the sequences for two restriction enzyme Xho-I and EcoR-I. Once amplified, multiple attempts were taken to clone this into the MSCV vectors (intermediate vector) or directly into the pINDUCER Tet-off vector. The amplified insert however did express the appropriate restriction sites and underwent proper restriction digestion as verified once this successfully cloned into the pBluescript plasmid and sequenced (see Appendix 1). After this attempt three custom dog matriptase-targeting shRNA sequences (st1, st2 and st3), st3 being the same sequence used for the siRNA knockdown experiments, and fourth Non Target Control (NTC) sequence, were cloned into the vector pLKO.1, which included a GFP reporter gene by Sigma (Figure 3.18 A). The provided plasmids were used to generate lentivirus particles for transduction of MDCK cells to generate stable cell lines with matriptase knockdown.

3.2.6.1 Generating stable MDCK-I cells with mission PLKO.1 shRNA lentivirus system

Three stable MDCK-I cell lines expressing each of the PLKO.1 st1, st3 and NTC vectors were generated by transfection using Lentivirus transduction particles packaged through HEK293T cells (Figure 3.18 A). Initially following particle synthesis and harvest, GFP expressed by pLKO.1 vectors was used to determine virus titre. To determine virus concentration, 50, 100 and 200 μ l were added to MDCK-I cells seeded at 1×10^5 in 6 well plates for 2 days. This showed that 200 μ l of

viral particles generated approximately 50% infection (Figure 3.17). Therefore to generate stables, MDCK-I cells were incubated with 400 μ l of particle containing medium for 24 hrs, and allowed to grow for 2 days before splitting and placing under selection with 2.2 μ g/ml puromycin. This concentration of puromycin was determined through concentration kill curve (Figure 3.16) showing complete cell death at day 5 at the highest concentration used of 2.4 μ g/ml and very low death at concentrations below 2 μ g/ml (Figure 3.16).

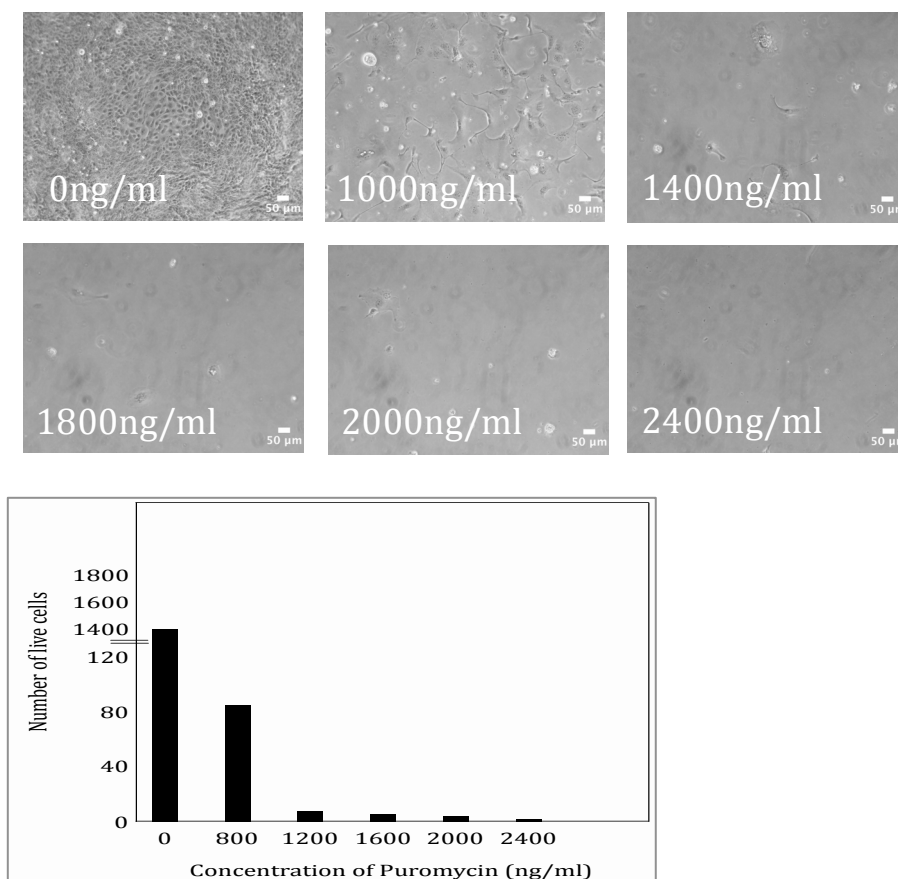


Figure 3.16 Puromycin kill curve on MDCK-I cells.

A range of puromycin concentrations (0-2400 ng/ml) was added to MDCK-I cells seeded at 2×10^4 in 6 well plates. The cells were maintained under treatment with puromycin for 6 days.

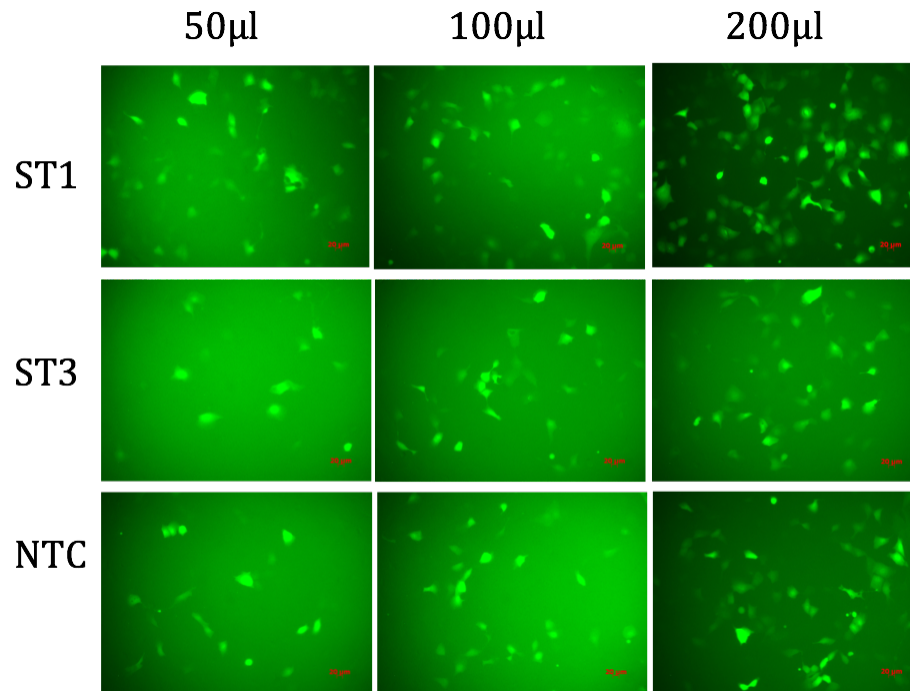


Figure 3.17 Determining packaged Mission PLKO.1 lentivirus titer using GFP signal. Packaged lentivirus was added at 50, 100 and 200 μ l with 8 μ g/ml hexadimethrine bromide. Microscope images of GFP expressed by the PLKO.1 vectors carried by lentivirus after 1 day of transfection were taken at x20 objective.

3.2.6.2 Matriptase gene expression in stable pLKO.1-shRNA expressing MDCK-I cells

RNA from stable PLKO.1 st1, st3 and NTC expressing MDCK-I cells selected with puromycin was obtained and used to determine the level of matriptase expression by qRT-PCR. Approximately 44% knockdown was observed upon the expression of the st1 shRNA sequence compared to NTC and regular control cells. However no significant decline in matriptase mRNA was observed with st3 shRNA expression (Figure 3.18) B). MDCK-I cells expressing the targeting sequence st3 did not show significantly different level of mRNA expression relative to the NTC cells and NTC MDCK-I cells (Figure 3.18 B).

A

Vector clone ID	DNA restriction digest	Sequence	Synthesis of lentivirus particles	Final Volume(ul)
pLKO.1-puro-CMV-tGFP	st14-1	GTGGGCTTCAGTGTGTATT	yes	400
pLKO.1-puro-CMV-tGFP	st14-2	CATGCGGGTTCAGAAGATCTT	no	---
pLKO.1-puro-CMV-tGFP	st14-3	TGCAAGAACAAGTTCAGCAAG	yes	400
pLKO.1-puro-CMV-tGFP	Non-target control	unknown	yes	400

Matriptase expression

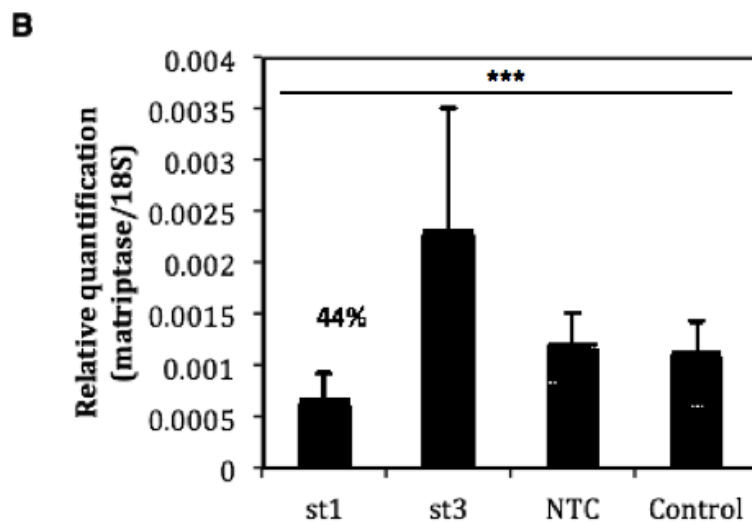


Figure 3.18 Effect of stable PLKO.1 shRNA expression on levels of endogenous matriptase expressed by MDCK-I cells.

A) Table representing the four designed Mission custom shRNA vectors provided and displaying the sequence of the matriptase targeting shRNA. Lentiviruses carrying the st1, st3, NTC but not st2 vectors were generated and 400 μ l final volume was added MDCK-I cells to generate stable cells. B) st1, st3 and NTC stable MDCK-I cell lines were generated and knockdown tested after 1 week growth in culture. Matriptase gene expression analysis conducted through qRT-PCR and quantification were conducted relative to the 18S house keeping gene. Analysis was carried on triplicate samples, (n=3). *** = $P < 0.05$.

3.3 Discussion

The literature so far clearly highlights that loss of or reduced matriptase activity significantly impaired the integrity of the epidermal and intestinal barrier epithelia, and further findings suggest that perhaps this is mediated through different regulatory mechanisms amongst these tissues (Buzza et al., 2010, List et al., 2007a, List et al., 2002, Netzel-Arnett et al., 2012).

The aim of this thesis was to investigate further the role of matriptase in regulating epithelial barrier function and behavior. Utilizing a distinctive *in vitro* model system to be used in the studies of matriptase and could therefore provide a descriptive analysis with regards to some of the most important aspects that contribute to barrier physiology. Following the early characterisation of MDCK cells by their growth, immunologic, and cytogenetic properties in 1966, they have become extensively used by researchers, in particular MDCK-II, as this is the best-characterized and easily available model for a variety of studies in cell biology. For a long time, much of our knowledge on epithelial barrier function and particularly tight junction function came from studies on MDCK-II cells, yet MDCK-I cells are less commonly known (Madin et al., 1957, Gaush et al., 1966).

The two available strains of MDCK cells, MDCK-I and MDCK-II develop similar structural barriers once cultured on filter inserts, yet they display different phenotypes in sub-confluent cultures. At sub-confluent level in a normal growth environment, MDCK-II cells were distinguished by a more adherent appearance. These cells are renowned by their adherent phenotype, as they immediately form small islands in culture from which they expanded and grew to establish a high confluence monolayer. They are also a preferred model for studies of cell migration and scattering due to the adherent appearance and distinguished response to motogenic factor stimulation (e.g. HGF scatter assays) (see review (Dukes et al., 2011)). In contrast, sub-confluent MDCK-I cells are morphologically distinct to MDCK-II cells. They maintained isolation from surrounding cells prior to approaching high confluence (90-100%), at which point neighboring cells adhered

and assembled into one monolayer structure uniform with confluent MDCK-II cells.

MDCK-I and MDCK-II monolayer cells exhibit similar expression and co-localisation of adhesion proteins such as E-cadherin and β -catenin and express similar apical-basal microtubule array and tight junction polarity on permeable support filters. However, although barrier properties and MDCK cell polarity require tight junction polarization, their overall paracellular permeability and TEER is more so defined by the expression ratio of the different claudin proteins. Paracellular permeability and TEER are real-time measures used to evaluate barrier status that is directly related to the properties of the tight junction, and functional integrity upon stimulus. Despite the structural similarities of their apical tight junctions, MDCK-I and MDCK-II monolayer permeability was markedly different, as reflected by the overall physiological permeability to macromolecular 4 kDa FITC-dextran and TEER. These measures significantly vary due to differences in the expression ratio of tight junction protein component, claudin-2.

The high TEER of $>2000 \Omega \cdot \text{cm}^2$ established by MDCK-I cells is caused by the expression of much tighter tight junction strands that highly restrict paracellular flow of ions, solute and water across, compared to MDCK-II cells, which develop low TEER ($<100 \Omega \cdot \text{cm}^2$). MDCK-II cells thus express leaky tight junctions, reflected in the high detection of claudin-2 at both the mRNA and protein level. Claudin-2 is known to increase selective permeability to cations and weaken interactions between neighboring cell strands in MDCK-II cells (Furuse et al., 2001), despite that these cells were found to express higher levels of other tight claudins such as claudin-1. However, the high abundance of claudin-2 protein has been previously shown to weaken the hydrophobic interactions of claudin-1 and claudin-4 at the tight junctions (Furuse et al., 2001), therefore despite the higher abundance of claudin-1, its tight properties are likely altered in MDCK-II cells resulting in low TEER measurements. Although previous studies showed increased or decreased claudin-2 expression has no significant influence on the paracellular permeability to macromolecules such as 4kDa FITC dextran, in comparing physiological permeability of both MDCK-I and MDCK-II barriers in culture inserts, we showed

MDCK-I barriers have tighter restriction to the paracellular passage of 4kDa FITC-dextran compared to MDCK-II (MDCK-I, ~19ng/ml/hr or, MDCK-II ~271ng/ml/hr) (Ikari et al., 2011, Suzuki et al., 2011).

Matriptase has been previously shown to alter physiological permeability and TEER of intestinal cells *in vitro* (Buzza et al., 2010). However, to be able to examine whether matriptase function is necessary for regulating the permeability of MDCK-I and MDCK-II cells in later experiments, the level of dog matriptase gene expression in these cells was determined. Although the detection of the dog protein was unsuccessful due to lack of available dog antibodies, a similar mRNA expression between MDCK-I and MDCK-II cells was clearly illustrated through the design of dog specific PCR primers for matriptase. Quantitative PCR analysis also indicated high level of expression of intrinsic st14 mRNA as amplification showed low cycle threshold for rising mRNA detection signal (<26C^t). Although expression was not found to be significantly different between the different barrier forming MDCK-I and MDCK-II cell lines, this does not necessarily mean that matriptase function does not play a part in their barrier function and TEER establishment. Matriptase activity may in fact convey different functions in both cell lines judged by various biological aspects including substrate availability and surface activation, such as HGF, which is an important factor is triggering cell migration more so shown in MDCK-II cells (Webb et al., 1996).

MDCK-I cells forming high TEER monolayers with high integrity toward diffusion of macromolecules on culture inserts could be used alongside MDCK-II cells, which express lower TEER and higher physiological permeability, to investigate the effect of matriptase function on these barrier aspects. The difference in expression of claudin-2 between MDCK-I and MDCK-II cells and the resulting difference in TEER are two characteristics that would be used to provide further mechanistic insight into the cellular processes mediated by matriptase that are involved in barrier closure and establishment of the tight junction. MDCK cells therefore could also be used to investigate the role of matriptase on cell competency to fully regain integrity following injury, by measuring effects on the repair and reestablishment of monolayer TEER in a calcium switch model, which can be conducted on both

MDCK-I and MDCK-II cells. To be able to study the role of matriptase it is important to utilize different experimental approaches to examine the effect of insufficiency on barrier function. In the following chapter, we investigated this using several specific methods for reducing activity (specific catalytic inhibitor approach) and utilize the knockdown system (transient and stable) developed for targeting the dog st14 gene expression, which is described in this chapter section 3.2.6.2.

3.4 Conclusion

In summary, we have validated a model utilizing two strains of MDCK cells, MDCK-I and MDCK-II to study barrier function and determine physiological permeability under specific culture conditions. These cells show similar structural and permeability adaptations in response to calcium switch and have an effective repair mechanism, shown by TEER reformation reestablishment of selective paracellular diffusion. Although we and others have shown that these form differential barriers in culture with regards to their overall paracellular permeability and TEER, primarily due to claudin-2 expression, we also showed that they have similar and high expression levels of matriptase at the mRNA level. Establishing a research tool to knockdown the gene expression of matriptase in the canine cells will be useful for investigating its role in both systems. This can be utilized along with other tools to inhibit matriptase activity either barrier function or other biological aspects of epithelial cells.

Chapter 4. Matriptase role in regulating MDCK barrier integrity and repair function

4.1 Introduction

Epithelial polarity program and process of recovery

In polarized simple epithelia, the paracellular junctions control monolayer integrity and dynamic function. The dynamic organization and assembly of adhesion molecules such as E-cadherin followed by the tight junctions is a well-described mechanism, which plays a critical role in restitution of barrier continuity once damaged (Momose et al., 2012, Wodarz, 2002, Nelson, 2003). Therefore epithelial barrier function can be arbitrated through the ability to rapidly recover a continuous and tight epithelial network to prevent infiltration of environmental toxins and pathogens (Colombo et al., 2012).

Although a great effort has gone into understanding the processes associated with barrier disruption and reassembly, the main regulatory pathways that dynamically control epithelial barrier behavior are still not well understood. Loss of barrier functions and increased barrier permeability in matriptase deficient epithelial monolayers presented a new potential regulator of barrier integrity, which led to a number of significant studies. Amongst these studies are those highlighting that altered matriptase function is necessary for epithelial barrier formation and maintenance both *in vivo* (e.g. hypomorphic mice) and *in vitro* (e.g. Caco2 cell line) (Buzza et al., 2010, Netzel-Arnett et al., 2012, List et al., 2007a, List et al., 2002).

The requirement of matriptase for postnatal survival demonstrated in knockout mice was dependent on its physiological role in the development and proper

maintenance of epidermal barrier epithelia and prevention of excessive loss of body fluids (List et al., 2002). However, conditional knockout mice were first to highlight a role for matriptase in the regulation of gut function and physiology (List et al., 2009). This was followed by the studies of hypomorphic mice (>1% mRNA), which confirmed this role as they developed weakened intestinal tissue with raised paracellular permeability and increased susceptibility to injury (Buzza et al., 2010). These mice illustrated an impediment in the epithelial repair function as indicated through an experimental colitis model (Netzel-Arnett et al., 2012). This function of matriptase is dependent on the catalytic activity as demonstrated *in vitro* barrier assays conducted on Caco-2 cells (List et al., 2007a, Whitson et al., 2006).

Matriptase catalytic function and control:

Catalytic function of matriptase includes the activation of growth factors, cell surface signaling receptors, and other serine proteases, most of which have been shown to play independent roles in the regulation of paracellular permeability and overall epithelial function (Watson et al., 2006, Buzza et al., 2013). The specific inhibition of matriptase activity in Caco-2 cultured epithelial monolayer was found to increase paracellular permeability, and the molecular changes associated with this include decreased PKC ζ phosphorylation and increased claudin-2 expression (Netzel-Arnett et al., 2012, Buzza et al., 2010).

In contrary using MDCK-I cell model, in which the acquisition of paracellular integrity is dependent on trypsin-like activity, the overexpression or treatment with recombinant HAI-2 was shown to accelerate the acquisition of functional tight junctions and in turn enhance TEER (Szabo et al., 2009). As HAI-2 serves as a cognate inhibitor for matriptase, this suggested that matriptase activity might be playing a different role in MDCK barrier model. Thus whether matriptase activity in MDCK cells is required for barrier function and paracellular integrity as previously observed in Caco-2 cell and hypomorphic model is still unknown (Buzza et al., 2010).

4.1.1 Matriptase inhibitor binding and function ablation

Several previous studies have shown a critical role for matriptase in cancer initiation and progression, through studies of transgenic mouse models as well as the found elevated expression in a variety of epithelial cancers (Oberst et al., 2002, List et al., 2005). Collectively, these data led to the recognition of matriptase as a novel and potential target for cancer therapy. Herein, several groups have worked on the discovery, design and synthesis of various types of inhibitors to be considered for suppression of matriptase induced tumor development. Our main approach to studying the function of matriptase in MDCK epithelial model cell line is by using these inhibitors specifically designed to target the catalytic activity of matriptase.

The structures of the active sites of matriptase and trypsin are very similar, with the major differences being in the loops surrounding the active site, particularly loop II, which are involved in both substrate and inhibitor binding (Quimbar et al., 2013). Although effective inhibition of protease activity is easily accomplished using synthetic small molecule inhibitors, selectivity of inhibition is much more difficult to achieve, particularly between closely related proteases. In this study we used three different types of inhibitors to investigate the role of matriptase in MDCK cells, in barrier recovery assays. Amongst these inhibitors are the high affinity cyclic cysteine knot peptide inhibitors known as *Momordica cochinchinensis* trypsin inhibitor-II (MCoTI-II), 3-amidinophenylalanine-based inhibitors CJ-730 and derivative inhibitor CJ-1737 and the peptidomimetic inhibitor with a ketobenzothiazole group (IN-1). It is important to mention that the majority of these inhibitors have been shown to distinguish between matriptase and hepsin, which have overlapping substrate specificities, and both found to be up-regulated in various cancers.

Cyclic cysteine knot peptide inhibitors

Momordica cochinchinensis trypsin inhibitor-II (MCoTI-II) is a miniprotein trypsin inhibitor from Vietnamese squash that contains a disulphide-rich cyclic backbone

of 34 residues, established by Robin Leatherbarrow and Ed Tate at Imperial College London (Thongyoo et al., 2006)(Figure 4.1). The so-called “knottin” cysteine-rich cyclic scaffold is developed through the formation of three-disulphide knots, which create a thermodynamically stable peptide with low sensitivity to proteolytic degradation, and provide high stability *in vivo* (Werle et al., 2007). New methodology was developed that allows for the total chemical synthesis of MCoTI-II, which serves as a scaffold for introducing sequence variations, developing structural analogs with modulated target affinity and specificity of inhibition (Thongyoo et al., 2006, Thongyoo et al., 2007).

In our initial examination the potency of MCoTI-II toward matriptase, hepsin and other serine proteases was tested against four other derivatives that carry variation in sequence around the reactive center residue. The MCoTI-II was found to have the highest selectivity for inhibiting matriptase activity with a K_i value of 9 nM, at least 1000-fold lower than that observed for the closely related TTSP, hepsin (Gray et al., 2014).

As mentioned previously matriptase mediates its biological activity via the proteolytic activation of many substrates, some of which are well defined and also serve as substrates for hepsin, such as pro-HGF (Owen et al., 2010). In our lab we used both purified and cell based assays to demonstrate the efficiency of MCoTI-II (generated by total chemical synthesis) at inhibiting matriptase activity relative to hepsin. Here, we showed that MCoTI-II effectively inhibited the proteolytic activation of pro-HGF and pro-HGF mediated cell scattering in MDCK-II cells by matriptase but not by hepsin. Also this was able to selectively inhibit matriptase-expressing prostate cancer cell invasion. These observations highlight the strong potency and selectivity of MCoTI-II in the inhibition of matriptase in biological systems and that this potency is retained for the inhibition of dog matriptase, which is useful for further studies that use MDCK model assays (Gray et al., 2014).



Figure 4.1 MCoTI-II structure and inhibition properties.

The figure represents MCoTI-II inhibitor structure displaying the cyclic 3 disulphide bridges (in yellow) formed by the side chains on 6 cysteine residues. The table documents the inhibition constant (K_i) of MCoTI-II and relative fold selectivity for both matriptase and the related protease hepsin (Thongyoo et al., 2008).

Bis-benzamide-based tripeptide mimetic inhibitors

The CJ-730 (Compound 8) and CJ-1737 (Compound 59) inhibitors are analogues based on the bis-basic secondary amides of sulfonylated 3-amidinophenylalanine, developed by the group of Torsten Steinmetzer, at the University of Marburg (Steinmetzer et al., 2009, Steinmetzer et al., 2006)(Figure 4.2). These inhibitors contain an additional basic group at their C-terminus found to enhance selectivity and potency for matriptase. X-ray structural analysis revealed accommodation of the C-terminal aminoethyl group at the “cation cleft” between the 60-insertion loop and the surface of matriptase while the arylsulfonyl group was suggested to occupy the S4 binding site (Steinmetzer et al., 2006).

Our lab group previously tested the potency of CJ-730 using recombinant proteases and a specific fluorogenic peptide substrate (for matriptase and hepsin). This revealed a 40 nM K_i for matriptase, and a higher K_i (185 nM) for hepsin (Owen et al., 2010). Steinmetzer *et al*, showed CJ-1737 to have a higher potency for matriptase than CJ-730 (>100 fold) with a K_i of 0.6 nM, and a high selectivity when compared against other serine protease such as uPA and thrombin (Steinmetzer et al., 2006).

Both of these compounds were studied in an orthotopic xenograft mouse model of prostate cancer and found to reduce tumor growth and metastasis (Steinmetzer et al., 2006). Both of these inhibitors were found to reduce tumour growth in an

orthotopic xenograft mouse model of prostate cancer, as well as reduce pro-uPA and proHGF activation and mediated cell invasion and scatter in PC3 (prostate cancer cells) and MDCK-II cells (Forbs et al., 2005, Steinmetzer et al., 2006, Owen et al., 2010).

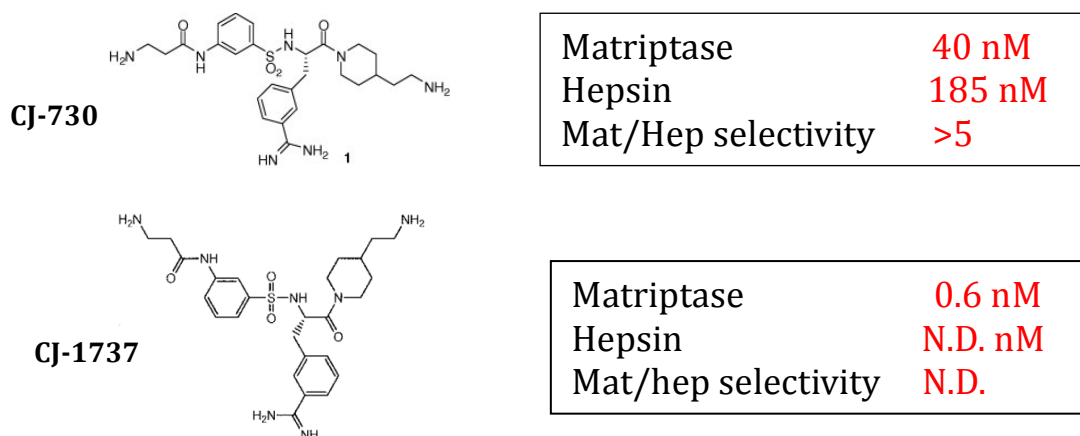


Figure 4.2 Chemical structures and inhibition properties of CJ-730 and CJ-1737.

This figure represents chemical structure of CJ-730 and CJ-1737. The tables document the inhibition constant (K_i) of CJ-730, CJ-1737 and relative fold selectivity for matriptase related protease hepsin. CJ-730 relative selectivity against hepsin is UD, however this has higher selectivity for matriptase (>100-fold) and other serine proteases such as uPA and thrombin compared to CJ-730 (Kotthaus et al., 2010, Steinmetzer et al., 2006).

IN-1-peptidomimetic inhibitor with ketobenzothiazol serine trap (IN-1)

IN-1 is a matriptase inhibitor developed by Eric Marsault's group at Sherbrooke University in Quebec, that belongs to the potent and selective peptidomimetic inhibitors of matriptase mimicking the P4-P1 (Arg-Gln-Ala-Arg) autoactivation sequence (Colombo et al., 2012) (Figure 4.3). The inhibitory function comes from the reversible covalent attachment of a ketobenzothiazole group to the catalytic serine residue in the matriptase active site, to prevent substrate binding and cleavage (Colombo et al., 2012).

The K_i value for the inhibitor was determined as 0.011 nM using the method of Morrison for slow, tight-binding inhibition (Colombo et al., 2012). This extremely low K_i does not reflect the initial binding of the inhibitor, but the function of the ketobenzothiazol trap that binds covalently, but reversibly, to the catalytic serine

residue of matriptase. The biological activity of the inhibitor has been demonstrated through its ability to block H1N1 influenza virus replication, mediated by matriptase, in Calu-3 human bronchial epithelial cells (Beaulieu et al., 2013). Under these conditions the efficiency of the inhibitor was greatly reduced, with a half-maximal effective concentration (EC₅₀) of 5.64 μ M and > 5 orders of magnitude higher than the K_i value (Beaulieu et al., 2013).

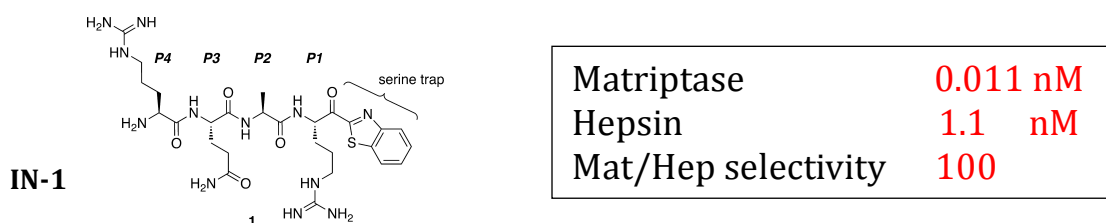


Figure 4.3 Chemical structure and inhibition properties of IN-1.

The figure represents IN-1 inhibitor chemical structure containing the ketobenzothiazole group, which forms the serine trap. The table documents the inhibition constant (K_i) of IN-1 and relative fold selectivity for matriptase and related protease hepsin (Colombo et al., 2012).

4.1.2 Matriptase approach to study its role in MDCK model of epithelial barrier

So far multiple studies have highlighted the critical role of matriptase in regulating the integrity and function of epidermal and intestinal barrier epithelia, which is mediated through different mechanisms, which is dependent on its catalytic activity. The proteolytic function of matriptase encompasses the activation of protease and non protease targets to regulate epithelial integrity. This mechanism remains unclear in the simple intestinal epithelia, whereby one group linked matriptase activity to the regulation of tight junctions, in particular claudin-2 expression (Buzza et al., 2010). Therefore in this study we aim to investigate the role of matriptase in two strains of MDCK cells, which present a well-defined model of the simple barrier epithelia in culture. Here we utilize the aforementioned inhibitors of matriptase and compare this effect using and si/shRNA knockdown approach.

4.1.3 Aims and objectives

In this chapter we aim to:

- Study the role of matriptase in regulating the function and integrity of MDCK barrier epithelia. To achieve this, *in vitro* barrier permeability assays will be used to study the effects of three different matriptase inhibitors, MCoTI-II, CJ-730/CJ-1737 and IN-1 on the ability of MDCK-I and MDCK-II to develop or reestablish (following calcium switch) fully functional barrier systems.
- Determine whether matriptase inhibition and its effect on paracellular permeability is cofounded by changes in the expression or resealing of the barrier determining paracellular junctions, including the tight junctions, adhesion junctions, and associated cytoskeleton.

4.2 Results

4.2.1 Effect of matriptase inhibition on MDCK-I and MDCK-II pro-HGF activation induced cell migration

To determine the effectiveness of the various matriptase inhibitors on MDCK cells, we studied their ability to inhibit the activation of proHGF, a process we have previously shown to be mediated by matriptase, more formally in PC3 cells. Here we apply recombinant proHGF in the presence of the matriptase inhibitors and determine their function through analysing their effects on HGF induced cell migration and scatter.

The recombinant pro-HGF used for this study, has been synthesized in our lab with a C-terminal V5-tag expressed by *Drosophila* S2 cells (Owen et al., 2010). Initially six different preparations were analysed by western blotting, to determine which sample comprised the least amount of active HGF (30 kDa band). Antibody to the V5-tag was able to detect the activated form once the samples were treated with the reducing agent β -mercaptoethanol before running on SDS-PAGE. Sample 15 exhibited the least active HGF contamination relative to the levels of pro-HGF as shown in Figure 4.4. This preparation was therefore used for further studies to determine the effect of matriptase activity on different aspects of cell behavior mediated by activation of pro-HGF.

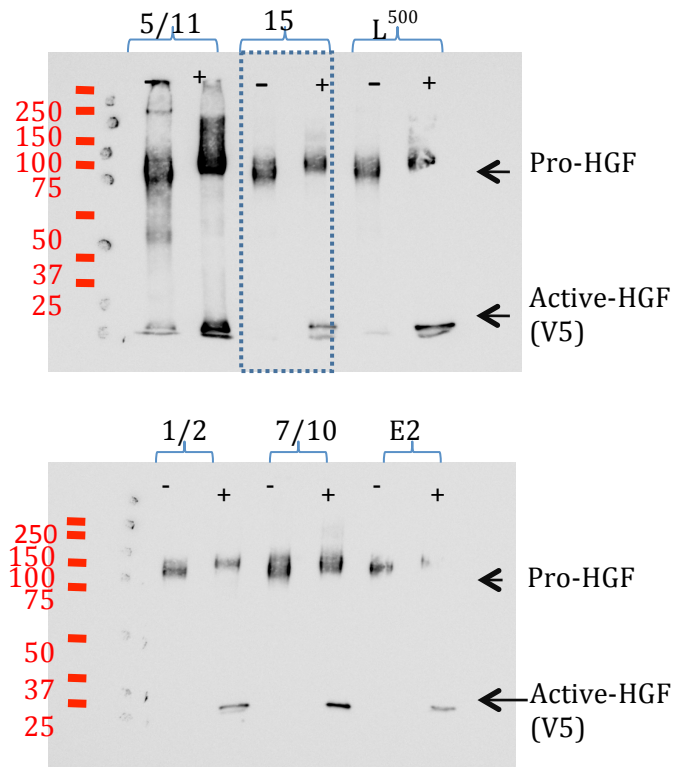


Figure 4.4 Examination of different sample preparations of recombinant proHGF.

Six different preparations of proHGF expressed by *Drosophila* S2 cells and named 5/11, 15, L500, 1/2, 7/10 and E2, were analyzed by western blots under non-reducing (-) and reducing (+) conditions to determine the relative level of active HGF to inactive proHGF. The active HGF is represented by the 30 kDa band present in the reduced samples that refer to the β -chain, which connects to the α -chain by a single disulphide bond once activated. The smaller β -chain holds the V5 epitope, and therefore the V5 antibody only detects this and not the separated α -chain (~69 kDa). Sample 15 expressed the least amount of active HGF relative to inactive (92 kDa).

CJ-1737

To determine the efficiency of CJ-1737 as an inhibitor of matriptase in cell culture, HGF-stimulated MDCK-I cell migration was studied by time-lapse microscopy. Images of cells were collected every 10 minutes for a total period of 16 hours to generate a short time-lapse video showing cell movement. MDCK-I cells were treated with proHGF and CJ-1737 (100 μ M), 10 minutes before imaging was initiated. MDCK-I cell showed enhanced cell migration in the presence of pro-HGF. The enhanced cell migration initiated by treatment with pro-HGF was repressed

upon matriptase inhibition with CJ-1737. Treatment of MDCK-I cells with inhibitor alone showed similar migration velocity to control conditions (Figure 4.5)

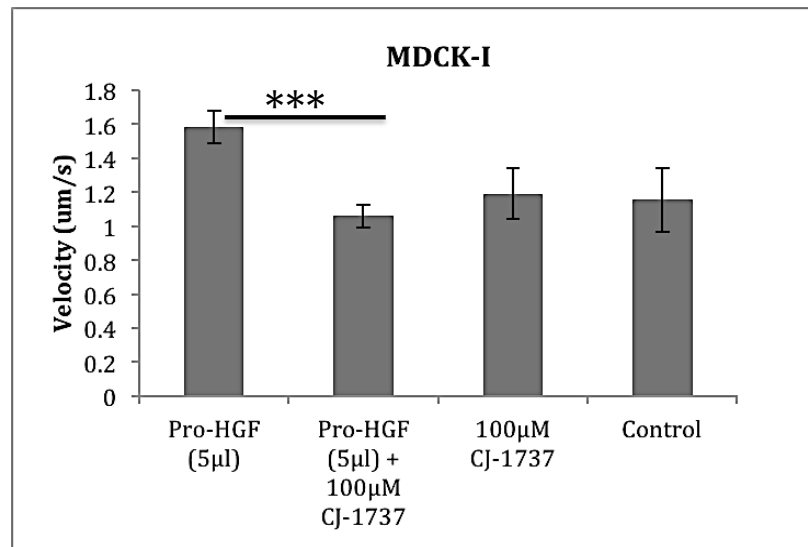


Figure 4.5 Effect of CJ-1737 on proHGF induced cell migration in MDCK-I cells.

MDCK-I cells were seeded at 8000 cells per well. Cells were treated with pro-HGF (5µl from preparation 15) in 500 µl DMEM-serum free in the presence of CJ-1737 (100 µM) for 16 hours at 37°C. Cells were treated with proHGF (5-µl), without pro-HGF treatment and CJ-1737 (100 µM) alone served as positive and negative controls respectively. The migration assay was done in triplicates (n=3) and analysis of cell movement and velocity were carried out using image J software tracking for 3 cells from each repeat (therefore a total of 9 cells for each conditions). *** = $P < 0.05$.

MCoTI-II

Preliminary data on the effect of MCoTI-II on cultured cells were generated from the treatment of sub-confluent MDCK-II cells with pro-HGF or active HGF with matriptase inhibitor MCoTI-II at 100 and 500 nM (Gray et al., 2014). Data confirmed the potency of MCoTI-II in inhibiting pro-HGF induced cell scatter at both low and high concentrations of the inhibitor. As expected, MCoTII had no effect on cell scattering upon stimulation with active-HGF demonstrating that matriptase expressed on the surface of MDCK-II cells was responsible for pro-HGF activation and the cell scattering response (Figure 4.6).

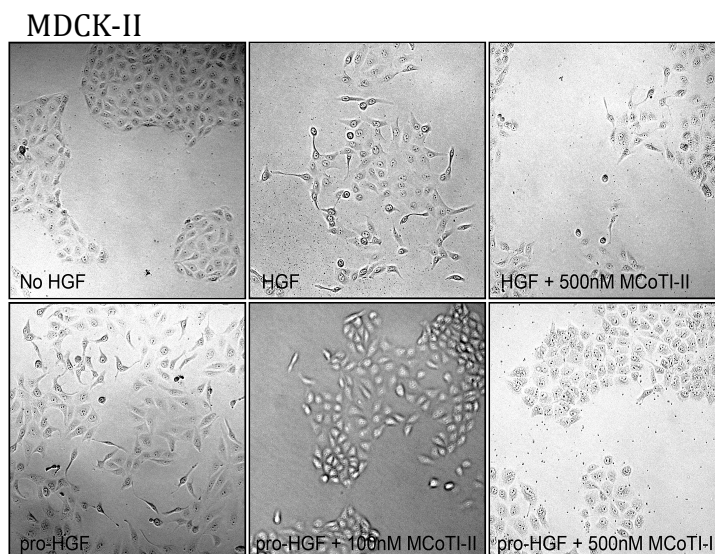


Figure 4.6 MDCK-II HGF cell scatter assay with MCoTI-II inhibitor.

MDCK cells were seeded at a density of 10^3 cells per well. Cells were treated with pro-HGF (10 ng/ml) in serum-free medium in the presence of 100 nM or 500 nM MCoTI-II for 24 h at 37°C. Cells treated with active HGF (10 ng/ml) and cells without HGF treatment served as positive and negative controls respectively. Cells were fixed with ice-cold methanol for 5 min and images taken using the Zeiss CCD inverted microscope using an x10 magnification (Gray et al., 2014).

4.2.2 Effect of matriptase inhibition on MDCK-I and MDCK-II barrier integrity and TEER

The TEER assays were carried to investigate the effect of matriptase inhibition on the re-establishment of paracellular integrity, following calcium switch, in MDCK-I and MDCK-II cells. Previously our group studied the effect of MCoTI-II on the development of barrier TEER in MDCK-I cells, which showed no significant alteration in TEER development but showed a small reduction in maximum TEER (Gray et al., 2014). However, this effect was also examined when calcium switch was applied to study TEER recovery and barrier repair, which signifies a well functioning barrier system. Cultured MDCK-I and MDCK-II cells, which form high and low TEER monolayers, respectively, both display an ability to repair following injury induced by depletion of extracellular Ca^{2+} , as demonstrated in Chapter 3 (section 3.2.2 and 3.2.3). Treatment of MCoTI-II inhibitor, strongly delayed the

recovery of TEER in MDCK-I monolayer, but interestingly did not alter MDCK-II barrier TEER recovery. This data implied a much more prominent role of matriptase activity on the functional aspect of barrier repair following injury in MDCK-I cells (Figure 4.7).

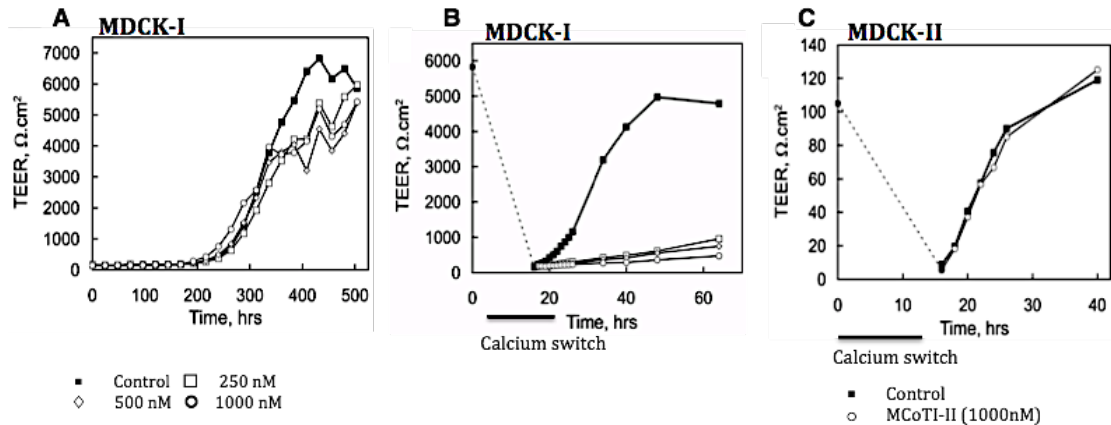


Figure 4.7 Matriptase MCoTI-II inhibitor affect on TEER establishment and re-establishment in MDCK-I and MDCK-II cells.

A) MDCK-I cells seeded on Transwell support expressed a normal monolayer TEER that was mildly affected by treatment with 250, 500 and 1000 nM MCoTI-II added at the start and replenished ever 24 hours. B) Treatment of MDCK-I cells with the same concentration range of MCoTI-II induced a significant ablation in barrier TEER repair property. C) MDCK-II cells treated with 1000 nM MCoTI-II expressed normal TEER repair function following disruption of barrier by calcium switch. Each TEER assay was done in triplicate (n=3). Data was collected in collaboration with Dr Kelly Gray and Dr Roman Szabo.

CJ-730 and CJ-1737

The effect of the two synthetic small-molecule inhibitors, CJ-730 and CJ-1737 on MDCK-I and MDCK-II barrier recovery was also studied. Here, the concentrations applied to MDCK cells were based on the 5 μM IC_{50} value previously determined for CJ-730, while studying the efficiency of inhibition of proHGF activation by PC3 cells, which was 100 fold higher than the K_i value (Owen et al., 2010). Initially MDCK-I cells were treated with 50 and 100 μM of CJ-730 following calcium switch. MDCK-I cells treated with 50 μM of CJ-730 inhibitor expressed a smaller delay in TEER recovery, compared to 100 μM . Furthermore, the efficiency of CJ-1737 on

delaying barrier TEER recovery in MDCK-I cells was very similar to CJ-730, despite the chemical modification previously shown to increase its potency by 100 fold in recombinant systems (Jacobson et al., 2006). This significant delay of TEER recovery by MDCK-I cells was not seen following treatment of MDCK-II cells similar to the MCoTI-II observation.

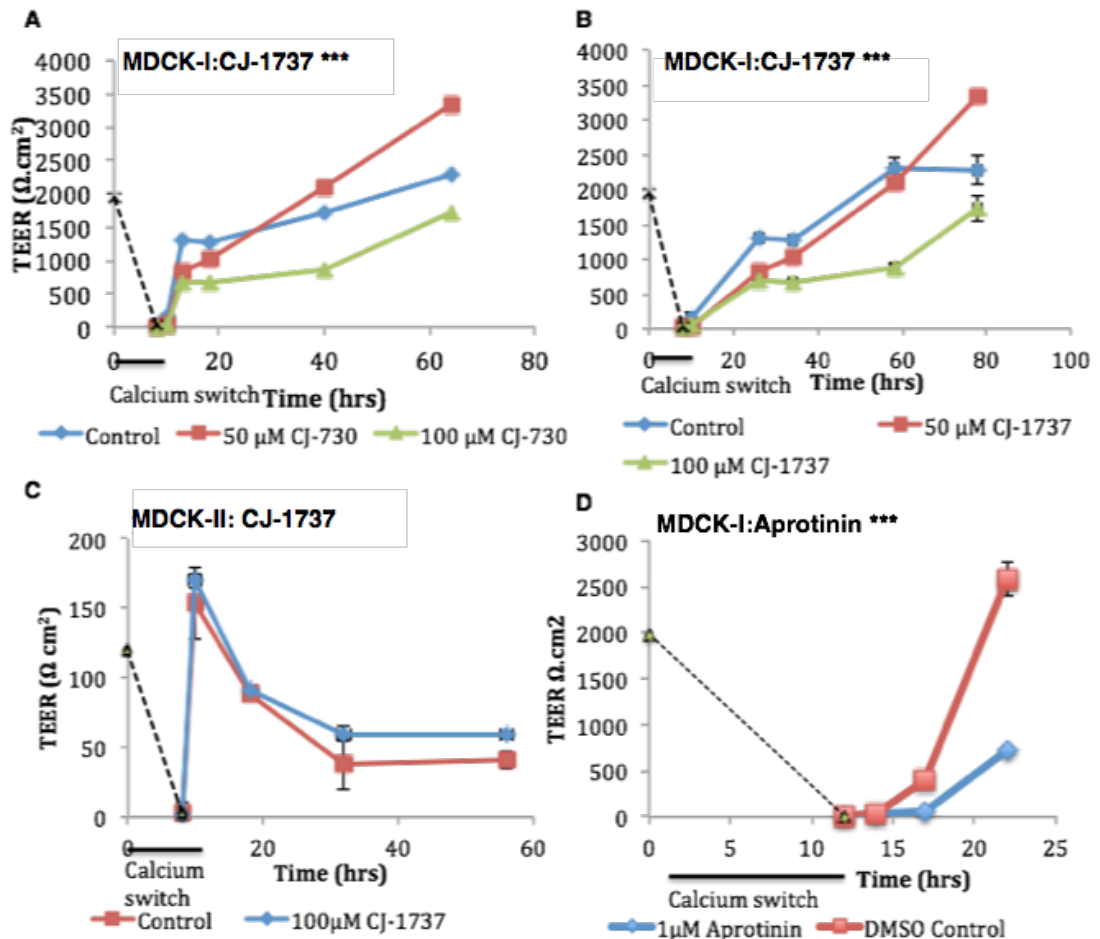


Figure 4.8 Effect of matriptase inhibitors CJ-730 and CJ-1737 and general inhibitor Aprotinin on TEER re-establishment in MDCK-I and MDCK-II monolayer.

A) and B) MDCK-I cells seeded on 6.5 mm Transwell support filters at 5×10^4 , were allowed to develop maximum TEER (day 4) prior to calcium switch. Subsequent to TEER loss, MDCK-I cells were treated with serum free calcium containing medium in the presence of 50 and 100 μM CJ-730 or CJ-1737 or water control. C) MDCK-II cell in a monolayer seeded on 6.5mm Transwell support filters at 5×10^4 , were allowed to develop maximum TEER (day 4) before calcium switch and repletion with 100 μM CJ-1737 or water control. D) MDCK-I cells following TEER establishment were subject to calcium depletion and repletion in the presence of 1 μM Aprotinin or DMSO control. MDCK TEER assays with CJ-730 and CJ-1737 treatment were done on triplicate inserts and multiple biological repeats were for CJ-1737. ***= $P < 0.05$. Aprotinin treatment was applied to duplicate inserts.

IN-1

To examine the effect of the new matriptase inhibitor, IN-1 on MDCK-I and MDCK-II cell monolayer ability to re-establish TEER, different concentrations were applied to each monolayer following calcium switch. Treatment of MDCK-I with 1, 15, 30 and 60 μM showed a dose-dependent response with regard to TEER recovery. Treatment of the highest concentration of 60 μM IN-1, inhibited TEER recovery more effectively than lower concentrations, and this showed double the inhibitory effect relative to half the concentration i.e. treatment of 30 μM (figure 4.9 A). The 50 μM concentration was adopted for further experimentation, proving a significant inhibition in TEER re-establishment in MDCK-I cells.

Furthermore, when we examined the effect of IN-1 on recovery of MDCK-II barrier TEER we found that treatment with different concentrations of IN-1 did not affect the initial rate of TEER recovery. However, it is worth mentioning that often TEER overshoot is observed shortly after calcium repletion and this is prevented here upon treatment with higher concentrations of IN-1, which was not prevented upon treatment with CJ-730 or CJ-1737 (figure 4.9 B and C).

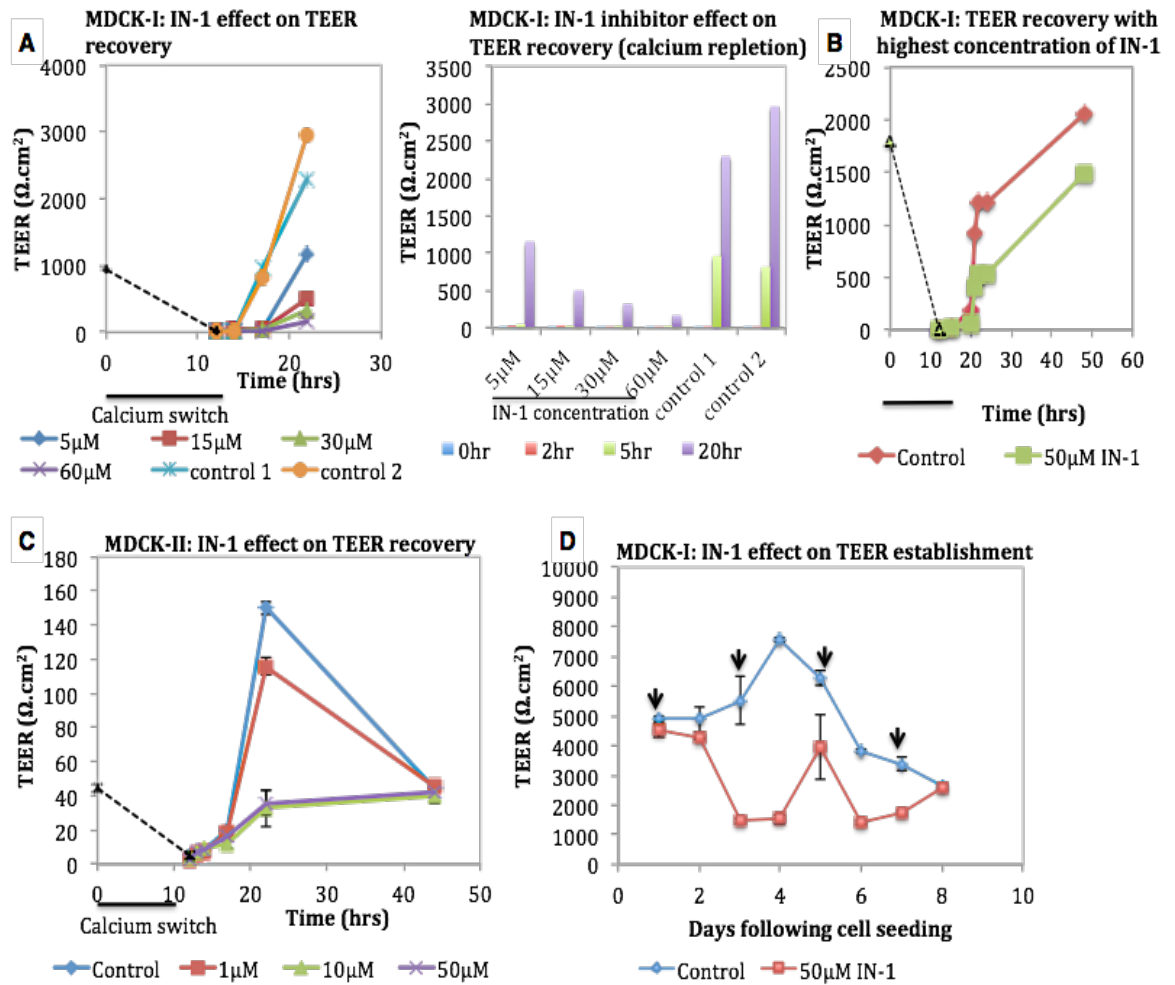


Figure 4.9 Matriptase inhibitor IN-1 effect on TEER re-establishment in MDCK-I and MDCK-II cells.

A) MDCK-I cells seeded on 6.5 mm Transwell support filters at 5×10^4 were allowed to develop until maximum TEER is achieved (day 4). Monolayers are subject to calcium switch and treated with serum free calcium medium containing 5, 15, 30 and $60 \mu\text{M}$ IN-1 inhibitor or water control (control 1 and 2 are with the same treatment). B) Treatment of MDCK- cells with $50 \mu\text{M}$ IN-1 during recovery from calcium switch. C) MDCK-II seeded on 6.5mm Transwell support filters at 5×10^4 cells per insert similar to MDCK-I. Once cell monolayers are well established, a calcium switch was carried and repletion of calcium was done with $1 \mu\text{M}$, $10 \mu\text{M}$, and $50 \mu\text{M}$ IN-1 or water control. Measurement of TEER recovery was taken up to 32 hours following calcium switch. D) MDCK-I cells seeded on to Transwell inserts with $50 \mu\text{M}$ IN-1 and inhibitor was replenished every 2 days (indicated by black arrows) in fresh medium. TEER development was measured every 24 hours up to day 8. Each TEER assay was done in triplicate repeats. ***= $P < 0.05$.

Aprotinin

Once the effect of the specific inhibitors of matriptase on MDCK barrier function was determined, we used the wide-spectrum inhibitor of serine proteases, aprotinin, to elucidate the general role of serine proteases in barrier recovery. Treatment of MDCK-I cells with 1 μ M aprotinin caused a significant delay in TEER recovery of MDCK-I monolayer (Figure 4.8D).

To summarise, all specific inhibitors of matriptase used in this study were effective at reducing TEER recovery in MDCK-I cells, following calcium switch. However, a single assay does not allow for meaningful conclusion over examining the effects of matriptase inhibition on paracellular integrity. TEER alone defines ion and water permeability but does not reflect the overall physiological paracellular integrity, therefore it is important to consider this by conducting size selective tracer diffusion assays.

Due to a limited supply of inhibitor MCoTI-II, further biological assays with matriptase inhibition were conducted using CJ-730, CJ-1737 and IN-1.

4.2.3 Influence of matriptase inhibition on recovery of barrier paracellular integrity and restricted permeability to macromolecules: 4 kDa FITC-dextran flux assay.

MDCK-I and MDCK-II cells express similar tight junctions with the exception of claudin-2, which is highly abundant in MDCK-II cells, as confirmed in Chapter 3 (section 3.2.2.1). As demonstrated in the previous chapter, these have a large disparity in TEER, reflecting differences in permeability to ions but not necessarily larger solutes. To determine whether matriptase inhibition affects the recovery of not just TEER but also physiological paracellular integrity in MDCK cells, we studied effects on the paracellular flux of 4 kDa-FITC-dextran.

During normal recovery at 5, 10 and 32 hours following calcium switch, the diffusion of dextran through from the apical to the basolateral medium of MDCK-I cells is low, signifying a very tight and prompt regain of closure of the paracellular

space. However, a significant increase in the apical to basolateral flux of dextran in MDCK-I cells following 5, 10 and 32 hours of recovery from calcium switch was observed upon treatment with matriptase inhibitor CJ-1737 and at 5 and 10 hours of recovery for IN-1 treated cells (Figure 4.10 A and B). During matriptase inhibition, also a gradual decrease in dextran diffusion with increasing recovery time was shown, despite this being much slower recovery than control. Thus, the functional ability of MDCK-I cells to regain paracellular integrity was delayed, which may be due to altered formation or recovery of paracellular junctions, which are essential for sealing paracellular space and limiting the diffusion of macromolecule between cells in such tight epithelial barrier system.

It is important to note however that, the flux of FITC-dextran across MDCK-II monolayers during barrier recovery was not significantly affected by matriptase inhibition, contrast to that of MDCK-I cells (Figure 4.10 Ci). Here the calculated percentage of dextran diffusion was similar at 5 and 10 hours recovery with and without IN-1 treatment (Figure 4.10 C and Ci).

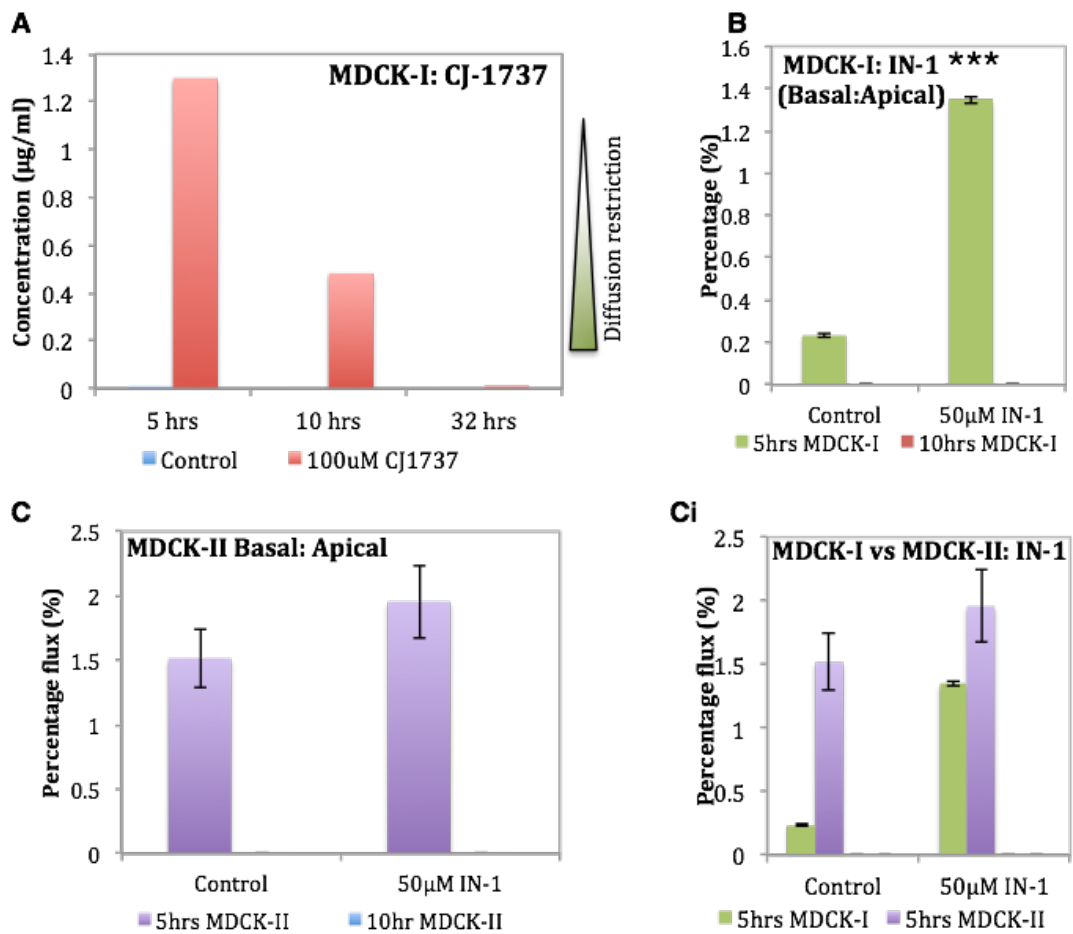


Figure 4.10 Matriptase inhibition effect on recovery of restricted paracellular integrity toward 4kDa FITC-dextran in MDCK-I and MDCK-II cells.

A) Following calcium depletion, MDCK-I cells were incubated with calcium medium and allowed to recover with and without CJ-1737 for 5, 10 and 32 hours. At each time point 50µg/ml FITC dextran applied to medium of the apical chamber of the 6.5mm inserts, for 1 hour at 37°C and 5%CO₂. Medium from the basolateral chamber was collected and absorbance measure at 530nm to determine concentration using a standard curve. B) MDCK-I cells were treated with 50µM IN-1 during calcium repletion, and FITC-dextran was added a 5 and 10 hours. Here absorbance of dextran was measured in both the apical and basolateral medium and relative percentage of diffusion was calculated. C) Relative level of diffusion was measured for MDCK-II monolayers at 5 and 10 hours of recovery from calcium with, with and without IN-1. D) Bar graph comparing both relative diffusion data from MDCK-I and MDCK-II cells. Triplicate repeats (n=3) were established for each experiment (only two repeats for CJ-1737, n=2), and samples are presented with SE. ***= $P < 0.05$.

4.2.4 Matriptase expression in MDCK-I and MDCK-II cells before, during and after calcium switch

Analysis of matriptase mRNA expression was conducted to quantify relative levels of gene expression at different stages of the TEER assay. In MDCK-I cells the expression of matriptase mRNA was not influenced by loss of barrier TEER induced by depletion of extracellular calcium (Figure 4.11A). Also no significant change was observed at 5, 10 and 32 hours of MDCK-I barrier recovery and C_t measurements are within approximately 24.5 ± 0.6 (Figure 4.11 A). Furthermore, analysis of the expression of matriptase in MDCK-II cells, during calcium switch and barrier recovery, does not show any regular change and no drastic shift within each C_t value ($C_t \sim 25.9 \pm 0.4$) are observed (Figure 4.11 B).

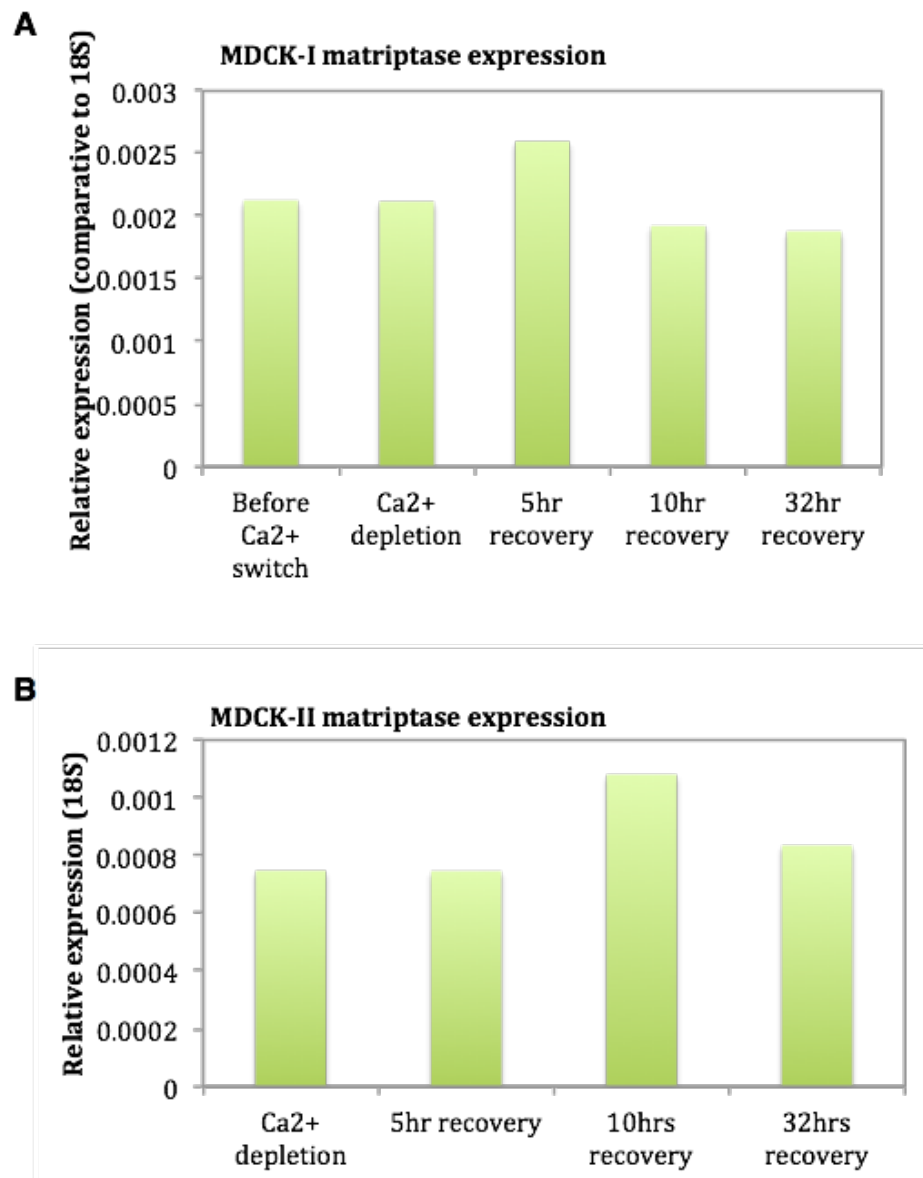


Figure 4.11 Matriptase expression in MDCK-I cells before and after calcium switch.

A) Matriptase gene (ST14) expression was quantified with qRT-PCR in MDCK-I monolayer after 4 days of establishment on Transwell filters (before calcium switch), during calcium depletion and at 5, 10 and 32 hours of recovery in regular calcium medium in the absence of serum. B) Matriptase gene expression was measured in MDCK-II monolayer during calcium depletion, and at 5, 10 and 32hours of recovery in regular calcium medium in the absence of serum. For MDCK-I and MDCK-II qRT-PCR of st14 mRNA expression analysis was conducted on duplicate samples for each condition (n=2).

4.2.5 Effect of matriptase inhibition on the expression of the major components of tight junctions and adhesion junctions in recovering MDCK-I cells monolayers

During barrier recovery the tight junctions and the adhesion junctions rapidly reconstitute at the cell membrane and form the cell-cell junctions. In MDCK-I and MDCK-II cells calcium-depletion causes the disassociation between these junctions and loss of barrier integrity, polarity and TEER. It was shown in the previous chapter that MDCK-I cells express various tight junction and adhesion junction proteins, but lacked endogenous expression of claudin-2, which is exclusively responsible for the TEER difference compared to MDCK-II cells.

From our barrier permeability assays I discovered that matriptase inhibition affects the recovery of MDCK-I cells that do not express claudin-2. However, this is not consistent with the findings with CaCo-2 cells, which showed that matriptase inhibition or suppression reduced barrier TEER through increased claudin-2 expression (Buzza et al., 2010). Therefore, to investigate whether matriptase inhibition in MDCK-I cells and delay in barrier recovery is due to claudin-2, we investigated whether its expression is switched on. At different times of recovery, with and without matriptase inhibitors CJ-1737 and IN-1, we did not observed an up regulation in claudin-2, and expression remains suppressed in those cells (Figure 4.12 A and B). This suggested that the matriptase mediated barrier restitution process is likely independent of claudin-2 in MDCK-I cells. However, because matriptase only affect MDCK-I and not MDCK-II cells, which express high levels of claudin-2, we aimed to investigate the importance of claudin-2 further by analysing the effect of matriptase inhibition on MDCK-I cells in the presence of this protein.

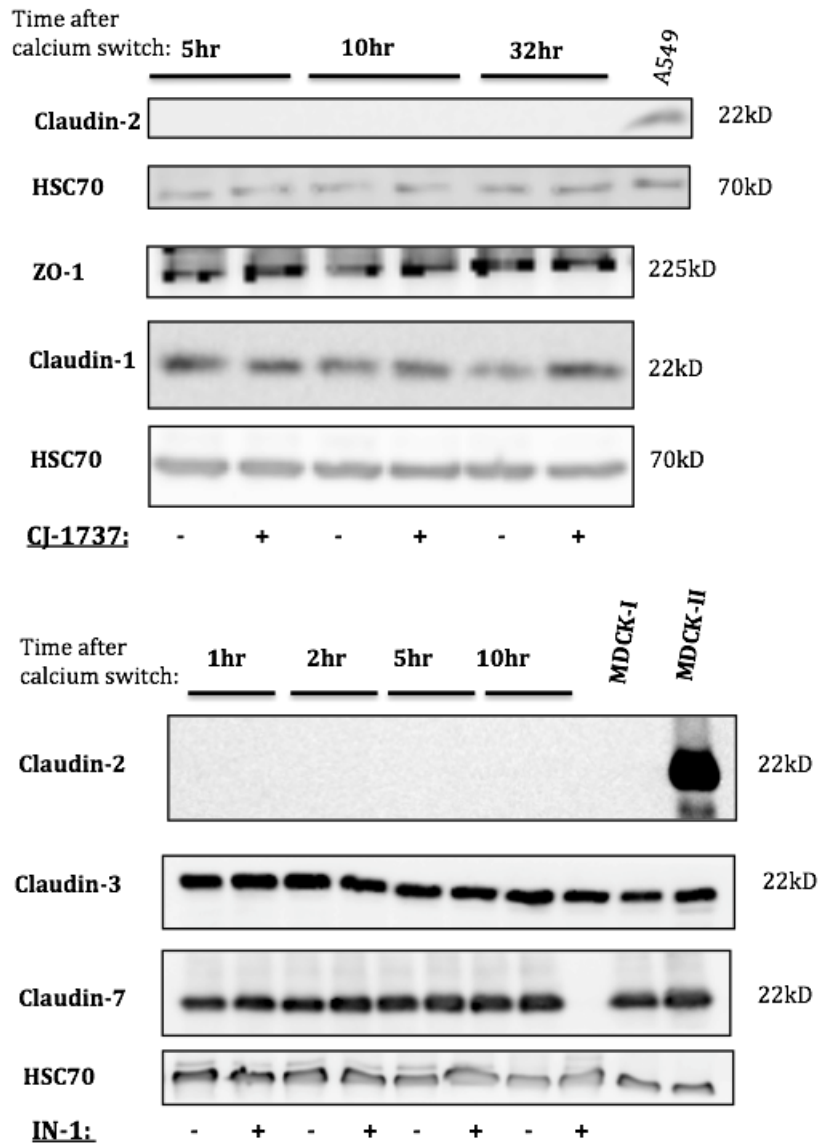


Figure 4.12 Tight junctions protein expression in MDCK-I monolayers, following calcium switch and during matriptase inhibition.

A) Immunoblot analysis of tight junction proteins present in total cell lysates of MDCK-I cells following 5, 10 and 32 hours of calcium repletion. Shown are lysates either from cell treated with 100 μ M matriptase inhibitor CJ-1737 (+) or no inhibitor (-). Immunoblot analysis of claudin-1, claudin-2 and ZO-1 during monolayer recovery, with HSC70 used to determine protein loading. A549 lung adenocarcinoma cells were used as a positive control for detection of claudin-2. B) Immunoblot analysis of claudin-2, claudin-3 and claudin-7 during MDCK-I recovery from calcium switch. Shown are lysates from 1, 2, 5 and 10 hour periods of recovery by calcium repletion with or without 50 μ M matriptase inhibitor IN-1.

4.2.6 Role of claudin-2 in the matriptase-dependent regulation of MDCK-I barrier integrity

To determine whether claudin-2 does or does not play a role in the matriptase dependent regulation of the MDCK-I barrier recovery, we studied matriptase inhibition on TEER recovery of MDCK-I model, with inducible claudin-2 expression, generated by Professor Alan Yu at the University of Kansas Medical Center (Yu *et al*, 2009). In the absence of tetracycline these cells express claudin-2 and develop significantly lower TEER compared to MDCK-I cells in the absence of claudin-2 (Figure 4.13 A and B). In the claudin-2 expressing MDCK-I cells the low TEER corresponds to that of MDCK-II monolayers (Figure 4.13 A and B). This finding is consistent with data from multiple studies, whereby claudin-2 overexpression in MDCK-I cells is shown to reduce TEER, and knockdown in MDCK-II cells has the adverse effect (Yu *et al*, 2009).

For this study MDCK-I-cld2 cells were seeded onto inserts with or without doxycycline. Once TEER was fully established, a calcium-switch was performed and recovery of TEER in the presence and absence of matriptase inhibitors CJ-1737 or IN-1 was studied. Both inhibitors were found to significantly reduce TEER recovery in both high TEER MDCK-I cells not expressing claudin-2 and low TEER MDCK-I cells expressing claudin-2 (Figure 4.12 C and D). Therefore suggesting that the effect of matriptase inhibition on barrier recovery is mediated through a mechanism that is independent of claudin-2, but only instrumental in MDCK-I cells.

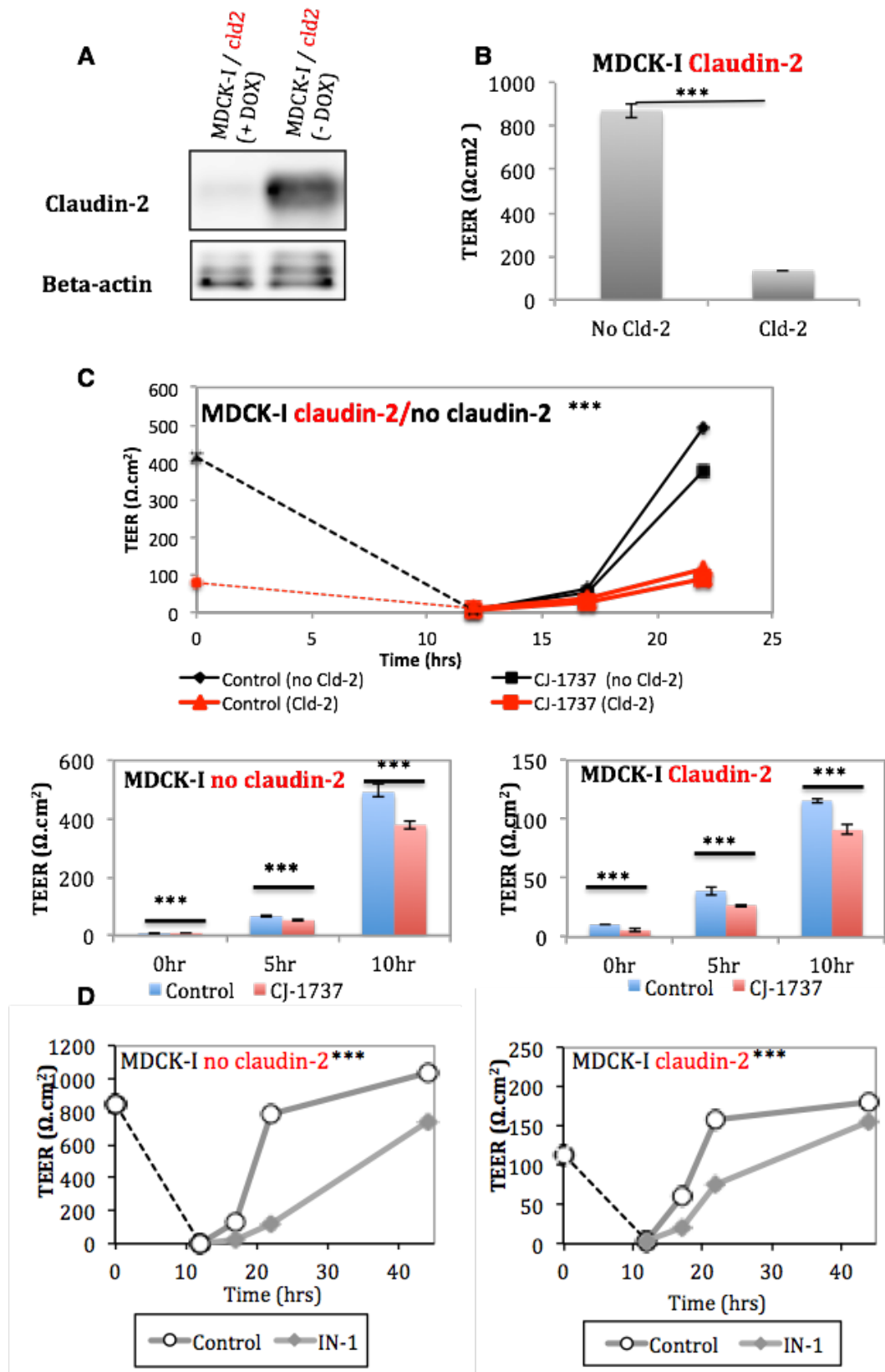


(figure legend on next page)

Figure 4.13 Effect of matriptase inhibition on claudin-2 expressing MDCK-I cells.

A) Immunoblot analysis of inducible claudin-2 protein expression in Tet-off MDCK-I cells. MDCK-I-claudin-2 Tet-off cells were seeded onto 10 cm petri dishes in with 10% tetracycline-free FCS in MEM. Doxycycline was added to cells to keep claudin-2 suppression (+Dox) or cells were grown without treatment (-Dox) to induce exogenous expression of claudin-2. β -actin was used to determine equal protein loading. B) Graph represents maximum TEER established by MDCK-I-claudin-2 Tet-off cells in the presence or absence of Dox. Cells were seeded at 5×10^4 onto 6.5 mm Transwell inserts and TEER was measured every 24 hours with constant replenishment of Dox treatment accordingly. C) TEER calcium switch assays were carried on MDCK-I cells in the absence (black line) or abundance (red line) of claudin-2. Cells were subject to calcium repletion with and without treatment of 100 μ M matriptase inhibitor CJ-1737, and TEER measurements were taken at 5 and 10 hours post treatment. TEER measurements at 0, 5 and 10 hours of recovery are also displayed in bar graphs. D) Similarly, TEER recovery assays, but with 50 μ M IN-1 inhibitor, were carried on MDCK-I cells in the absence or abundance of claudin-2. TEER measurements were taken at 5, 10 and 32 hours post treatment. TEER assays were conducted in triplicates for each condition. Each data point is presented with \pm SEM. ***. = $P < 0.05$

4.2.7 Effect of matriptase inhibition on tight junction and adhesion junction protein expression

To investigate whether matriptase function is dependent on the regulation of other junction proteins, we also analysed the expression of various components known to contribute to epithelial barrier integrity. Analysis of the expression of E-cadherin, β -catenin, ZO-1, and claudins 1, 3 and 7 showed no change between 5, 10 and 32 hours of recovery with and without matriptase inhibition (Figure 4.12 and Figure 4.14). The expression data suggested that matriptase's role in barrier restitution is not mediated through the expression of these components per se. However, during barrier recovery these proteins quickly reconstitute at the cell surface to ensure paracellular closure and although their expression is important in barrier development, dynamic localisation is also key and must be studied during matriptase inhibition.

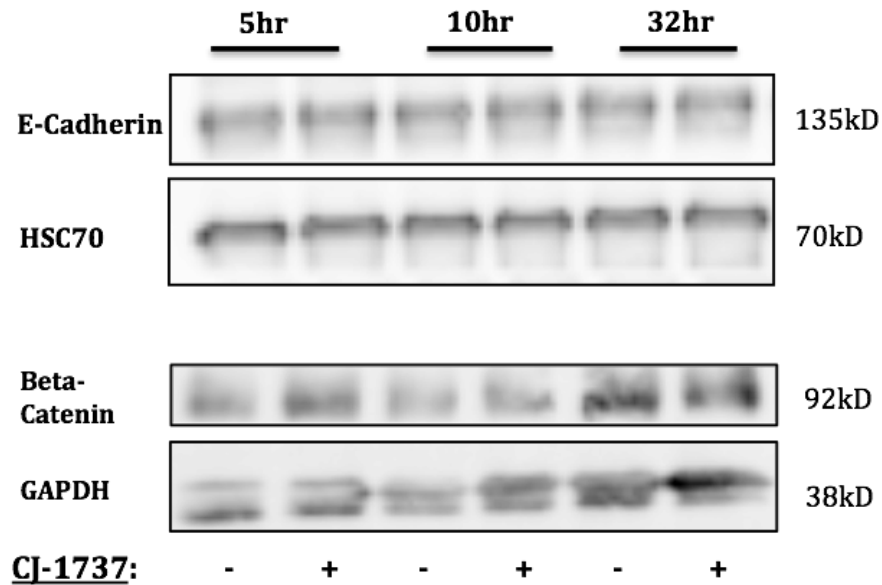


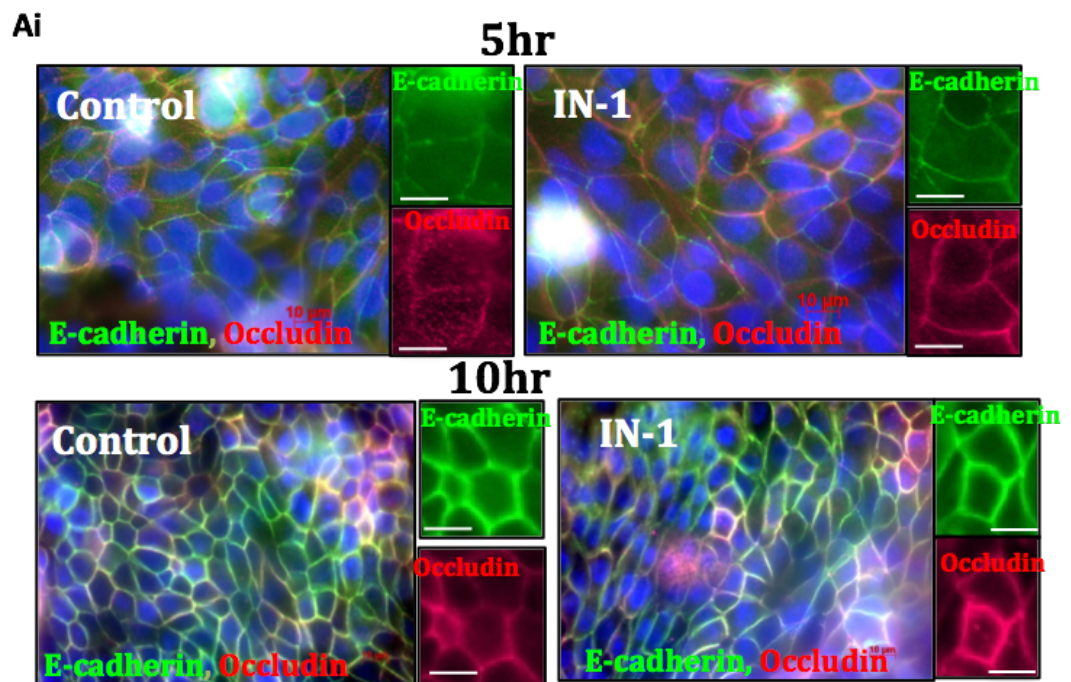
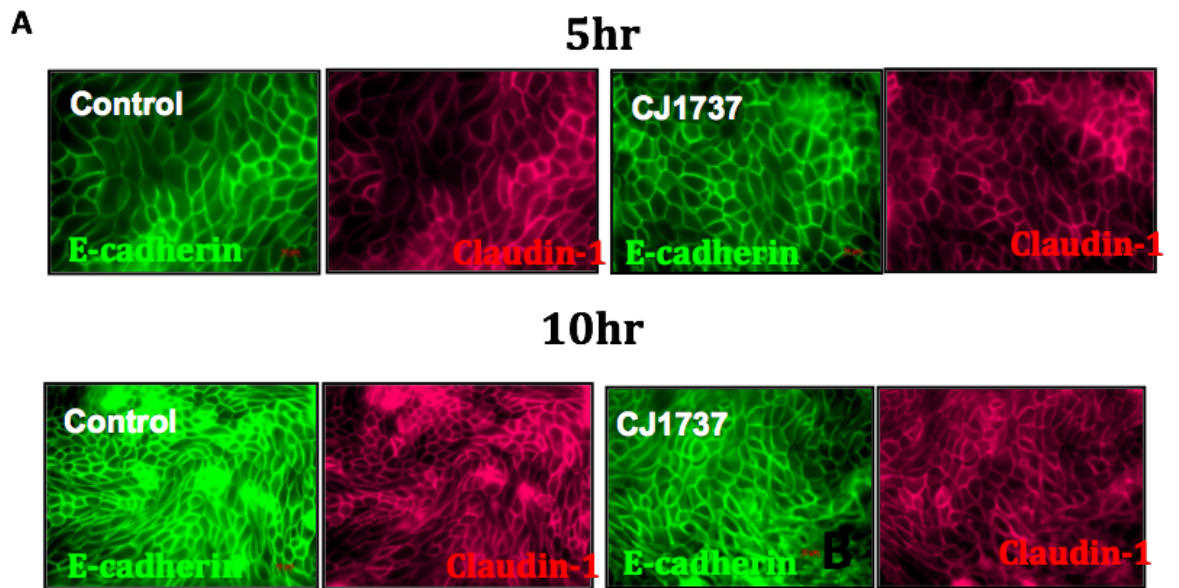
Figure 4.14 Effect of matriptase inhibition on adhesion junction protein expression in MDCK-I monolayers, during recovery from calcium switch.

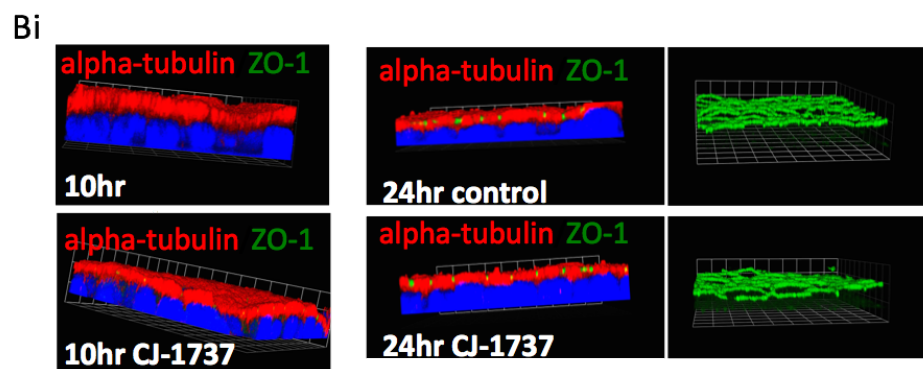
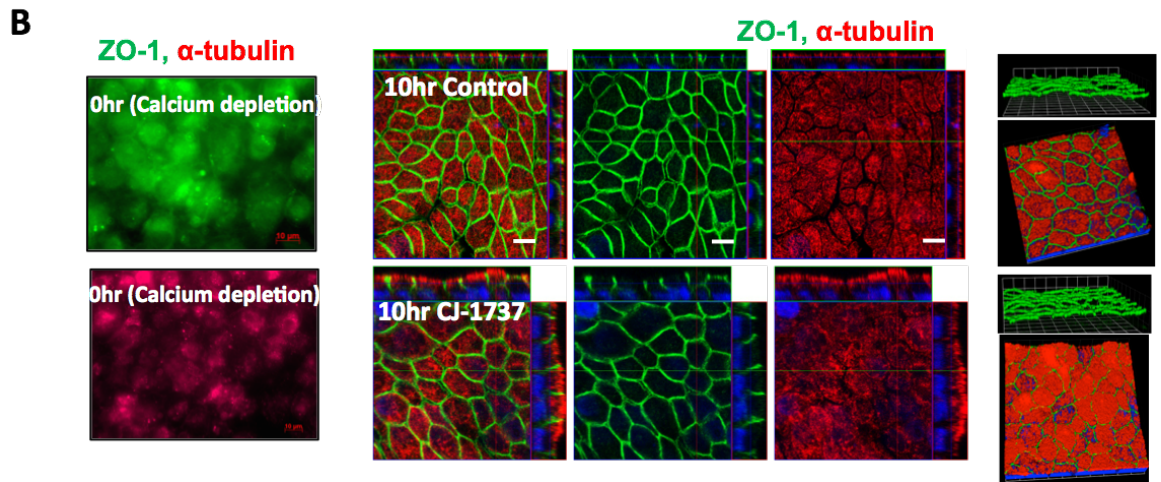
Immunoblot analysis of adhesion junction proteins present in total cell lysates of MDCK-I cells following 5, 10 and 32 hours of calcium repletion. Shown are lysates either from cells treated with 100 μ M matriptase inhibitor CJ-1737 (+) or no inhibitor (-). Immunoblot analysis of E-cadherin and β -Catenin during monolayer recovery with HSC70 and GAPDH was used to determine protein loading.

4.2.8 Effect of matriptase inhibition on the re-establishment of intracellular junctions in MDCK-I cells

Polarised MDCK-I epithelial monolayer with maximum TEER, display a well-defined apical-basolateral organization that is demarcated by the apical localisation of the tight junctions and the formation of an apical-basolateral microtubule system (see Chapter 3, Figure 3.7). During calcium depletion the establishment and organization of these structure is rapidly lost, but quickly recovered after restitution of calcium. To determine whether these structures are affected by matriptase inhibition during barrier recovery, an immunofluorescence approach was used to observe the reassembly of various components of the tight junction, adhesion junction and the cytoskeleton.

Labeling of tight junction proteins, ZO-1, claudin-1, and occludin showed high intensity strands and peripheral localisation from 5 hours of barrier recovery and this was not altered during matriptase inhibition with either CJ-1737 or IN-1 (Figure 4.15A and B). Furthermore analysis of microtubule structure during recovery in MDCK-I cells revealed similar intensity and structural reestablishment and the development of an apical-basolateral microtubule array was not delayed during treatment with matriptase inhibitor CJ-1737 (Figure 3.15B and Bi).





FITC-Phalloidin

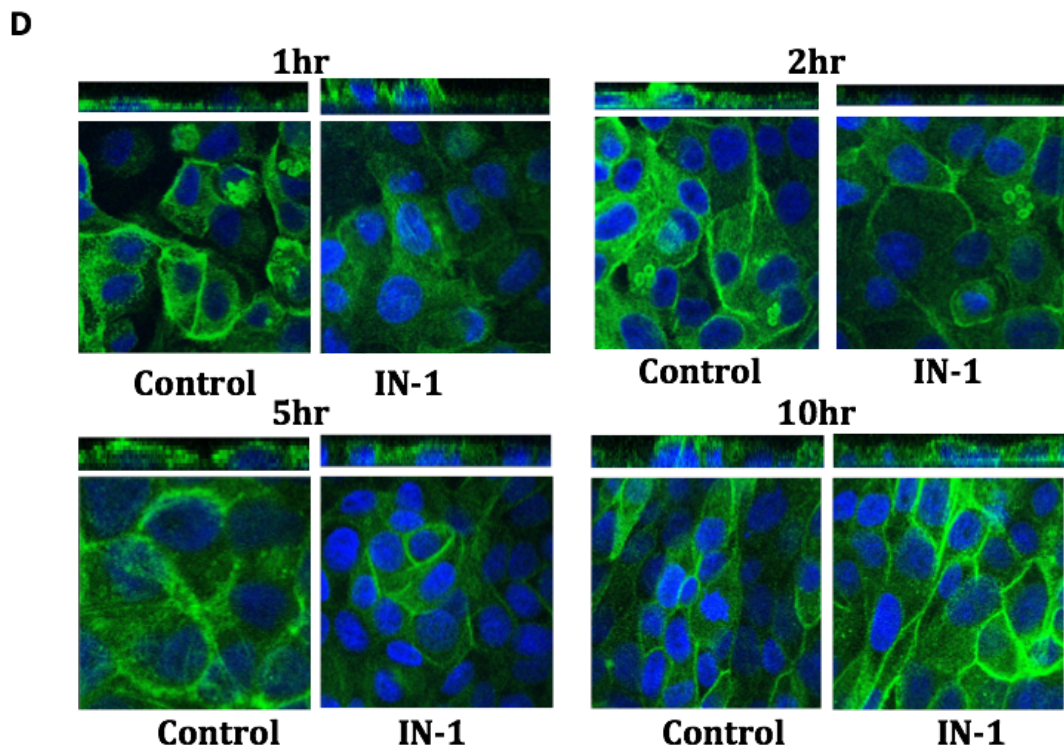


(Figure legend on the next page)

Figure 4.15 Immunofluorescence analysis of paracellular junctions and cytoskeletal structures in MDCK-I cells during TEER recovery assay.

A) Upright images showing MDCK-I cells labelled for E-cadherin (Alexa-488- green) and claudin (Alex-647- far red) one, after 5 and 10 hours of recovery from calcium switch with and without matriptase inhibitors CJ-1737. Ai) MDCK-I cells labelled for E-cadherin (Alexa-488- green) and Occludin (Alex-647- far red) after 5 and 10 hours of recovery with and without the matriptase inhibitor, IN-1. B) Confocal images showing microtubule (red) and ZO-1 (green) structure and polarisation in MDCK-I after calcium depletion (0hr) and after 10 hours of barrier recovery with and without treatment with CJ-1737. Bi) 3D confocal images showing ZO-1 and microtubule structures and polarization in control and treated MDCK-I cells, following 10 and 24 hours of barrier recovery from calcium switch. C) Confocal images of actin shown via staining with Phalloidin-488 (1:2000) at 1, 2, 5 and 10 hours of MDCK-I TEER recovery. Images captured with x63 objective. A) Represents triplicate separate experiment, while B) and C) are taken from a single experiment with triplicate sample repeats from each time point. Scale bar =10µm.

**4.2.9 Specific depletion of matriptase by siRNA in MDCK cells:
Effect on barrier formation and TEER re-establishment in
MDCK-I cells.**

As previously shown, under treatment with various matriptase inhibitors, MDCK-I monolayers show loss of ability to recover full barrier integrity following disruption by calcium depletion. As these inhibitors were effective at much higher concentrations than those used to determine K_i , the alternative genetic approach of RNA interference was adopted to further validate the inhibitor effect. Initially we developed a custom siRNA targeting the dog st14 gene, which was designed with the potential of developing a stable (possibly inducible) system for matriptase knockdown in MDCK cells, to study the effect of transient knockdown on MDCK-I barrier recovery.

4.2.9.1 Transient knockdown affect on TEER in MDCK-I cells

In chapter 3, we illustrated an efficient knockdown (>95%) of matriptase by transient transfection with the siRNA sequence into MDCK-I cells. To investigate the effect of matriptase knockdown on TEER establishment and re-establishment, MDCK-I cells were initially double transfected with st14 1 siRNA, NTC and transfection reagent without siRNA and seeded at high density (1×10^5) on small culture inserts. Cells transfected with NTC sequence, no siRNA or with the targeting sequence displayed similar development in TEER and showed no differences in TEER recovery (Figure 4.16 A). Surprisingly, MDCK-I cells transfected with scrambled NTC showed a delay in the recovery of TEER compared to ST14 1 and control (Figure 4.16A)

To investigate whether the knockdown by st14 1 siRNA was maintained during the TEER assay, the RNA was harvested and pooled from the monolayer MDCK-I cells at the end of the TEER assay and qRT-PCR for analysis of matriptase expression showed similar expression relative to NTC, but higher expression in no siRNA control (Figure 4.16 B)

As matriptase knockdown before the seeding of MDCK-I cells onto inserts failed to show an effect on TEER, as the knockdown was likely not maintained for the period of the assay, an attempt was made to investigate ability to knockdown matriptase in established MDCK-I monolayers growing on culture inserts prior to calcium switch. The high TEER MDCK-I monolayers were treated either twice for 48 hours or three times for 72 hours with targeting st14 siRNA, scrambled NTC or transfection reagent alone before investigating the effect on TEER recovery following calcium switch. The data obtained showed that the targeting siRNA not only had no effect on maximum TEER of the established monolayer but also TEER recovery was not affected (Figure 4.16 B and C). However following the TEER assay (triple transfections), qRT-PCR for matriptase mRNA after 72 hours revealed no knockdown in mRNA expression relative to NTC and no siRNA control (Figure 4.16C)

Due to the lack of effectiveness of the siRNA approach, stable cell line expressing targeting and non-targeting shRNA for matriptase transcript knockdown was developed.

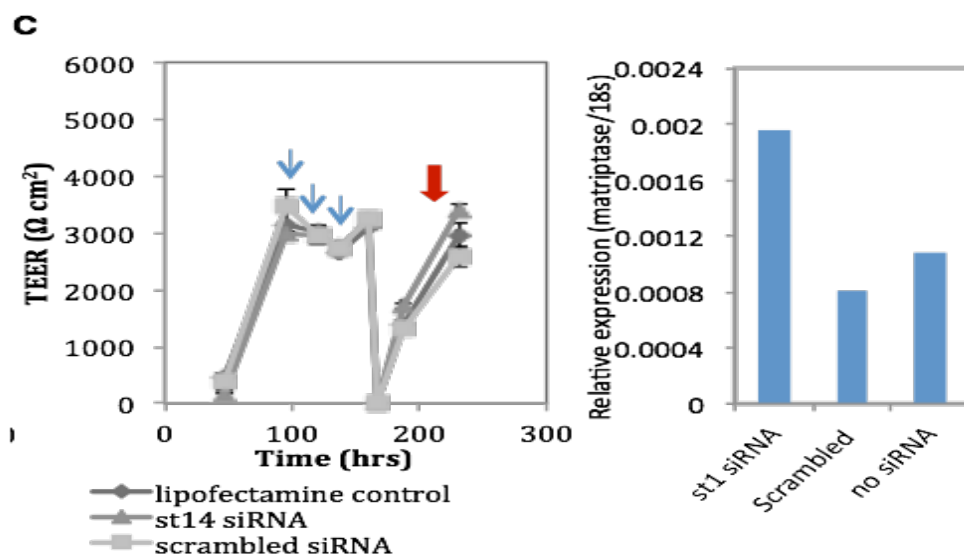
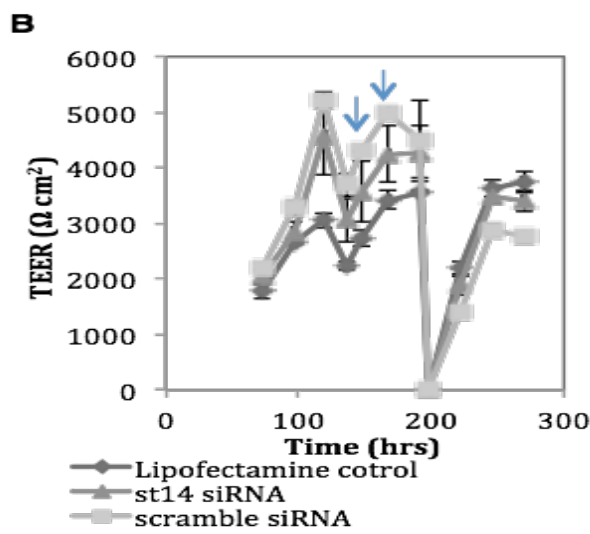
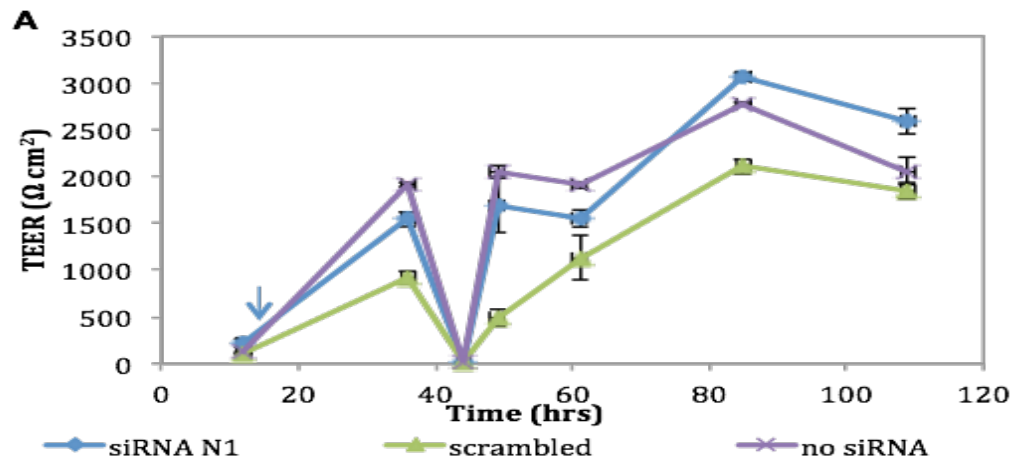


(Figure legend on the next page)

Figure 4.16 Effect of transient knockdown of matriptase in MDCK-I epithelial monolayers during TEER development and reestablishment.

A) MDCK-I cells were double transfected with 50 nM st14 siRNA, scrambled NTC or just treated with transfection reagent, lipofectamine alone (no siRNA control), prior to seeding on 6.5mm inserts at a density of 1×10^5 . After 2 days from seeding, a calcium switch was conducted and TEER recovery measured. B) TEER established MDCK-I monolayers were transfected twice with 50nM st14 target siRNA, scrambled NTC siRNA or Lipofectamine alone (i.e. no siRNA), 2 days before a calcium switch was applied. TEER recovery was measured up to 72 hours. C) Established MDCK-I monolayers cells transfected three times with 50nM matriptase targeting siRNA, scrambled NTC siRNA or Lipofectamine alone (i.e. no siRNA), 3 days before a calcium switch was applied. TEER recovery was measured up to 72 hours. Ci) RNA was collected after TEER recovery and matriptase mRNA level was analysed via qRT-PCR, carried on pooled RNA from 3 insert. TEER data presented as mean \pm SEM from triplicate inserts for each condition.

4.2.9.2 Effect of matriptase stable knockdown on the establishment and re-establishment of MDCK-I barrier integrity

TEER assays were carried on MDCK-I cells stably expressing matriptase-targeting shRNA st1 and st3 along with the non-targeting control cells to investigate the effect of matriptase down-regulation on TEER, before and after calcium switch. MDCK-I cells expressing the st1 shRNA targeting sequence, which showed matriptase knockdown developed lower TEER on days 3 and 4 following seeding onto inserts (Figure 4.17 A). These cells also had slower recovery as compared NTC stable cells (Figure 4.17 B). MDCK-I st1 cells also showed slower recovery of TEER at 5 and 10 hours following calcium repletion, however by 32 hours the TEER value was not significantly lower than NTC expressing cells and regular control cells (Figure 4.17, B and C), possibly due to the low knockdown efficiency of approximately 44% as demonstrated in chapter 3 section 3.2.6.2. It is important to also highlight that, as expected, st3 expressing MDCK-I cells, which show no matriptase knockdown (see chapter 3), showed no difference relative to NTC.

Although the knockdown was relatively inefficient compared to the inhibition of catalytic activity that can be achieved, this still showed a consistent delay on TEER reestablishment in st1 stable MDCK-I cells.

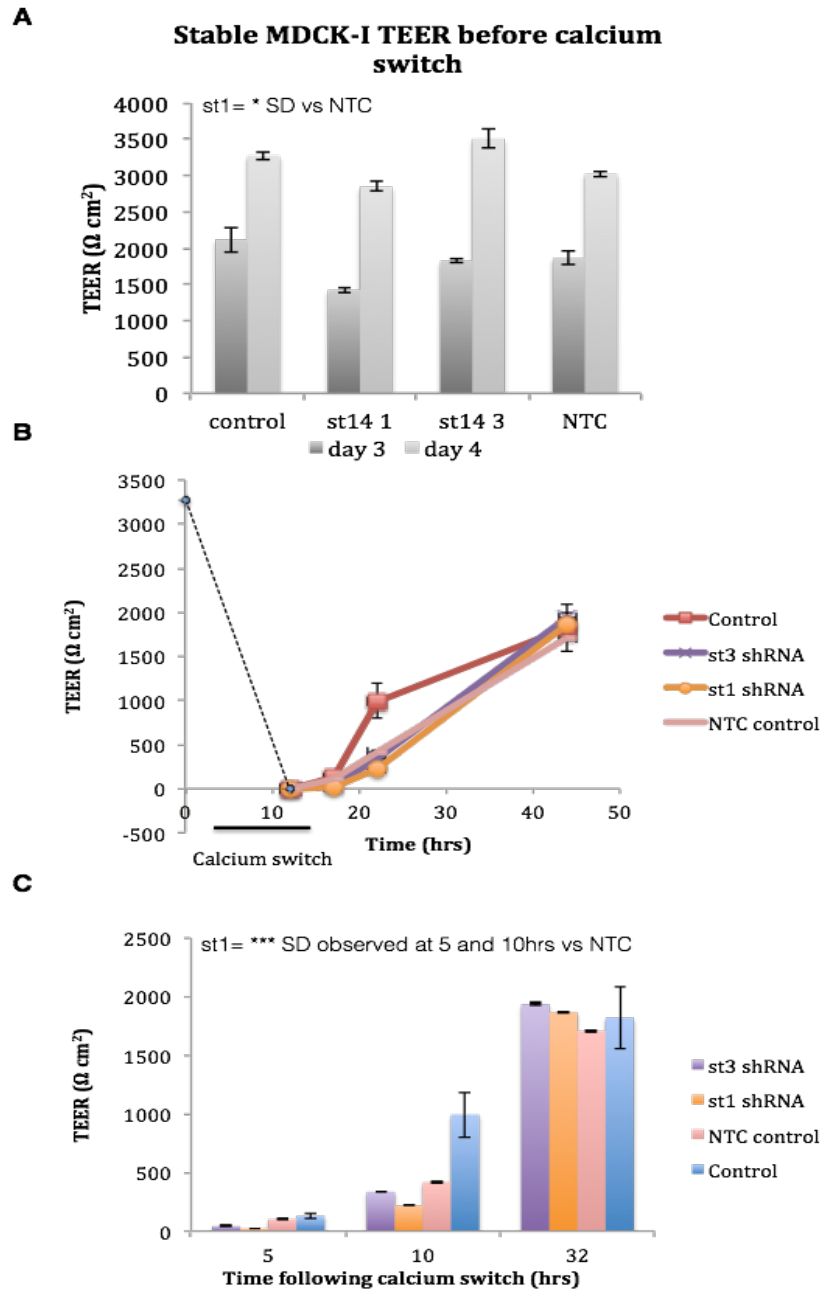


Figure 4.17 Effect of stable knockdown of endogenous matriptase expression on MDCK-I TEER recovery.

A) MDCK-I stably expressing the st1, at3 and NTC shRNA sequences were seeded onto Transwell inserts at 5×10^4 and TEER measured up to 4 days. TEER measurements are presented at day 3 and 4 of barrier after seeding. B) MDCK-I cells were subject to calcium switch at day 4 and repletion was conducted after 12 hours with serum free calcium high MEM. B and C) TEER measurements were taken 5, 10 and 32 hours post calcium switch. TEER data presents as mean \pm SEM from triplicate inserts for each condition. ***= $P < 0.05$.

4.3 Discussion

The main aim of this chapter was to determine the role matriptase plays in epithelial barrier function in two strains of MDCK cells, MDCK-I and MDCK-II, which had/displayed different paracellular diffusion properties. We initially showed that matriptase activity is important in both cell lines, where it functions as a potent surface activator of pro-HGF and induced cell motility. Therefore various peptide inhibitors of matriptase were used to study whether matriptase activity in these cells is essential for maintaining barrier function and integrity. TEER and dextran flux assays for analyses of paracellular permeability showed that the restitution of MDCK-I barrier integrity, following disruption by calcium depletion, is significantly delayed during matriptase inhibition. However, matriptase activity is not essential in MDCK-II barrier recovery. This effect on MDCK-I was later confirmed with knockdown, once stable MDCK-I cells expressing matriptase-targeting shRNA were generated. Initially the aim was to generate an inducible system, to be able to maintain normal expression of matriptase and induce shRNA knockdown at desired time points, during the TEER assay. However, as insert failed to clone into the desired vector this method was ended and instead a stable pLKO.1 Mission system was designed (see Appendix 2 for detail on the initial attempted development of inducible system).

The role of claudin-2 in the matriptase-mediated effect on MDCK-I barrier integrity but not MDCK-II

MDCK-I cells are different to MDCK-II cells in their barrier paracellular properties as they form much tighter epithelial barrier systems. This has been shown to be due to the absence of claudin-2, a leaky tight junction protein, which was found overexpressed in the intestinal epithelium of matriptase hypomorphic mice and in Caco-2 cells during matriptase knockdown, resulting in raised barrier permeability and loss of TEER (buzza et al, 2010).

In general, and as previously highlighted tight junctions are essential for determining the paracellular properties of epithelial cells and hence investigations

were carried to determine whether matriptase was necessary for tight junction/barrier formation in MDCK-I cells. Initially experiments conducted to establish whether the expression of claudin-2 or even the phosphorylation of its regulator kinase, PKC ζ , are altered during MDCK-I barrier recovery, and found no upregulation in claudin-2 expression or change in PKC ζ phosphorylation during matriptase inhibition at different recovery time-points. However, because matriptase activity only affected MDCK-I barrier ability to reestablish and not the claudin-2 expressing MDCK-II, a TEER recovery study on MDCK-I cells which expressed claudin-2 exogenously, in an inducible fashion was conducted. This was done to show whether this effect was either dependent or independent of the preexistence of claudin-2 and if this effect ultimately is MDCK-I specific. Here, the inhibition of matriptase in claudin-2 expressing MDCK-I cells still altered barrier recovery supporting an independent mechanism. However this does not rule out that matriptase still affects barrier integrity through other junction proteins.

Effect of matriptase inhibition on paracellular junction molecules

It is important to also note that the MDCK-II data, showed that matriptase certainly was not “essential” for their integrity and TEER, and the same has been surprisingly discovered in humans who had a loss of function mutation in matriptase, which only developed a skin barrier defect (Desilets et al., 2008, List et al., 2007a). However, matriptase activity is linked to various epithelial substrates, some of which have been previously shown to regulate various aspects of cellular junctions including protein expression. Distinct to claudin-2, most of the tight junction proteins have sealing functions such as claudins 1, 3, and 7 and occludin, which are abundant in most epithelia (Gunzel and Yu, 2013). Recently Szabo *et al* showed that combined matriptase and substrate PAR-2 function is essential for the establishment of the placental barrier function associated with claudin-1 expression (Szabo et al., 2014). Other substrates such as HGF/c-met, have also been shown to regulate expression of both tight junction and adhesion proteins in epithelia (Nusrat et al., 1994). Often effects on tight junction proteins can be indirect, for example proteins can be altered by inflammation subsequent to epithelial injury, as predicted for claudin-2 during loss of matriptase in *in vivo*

study and colitis model (Netzel-Arnett et al., 2012). Therefore when analysing tight junctions in MDCK-I cells, it was found that the changes in paracellular permeability of MDCK-I cells by matriptase inhibition were not cofounded by changes in the levels of either sealing tight junction proteins (ZO-1, occludin, claudin-1, 3, and 7) or adhesion proteins (E-cadherin, β -catenin). However we cannot exclude the possibility that the expression of other unexamined molecules could be affected, as sometimes barrier defects can be associated with a selective deficiency in the expression of the tight junction molecules.

It is well established that the modulation of expression as well as intracellular localisation of tight junction molecules results in key changes in tight junction barriers. Aberrant localisation of tight junction and adhesion junction proteins often is linked with polarity defects in epithelial cells, which are profoundly abundant in cancer and promote cell invasion (see review: (Martin and Jiang, 2009)). In matriptase conditional knockout mice the loss of matriptase function was associated with severe epithelial demise due to the focal loss of occludin, ZO-1 and claudin-1 while E-cadherin remains unaltered (List et al., 2009). During restoration of MDCK-I cell barrier integrity the reconstruction of junction proteins is very prompt, and despite the delay in TEER recovery caused by matriptase inhibition immunofluorescence, data showed this was not due to altered localisation of occludin, ZO-1 and claudin-1. These proteins, similar to E-cadherin, showed normal redistribution at the intracellular space shortly after calcium repletion and at later recovery time points during matriptase inhibition. Overall, from the observed unaltered expression and peripheral localisation of junction proteins during matriptase inhibition, it can be concluded that delayed MDCK-I barrier recovery through matriptase inhibition is not associated with incorrect construction and abundance of barrier sealing tight junction molecules and adhesion junctions.

Effect of matriptase inhibition on the reorganization of the cytoskeletal proteins

The experimental analysis of the structure of the MDCK-I barrier, via the cytoskeleton, illustrated that the inhibition of matriptase does not alter the ability

of these microtubules to repolarize during MDCK-I epithelial barrier repair. Here, similar apical-basolateral polarization of the microtubules and therefore association with the lateral junction proteins was observed during and without matriptase inhibition in MDCK-I cells, therefore proposing no obvious alterations to the cytoskeletal polarisation and therefore probably illustrating the effect of matriptase inhibition of barrier recovery is not due to direct disruption to cellular polarity. Meanwhile, although it was difficult to achieve complete and well-defined staining of actin during the recovery assay, but nevertheless fluorescence also revealed no difference in terms of intensity and organization of actin, between matriptase inhibitor and control samples, at early and different hours of monolayer recovery. The polarization and proper structuring of microtubules and actin cytoskeletal filaments is essential for providing mechanical barrier strength. Microtubules dynamics have an important role in regulating the concentration of the adhesion junctions' proteins such as E-cadherin at cell-cell contact sites, which also showed normal assembly even during matriptase inhibition.

Contrary to the previous findings in the conditional knockout and hypomorphic mice that highlighted matriptase's role in the establishment of the simple intestinal epithelial barrier, this study strongly argues a primary role of matriptase in the restoration of barrier integrity rather than development, in MDCK-I model cell line. This role was strongly accentuated by four specific inhibitors of matriptase and through the development of a stable system for specific knockdown of matriptase in MDCK-I cells.

Surprisingly, inhibition of matriptase activity in MDCK-II cells, although essential for pro-HGF activated signalling and induction of cell scatter, did not alter barrier integrity and ability to re-establish following calcium switch. The role of matriptase in regulating barrier integrity therefore is only relevant in MDCK-I cells and is not dependent on the difference in intrinsic expression of claudin-2 unlike previous findings in Caco-2 cells (Antalis et al 2013, Buzza et al., 2010). Here, MDCK-I expressing claudin-2 exogenously still displayed a significant delay in barrier recovery and claudin-2 expression during barrier recovery remained suppressed with matriptase inhibition.

Furthermore, we found the effect of matriptase inhibition was not cofounded by changes in sealing tight junction proteins (ZO-1, occludin, claudin-1, 3, and 7), adhesion proteins (E-cadherin, β -catenin) or cellular cytoskeletal network. According to the matriptase hypomorphic mice with a leaky intestinal epithelial the unaltered expression in some of these proteins such as claudin-1, 3, 4 and ZO-1 correlated with the no-change found in MDCK-I (Buzza et al., 2010).

Therefore matriptase is likely maintaining barrier function through a tight junction and adhesion junction independent mechanism. Cell surface proteolysis by matriptase is part of a large signaling cascade involving a number of epithelial surface linked substrates, with key published implication in epithelial tissue maintenance and function.

4.4 Conclusion

In summary, this chapter discussed a role for matriptase expression and activity in the regulation of epithelial barrier integrity in MDCK-I cells. Interestingly, matriptase was found to play a prominent role not in the development of these MDCK-I barrier but monolayer ability to regain function and integrity following disruption, as shown, by calcium depletion. This effect was not perceived by MDCK-II cells, and was not dependent on claudin-2, which is differentially expressed between these cells and serves as the major determinant of the difference in their permeability. The matriptase-induced delay in MDCK-I barrier restoration of TEER as well as physiological integrity, was not due to altered expression or localisation of sealing tight and adhesion proteins, therefore suggesting a specific change that is represented by alteration in a single pathway which can affect barrier permeability but not cause an overall detrimental effect on physiology of MDCK-I barrier epithelia.

Chapter 5. Investigation into the mechanism of matriptase in epithelial barrier function and restitution in MDCK cells using a candidate substrate approach

5.1 Introduction

As matriptase is one of the best characterised TTSPs, several protein substrates have been identified, most through substrate preference studies, after analysis of preferred peptide substrate cleavage sequence (Chen et al., 2008, Netzel-Arnett et al., 2006, Takeuchi et al., 2000, Lee et al., 2007). Putative substrates of matriptase have been identified biochemically and using multiple *in vivo* and *in vitro* models and most of these substrates also show strong associations with cancer development and progression.

A previous analysis of the peptide substrate preference of matriptase was studied by our group using the Positional Scanning-Substrate Combinatorial Library (PS-SCL) technique, identifying preference for basic P1 residues (Lys/Arg), small residues (Ser/Ala) or Phe for P2, basic residues (Lys/Arg) for P3 and basic residues at P4 (Lys/Arg) (Owen et al., 2010). This specificity corresponds well with the cleavage sequence particularly for the substrates pro-uPA, pro-HGF, PAR-2, pro-prostasin and even pro-matriptase (Chen et al., 2008, Netzel-Arnett et al., 2006, Takeuchi et al., 2000, Lee et al., 2007). As mentioned in the previous chapter, matriptase and another TTSP, hepsin, share similar protein substrate specificities, and expression and activity of both enzymes are highly correlated with malignancy and progression particularly in prostate cancer (Riddick et al., 2005, Klezovitch et al., 2004). HAI-1 and HAI-2 play a key role in balancing this enzymatic activity to ensure correct substrate activation and signaling, as well as acting as key regulators of other proteases.

All known matriptase substrates, which include the zymogens of prostaticin, HGF, and uPA, as well as EGFR and ENaC, are abundant in epithelial barrier tissues in which they have been shown to independently regulate key aspects of development, differentiation and maintenance (Owen et al., 2010, Kilpatrick et al., 2006, Lee et al., 2000). Some of these particularly present a specialised role in polarised simple epithelial barriers in organs such as the intestine and kidney, where they help maintain paracellular integrity and TEER. Despite the current understanding of how these substrates aid simple barrier formation and maintenance, it is not yet clear if this occurs as a consequence of matriptase function. During re-establishment of epithelial barrier integrity and therefore epithelial repair, growth factor receptors such as the EGFR have been shown to promote mucosal wound healing and altered function has been linked to ulcerative colitis similar to matriptase. Therefore because EGFR was thought to have a role in the onset and progression of ulcerative colitis, it became considered as a therapeutic target (Sinha et al., 2003).

5.1.1 Matriptase substrates and role in epithelial tissue function

The leaky intestinal barrier caused by a reduction in matriptase expression and activity, was associated with disruption of the paracellular tight junctions by increasing claudin-2 expression (Buzza et al 2010). So far the findings in this thesis demonstrate that matriptase function is required for the development and re-establishment of barrier function in different model systems, which display well-polarized features and develop high TEER, as demonstrated in the MDCK-I model. In this model, we have shown that this function is independent of claudin-2 expression, possibly indicating alternative pathway(s) with different effector targets for matriptase activity. Several of the proteins that have been shown to be substrates for matriptase have well-established roles in epithelial maintenance and repair. Therefore in this chapter a candidate substrate approach has been used to investigate the role of matriptase in MDCK-I barrier function.

5.1.2 Prostasin

As mentioned previously in chapter 2, prostasin enzyme is synthesized as a 40 kDa zymogen that requires proteolytic cleavage by other serine proteases at Arg-44 within the QPR⁴⁴ITG amino acid sequence (Friis et al., 2013, Yu et al., 1995). Activation results in a two-chain form linked together by a disulphide bond that is broken under reducing conditions to give a 37 kDa protein, which represents the 299-aa heavy chain, that can be detected by western blots (Takeuchi et al., 2000, Netzel-Arnett et al., 2006).

Analysis of human tissue expression of prostasin showed highest abundance in the prostate gland as well as moderate expression in the colon, lung, liver kidney, pancreas and most all other epithelia (Yu et al., 1994). In the epidermis, prostasin is co-localised with matriptase in the transitional layer where keratinocytes undergo terminal differentiation. Here, matriptase-mediated terminal tissue differentiation involves the activation of prostasin to facilitate the processing of pro-filaggrin, which is lost in mice with deficiencies in either of the proteases independently (List et al., 2007b, Netzel-Arnett et al., 2006, List et al., 2003). These mice presented with a plethora of epithelia-related defects including the malformation of the stratum corneum and follicular hypoplasia, ultimately leading to loss of epidermal differentiation and integrity (Takeuchi et al., 2000, Leyvraz et al., 2005). They also show defects in the formation and function of the paracellular tight junctions, leading to excessive loss of water (List et al., 2002, List et al., 2009).

Whether prostasin activation by matriptase is necessary for matriptase-mediated intestinal barrier integrity, which is lost in matriptase hypomorphic mice and *in vitro* systems with loss of matriptase function, is yet to be determined. In the polarized epithelia, prostasin and matriptase are controlled by topological separation on the plasma membrane, where prostasin, in common with most GPI-anchored proteins, is associated with the apical membrane while matriptase is located at the basolateral membrane (List et al., 2007b). Yet, protein targeting studies have provided evidence suggesting brief co-localisation between prostasin and matriptase at the basolateral plasma membrane, where it can become

activated by matriptase before transport to the apical surface (Friis et al., 2011). Overall, the synchronized expression of prostasin and matriptase in well-differentiated epithelial tissue indicates a coordinated role in tissue physiology. A study by Buzza et al (Buzza et al., 2013) recently showed that prostasin is required for barrier paracellular integrity, similar to matriptase. Here, depletion of prostasin was found to inhibit barrier development similar to matriptase knockdown and inhibition. However, in the absence of matriptase, prostasin does not stimulate barrier formation, therefore suggesting it has a function upstream to activate matriptase in the intestinal epithelia. Therefore this study further highlighted the role of matriptase as the direct mediator of intestinal barrier development (Friis et al., 2013, Buzza et al., 2013).

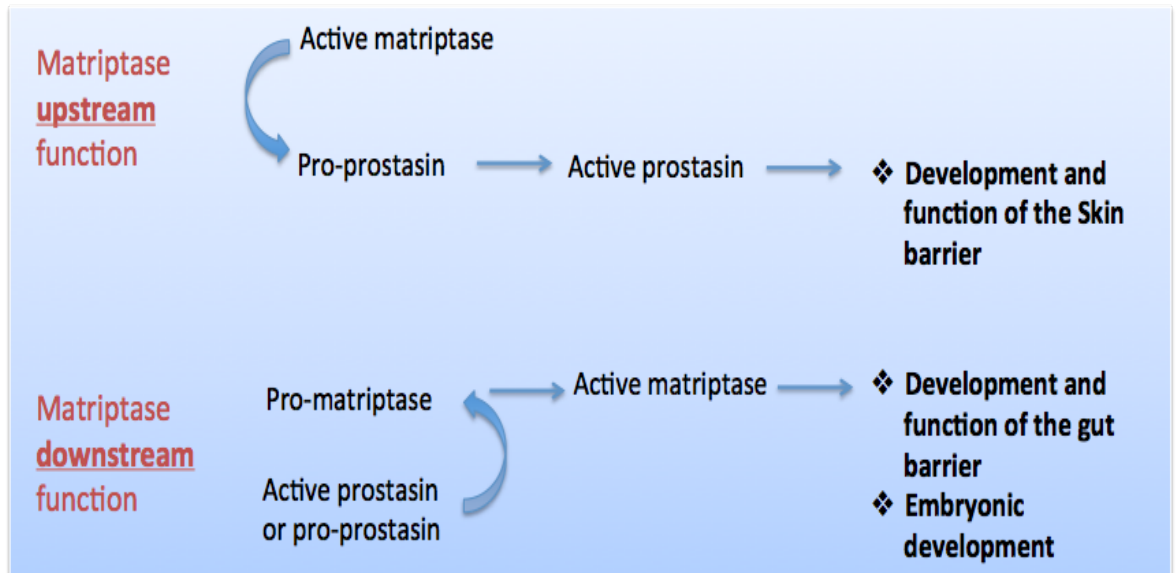


Figure 5.1: A schematic describing the upstream and downstream activation functions of the reciprocal complex between matriptase and prostasin.

Several studies have converged to illustrate this strong mechanistic interrelationship between matriptase and prostasin in simple epithelial tissue (Figure 5.1) demonstrating their participation in a single proteolytic pathway required for barrier formation (Buzza et al., 2013). This complex presented features that suggest prostasin may function as a non-enzymatic cofactor for the conversion of the matriptase zymogen to active enzyme, which becomes capable of

activating prostaticin (Friis et al., 2013).

Prostaticin has a few potential substrates that are strongly associated with maintenance of epithelial permeability. It displays trypsin-like activity and this plays an important role in the activation of regulatory molecules, also shared by matriptase, such as the ENaC, EGFR and PAR-2 (Adachi et al., 2001, Vuagniaux et al., 2002, Chen et al., 2008, Bruns et al., 2007, Friis et al., 2013). Prostaticin activity is also tightly controlled in a similar way to matriptase by forming interactions with cognate surface inhibitors HAI-1 and HAI-2, and also protease nexin-1 (PN-1), which is a potent thrombin inhibitor, known to participate in renal epithelial injury repair (Moll et al., 1996). The strong and complex interrelationship between matriptase and prostaticin make it an important candidate in the study of the mechanism of matriptase in mediating MDCK barrier epithelial function.

Epithelial sodium channel (ENaC) function in epithelial barriers

ENaC is a membrane-associated ion channel that is expressed at the surface of epithelial cells in many tissues including the kidney, intestine, lung, and skin (Renard et al., 1995, Voilley et al., 1994, Brouard et al., 1999). ENaC is a constitutively active and highly selective channel that functions in regulating body Na⁺ homeostasis. This function is particularly essential in the lung to drive airway fluid clearance as revealed through knockout studies and studies of cystic fibrosis (Tong et al., 2004, Fang et al., 2002, Hummler et al., 1996).

Previous electrophysiological studies revealed functional heterogeneity of ENaC in different tissues based on biophysical effects, including ion selectivity and sensitivity to channel inhibitory drug and potassium-sparing diuretic amiloride (Palmer, 1992). The importance of Na⁺ balance, in maintaining water homeostasis was demonstrated in many barrier epithelia and dysregulation has been shown to drive loss of barrier integrity. This was particularly shown in ENaC deficient mice, which developed epidermal barrier defects that led to dehydration due to excessive loss of water from the body (Planes et al., 2010).

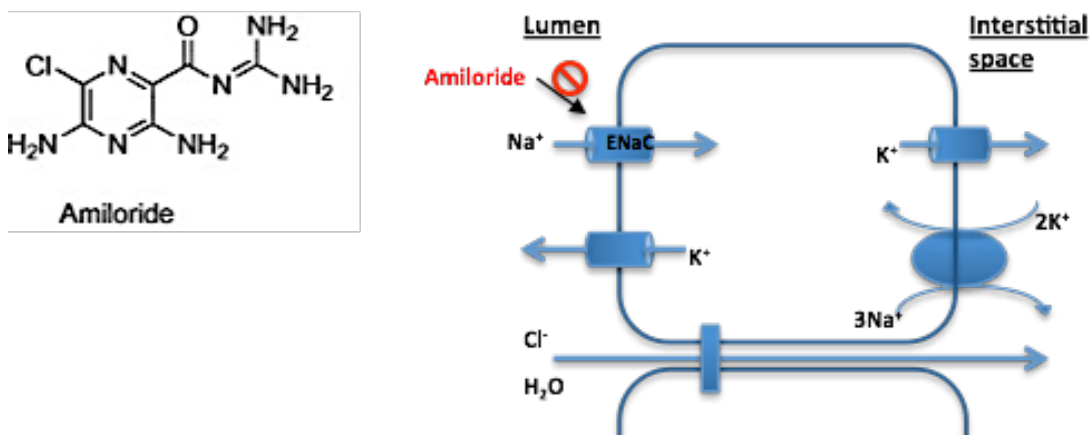


Figure 5.1 Schematic representation of mechanism of Na⁺ reabsorption and fluid balance mediated by the amiloride-sensitive ENaC at the surface of epithelial cells.

Transepithelial transport of Na⁺ by ENaC is accomplished together with the Na⁺/K⁺ ATPase, and maintain electrolyte and osmotic pressure in the extracellular space. The chemical structure of the diuretic amiloride (which also inhibits uPA) is also displayed (Massey et al., 2012).

The structure of ENaC consists of three domains termed α , β and γ . Full channel function essentially requires proteolytic cleavage of the γ domain by furin followed by a second cleavage by serine proteases such as prostasin at a distal site (Bruns et al., 2007). The γ subunit is important for channel gating and interaction with the amiloride (Shi and Kleyman, 2013). During the characterization of MDCK cells in culture, they were shown to display amiloride sensitivity observed through changes in ion current and TEER, which was comparable to other kidney epithelial cell lines (Mauro et al., 2002, Charles et al., 2008). The role of matriptase in regulating MDCK-I cell barrier recovery may therefore involve ENaC function, as a mediator of ion and fluid balance. Therefore ENaC is a potential candidate substrate for both matriptase and prostasin in the maintenance of epithelial barrier integrity and function.

EGFR role in maintenance of epithelial function

EGFR is another potential cell surface substrate that is found in all epithelia, and displays key roles in regulating barrier function of simple tissues (reviewed in: (Melenhorst et al., 2008). EGFR knockout mice suffer from impaired epithelial development that leads to abnormalities in multiple organs, including the kidney, affecting electrolyte homeostasis. More studies also highlight that EGFR activation and signaling can enhance TEER in MDCK-II cells by affecting claudin expression and tight junction assembly (Singh et al., 2007).

One study by Chen et al published in 2008, described the proteolytic activation of EGFR requiring prostatic and matriptase activity (Chen et al., 2008). They demonstrated the ability of both enzymes to directly cleave EGFR leading to constitutive phosphorylation and loss of EGF stimulation. This again provides further indications toward a matriptase and prostatic pathway (and possibly EGFR), in MDCK-I barrier repair.

5.1.3 The HGF/SF-c-Met signaling axis

Endogenous matriptase on the surface of epithelial cells is critically involved in pro-HGF activation, facilitating downstream signaling via c-Met and eliciting many cellular responses, including cell growth and migration (Szabo et al., 2011, Owen et al., 2010). In transgenic mouse models, matriptase overexpression has been found to facilitate c-Met mediated oncogenesis in the skin and to increase susceptibility to carcinogens through increased proteolytic activation of pro-HGF (Szabo et al., 2011). Although HGF plays an important role in breaking associations between neighboring epithelial cells, in well-differentiated simple epithelial tissues, as discovered in MDCK-II cells, it has also been shown to play a critical role in tissue differentiation and maintenance (Gherardi et al., 1989, Stoker et al., 1987). A few studies also have published data showing HGF and c-Met up-regulation during organ injury, contributing to their repair (Itoh et al., 2004, Schmassmann et al., 1997). This HGF/C-MET signaling has been particularly shown to play an important role in liver regeneration and repair (Huh et al., 2004).

From our findings it can be concluded that matriptase activity is required for HGF-mediated cell scattering responses in both MDCK-I and MDCK-II cells (Gray et al., 2014). This could mean that HGF/c-Met signaling is also induced by matriptase activity during epithelial cell monolayer recovery and mediates the observed monolayer and TEER reestablishment after calcium switch. A role for HGF in regulating tight junctions is supported by a study of its effect on MDCK TEER development, demonstrating that polarized MDCK-II cell monolayers displayed an increase in TEER when subject to HGF stimulation. This effect on TEER was mediated through downstream pERK 1/2 signaling and was only observed in MDCK-II cells, as HGF had no effect MDCK-I monolayers which were shown to have high intrinsic pERK activation (Lipschutz et al., 2005). This study illustrates that the higher level of intrinsic pERK activity in MDCK-I cells limited cell line sensitivity to HGF stimulation, and also facilitated the difference in tight junctions and development of TEER (Lipschutz et al., 2005). So far however, the literature highlights various effects of HGF on barrier function, particularly in different epithelial models, demonstrating either a negative or positive influence on barrier integrity and TEER (Jiang et al., 1999, Nusrat et al., 1994). Whether HGF plays a role in matriptase mediated recovery of MDCK-I cultured epithelial monolayers is yet to be elucidated.

c-Met, similarly to matriptase, is widely expressed in most epithelia and performs at the same polarised epithelial domain, as it is predominantly associated with the basolateral surface of polarised epithelial cells. Therefore matriptase is in the right place to activate pro-HGF once bound to c-Met. Thus the activation of c-Met maybe required for epithelial repair and may play a role in MDCK-I barrier function and repair.

5.1.4 Protease activated receptor-2 activation and physiological function

Matriptase is also a direct proteolytic activator of the tethered-ligand G-protein-coupled receptor PAR-2, which has pleiotropic functions in development and maintenance of postnatal homeostasis in vertebrates. This receptor is encoded by

the F2RL1 gene, which is widely found in different human tissues, including the epithelial tissues, such as the skin and intestine (D'Andrea et al., 1998). Matriptase is not the only activator of PAR-2, as many other trypsin-like serine proteases also activate this receptor (Chokki et al., 2004, Wilson et al., 2005, Camerer et al., 2010, Takeuchi et al., 2000). Thus PAR-2 functions as part of a proteolytic enzyme sensory mechanism during infection, and it is associated with various common human diseases and contributes to inflammation (Rothmeier and Ruf, 2012). Therefore selective and potent agonists and antagonists of PAR-2 have been established as tools for studying its biological role using *in vivo* and *in vitro* systems.

Several studies have provided evidence for the role of PAR-2 in modulation of epithelial tissue function and barrier paracellular integrity, particularly by regulating tight junctions (Vesey et al., 2013, Enjoji et al., 2014, Yoshida et al., 2011). However, most evidence shows that PAR-2 activation resulted in impaired epithelial barrier, and enhanced paracellular permeability (Yoshida et al., 2011). This effect was also observed in human kidney tubular epithelial cells, whereby PAR-2 activation by an agonist peptide added at the basolateral surface led to increased expression of inflammatory genes, and a 5-fold decrease in TEER (Vesey et al., 2013). The predication from these studies is that if matriptase has a role in PAR-2 activation during barrier recovery, inhibition of matriptase activity would be expected to lead to an increase in recovery; the opposite to what we have observed. Nevertheless, it is important to consider PAR-2 as a candidate, particularly as these studies have focused on PAR-2 agonists rather than direct proteolytic activation. Interestingly it has also been demonstrated that this receptor can be activated downstream of prostatic activity. Ectopic expression of prostatic in the skin of transgenic mice leads to ichthyosis phenotype, which can be completely rescued by ablation of PAR-2 (Frateschi et al., 2011). However, as it has been demonstrated that prostatic cannot directly activate PAR-2, prostatic may therefore be acting as an upstream activator of matriptase (Camerer et al., 2010).

In this chapter the aim has been to identify whether any of the proteins discussed here play a role in MDCK-I barrier recovery, and are therefore potential candidates substrates for matriptase. Particularly we question their role in the matriptase

pathway for maintaining MDCK-I integrity and promoting barrier recovery following disruption of barrier integrity. Overall the candidate substrate approach was carried in an attempt to elucidate the mechanism through which matriptase mediates epithelial barrier integrity and function.

5.2 Results

5.2.1 Expression of prostasin, hepsin and PAR-2 in MDCK-I and MDCK-II cells

As demonstrated in Chapter 3, a similar level of expression of matriptase mRNA is found in MDCK-I and MDCK-II cells. MDCK-II are the most widely used in epithelial studies and the literature on expression of the candidate matriptase substrates is mainly restricted to these cells. As we aimed to investigate the function of potential matriptase substrates in MDCK barrier function, their relative expression was examined in both strains. Quantitative TaqMan PCR was carried out to analyse the expression of prostasin and PAR-2, as well as the structurally and functionally related TTSP, hepsin in MDCK-I and MDCK-II cells. Quantification of mRNA expression was determined relative to 18S ribosomal RNA as a housekeeping gene. MDCK-I and MDCK-II cells expressed similar levels of *F2RL1* mRNA coding for PAR-2, with a low C_t for amplification around 26.3 ± 0.06 , suggesting high mRNA content (Figure 5.3 A). High and similar mRNA detection for PAR-2 suggested that MDCK-I and MDCK-II cells have an endogenous expression of the receptor. Furthermore, levels of *Prss8* mRNA coding for prostasin revealed similar expression between MDCK-I and MDCK-II cells. The average C_t values for expression of prostasin were 27.6 for MDCK-I and 28.5 for MDCK-II cells, indicating high endogenous expression in both cell lines (Figure 5.3 B).

To analyse prostasin expression at the protein level in the two strains of MDCK cells the same antibody was used as in a previous study identifying prostasin localization in human airway epithelial cells (Nimishakavi et al., 2012). Lysates from A549 cells for human positive control were run on SDS PAGE without a

reducing agent, using Hsc-70 as a loading control. Protein bands were observed in both MDCK-I and MDCK-II cells at the same molecular weight as the control, confirming recognition by the antibody (Figure 5.4 A). Therefore, further analysis of prostatic protein expression in MDCK-I and MDCK-II cells confirmed the PCR data, showing no difference in total protein levels. Two closely-spaced bands were detected, possibly indicating the 40k Da inactive form and the 37 kDa activated form of prostatic. However this was observed in the absence of a reducing agent, which is required to break the disulphide bridge between the two-chain proteolytically activated form of the enzyme.

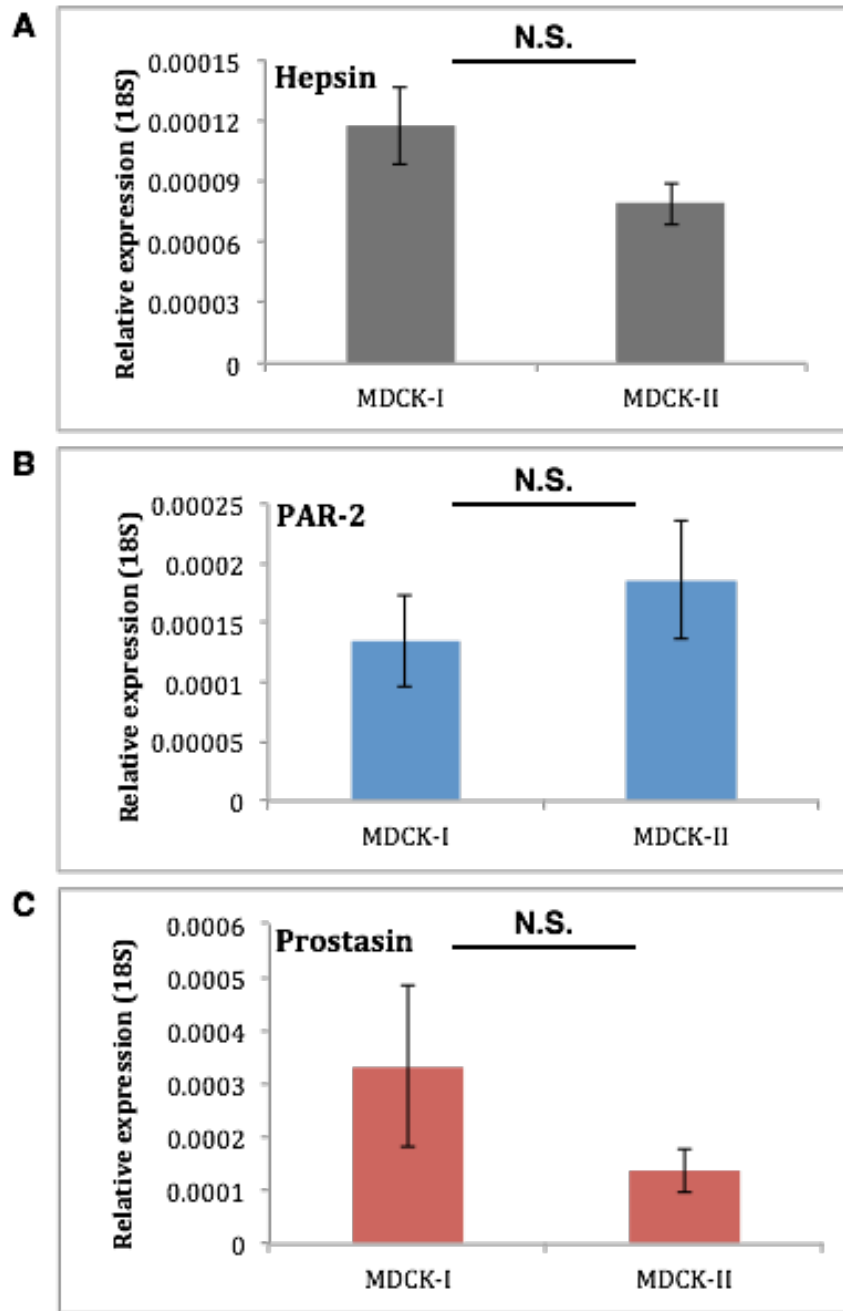


Figure 5.2 Quantitative mRNA expression of hepsin, PAR-2 and proastasin in MDCK-I and MDCK-II cells.

RNA was harvested from MDCK type I and II cells grown on 6 well plates for 4 days. qRT-PCR analysis of A) hepsin, B) PAR-2 and C) proastasin expression levels using specific TaqMan primers and probes. Levels of expression were calculated relative to the 18S rRNA as a house keeping gene using the $2^{-\Delta C_t}$ method. TaqMan qPCR data are expressed as mean \pm S.E. (n=9). N.S. p > 0.05.

5.2.2 Prostasin expression and function in MDCK-I barrier epithelia

5.2.2.1 Relative quantification of prostasin mRNA expression in MDCK-I barrier: influence of calcium switch

TaqMan qRT-PCR for prostasin was conducted on mRNA samples harvested from MDCK-I cells before, during and after calcium switch-induced barrier disruption and recovery. The relative quantification of prostasin expression revealed no significant change upon calcium depletion, at the time-point when there is a substantial loss of TEER (graph indicates lower expression however the original C_t values were very similar; 25.84 ± 0.3). Furthermore, no changes in prostasin mRNA levels were detected during barrier recovery following calcium switch. Here mRNA levels were similar at 5, 10 and 32 hours of recovery from calcium depletion, which suggested that prostasin gene is unaltered during the breakdown of MDCK-I barrier and in normal recovery (Figure 5.4B).

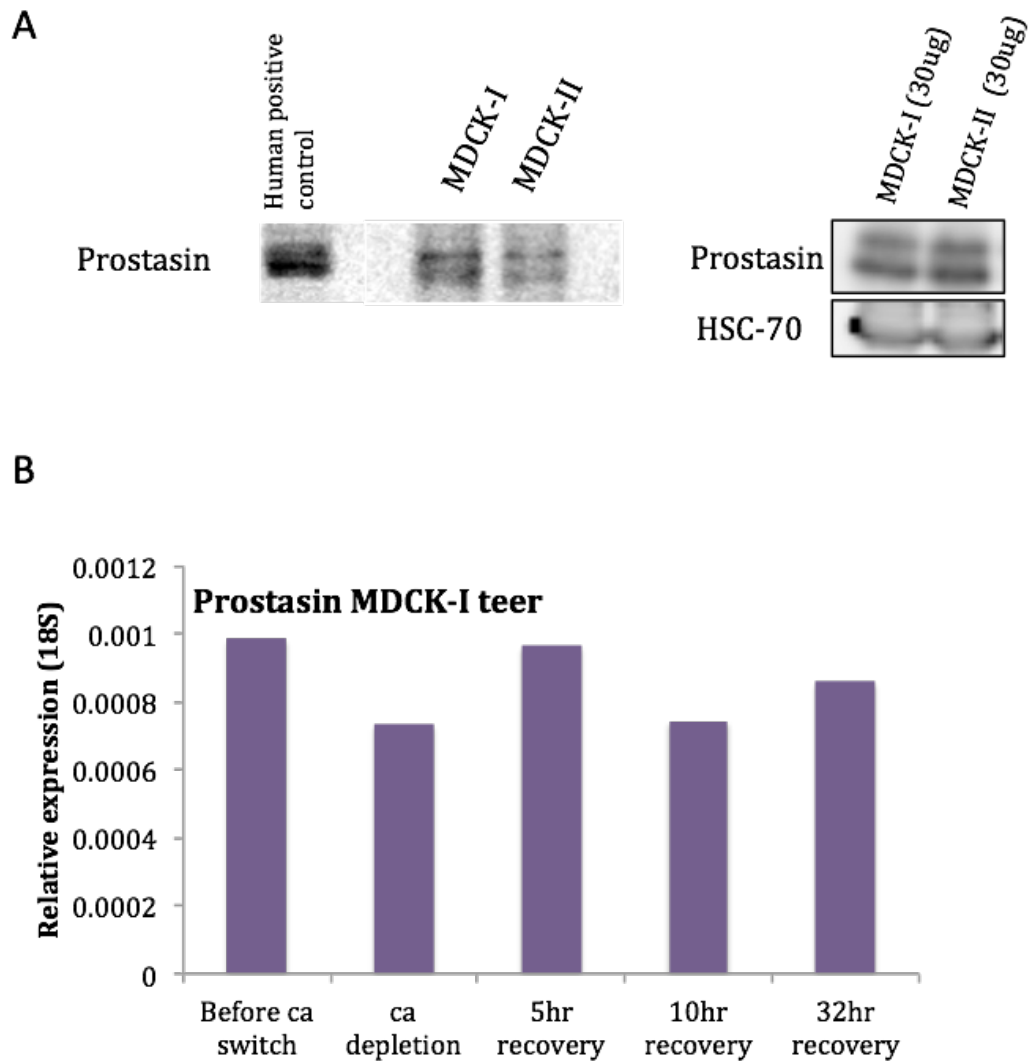


Figure 5.3 Expression of prostatin mRNA and protein in MDCK-I and MDCK-II during and after calcium switch in MDCK-I cells.

A) Prostatin protein expression level was similar between MDCK-I and MDCK-II cells displaying double band around 38 kDa. A549 cell line served as a human positive control for confirmation of band size. B) qRT-PCR to show prostatin expression, using dog specific TaqMan primers and probe, during calcium switch and at 5, 10 and 32 hours calcium repletion and TEER recovery without any treatment conditions. Data are expressed as average from duplicate samples.

5.2.2.2 Effect of matriptase inhibition on prostasin mRNA levels in MDCK-I monolayers

To investigate whether mRNA expression level of prostasin is altered when matriptase is inhibited in MDCK-I monolayers during recovery from calcium switch, RNA samples were harvested at different time points of recovery with and without the matriptase inhibitor IN-1 (the benzothiazole-containing IN-1-peptidomimetic). Figure 5.4 A for prostasin expression revealed no significant change between control and inhibitor samples at 1, 2, 5 (slightly higher in control but not statistically significant, p-value=0.65) and 10 hours of barrier recovery compared to inhibitor treated cells (Figure 5.5 A).

Prostasin protein expression was also investigated in lysate samples collected from MDCK-I monolayers treated with CJ-1737 (an amidinophenylalanine-based inhibitor) at the 5, 10 and 32 hours recovery time points. Running of 30µg of protein sample onto 10% SDS-PAGE and analysis by western blot showed expression of two bands in during barrier recovery. The upper band intensity increases with time of recovery, but the strongest observation was an increase in the intensity of the lower prostasin protein band (~37kDa) at early recovery points (5 and 10 hours), which was quantified through band densitometry. However, it is difficult to define whether this is the active form of the enzyme since the samples were not subjected to a chemical reducing agent (Figure 5.5 B).

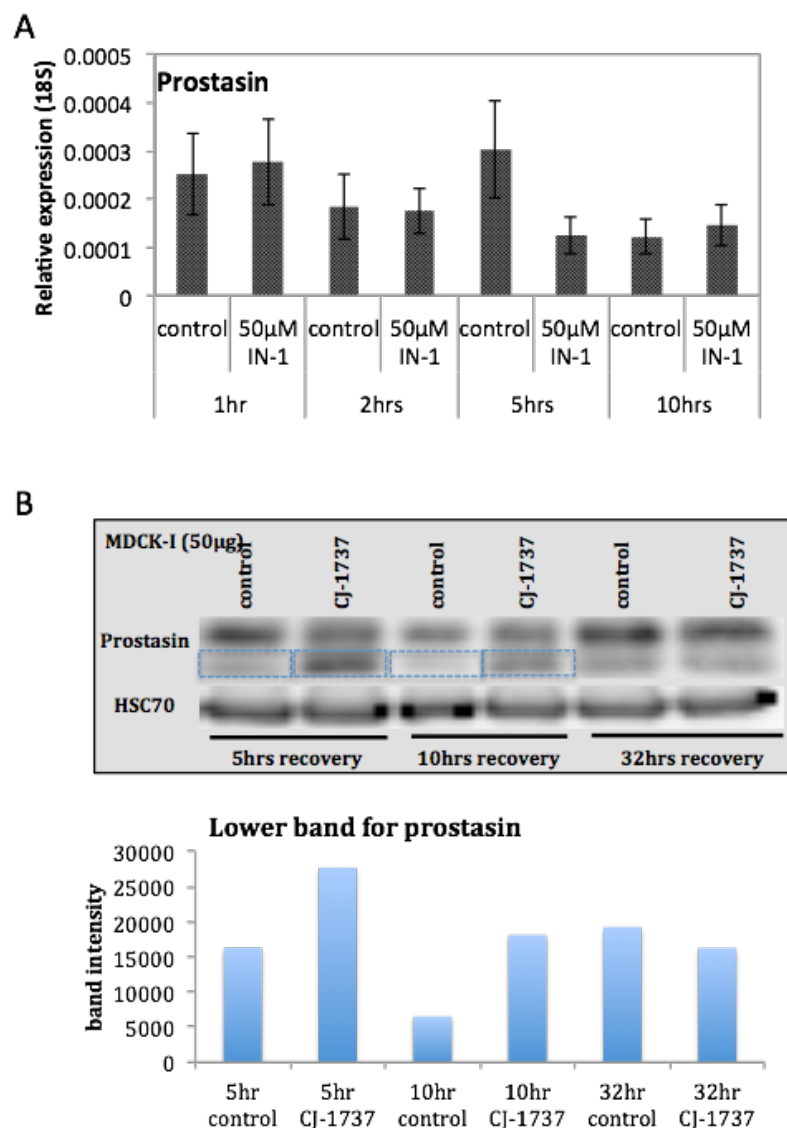


Figure 5.4 Effect of matriptase inhibition on prostasin expression in MDCK-I during monolayer recovery from calcium switch.

A) Expression of prostasin mRNA levels during MDCK-I monolayer re-establishment in a TEER assay conducted under treatment with 50 μ M matriptase inhibitor, IN-1. mRNA samples were collected at 1, 2, 5 and 10 hours recovery from calcium switch. B) Prostasin protein expression in MDCK-I cells following calcium switch and recovery at 5, 10 and 32 hours with and without 100 μ M CJ-1737. Proteins were loaded without reducing agent on 10% acrylamide gel. The intensity of the lower of the two prostasin bands was quantified by densitometry and shown in the graph. In A) samples TaqMan qPCR data are expressed as mean \pm S.E. (n=9). N.S. $p > 0.05$.

5.2.2.3 Attempt to analyse prostatic activity and complex binding in MDCK-I cells

The proteolytic activation of prostatic can be studied by analysing its conversion from a single-chain to a two-polypeptide chain complex, which remains connected via a disulfide bond between the side chains of Cys-5 and Cys-122. In studies that reveal changes in prostatic activity, in both humans and mice, an increase or decrease in the intensity of the heavy chain band at ~37 kDa is observed (the light-chain, being only 12 amino acids, is too small to detect in SDS-PAGE). In MDCK-I cells the amount of activated prostatic was shown directly by the detection of the 37 kDa fragment (in comparison to 41 kDa zymogen) after reduction of the samples and separation in SDS-PAGE gels and probing with prostatic antibody. Reduced lysates from MDCK-I barrier recovery assays, conducted with or without treatment with the matriptase inhibitor CJ-1737, showed a well-defined upper prostatic band with no difference in protein levels observed between the control and inhibitor samples at each of the time points 5, 10 and 32 hours post calcium switch (Figure 5.6A). This prostatic band observed under reduced conditions ran as a slightly higher molecular weight compared to non-reduced control (control used was from lysate collected at 0 hours after calcium switch i.e. end of calcium depletion). A fainter active form band also can be observed in samples treated with reducing reagent, but this does not show a similar change in band intensity with time of barrier recovery and inhibition with CJ-1737, as seen without reducing agent, suggesting that the previous altered band is unlikely to be the active form of prostatic. This could be confirmed by testing whether prostatic in MDCK-I cells forms higher molecular weight complexes with endogenous inhibitors.

Prostatic enzymatic activity can be also determined by studying the formation of a covalent complex with the serpin, PN-1. The ability to form this 82 kDa complex during barrier recovery from calcium switch in MDCK-I cells with and without matriptase inhibitor was tested. Non-boiled lysate samples run on 8% SDS-PAGE later showed an immuno-reactive band at the correct molecular weight, which did not vary in intensity across all the samples representing the time point of recovery and treatment with CJ-1737. This indicates that prostatic-PN1 complex formation

likely does not occur in the matriptase mediated role in barrier repair in MDCK-I cells (Figure 5.6B). Further, unidentified lower-molecular weight bands are observed in the non-boiled samples but they also have similar intensity between all samples. Therefore, there is no evidence that prostaticin is activated during barrier disruption or recovery and during matriptase inhibition.

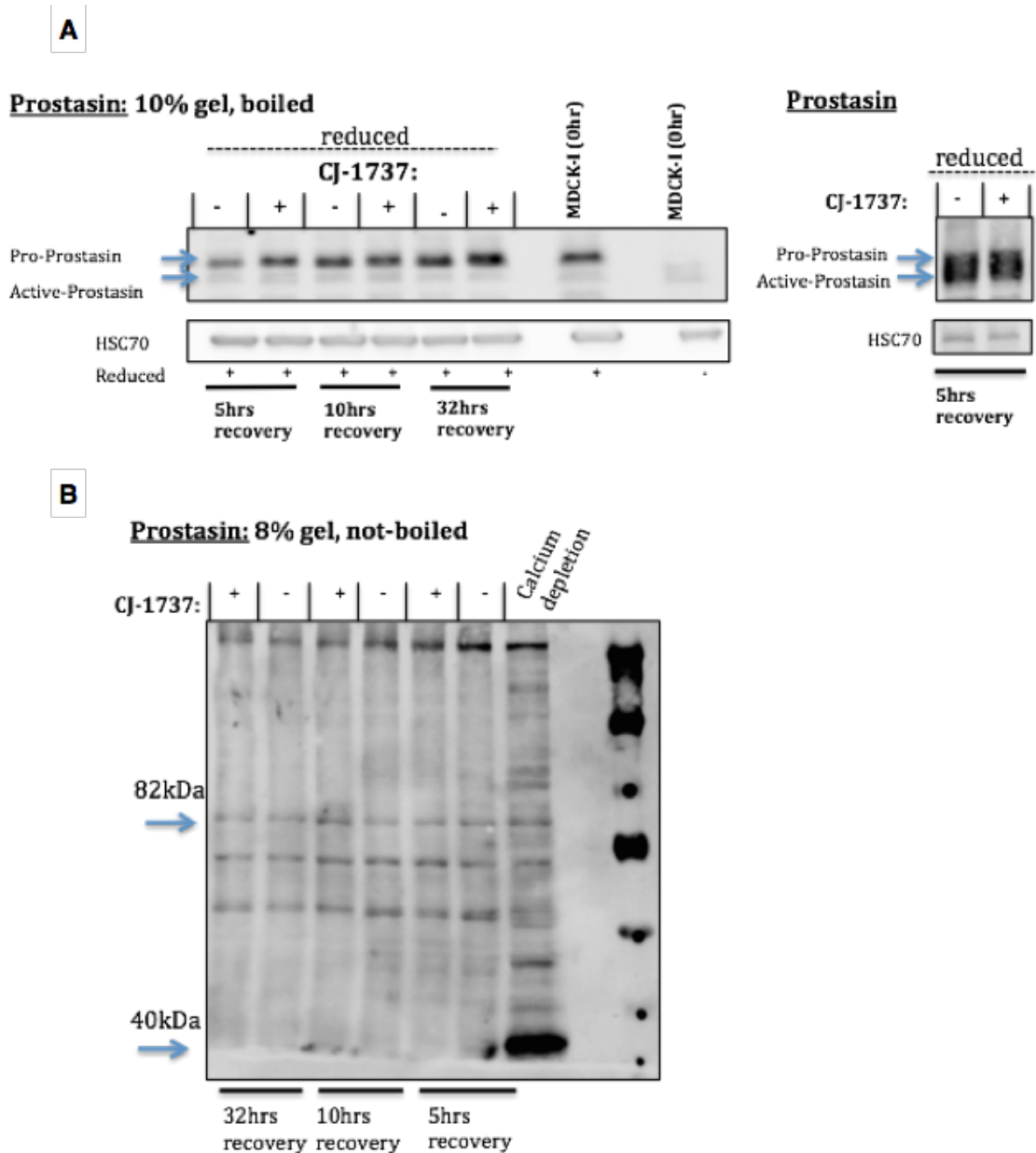


(figure legend on the next page)

Figure 5.5 Effect of matriptase inhibition on prostasin activation and endogenous inhibitor complex formation during MDCK-I barrier restitution.

A) Prostasin protein conversion from single-chain to two-chain was analysed following the reduction of protein samples with β -mercaptoethanol. The proteins were run on a 10% polyacrylamide gel and probed western blots revealed two bands at approx. molecular weight of 41 kDa and 37 kDa. Protein sample from MDCK-I cells at 0 hr recovery, both reduced and non-reduced, are shown as controls. The blot on the far right shows a repeat of the 5 hr time point. B) Activity of prostasin examined by the formation of higher molecular weight complexes with endogenous inhibitors (e.g. 84 kDa complex with PN-1). MDCK-I cell lysates from the barrier recovery assays conducted under matriptase inhibition with CJ-1737. Protein samples following 0 hr, 5 hr, 10 hr and 32 hr recovery were run on 8% polyacrylamide gels without boiling to preserve protein-protein complexes.

5.2.3 Influence of amiloride, an inhibitor of uPA and ENaC, on MDCK-I barrier function

Amiloride, is a pyrazinoylguanidine drug, Known for its potency against the sodium channel as well as the Na^+/H^+ exchanger and $\text{Na}^+/\text{Ca}^{2+}$ exchanger (Kleyman and Cragoe, 1988). This was also found to inhibit uPA. To test whether amiloride, inhibitor of ENaC and uPA altered TEER recovery in MDCK-I cells, monolayers were treated with amiloride during calcium repletion.

MDCK-I cells were treated with 10 μM amiloride, as this concentration has previously been shown to affect TEER responses in MDCK-II cells (Chen et al., 2013). Amiloride-treated cells showed normal TEER recovery (similar to DMSO control), in comparison to matriptase inhibitor (CJ-1737) treated cells, which displayed the expected slow recovery from calcium switch (Figure 5.7A). A higher concentration of amiloride (50 μM) often promoted an increase in maximum TEER following complete recovery, compared to 10 μM amiloride and control, yet no increase was observed during early recovery of TEER (data not shown). Amiloride also had no effect on recovery of MDCK-II TEER (data not shown), suggesting ENaC function is unlikely to be essential for the reformation of MDCK barrier TEER, particularly following injury induced by calcium depletion.

5.2.4 EGFR function during recovery of MDCK-I monolayer

To determine whether EGFR auto-phosphorylation is required for barrier repair function following disruption by calcium switch in MDCK-I cells, the cells were treated with AG1478, a potent inhibitor of the EGFR kinase activity and auto-phosphorylation. Cells were treated immediately before and during calcium repletion

AG1478 treatment presented no effect on early recovery of barrier TEER in MDCK-I cells but slightly increased the overall TEER at time points from 32 hours onwards (Figure 5.7B). Investigating the level of EGFR phosphorylation at residue Tyr-1068, representing the binding site for Grb2, during barrier recovery with and without matriptase inhibition with CJ-1737, was conducted by western blotting. Analysis of cell lysates treated with phosphatase inhibitors, revealed no significant changes in the level of p-EGFR between matriptase inhibition and control samples following 5, 10 and 32 hours of recovery after calcium repletion (Figure 5.7C). This along with the lack of effect of AG1478 on TEER suggests that it is unlikely that EGFR activity is related to the function of matriptase in mediating recovery of MDCK-I barriers. Subsequently the effect of EGFR inhibition was examined on the ability of MDCK-II cells to recover after calcium switch. No significant effect was observed compared to control DMSO treated monolayers, suggesting that EGFR activation is not relevant for barrier reestablishment for either strain of MDCK cells.

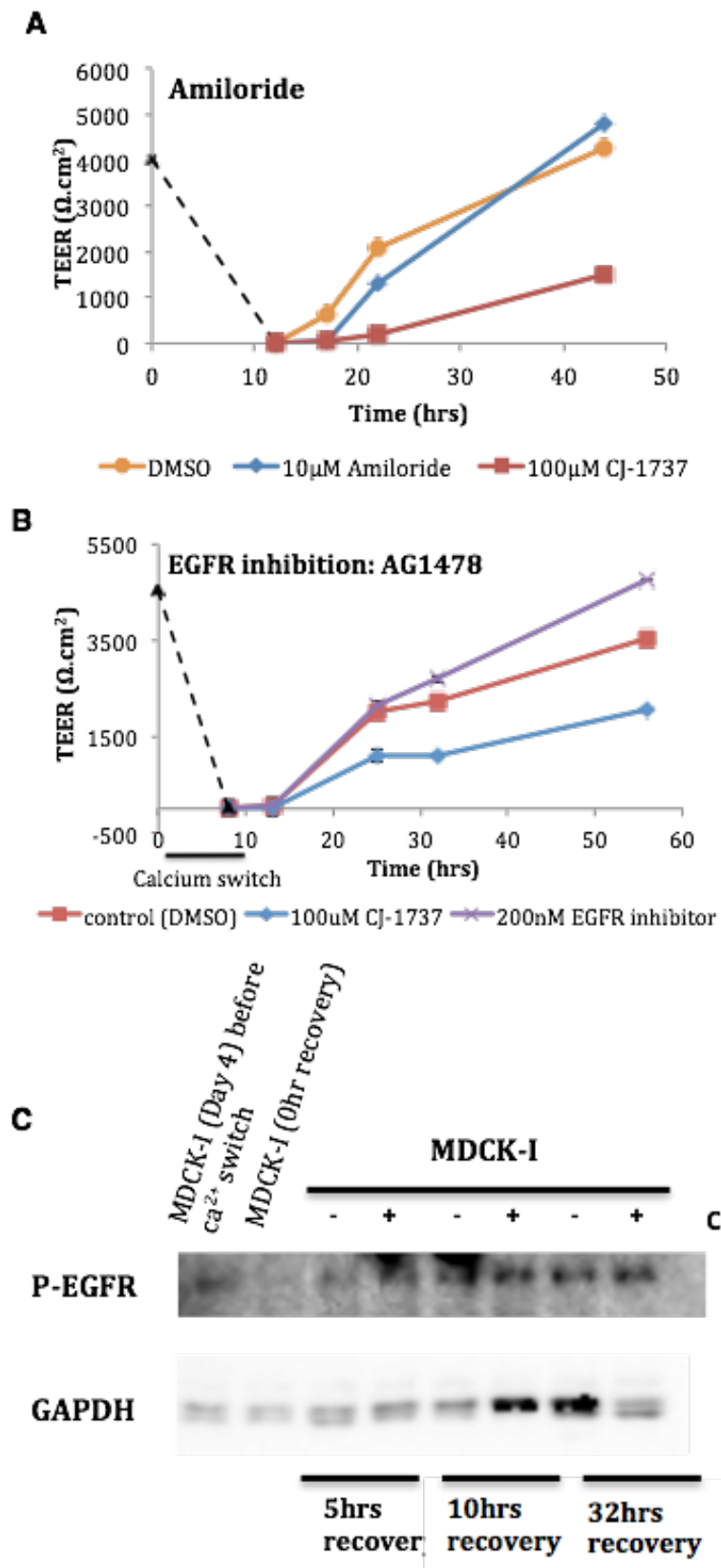


(Figure legend on the next page)

Figure 5.6 Effect of amiloride and EGFR inhibitor on TEER recovery of MDCK-I monolayer.

A) MDCK-I monolayers were subject to calcium switch after establishing maximum barrier TEER, before addition of amiloride or DMSO for treatment control. Amiloride (10 μ M) was applied 30 minutes before calcium repletion and inhibitor or CJ-1737 were reapplied in calcium repletion medium. B) MDCK-I monolayer cells were treated with EGFR inhibitor AG1478 (200 nM) applied 30 minutes before calcium repletion and during barrier recovery following calcium repletion. This treatment was also conducted alongside matriptase inhibition with CJ-1737 and DMSO control. TEER data are expressed as mean \pm S.E. (n=3). C) Samples at various recovery time points were probed for pEGFR by western blot with GAPDH used as a loading control.

5.2.5 PAR-2 effect on TEER recovery in MDCK-I cells

5.2.5.1 Relative expression of PAR-2 (F2RL1) during matriptase inhibition with IN-1

To investigate whether mRNA expression level of PAR-2 is altered with matriptase inhibition in MDCK-I monolayers during recovery from calcium switch, RNA samples were harvested at different time points of recovery with and without the matriptase inhibitor IN-1 (50 μ M). Following the previous data for prostasin expression, PAR-2 revealed no significant changes between control and inhibitor samples at 1, 2, 5 and 10 hours (Figure 5.5A). Interestingly a similar pattern was observed for PAR-2 mRNA, which overall showed a decline in expression in both control and inhibitor treated cells with increasing recovery times, similar to the observation for prostasin.

Analysis of PAR-2 protein expression was inconclusive due to failure to detect PAR-2 protein in MDCK cells using an antibody recognizing human PAR-2.

5.2.5.2 Influence of PAR-2 antagonists and agonists on TEER restoration in MDCK-I cells

PAR-2 activation by trypsin has been shown to modulate inflammation and cytoprotection, particularly in the intestinal and airway epithelia (Bueno and Fioramonti, 2008, Shan et al., 2012). Various studies have demonstrated that PAR-2 activation can influence epithelial tissue integrity and TEER. To determine whether activation of PAR-2 is important in MDCK-I TEER recovery, MDCK-I cells were treated with 5 μ M 2-furoyl-LIGRL-NH₂ peptide agonist (5 μ M) in the presence and absence of the matriptase inhibitor CJ-1737. The PAR-2 agonist on its own had no effect on TEER recovery after calcium switch (Figure 5.8 C), and in its presence CJ-1737 still caused a significant delay in TEER recovery (Figure 5.8 D). Furthermore, MDCK-I cells were treated with the PAR-2 antagonist ENMD-1068 (1 and 1.5 mM), which also have no effect on MDCK-I barrier TEER re-establishment (Figure 5.8 B).

Therefore, neither PAR-2 agonists nor antagonists were observed to have an effect, suggesting that PAR-2 is not involved in TEER recovery in MDCK-I cells. The inability of the PAR-2 agonist to restore TEER recovery in the presence of matriptase inhibition also supports this.

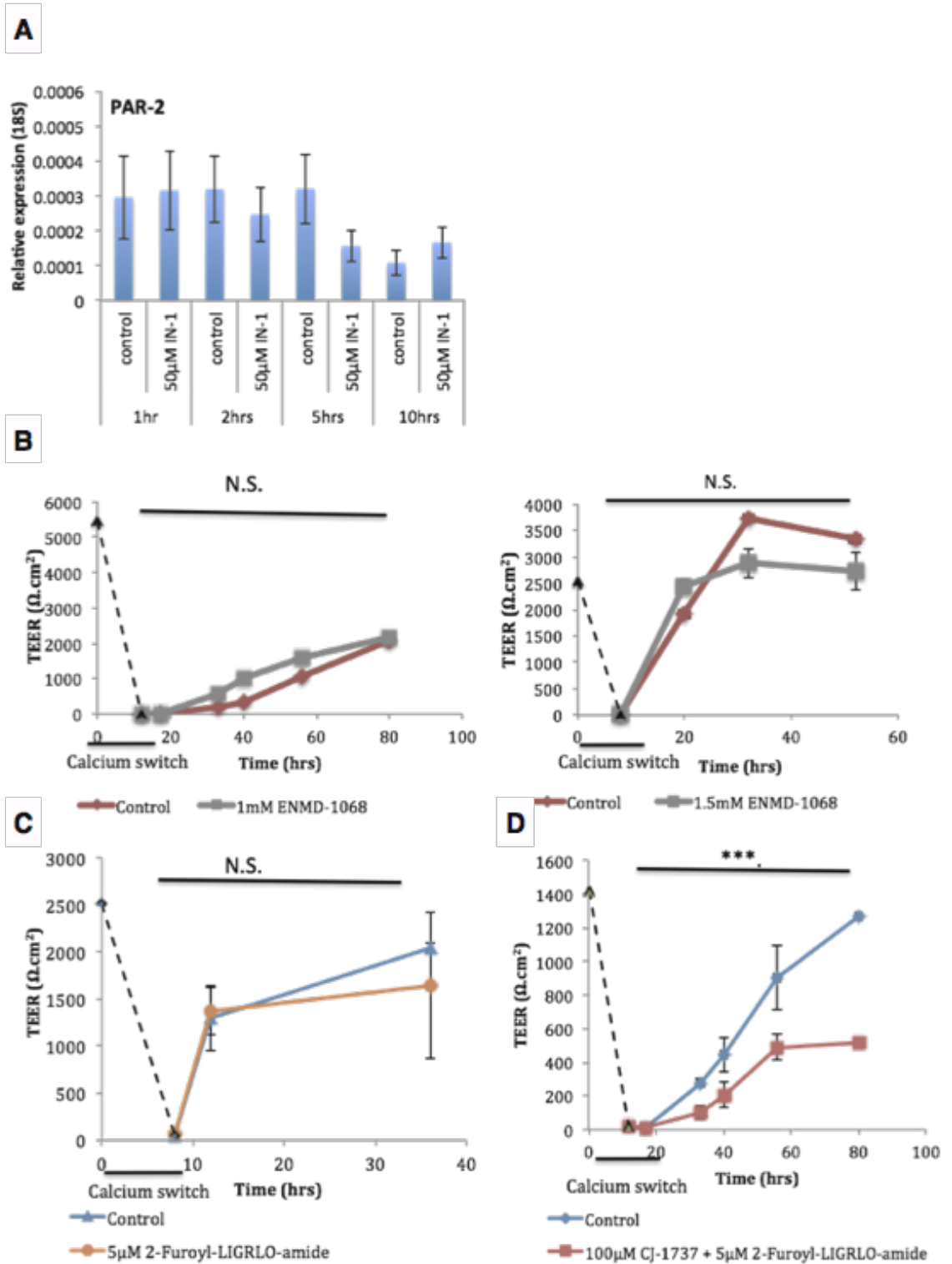


(Figure legend on the next page)

Figure 5.7 PAR-2 function and role in matriptase mediated MDCK-I barrier reestablishment.

A) Expression level of PAR-2 (F2RL-1 gene) mRNA in MDCK-I cells following 5, 10 and 32 hours of recovery from calcium switch was analysed using dog specific TaqMan primers and probe. Quantification was calculated relative to the 18S rRNA as a house keeping gene, and using the $2^{-\Delta C_t}$ method. B) MDCK-I cells were treated with 1 mM and 1.5 mM of the PAR-2 antagonist ENMD-1068 following calcium switch and recovery measured by TEER. C) MDCK-I cells were also treated with the PAR-2 peptide agonist 2-furoyl-LIGRLO-amide (5 μ M) cells following calcium switch. D) MDCK-I monolayers treated with both PAR-2 agonist and matriptase inhibitor CJ-1737 following calcium switch. All TEER data are expressed as mean \pm S.E. (n=3). N.S. $p > 0.05$. and ***= $P < 0.05$.

5.2.6 HGF/c-Met signaling function in MDCK barrier epithelia

5.2.6.1 Function of intrinsic pERK 1/2 activity on TEER and claudin-2 expression

The MAP kinase ERK 1/2 serves as a significant downstream signaling molecule in several of the potential matriptase substrate pathways. Its activation has been implicated in many mechanisms for epithelial regulation, including the EGFR, PAR-2, VEGF and HGF/c-Met signaling pathways. As mentioned earlier, one study clearly illustrated that a significant difference in the intrinsic level of activated pERK between MDCK-I and MDCK-II cells was the main factor mediating the established difference in TEER between these cells, that is due to differences in claudin-2 expression (Lipschutz et al., 2005). Following the findings in that particular study, we investigated the effect of inhibition of pERK on claudin-2 expression using the selective kinase inhibitor u0126, in both strains of MDCK cells.

Confluent cell grown on plastic culture plates (6 well plates) were treated with u0126 (10 μ M) for either 1 or 3 hours and cell lysates collected. Western blotting showed a higher level of activated pERK in MDCK-I cells compared to MDCK-II cells (Figure 5.9), while total ERK levels were not changed amongst the different cell line (data not shown). Furthermore treatment with u0126 almost completely abolished phosphorylation in both cell lines, as observed by the disappearance of the bands for each cell line and time point. These observations are consistent with

the previous study, although a much larger difference in activated ERK between the two cell lines was shown (Lipschutz et al., 2005). When the effect of u0126 on claudin-2 expression was observed, no increase in claudin-2 expression by MDCK-I cells was found, despite the complete inhibition of pERK (Figure 5.9). Similarly no change in claudin-2 expression in MDCK-II cells was observed, remaining unaltered and not different to the control for each cell line upon pERK inhibition (Figure 5.9). Furthermore stimulation of pERK levels by treatment with recombinant pro-HGF was clearly observed in MDCK-II cells, yet this did not lead to a reduction in the level of claudin-2 expression. Both of these observations are in sharp contrast to those previously published (Lipschutz et al., 2005), and suggest that signaling through ERK 1/2 has no role in claudin-2 expression in MDCK cells.

To confirm this lack of effect on claudin-2 expression, another experiment was conducted to determine the effect of long term pERK inhibition in MDCK-I and MDCK-II cells. Cells were treated with 10 μ M u0126 for a period of 8 or 24 hours before collecting cell lysate. During the treatment inhibitor was frequently replenished. Reduced ERK phosphorylation was confirmed for both time points and compared to total ERK levels, which remained constant. With longer treatment with u0126, claudin-2 protein expression still remained unaltered in both MDCK-I and MDCK-II cells (Figure 5.10A).

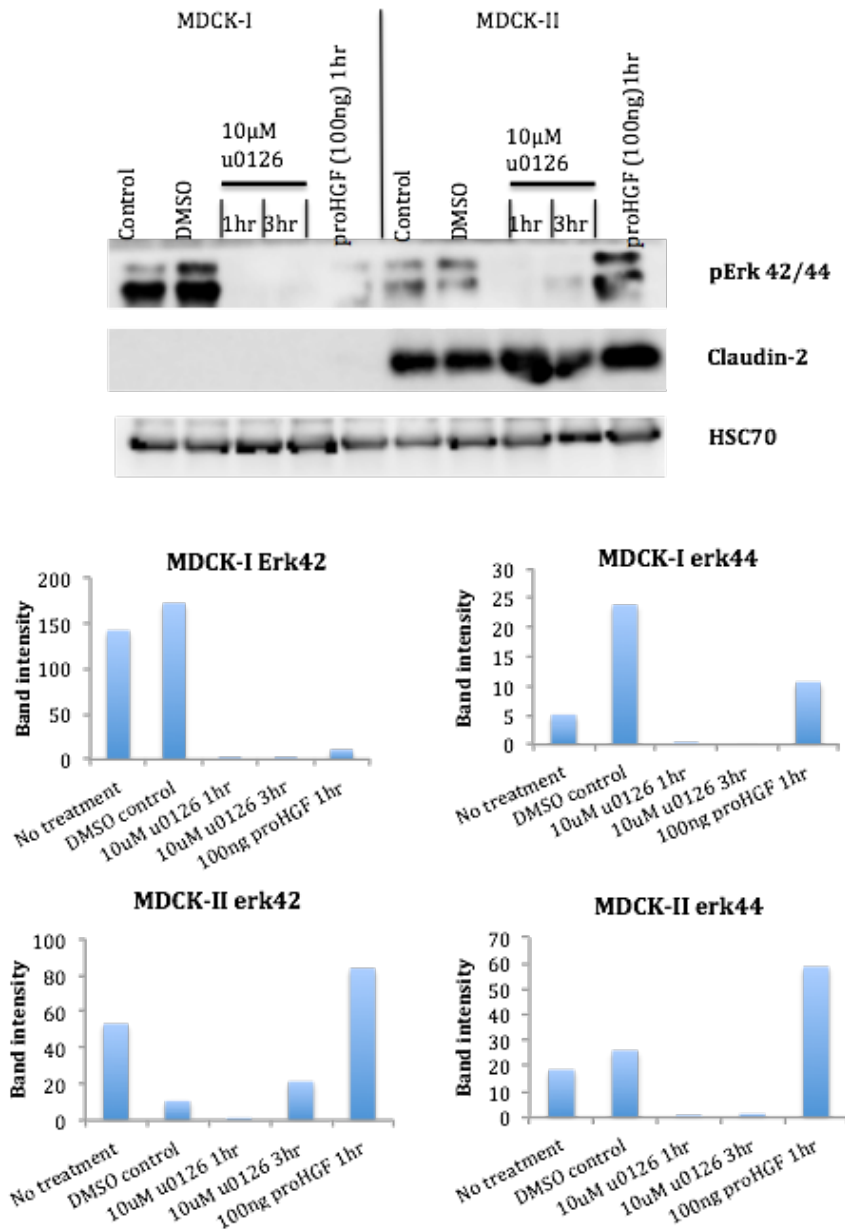


Figure 5.8 Intrinsic pERK activity and effect on claudin-2 expression in MDCK-I and MDCK-II cells.

Levels of intrinsic p-ERK p42/p44 were detected by western analysis of whole cell protein lysate samples from confluent MDCK-I and MDCK-II cell cultures. MDCK-I and MDCK-II cells were subject to either 1 or 3 hour treatment with u0126 (10 µM) for inhibition of pErk or 1 hour stimulation by pro-HGF (100 ng/ml). Western blots were probed with pERK and claudin-2 antibodies using non-reduced samples, with HSC-70 used as a loading control. Intensity of individual bands was measured using Image-J software and presented in the bottom bar charts.

5.2.6.2 Pro-HGF activation, stimulation and regulation of claudin-2 expression in MDCK-I and MDCK-II cells.

The intrinsic activity of pERK was determined to be significantly higher in MDCK-I cells compared to MDCK-II cells, which is thought to reduce cell line sensitivity to HGF stimulation and was shown to be required for their high TEER. As HGF activation is directly influenced by matriptase activity, further analysis to determine response to HGF signaling and its effect on pERK and claudin-2 expression in MDCK cells was carried out. Prolonged treatment of MDCK-I and MDCK-II cells seeded on 6 well culture plates with pro-HGF (sample 15 from S2 cells) for 1 or 8 hours, induced a small increase in pERK in MDCK-I cells (better seen in Figure 5.10C) although a much higher induction was found in MDCK-II cells, but this disappeared by 8 hours, despite growth factor replenishment every 2 hours (Figure 5.10B). However, stimulation by pro-HGF did not lead to a decrease in claudin-2 expression, as this remained unchanged in both cell lines at all time-points. Again, this is in contrast to the previous published observations (Lipschutz et al., 2005).

5.2.7 c-Met activity and function in MDCK-I and MDCK-II cells

To determine whether the lower HGF sensitivity and the intrinsic phosphorylation of pERK in MDCK-I cells is due to c-met phosphorylation, the levels of active c-Met and effect of inhibition on pERK and claudin-2 were examined. Also if these were found higher in MDCK-I cells it may explain their lower sensitivity to HGF stimulation and high intrinsic pERK activity. Phosphorylation of c-Met at tyrosine 1234/1235, present in the kinase domain and required for receptor biological activity was examined to investigate the level of activity under normal serum or serum-free conditions in MDCK-I and MDCK-II cells. Western blot analysis of Tyr-1234/1235 phosphorylated c-Met showed significantly higher phosphorylation in MDCK-II cells compared to MDCK-I in serum (Figure 5.10D). In the absence of serum this difference in the level of c-Met phosphorylation was not observed as indicated by measurements of protein intensity relative to Hsc-70 loading control (Figure 5.10D).

Therefore, surprisingly c-Met phosphorylation is found much higher in the presence of serum (as it probably contains HGF), in MDCK-II cells, which express lower pERK activation compared to MDCK-I cells. While phospho-c-Met levels became similar under serum free conditions between those cells, inhibition of its tyrosine kinase activity in MDCK-I cells using the chemical inhibitor PHA66752 was found to exclusively reduce intrinsic activity of pERK, more so than MDCK-II cells, and without altering claudin-2 expression (Figure 5.10D). These data suggest that the higher intrinsic phosphorylation of ERK in MDCK-I cells is largely dependent on the intrinsic activation of c-Met.

Therefore although the difference in c-Met phosphorylation appears to underlie the higher levels of pERK in MDCK-I cells, this was not the same for MDCK-II cells despite showing similar levels of the activated receptor without serum. This difference in c-Met therefore probably suggests a role for the receptor in barrier TEER formation in MDCK-I cells. Overall these findings support the observation with the u0126 inhibitor experiments, which represent findings that are distinct to those by Lipschutz et al, which declare the HGF pathway as a mediator of the difference in claudin-2 dependent TEER in MDCK-I and MDCK-II cells (Lipschutz et al., 2005).

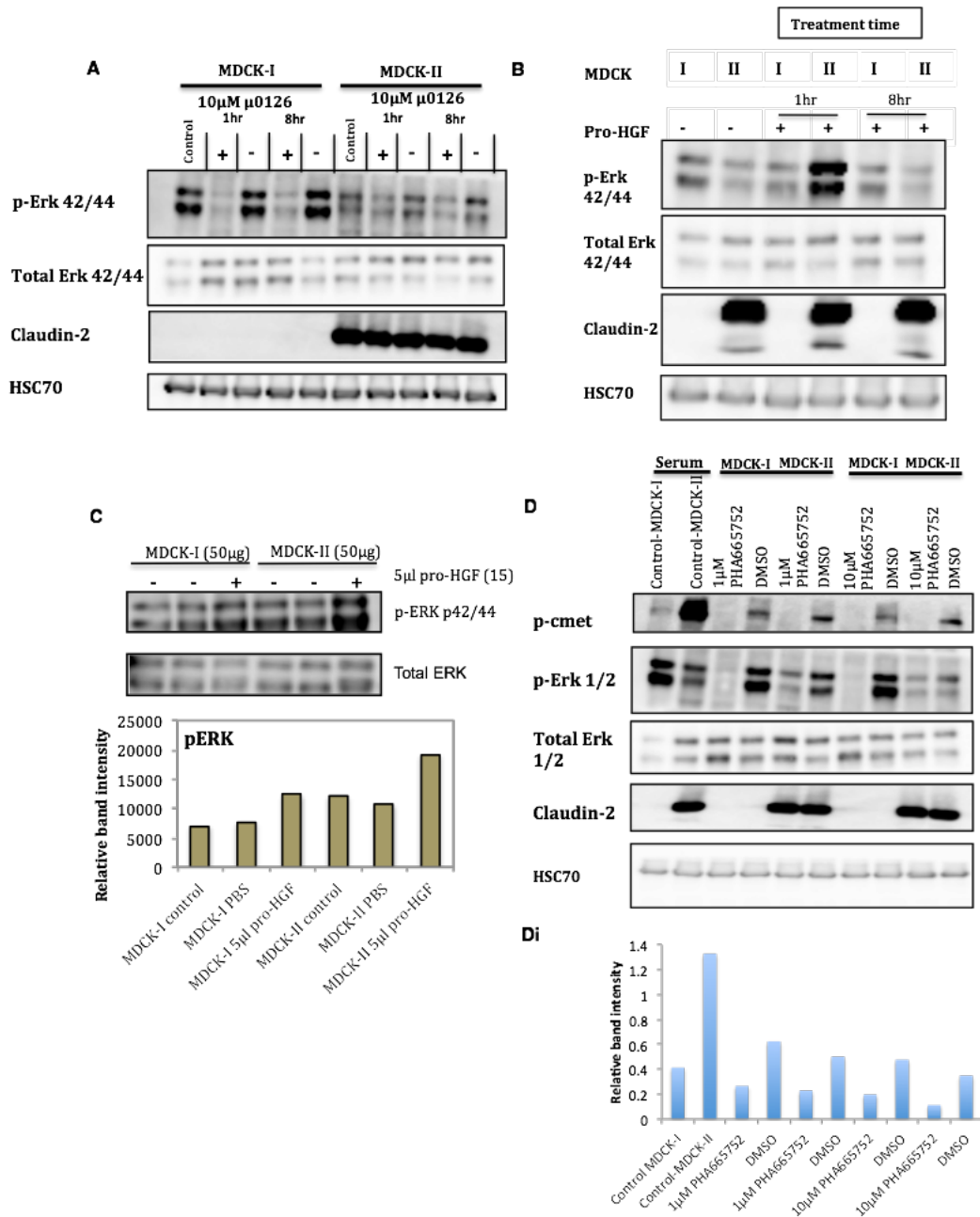


Figure 5.9 Intrinsic c-Met and p-ERK activity and regulation of claudin-2 expression in MDCK-I and MDCK-II cells.

A) Inhibition of intrinsic ERK phosphorylation with u0126 (10 µM) for 1 and 8 hours, after 4 hours serum starvation. Control MDCK-I and MDCK-II samples represent cells treated with DMSO for 8 hours. B) Serum-starved (4 hours) MDCK-I and MDCK-II cells were treated with recombinant pro-HGF (5 µl batch15 from S2 cells) for a period of 1 or 8 hours (with replenishment every 2 hours). Western blots for protein expression were analysed for p-ERK, total ERK and claudin-2. C) Repeated experiment for pERK following stimulation of MDCK-I and MDCK-II with pro-HGF for 2 hours. D) Effect of the c-Met inhibitor PHA665752 (1 and 10 µM) on levels of phosphorylated c-Met (Tyr1234/1235), p-ERK and claudin-2. Data are shown for MDCK-I and II cells. Di) Intensity of individual bands, relative to HSC-70 loading control was measured using Image-J software and presented in the bottom bar charts.

5.2.7.1 Function of intrinsically active pERK in MDCK-I barrier TEER development and recovery

Having established that that the selective MEK inhibitor u1026 was effective at lowering the levels of intrinsic pERK activity in MDCK-I cells, the role of pERK activity on initial epithelial barrier development was investigated by measurements of TEER. Initially, cells seeded on inserts were treated with 10 μ M u0126 (replenished every 24 hours) and TEER development showed an increase compared to control, however this was only conducted on duplicate inserts so no significant analysis was carried (Figure 5.11A). During calcium switch and recovery, MDCK-I treated with u0126 often showed a small delay in TEER during early recovery (up to 5 hours), however this delay was very small and therefore it was difficult to calculate the significant value. Soon after, TEER recovery became similar to control treated MDCK-I cells (Figure 5.11 B). However MDCK-II cells treated with 10 μ M u0126 also showed a small delay during early recovery of TEER, but later appear to recover to reestablish higher TEER compared to control treated cells (Figure 5.11 C).

Furthermore, during barrier recovery of MDCK-I cells treated with or without the matriptase inhibitor CJ-1737, no significant change in the levels of activated pERK were observed throughout the time course between the two conditions (Figure 5.12C). However pERK activation levels did appear to be slightly increased by calcium depletion and loss of TEER compared to the initial fully polarized. Therefore it appears that levels of intrinsic pERK have little or no effect on the establishment or recovery of barrier integrity.

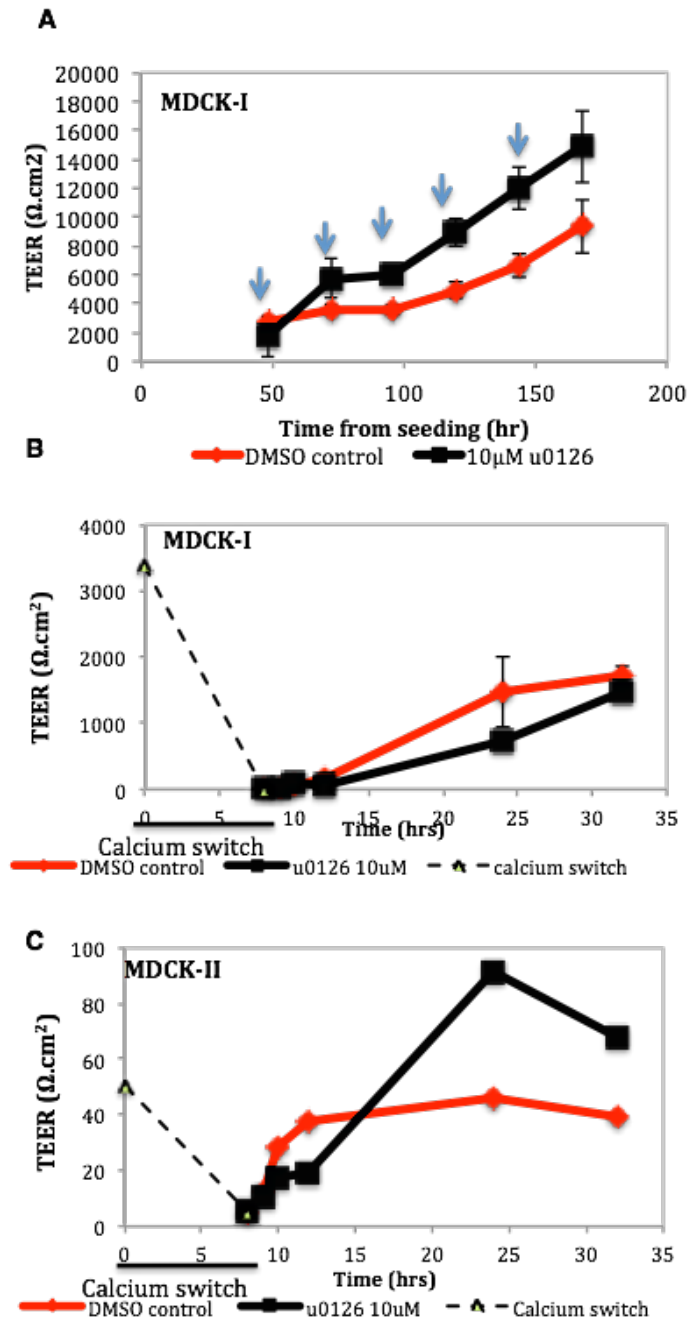


Figure 5.10 Intrinsic p-ERK inhibition during MDCK-I barrier development and repair in MDCK-I and MDCK-II cells.

A) MDCK-I cells were seeded at 50000 cells per insert and treated with u0126 (10 μM) 30 minutes before calcium repletion. u0126 was replenished every 24 hours (after each TEER measurement), as shown by arrows. B and C) MDCK-I and MDCK-II cells were subject to calcium switch after the establishment of maximum TEER and treated with u0126 30 minutes before calcium repletion and during calcium repletion. Data are expressed as mean \pm S.E. (A n=2, B n=3 C n=4 : D n=1).

5.2.7.2 c-Met role in MDCK-I and II barrier recovery following calcium switch

Having found that inhibition of c-Met activity affects intrinsic pERK levels in MDCK-I cells, its effect on barrier recovery following calcium switch was studied. Some studies divide over whether c-Met functions in promoting paracellular integrity or is involved in the loss of permeability in polarised epithelia. In our experiments treatment of MDCK-I monolayers with the c-Met inhibitor PHA665752 (referred to as c-Meti) at 0.2, 1 or 10 μM final concentration, added both 30 minutes before and during calcium repletion, led to a short delay in TEER recovery (Figures 5.12A, Ai and Aii). At 1 and 10 μM treatment with PHA665752, a small delay in TEER recovery was induced in MDCK-I cells up to 5 hours of recovery. TEER measurements after 5 hours were not significantly different from the control (Figure 5.12A). Inhibition of c-Met activity in MDCK-II cells however, had no effect on TEER recovery (Figure 5.12C).

Although the effect of c-Met inhibition of MDCK-I barrier recovery was smaller to that shown by the matriptase inhibitors CJ-1737 and IN-1, it could still play a role. Therefore, to link the function of c-Met to matriptase, level of c-Met receptor phosphorylation during barrier recovery of MDCK-I cells treated with or without matriptase inhibitor CJ-1737 was analysed by western blots. This showed no consistent change between the treated and untreated samples at different time points. Although, it is worth mentioning that one western blot showed a slightly more intense band for phosphorylated c-Met at 5 hours in the presence of matriptase inhibitor, but the bands from different time points do not appear to differ much in intensity (Figure 5.12B). However it was difficult to confirm this as often we struggle to detect any bands from TEER lysates using the same antibody used on extracts from cells not used in Transwell experiments.

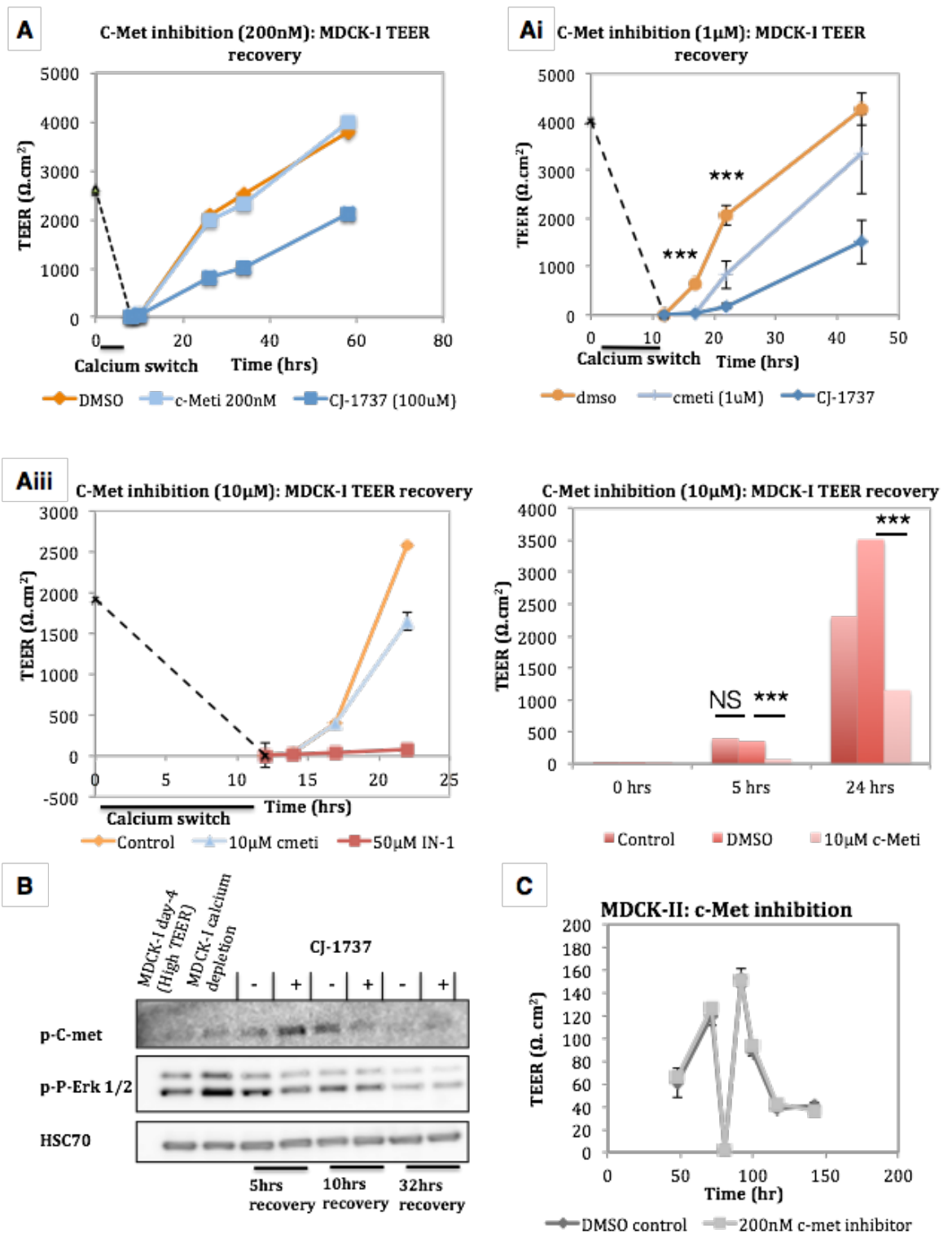


(Figure legend on the next page)

Figure 5.11 Intrinsic c-Met activity and p-ERK levels control over claudin-2 expression in MDCK-I and MDCK-II cells.

A, Ai and Aii) The c-Met inhibitor PHA665752 or the matriptase inhibitors CJ-1737 and IN-1 were applied to MDCK-I cell monolayers 30 minutes before and during calcium repletion at 200nM, 1 μ M and 10 μ M (also presented in bar graph). Control cells were treated with DMSO. B) Phosphorylation of c-Met at Tyr 1234/1235 in the kinase domain of the receptor was analysed on western blots of MDCK-I lysates from before and during calcium switch, and during recovery with and without CJ-1737. Samples were taken from the TEER experiments. pERK and HSC-70, as a sample loading control, are also shown. C) Monolayer recovery assays carried on MDCK-II cells subject to treatment with PHA665752 (200 nM) following calcium switch (indicated by arrow). N.S. $p > 0.05$ and ***= $P < 0.05$.

5.2.8 HGF stimulation effect on MDCK barrier recovery and role during matriptase inhibition

To investigate further into whether the c-Met pathway plays a role during matriptase mediated MDCK-I TEER recovery, the role of HGF activity was investigated further by treating the cells with active human HGF (rhHGF, 100 ng/ml). This was done with and without matriptase inhibitors, with the aim of determining whether HGF could reverse the effect of matriptase inhibition on barrier recovery. Analysis of TEER showed that MDCK-I cells displayed the expected delay in TEER reestablishment when inhibited by either of the matriptase inhibitors (CJ-1737 or IN-1), and that HGF treatment did not reverse this effect caused by matriptase inhibition (Figure 5.13). In these experiments TEER recovery was not significantly different to matriptase inhibitor alone despite rhHGF treatment. Additionally, HGF treatment alone did not have any effect on TEER compared to controls, in contrast to the previous findings (Lipschutz *et al.*, 2005).

Overall, these experiments appear to rule out HGF as a signaling target in the matriptase pathway to promote MDCK-I barrier recovery from injury induced by calcium depletion.

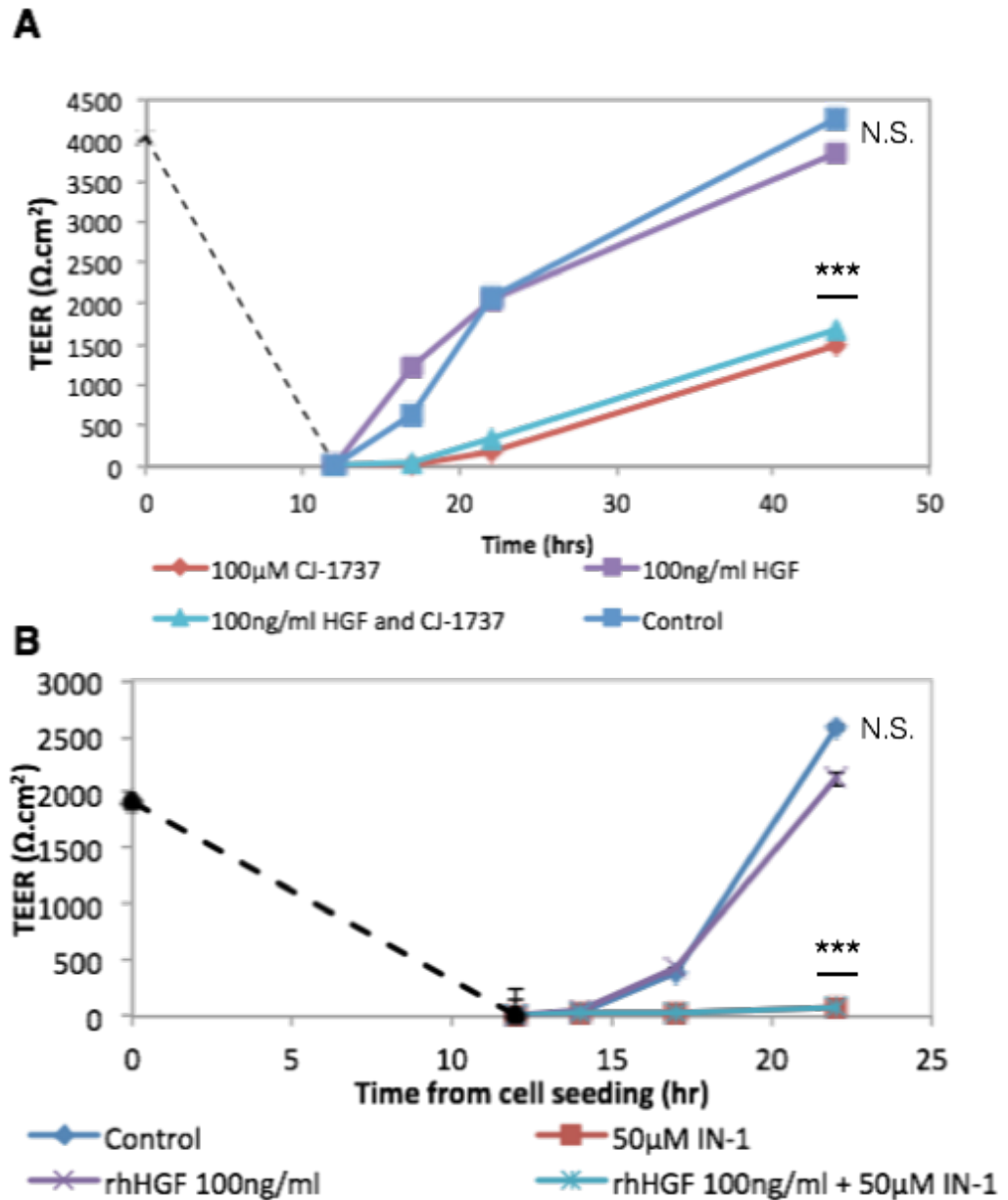


Figure 5.12 Role of HGF signaling in recovery of TEER in MDCK-I monolayers.

A) MDCK-I monolayers were treated with either active HGF (100 ng/ml), CJ-1737 (100 µM) or both, 30 minutes before calcium depletion and during calcium depletion. B) MDCK-I monolayers were treated with either active HGF (100 ng/ml), IN-1 (50 µM) or both, 30 minutes before calcium depletion and during calcium depletion. Control monolayers were treated with PBS/BSA. Data are expressed as mean ± S.E. (n=3). N.S. p > 0.05 and ***= P<0.05.

5.2.9 Effect of matriptase inhibition on receptor tyrosine kinase phosphorylation in MDCK-I cells during recovery from calcium switch

In a further attempt to dissect the potential mechanism through which matriptase mediates barrier re-establishment of MDCK-I cells, a chemiluminescence-based RTK protein detection array was used to determine phosphorylation of these kinases. The protein samples used were taken from TEER assays conducted with the matriptase inhibitors CJ-1737 and IN-1, as previously described. Protein from control and inhibitor treated MDCK-I cells at varying time points of recovery from calcium switch were applied to membrane arrays spotted with antibodies to a range of phosphorylated kinases. Following the manufacturer's guidelines, the antibody signal was detected using HRP-conjugated streptavidin and chemoluminescent detection, which revealed an organised array of dots with varying intensities (Figure 5.14A). An initial analysis with the CJ-1737 treated samples, which come from longer recovery time points (5, 10 and 32 hours) an increase only in STAT-1 was observed. STAT-1 is very much influence by IFN α (interferon- α) and IFN- γ , often elevated in response to cell stress (Dudley et al., 2004). However, when later examined with an independent western blot there was no detection of STAT-1 phosphorylated at Tyr-701 (Figure 5.14B). A positive control of IFN- γ treated MDCK-I cells was used in this experiment. Furthermore, STAT-1 showed no differences when the Pathscan array conducted for IN-1 treated MDCK-I cells.

Pathscan array was also conducted on protein samples from MDCK-I cells treated with IN-1 matriptase inhibitor. Samples taken at 1, 2, 5 and 10 hours post calcium switch displayed no consistent change in phosphorylated protein signal (Figure 5.15). Matriptase inhibitor treated samples did not display any differences in dot intensity at any of the time points, suggesting that none of the array signal pathways are likely downstream targets of matriptase in MDCK-I cells, particularly in promoting MDCK-I epithelial barrier recovery after disruption. It should be

noted however that this antibody array is designed for the detection of phosphorylated human proteins, and that although a positive signal was observed for many of the proteins, some of the negative signals could potentially be due to lack of recognition of the dog proteins.

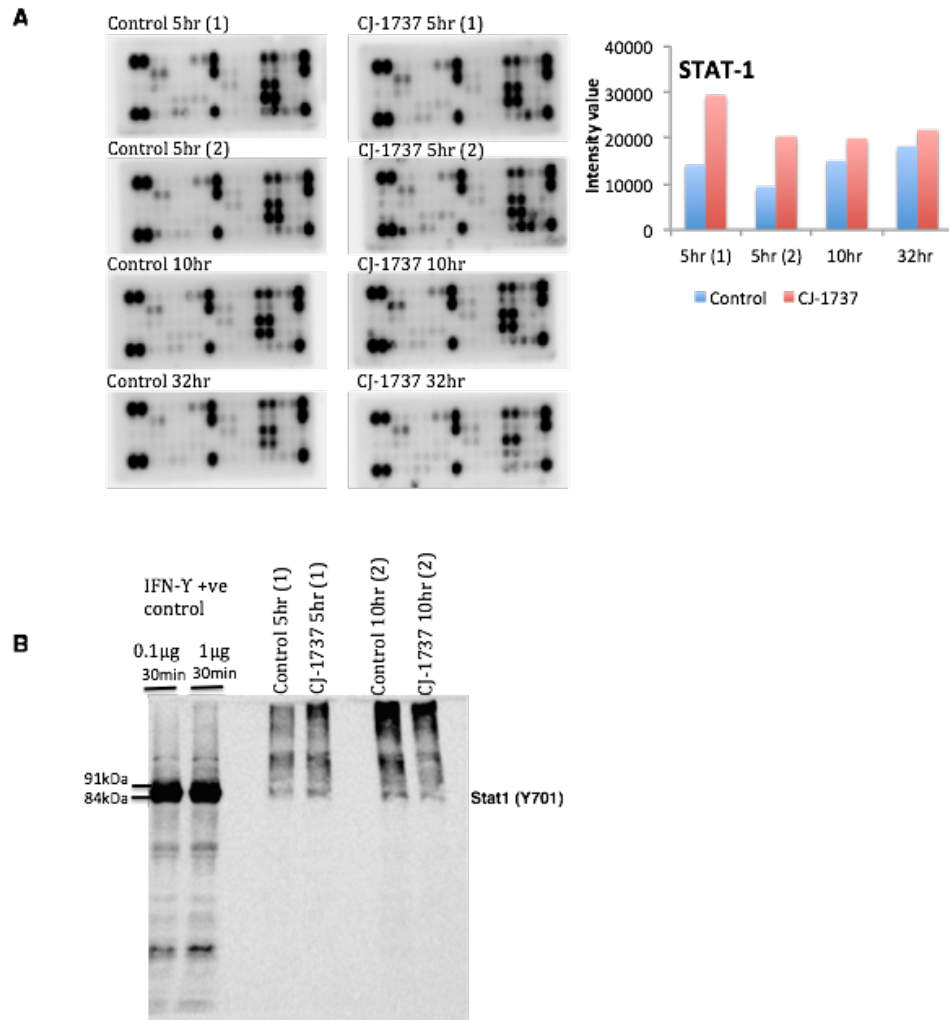


Figure 5.13 Effect of matriptase inhibition with CJ-1737 on protein kinase phosphorylation (Pathscan array).

A) Lysate was gathered from MDCK-I monolayers at 5 (repeated twice with lysates from independent samples), 10 and 32 hours recovery from calcium switch, with and without the matriptase inhibitor CJ-1737 (100 μ M). 150 μ g total protein (BCA assay) was applied to each membrane constructed with an array of antibodies to receptor tyrosine kinases and related signaling nodes. The assay was completed according to the manufacturer's instructions and membranes were imaged using HRP and chemiluminescence detection to reveal multiple dots with a range of intensities. B) Western blot for analysis of STAT-1 expression during barrier recovery with and without CJ-1737 in duplicate samples repeat of the 5-hour recovery time point. IFN- γ stimulated MDCK-I cells were used as positive control.

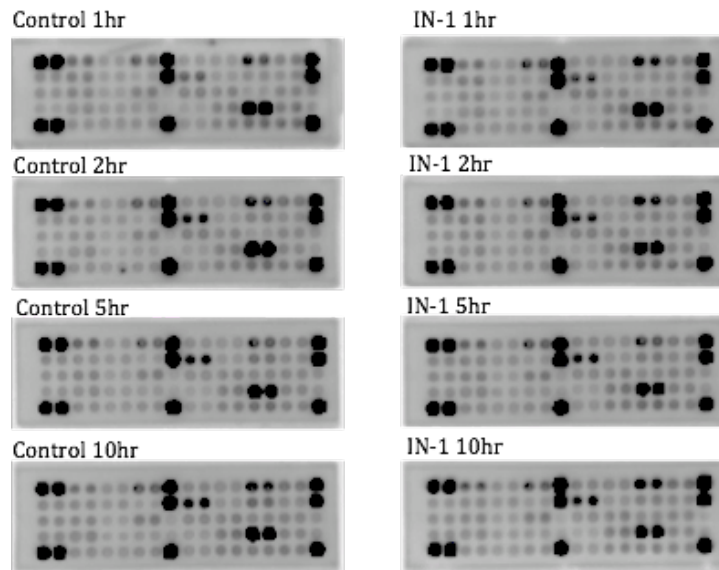


Figure 5.14 Effect of matriptase inhibition with IN-1 on protein kinase phosphorylation (Pathscan array).

Cell lysates gathered from MDCK-I monolayers at 1, 2, 5 and 10 hours recovery from calcium switch with and without treatment with the matriptase inhibitor IN-1 (50 μ M). 150 μ g total protein (BCA assay) was applied to each membrane constructed with an array of antibodies to receptor tyrosine kinases and related signaling nodes. The assay was completed according to manufacturer's instructions and membranes were imaged using HRP and chemiluminescence detection to reveal multiple dots with a range of intensities.

5.2.10 Cytokine and inflammatory receptor 384 Gene analysis array

Over the past decade, there has been an increasing recognition of an association between altered epithelial barrier tissue integrity and inflammation. Often clinical and experimental evidence shows that barrier dysfunction results in persistent inflammatory conditions, such as IBD. However, altered protein and enzyme function can also trigger innate inflammatory responses by epithelial cells, which can cause or enhance damage to the epithelial barrier system. The activity of some proteins is required for protection from cytokine damage, as previously proposed for matriptase. There appears to be a close relationship between matriptase and altered inflammatory cytokine expression, particularly in the intestine, as *in vivo* and *in vitro* studies have shown that reduced matriptase function results in a

persistent increase in inflammation after DSS-induced colitis (Netzel-Arnett et al., 2012). To study whether the effect of matriptase inhibition on MDCK-I epithelial recovery is mediated by cytokine signaling, a commercially available dog inflammatory cytokine qRT-PCR array was used to determine the expression of a wide range of cytokines.

This system uses SYBR Green detection that provides simultaneous analysis of 84 different genes from dog RNA samples (see Appendix 2). To study cytokine expression, RNA samples from control and IN-1 treated MDCK-I cells were collected at 1, 2, 5 and 10 hours recovery time points and equally loaded into the appropriate wells pre-printed with primers for the amplification of cytokine genes in dog. Following the manufacturer's instructions, analysis of the SYBR Green array data was determined relative to 18S rRNA as a housekeeping gene, based on the $2\Delta C_t$ method. Some of the relative expression measures for individual genes are presented in table A from Figure 5.16. The graphs in the right column provide a visualisation of the changes based on the relative expression between the different samples. Based on this, the array showed a strong decline in IL-1 β when MDCK-I cells were treated with the IN-1 matriptase inhibitor, and this was observed at the 1, 2 and 5 hour time points of recovery (Figure 5.16C). A small decrease was also observed for complement component 5 (C5), during early recovery time points of 1, 2, and 5 hours as demonstrated in Figure 5.16D. This protein is part of the both the classical and alternative complement pathways, which are part of the innate immune system. The levels of both of these genes (IL-1 β and C5) declined gradually during the recovery process in control cells.

The only gene that showed a significant increase in expression when matriptase was inhibited with IN-1 was IL-13. This had the largest effect at 1 hour of recovery, with smaller increase in expression observed at the 2 and 5 hours of recovery (Figure 5.16B).

An overall analysis of the array data, determined both as the raw C_t values and relative to 18S, showed that for many of the cytokines, expression was highest at the start of recovery, and this declined gradually as recovery increased. This indicates increased cytokine expression triggered by calcium depletion and loss of

MDCK-I barrier integrity, which decline upon barrier restitution. However, inhibition of matriptase only affected the expression of three cytokine genes, with IL-13 being increased and IL-1 β and complement component C5 being decreased.



(figure continues on next page)

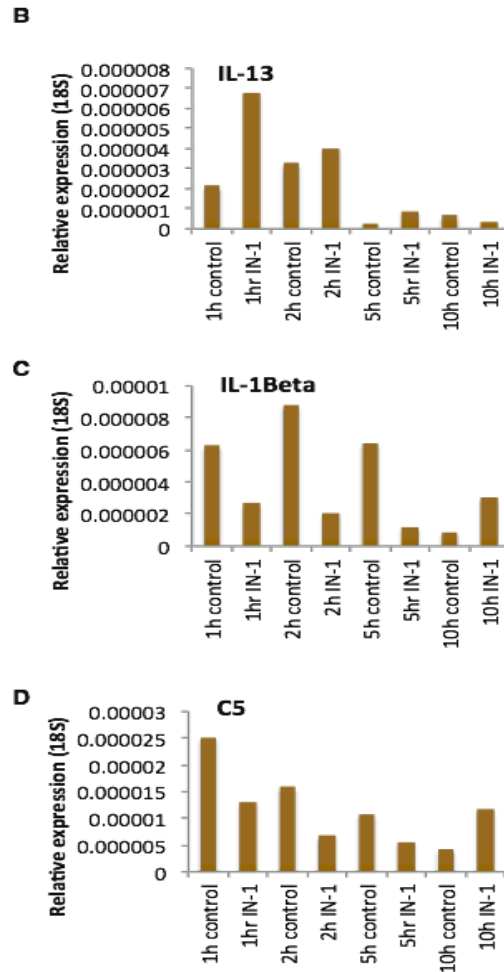


Figure 5.15 Effect of matriptase inhibition on the expression of inflammatory cytokines during MDCK-I barrier recovery assay.

A) MDCK-I total RNA was collected from inserts 1, 2, 5 and 10 hours following calcium repletion with and without treatment with the matriptase inhibitor IN-1 (50 μ M). Expression of cytokines was characterized using the inflammatory cytokine RT2 Sybr green gene profiler array designed specifically for detection of dog sequences. Detection was carried out according to the manufacturer's instructions. Dissociation (melting curve) curve analysis was also performed (see appendix 2). Expression was quantified relative to 18S rRNA as a house keeping gene and using the $2^{-\Delta C_t}$ method. The heat map table in A) displays genes that showed relatively high expression, determined through C_t values, and expression in each sample is highlighted from light to dark amber, with dark referring to higher expression (lower $C_t < 24$). Graphs on the right represent the changes in C_t values for each gene, with a higher C_t value representing lower expression. B) Bar charts representing the relative expression of selected genes, which showed a consistent change between control and matriptase inhibition. These were C5, IL-1 β , and IL-13 (see appendix 2 for table display of C_t values for every gene examined on the array).

5.3 Discussion

To summarize the main findings of this chapter:

- The cell surface substrates for matriptase previously shown to have a role in the regulation of epithelial barriers, PAR-2, prostasin and hepsin, are similarly expressed between MDCK-I and MDCK-II cells. In addition, no major changes in the mRNA expression levels of these substrates were observed during MDCK-I barrier recovery from calcium switch.
- Matriptase inhibition using two distinct types of inhibitor (CJ-1737 and IN-1) and the consequent delay in TEER recovery was not mediated by changes in prostasin activation. Protein analysis of prostasin expression and activation illustrated no difference during matriptase inhibition and barrier recovery. Western analysis of prostasin-inhibitor complexes, by avoiding heat denaturing, also revealed no change in protein intensity level between treated and control samples across all time points of recovery.
- The effect of amiloride and Inhibitor of uPA and ENaC during MDCK-I epithelial barrier reestablishment, showed no disruption to TEER recovery. However, occasionally a further increase in maximum TEER once the monolayers had fully restored was observed. This may be due to Na^+ and H^+ accumulation and inhibition of H^+ secretion attributed to hyperpolarization, as amiloride has been shown to also inhibit the Na^+/H^+ antiporter.
- Neither pro-HGF nor active HGF treatment of disrupted MDCK-I monolayers led to a significant effect on TEER recovery, despite pro-HGF facilitating cell migration in both strains of MDCK cells through matriptase activity. MDCK-I cells treated with both a matriptase inhibitor and active rhHGF still exhibited the same delay in TEER as those treated with matriptase inhibitor alone, suggesting that HGF is not relevant for barrier reestablishment following disruption by calcium switch.

- Intrinsic ERK phosphorylation was found to be significantly higher in MDCK-I compared to MDCK-II, yet Inhibition of pERK activity in MDCK-I cells was not found to be necessary for development, reestablishment of TEER or expression of claudin-2, in contrast to what has been published by one study, that particularly focused on this role (Lipschutz et al., 2005). Although a small delay during very early recovery of TEER in MDCK-I cells was detected upon the inhibition of c-Met, this was not the pathway of matriptase, as no changes were found in either the phosphorylation of c-met or pERK following matriptase inhibition.
- Further investigations into the role of PAR-2 downstream of matriptase were carried out. Treatment of cells with antagonist and agonist of PAR-2 had no significant effects on MDCK-I monolayer re-establishment from calcium switch.
- Analysis of dog inflammatory cytokine expression (96 genes) in MDCK-I cells during barrier recovery revealed a reduction in C5 and IL-1 β expression in MDCK-I cells treated with the matriptase inhibitor IN-1, while an increase in IL-13 was also observed. A higher expression of most cytokine genes was observed in recovering monolayer cells shortly after calcium switch, which declined as the barrier was re-established.

Data presented in Chapter 4 illustrated that proteolytic activity of matriptase plays a key role in maintenance of MDCK-I barrier integrity by promoting efficient recovery following disruption by calcium depletion. A similar effect has previously been observed in Caco-2 cells and attributed to an increase in claudin-2 expression (Buzza et al., 2010). However, this does not appear to be the mechanism in MDCK-I cells, as they have undetectable levels of claudin-2. In order to fully appreciate the role of matriptase in promoting MDCK-I barrier restitution following injury by calcium depletion, we must pursue a different mechanism. This candidate substrate approach study was conducted to provide insight into whether any of

the well-defined substrates of matriptase are involved in this epithelial recovery process mediated by matriptase expression and activity.

HGF/c-Met pathway:

Our group demonstrated the role of matriptase as an authentic activator of pro-HGF at the cell surface (Owen et al., 2010). Matriptase function in the HGF/c-Met signaling pathway has been strongly linked with matriptase-mediated epithelial oncogenesis, particularly highlighted in a study of human squamous cell carcinoma, where c-Met signaling is key (Szabo et al., 2011). HGF activation and signaling has multiple functions in epithelial cells, by regulating cell migration for processes such as wound healing, cell proliferation, and differentiation and maintenance of epithelial tissue integrity and homeostasis. Early studies of HGF highlighted its function in cell migration through MDCK-II cell scattering assays. We later showed that matriptase activity is key for this role, as the inhibition of the proteolytic activity in both MDCK-I and MDCK-II cells prevented pro-HGF mediated cell migration, but differences were found in downstream signal responses and sensitivities to pro-HGF stimulation.

Clearly, HGF plays a role in both MDCK-I and MDCK-II cells downstream of matriptase, but the aim here was to determine whether this activation is fundamental for barrier restitution by matriptase activity. In this chapter differences have been found in the sensitivity of MDCK-I and MDCK-II cells to HGF, whereby MDCK-I cells were less sensitive but displayed higher levels of activated pERK. This high intrinsic pERK activity is key in the ability of MDCK-I cells to differentiate and form tubules spontaneously in 3D culture independently of HGF, in contrast to the HGF-dependent process in MDCK-II cells (Webb et al., 1996). Furthermore, previous investigations into the different HGF sensitivities and levels of pERK activity concluded that these contributed to the differential development of TEER observed between MDCK-I and MDCK-II cells, by regulating claudin-2 levels (Lipschutz et al., 2005). It is worth noting that the literature contains multiple contradicting effects of HGF on barrier epithelia. Some indicate that HGF signaling is more important for cell-scattering and migration, while others show a

role in barrier differentiation and maintenance (Balkovetz et al., 1997, Pollack et al., 2004, Nusrat et al., 1994). As strong mediators of pro-HGF activation, MDCK cells provide a great model for studying the role of matriptase in HGF mediated epithelial barrier function. Therefore, the function of HGF, c-Met and pERK in MDCK-I barrier repair mediated by matriptase was investigated.

In MDCK-I monolayers, pERK activity did not appear to have a critical role in monolayer differentiation and TEER development, as inhibition of pERK had no effect on TEER formation, in contrast to what had previously been observed (Lipschutz et al., 2005). In a TEER recovery assay the inhibition of pERK or c-Met caused a small delay in early TEER recovery, in comparison to the powerful delay observed during matriptase inhibition. The total levels of both activated pERK and c-Met were not significantly changed by matriptase inhibition in recovering MDCK-I cells. This was also confirmed by the RTK Pathscan array, and neither were found to affect claudin-2 expression as had previously been proposed. Furthermore, HGF was not necessary for barrier recovery and did not change the effect of matriptase inhibition on MDCK-I TEER recovery, as shown when cells were treated with active HGF and matriptase inhibitors. From these finding and analysis of claudin-2 it can be concluded that this matriptase function in MDCK-I barrier maintenance is likely to be mediated by a mechanism independent of the HGF pathway.

Future studies may be directed to investigate whether matriptase activity takes part in the spontaneous initiation of primary tubulogenesis in MDCK-I cells and whether inhibition and knockdown alter tubule development, and therefore does loss of matriptase activity alter cell barrier formation in 3D cultured tubules. This could be studied using the stable knock down system developed here, where matriptase is permanently suppressed by shRNA in MDCK-I and MDCK-II cells.

Prostasin pathway:

Prostasin has been shown to work with matriptase as part of a single proteolytic pathway on the surface of epithelial cells, and carry a critical role in regulating epithelia development and homeostasis (Buzza et al., 2013, Chen et al., 2010b).

Prostasin activity is also tightly regulated in a similar fashion to matriptase, by the inhibitors HAI-1 and HAI-2 (Fan et al., 2005, Shipway et al., 2004). However, a number of studies have suggested that the hierarchical placement of matriptase and prostasin in the pathway differs between different epithelial barrier tissues (Friis et al., 2013). In polarised simple epithelial tissue, such as the intestine and kidney, matriptase and prostasin are separated by the apical and basal domains (Tsuzuki et al., 2005). It is not clear whether these proteases function together in mediating tissue function and maintenance, but one study showed evidence for matriptase transport to the apical surface, mediated by HAI-1 (Godiksen et al., 2008, Friis et al., 2011). However, it also is possible that during loss of tight junctions and domain separation, direct contact occurs between prostasin and matriptase, which may be part of an essential trigger for signaling toward epithelial repair that would either promote prostasin activation by matriptase and induced signaling or vice versa.

Although the same prostasin antibody used to detect prostasin activation in human and mouse protein samples by western blot also recognized the dog protein from MDCK cells, no change in the activated form was observed as a band of lower molecular weight (~37 kDa) in reducing conditions. This was analysed at 5, 10 and 32 hours of recovery from calcium switch and during matriptase inhibition. Analysis of the intensity of higher molecular weight bands in samples not subject to heat denaturation, to study active prostasin complex formation with endogenous inhibitors such as PN-1 of the serpin family, also revealed no specific difference between control and matriptase inhibition.

No evidence has been found to suggest that prostasin is activated by matriptase in MDCK cells, and from this it cannot be concluded that this is playing a role in MDCK-I barrier epithelia, particularly in MDCK-I barrier reestablishment. To study this further a construct could be developed for overexpression of PN-1 and further inhibitor complex interaction studies could be carried to determine if the activity of endogenous prostasin is affected by matriptase inhibition and plays a role during barrier reestablishment. Studies of the mechanistic and dynamic behaviour of both enzymes as well as their interactions in polarised cells and during MDCK-I

barrier recovery, will provide greater understanding of their role in such epithelia. Determining their localisation during barrier depletion and re-establishment with and without matriptase inhibition might illustrate whether these proteins can interact when the barrier is disrupted and cell polarity is compromised. With the future availability of specific prostasin and matriptase antibodies for detection of dog matriptase, these could be utilized to study into the relevance of their reciprocal function and domain specific localisation in MDCK-I barrier development and maintenance. Furthermore, cell-surface biotin labeling or optimized PI-PLC release of GPI-anchored prostasin to determine level of protein expressed at the cell surface during TEER assay can be applied in the presence of the necessary tools for detection in these MDCK cells.

Prostasin enzymatic activity and GPI anchorage in the kidney epithelia has been shown to be essential in regulating transepithelial ion transport using model kidney collecting duct cells (M-1 cells) (Vergheze et al., 2006). In the airways and kidney, prostasin function is critical for regulating sodium homeostasis and fluid transport via activating ENaC (Tong et al., 2004). A previous study by Chen et al used amiloride, which is a potassium sparing diuretic, to further characterise the electrophysiological properties of MDCK cells, revealing that they expressed amiloride sensitivity that is comparable with other kidney cell lines such as the mouse principle cell of kidney cortical collecting duct (mpkCCD) (Chen et al., 2013). In the experiments described here, treatment of MDCK-I cells with amiloride did not inhibit the recovery of TEER as with matriptase inhibition, but ultimately raised the maximum TEER formed once the barrier was fully reestablished. Although the mechanism underlying this increase in maximum TEER is not well explored, it is generally accepted that a measured increase in TEER reflects an increase in ionic transfer across epithelia. This increase in maximum TEER is probably due to the accumulation of sodium and potassium cations in the apical medium, which also affects fluid flux consequently changing electrical resistance. Therefore, in MDCK-I cells, the ultimate inhibition of TEER recovery caused by loss of matriptase activity, is not likely to be driven by changes in sodium reabsorption or consequent loss of fluid homeostasis. Therefore regulation of ion driven fluid balance is unlikely to be the major factor in the

matriptase dependent function in the development or re-establishment of barrier integrity and TEER.

PAR-2 and inflammation:

Immune homeostasis is a key part of epithelial barrier regulation. The onset of uncontrolled inflammation has been previously associated with altered matriptase function and influences gut and skin barrier homeostasis (Netzel-Arnett et al., 2012). This inflammatory response requires the activation of PAR-2 at the cell surface, which plays a major role in mediating inflammatory signals. PAR-2 activation has been shown to play an essential role in matriptase driven pre-malignant progression of Ras-mediated squamous cell carcinomas, through induction of NF κ B (Sales et al., 2014). In endothelial cells activation of PAR-2 by exogenous matriptase was found to mediate pro-inflammatory IL-6 and IL-8 expression (Seitz et al., 2007), which have been implicated in tight junction regulation and permeability in endothelial and epithelial cells (Al-Sadi et al., 2014, Yu et al., 2013). Furthermore, activation of PAR-2 has been shown to mediate loss of epidermal barrier function and promote ichthyosis instigated by prostasin overexpression in transgenic mice (Frateschi et al., 2011). It is necessary to point out that although matriptase functions in promoting barrier integrity, in most epithelia PAR-2 activation promotes pro-inflammatory effects and a loss of barrier integrity. However, it has recently been shown that matriptase/PAR-2 mediated proteolytic signaling plays a critical role in placental epithelial establishment of a foeto-maternal epithelial barrier, involving regulation of the paracellular tight junction protein claudin-1 (Szabo et al., 2014).

In our analysis of PAR-2 signaling and its impact on barrier recovery during matriptase inhibition in MDCK-I cells, we show that inhibition of PAR-2 with the antagonist ENMD-1068 does not affect TEER recovery. Similarly the PAR-2 peptide agonist furoyl-LIGRL-NH₂ treatment did not alter TEER recovery following calcium switch in MDCK-I cells. PAR-2 activation by the peptide agonist also did not abolish or reduce the effect of matriptase inhibition on recovery of TEER in MDCK-I cells. These observations suggest that it is unlikely that PAR-2 activation has a role in

matriptase-mediated MDCK-I barrier reestablishment after disruption with calcium switch. An attempt was made to analyze PAR-2 protein expression in recovering MDCK-I cells, however, the antibody failed to detect protein in western blot possibly due to its species specificity. However gene expression analysis might suggest a small increase shortly after calcium repletion and TEER recovery (1, 2, and 5 hours), during matriptase inhibition with the IN-1 inhibitor.

Inflammatory cytokine expression during MDCK-I recovery

In the DSS-induced experimental colitis model carried out on matriptase hypomorphic mice, an induction of claudin-2 expression was observed in the leaky gut tissue, which may be an indirect effect resulting from prolonged injury and inflammatory response (Netzel-Arnett et al., 2012). Therefore, it remains unclear whether matriptase function is mediated through a common mechanism in the intestine *in vivo* and the MDCK-I cell model. Thus it was important to determine whether there is an innate inflammatory response to matriptase inhibition during recovery of MDCK-I cells is altered.

Cytokines can be produced by a wide variety of cells including epithelial cells, which also serve as paracrine target cells for cytokines. Cytokines can induce potent effects. Inflammatory cytokines have been shown to play a central role in inflammatory processes in many epithelial tissues, and particularly the intestinal epithelia. Previous studies have shown IL-1 β to increase tight junction permeability of intestinal epithelia *in vivo* and *in vitro*, acting through the NF κ B pathway (Al-Sadi et al., 2010, Al-Sadi et al., 2008). However, during matriptase inhibition and altered recovery of MDCK-I barrier integrity, IL-1 β expression was significantly down regulated in MDCK-I cells. This could mean that the intrinsic regulation of these cytokines can mediate different functions and responses, which may be protective and important in epithelial repair. However, a role for IL-1 β and other cytokines (e.g. TGF β) in restitution of epithelial wounds *in vitro* has also been shown (Dignass and Podolsky, 1993). Therefore the observed decrease in IL-1 β expression could be a compensatory mechanism to ensure non-persistent effects produced by pro-inflammatory signals on recovery of barrier integrity by

MDCK-I cells. Epithelial repair following short-term injury is a rapid response, independent of cell proliferation, and some cytokines have been shown to play a role in promoting this process and establishing the continuity of the epithelial surface. Therefore IL-1 β could be an important mediator downstream of matriptase during injury in MDCK-I cells. The expression of IL-1 β at the protein level needs to be confirmed during matriptase inhibition and recovery of TEER, and studied during injury by calcium depletion, to investigate whether its levels are affected immediately after matriptase inhibition in MDCK-I cells. Also recombinant IL-1 β could be used in these assays to elucidate its role in matriptase-mediated barrier repair function.

5.4 Conclusion

The substrate approach taken in an attempt to elucidate the mechanism through which matriptase regulates MDCK-I barrier recovery, excluded the involvement of the candidate substrates studied. Here, altering the activation and signaling of the candidate substrates pro-HGF, PAR-2, prostasin, ENaC, and EGFR in MDCK-I is not required for mediating barrier restitution following calcium switch. Additional analysis of the activity of various important signaling RTKs and downstream effector nodes did not display any significant changes upon early and late recovery during matriptase inhibition, potentially excluding many of these pathways as candidates in the mechanism through which matriptase mediates its effect. Yet, gene expression analysis of 84 proinflammatory cytokines in MDCK cells, presented some potential new candidates, likely not as substrates, but potentially as mediators of the effect in MDCK-I cells. The presented changes include elevated expression of IL-13, which has been shown to be key in ulcerative colitis and epithelial restitution.

Chapter 6. General discussion and future direction

Matriptase plays an important role in regulating epithelial barrier tissue development, function and maintenance. Studies have converged to highlight the significance of the tight regulation of matriptase activity in this tissue, as both insufficient and excess matriptase proteolytic activity are equally detrimental to mouse epithelia and result in tissue dysfunction and onset of diseases such as cancer, ichthyosis and inflammatory bowel disease. Dysregulation of matriptase has been shown to influence two main types of epithelial barrier tissues, the epidermis and the intestinal epithelia. However the mechanism through which matriptase mediates epidermal barrier function is better understood, as evidence merged supporting a matriptase-prostasin proteolytic cascade in terminal epidermal differentiation (Netzel-Arnett et al., 2006), however little is known mechanistically about how matriptase regulates simple epithelial barrier development and function. The aim of this work were to dissect the role of matriptase *in vitro* using MDCK model lines of simple barrier epithelia, using various inhibitor and through the generation of an shRNA knockdown model.

In the recent study published by our group describing the biological activity of the matriptase inhibitor MCoTI-II, we have used MDCK cells as a model to study HGF activation/scattering. Inhibition by MCoTI-II revealed intrinsic matriptase activity in MDCK-II cells, by preventing pro-HGF and activation and the resulting cell scatter (Gray et al., 2014). Therefore, as a model of tight junction assembly we addressed the question of whether matriptase had a role in barrier function in MDCK-I cells.

Is the effect of matriptase on MDCK barrier function dependent on the tight junction, and more importantly claudin-2?

In MDCK-I cells matriptase inhibition using the same specific inhibitor of matriptase used in the MDCK-II pro-HGF scatter assay, MCoTI-II, a cyclic microprotein from the squash *M. cochinchinesis* family of trypsin inhibitors, had no effect on the establishment of TEER and only a minor effect on the maximum TEER developed. A large effect however was observed during MDCK-I monolayer repair from disruption caused by calcium switch. Here, the inhibition of matriptase activity significantly delayed barrier recovery of TEER and the restoration of integrity toward diffusion of macromolecular 4 kDa FITC-dextran during calcium repletion. Previously, *in vivo* studies have shown that deficiency of matriptase altered the establishment of intestinal barrier integrity, and also weakened its response and tolerance to stress (Netzel-Arnett et al., 2012). Consequently, the tissue's ability to re-establish a similar level of integrity to that found prior to injury was compromised. This effect is a consequence of the establishment of leaky tight junctions correlating with an increased expression of claudin-2, which was proposed to be due to PKC- ζ (Netzel-Arnett et al., 2012; Buzza et al., 2010). These findings suggested a tight junction regulatory function for matriptase, involving claudin-2.

A major difference between MDCK-I and MDCK-II cells is the expression of claudin-2 and its incorporation into tight junctions in the latter, which is responsible for the large difference in TEER between these cells. The two strains of MDCK cells therefore potentially provide an excellent comparative model system for elucidating the roles of matriptase and claudin-2 in controlling their characteristic epithelial permeability. Although these two cell lines have similar levels of endogenous matriptase mRNA, it was observed that they did not respond in the same way to matriptase inhibition. Here, treatment of MDCK-I and MDCK-II cells with several inhibitors of matriptase with varying potencies and mechanisms of action only altered barrier recovery function in MDCK-I cells and not MDCK-II. Although this effect was initially thought to be due to the lack of claudin-2, which may be switched on with matriptase inhibition in MDCK-I cells, analysis of

protein levels during recovery showed no changes in control and inhibitor treated cells.

Due to the strong link previously observed between matriptase and claudin-2 (Buzza et al., 2010), we conducted studies to determine if matriptase function in MDCK-I cells is dependent on this protein. Inducible expression of claudin-2 in MDCK-I cells was found to significantly lower TEER, confirming previous studies (Yu et al., 2009), and we found that inhibition of matriptase activity affected MDCK-I barrier recovery of TEER occurs regardless of whether they expressed claudin-2 in a stable inducible model system. Therefore, contrary to previous findings, matriptase appears to be able to mediate tight barrier function and maintenance of paracellular integrity independently of claudin-2, based on these findings in MDCK cells (described in chapter 4).

Furthermore, close morphological and structural analysis of MDCK-I cells treated with matriptase inhibitors showed no effect on the total expression or distribution of other essential tight junction components, adhesion junction components and both microtubule and actin cytoskeleton structures. This suggested that matriptase function could be mediated via a specific molecular response pathway that provides an effect on paracellular integrity reestablishment following stress. Therefore we conducted a wide analysis using a phospho-signaling protein array examining some key RTKs and downstream signaling nodes. Although initially the array carried out on MDCK-I samples treated with the matriptase inhibitor CJ-1737 gave slight differences in protein intensities, the repeated assay using protein samples from cells treated with inhibitor IN-1 (IN-1) showed no significant changes. It is worth noting that some protein signals in the array did not show any reactivity. This could be explained either by lack of expression, failed detection of dog protein, or that the cells required stimulation by specific growth factors.

Is matriptase function in MDCK-I cells dependent on its known substrates?

- Prostasin

In stratified epithelia, matriptase function is dependent on the activation of prostasin and subsequent processing of pro-filaggrin and tight junction formation. Although pro-filaggrin is a skin associated molecule and is only found in that tissue, prostasin is not, and in fact it is found to be coexpressed with matriptase in most epithelial tissues (List et al., 2007b). In the polarised epithelia the activity of both proteases has been shown to regulate barrier integrity. One study by Buzza et al, discussed the reciprocal function of prostasin and matriptase in promoting barrier integrity in Caco-2 model (Buzza et al., 2013). Here they showed that matriptase promoted barrier integrity is independent of prostasin and yet inversely prostasin mediated barrier function is dependent on matriptase (Buzza et al., 2013).

Prostasin protein is abundant in MDCK-I cells, however expression and activation of prostasin in MDCK-I cells following recovery from calcium switch, was not changed during matriptase inhibition. However, under non-reduced conditions, often two bands close in molecular weight (40-37 kDa) were observed and during early (5 hours) and medium (10 hours) recovery time points a higher intensity lower band (~37 kDa) was observed. The nature of this band can be further examined by conducting an immunoprecipitation, requiring a validated antibody, and mass spectrometry, but it is unlikely to be the active form. The study of prostasin's function in a polarised epithelial system remains unclear. In these cells prostasin is clearly located at the apical surface, while matriptase is predominantly found at the basolateral surface. Although Friis et al showed that active matriptase can briefly localize with prostasin at the apical surface in Caco-2 cells, it is also plausible that they can colocalise during the loss of barrier polarization and after disruption (Friis et al., 2011). This could trigger reciprocal activation and signaling by the two enzymes and therefore may be important for barrier reestablishment, presenting possibly a new mechanism to study in this epithelial system.

A recent study by Buzza *et al* proposed an upstream function of prostasin to indirectly activate matriptase in the simple and polarised epithelia, proposing that matriptase is the primary effector of barrier assembly and integrity in Caco-2 cells and yet downstream signaling targets remain unknown (Buzza *et al.*, 2013). Therefore MDCK-I cells with stable matriptase knockdown can be utilized to study this mechanism further.

Furthermore, prostasin is a potent activator of the amiloride-sensitive ENaC, which is an important regulator of salt and fluid balance in the lung, kidney and epidermis (Verghese *et al.*, 2006, Bruns *et al.*, 2007, Hummler *et al.*, 1996, Tong *et al.*, 2004, Charles *et al.*, 2008). Therefore the role of prostasin and ENaC in mediating MDCK-I barrier TEER re-establishment was studied by treatment of MDCK-I monolayers with the ENaC inhibitor amiloride. However, this treatment did not show any delay in barrier recovery of TEER, suggesting that matriptase function in mediating MDCK-I epithelial barrier re-establishment is not enabled through the activation of ENaC. It is worth noting that matriptase was shown to increase the activity of ENaC directly when expressed in *Xenopus* oocytes (Vuagniaux *et al.*, 2002). The two proteins however are expressed at different membrane domains in polarised epithelial cells with prostasin being apically located together with ENaC (Nimishakavi *et al.*, 2012, Friis *et al.*, 2011, Clark *et al.*, 2010). ENaC activity is very important in the regulation of renal Na⁺ reabsorption and fluid homeostasis, therefore prostasin and matriptase may still function in the regulation of this channel function in MDCK-I cells, but this may be independent of role in maintenance of paracellular permeability.

-HGF

In epithelial cells HGF, which is directly activated by matriptase as part of surface proteolysis, has been shown to play a role in regulating barrier function and permeability. One particular study highlighted this role in MDCK cells where they found that HGF treatment enhanced barrier integrity and increased TEER of polarised MDCK-II epithelial monolayers due to p-ERK signaling (Lipschutz *et al.*, 2005). This study linked this effect with a change in claudin-2 expression, as found activation of the HGF/c-Met/p-ERK response inhibited the intrinsic expression of

claudin-2, causing an increase in TEER (Lipschutz et al., 2005). This study also found that the HGF pathway plays a role in enhancing TEER, and is relevant in MDCK-I cells, which form high TEER monolayers. These were shown to have high intrinsic p-ERK activity what was linked to the suppressed expression of claudin-2 and essential for their high TEER (Lipschutz et al., 2005). As matriptase is a very important activator of HGF and mediator of HGF/c-Met signaling with a relevant role in cancer, the effect of this pathway on MDCK TEER recovery was investigated.

Using the TEER recovery assay it was shown that treatment of both MDCK-I and MDCK-II monolayers with HGF or pro-HGF did not alter TEER recovery, nor counteracts the delay in recovery of TEER caused by matriptase inhibition in MDCK-I cells. However based on the protein analysis, which showed high intrinsic pERK activity in MDCK-I cells, which interestingly was found to be dependent on the intrinsic phosphorylation of c-Met, the role of c-Met and pERK inhibition on MDCK-I barrier recovery of TEER was investigated. Although the inhibition of c-Met often produced a slight delay in early TEER recovery, the analysis of c-Met phosphorylation upon TEER recovery with matriptase inhibitor revealed no change in activity, and similarly with pERK activity. Therefore c-Met and pERK activation is unlikely mediated downstream of matriptase during MDCK-I barrier reestablishment.

It is important to mention that the analysis of this pathway in MDCK-I and MDCK-II cells also revealed that inhibited or induced p-ERK activity by HGF stimulation, had no effect on claudin-2 expression in both MDCK-I and MDCK-II cells, contradicting previous findings by Lipschutz et al (Lipschutz et al., 2005). Overall this suggests that HGF function is not required for re-establishment of TEER in MDCK-I cells, and therefore that the proteolytic activation of HGF is not the mechanism by which matriptase exerts its effect.

However, the data presented in this study confirmed differences in HGF-mediated responses between MDCK-I and MDCK-II cells. Therefore, these model cells may provide a useful tool for future studies of the complexity of this pathway in relation to matriptase function possibly corresponding to different biological responses, for

example differences in HGF signaling and cell migration or tubulogenesis in a 3D environment.

The candidate-substrate approach, overall, demonstrated that matriptase function in mediating MDCK-I barrier recovery is independent of the activation of pro-HGF/c-Met, prostasin, ENaC, EGFR, uPA and PAR-2.

Does matriptase activity regulate MDCK-I barrier recovery through controlling inflammatory signals?

It is well known that the maintenance of the integrity of epithelial barrier tissue relies on many elements, including a highly controlled innate immune response. Often the loss of tissue integrity manifested in many pathological diseases including IBD, is accompanied by uncontrolled chronic inflammation (reviewed in (Pastorelli et al., 2013)). Reduced levels of matriptase expression have been linked with IBD, and a reduced tolerance in the intestinal epithelial tissue of matriptase hypomorphic mice during experimental colitis, due to persistent inflammation (Netzel-Arnett et al., 2012). This persistence colitis and loss of immune homeostasis is known to be responsible for facilitating further damage and prevention of tissue repair. Therefore, the loss of the ability of MDCK-I cells to recover a tight epithelial barrier, following calcium switch, when matriptase is inhibited could potentially be mediated via a persistent inflammatory signal. Conduction of a multiple inflammatory cytokine quantitative gene analysis on MDCK-I cells during recovery from calcium switch revealed a few deviations in some cytokines under matriptase inhibition. A persistent decline in complement component C5 and IL-1 β levels was observed as well as an increase in IL-13, all during early recovery at 1, 2 and 5 hours. A few studies have highlighted that elevation of these cytokines or inflammatory molecules can enhance epithelial barrier permeability (Al-Sadi et al., 2010, Al-Sadi et al., 2008, Saatian et al., 2013, Heller et al., 2005). In particular IL-13 is shown to be key in ulcerative colitis, shown to alter tight junctions and impair epithelia barrier function and restitution (Heller et al., 2005). Hence it could be involved in the mechanism through which matriptase mediates its effects on MDCK-I barrier integrity.

The observed decline in the expression of IL-1 β and C5 may be part of a compensation mechanism to prevent further epithelial damage and aid barrier recovery, and may be a consequence of the physiological state of the barrier monolayer rather than of matriptase inhibition. It is important to mention that these cytokines come from intrinsic gene activation; while *in vivo* these are mostly released by inflammatory cells rather than epithelial cells and therefore depending on origin these may be exerting different functions, and therefore their role here will require further investigation.

6.1 Conclusion and future work

To summarize, the experiments described in this thesis provide an insight into the function of matriptase in the MDCK model of simple polarised epithelial barriers. A fundamental role for matriptase in the re-establishment of barrier integrity in MDCK-I cells, which form a very tight epithelial barrier, was apparent, but not MDCK-II cells. Investigation into the influence of matriptase inhibition on barrier paracellular physiology revealed that the influence on MDCK-I cells is not due to altered expression and assembly of various components of the tight junction and adhesion junctions. In contrast to the observations in other cell lines we have also demonstrated that the increased barrier permeability and reduced ability of MDCK-I cells to recover when subjected to different types of matriptase inhibitors is independent of claudin-2 expression. Studies of substrate function also revealed that the effect on MDCK-I barrier function occurs independently of the known substrates of matriptase. Thus, a conclusion can be made that matriptase function in polarised epithelial barrier maintenance is conserved across multiple cell lines and that the mechanism is likely to be independent of known downstream cell-surface activation events, including those of pro-HGF/c-Met, PAR-2, ENaC, EGFR and uPA. Whether prostasin activation still holds a role in this function requires further investigation, with validated custom tools for studying the endogenous protease in MDCK-I cells.

Continuation of this work will include elucidating the primary function of matriptase; whether long term ablation (i.e. stable knockdown) of matriptase affects any aspect of the structural development of MDCK-I barriers; to study effect on important molecular component in barrier rescue, including the family of RhoGTPases, which serve as key components in the important mechanism of epithelial polarity. Additionally, further work is required to investigate whether matriptase affects other components of the tight junction complexes, and one such way is to study their expression by using designed arrays similar to the RT²profiler PCR array used on cytokines analysis. It is important to also confirm and further investigate the role of cytokines IL-13 and IL-1 β on barrier recovery in MDCK-I cells, during inhibition and knockdown of matriptase. Also, dog specific protein analysis tools for matriptase could be established to investigate clearly the dynamic behavior of matriptase during the establishment, loss and reestablishment of epithelial polarization. So far this work has answered several questions with regards to matriptase's role in different epithelial barrier systems. This work also raised further questions regarding this role but at the same time revealed further stepping stones to increase the understanding of the complex function of the widely important TTSP, Matriptase.

References

- ADACHI, M., KITAMURA, K., MIYOSHI, T., NARIKIYO, T., IWASHITA, K., SHIRAIISHI, N., NONOGUCHI, H. & TOMITA, K. 2001. Activation of epithelial sodium channels by prostasin in *Xenopus* oocytes. *J Am Soc Nephrol*, 12, 1114-21.
- AL-SADI, R., YE, D., BOIVIN, M., GUO, S., HASHIMI, M., EREIFEJ, L. & MA, T. Y. 2014. Interleukin-6 modulation of intestinal epithelial tight junction permeability is mediated by JNK pathway activation of claudin-2 gene. *PLoS One*, 9, e85345.
- AL-SADI, R., YE, D., DOKLADNY, K. & MA, T. Y. 2008. Mechanism of IL-1beta-induced increase in intestinal epithelial tight junction permeability. *J Immunol*, 180, 5653-61.
- AL-SADI, R., YE, D., SAID, H. M. & MA, T. Y. 2010. IL-1beta-induced increase in intestinal epithelial tight junction permeability is mediated by MEKK-1 activation of canonical NF-kappaB pathway. *Am J Pathol*, 177, 2310-22.
- ALEF, T., TORRES, S., HAUSSER, I., METZE, D., TURSEN, U., LESTRINGANT, G. G. & HENNIES, H. C. 2009. Ichthyosis, follicular atrophoderma, and hypotrichosis caused by mutations in ST14 is associated with impaired profilaggrin processing. *J Invest Dermatol*, 129, 862-9.
- AMASHEH, S., MEIRI, N., GITTER, A. H., SCHONEBERG, T., MANKERTZ, J., SCHULZKE, J. D. & FROMM, M. 2002. Claudin-2 expression induces cation-selective channels in tight junctions of epithelial cells. *Journal of Cell Science*, 115, 4969-4976.
- ANDERSON, J. M. & VAN ITALLIE, C. M. 1995. Tight junctions and the molecular basis for regulation of paracellular permeability. *Am J Physiol*, 269, G467-75.
- ANDREASEN, D., VUAGNIAUX, G., FOWLER-JAEGER, N., HUMMLER, E. & ROSSIER, B. C. 2006. Activation of epithelial sodium channels by mouse channel activating proteases (mCAP) expressed in *Xenopus* oocytes requires catalytic activity of mCAP3 and mCAP2 but not mCAP1. *J Am Soc Nephrol*, 17, 968-76.
- BACALLAO, R., ANTONY, C., DOTTI, C., KARSENTI, E., STELZER, E. H. & SIMONS, K. 1989. The subcellular organization of Madin-Darby canine kidney cells during the formation of a polarized epithelium. *J Cell Biol*, 109, 2817-32.
- BACHOVCHIN, D. A. & CRAVATT, B. F. 2012. The pharmacological landscape and therapeutic potential of serine hydrolases. *Nat Rev Drug Discov*, 11, 52-68.
- BALKOVETZ, D. F., POLLACK, A. L. & MOSTOV, K. E. 1997. Hepatocyte growth factor alters the polarity of Madin-Darby canine kidney cell monolayers. *J Biol Chem*, 272, 3471-7.
- BASEL-VANAGAITE, L., ATTIA, R., ISHIDA-YAMAMOTO, A., RAINSHTEIN, L., BEN AMITAI, D., LURIE, R., PASMNIK-CHOR, M., INDELMAN, M., ZVULUNOV, A., SABAN, S., MAGAL, N., SPRECHER, E. & SHOHAT, M. 2007. Autosomal recessive ichthyosis with hypotrichosis caused by a mutation in ST14, encoding type II transmembrane serine protease matriptase. *Am J Hum Genet*, 80, 467-77.

- BEAULIEU, A., GRAVEL, E., CLOUTIER, A., MAROIS, I., COLOMBO, E., DESILETS, A., VERREAULT, C., LEDUC, R., MARSAULT, E. & RICHTER, M. V. 2013. Matriptase proteolytically activates influenza virus and promotes multicycle replication in the human airway epithelium. *J Virol*, 87, 4237-51.
- BEHRENS, M. A., BOTKJAER, K. A., GOSWAMI, S., OLIVEIRA, C. L., JENSEN, J. K., SCHAR, C. R., DECLERCK, P. J., PETERSON, C. B., ANDREASEN, P. A. & PEDERSEN, J. S. 2011. Activation of the Zymogen to Urokinase-Type Plasminogen Activator Is Associated with Increased Interdomain Flexibility. *J Mol Biol*.
- BEN-YOSEF, T., BELYANTSEVA, I. A., SAUNDERS, T. L., HUGHES, E. D., KAWAMOTO, K., VAN ITALLIE, C. M., BEYER, L. A., HALSEY, K., GARDNER, D. J., WILCOX, E. R., RASMUSSEN, J., ANDERSON, J. M., DOLAN, D. F., FORGE, A., RAPHAEL, Y., CAMPER, S. A. & FRIEDMAN, T. B. 2003. Claudin 14 knockout mice, a model for autosomal recessive deafness DFNB29, are deaf due to cochlear hair cell degeneration. *Hum Mol Genet*, 12, 2049-61.
- BENAUD, C., DICKSON, R. B. & LIN, C. Y. 2001. Regulation of the activity of matriptase on epithelial cell surfaces by a blood-derived factor. *Eur J Biochem*, 268, 1439-47.
- BENSON, K., CRAMER, S. & GALLA, H. J. 2013. Impedance-based cell monitoring: barrier properties and beyond. *Fluids Barriers CNS*, 10, 5.
- BERGUM, C. & LIST, K. 2010. Loss of the matriptase inhibitor HAI-2 during prostate cancer progression. *Prostate*, 70, 1422-8.
- BLIKSLAGER, A. T., ROBERTS, M. C. & ARGENZIO, R. A. 1999. Prostaglandin-induced recovery of barrier function in porcine ileum is triggered by chloride secretion. *American Journal of Physiology-Gastrointestinal and Liver Physiology*, 276, G28-G36.
- BOCHEVA, G., RATTENHOLL, A., KEMPKES, C., GOERGE, T., LIN, C. Y., D'ANDREA, M. R., STANDER, S. & STEINHOFF, M. 2009. Role of matriptase and proteinase-activated receptor-2 in nonmelanoma skin cancer. *J Invest Dermatol*, 129, 1816-23.
- BOHM, S. K., KONG, W., BROMME, D., SMEEKENS, S. P., ANDERSON, D. C., CONNOLLY, A., KAHN, M., NELKEN, N. A., COUGHLIN, S. R., PAYAN, D. G. & BUNNETT, N. W. 1996. Molecular cloning, expression and potential functions of the human proteinase-activated receptor-2. *Biochem J*, 314 (Pt 3), 1009-16.
- BOTTARO, D. P., RUBIN, J. S., FALETTO, D. L., CHAN, A. M. L., KMIECIK, T. E., VANDEWOUDE, G. F. & AARONSON, S. A. 1991. Identification of the Hepatocyte Growth-Factor Receptor as the C-Met Protooncogene Product. *Science*, 251, 802-804.
- BROUARD, M., CASADO, M., DJELIDI, S., BARRANDON, Y. & FARMAN, N. 1999. Epithelial sodium channel in human epidermal keratinocytes: expression of its subunits and relation to sodium transport and differentiation. *J Cell Sci*, 112 (Pt 19), 3343-52.
- BRUNS, J. B., CARATTINO, M. D., SHENG, S., MAAROUF, A. B., WEISZ, O. A., PILEWSKI, J. M., HUGHEY, R. P. & KLEYMAN, T. R. 2007. Epithelial Na⁺ channels are fully activated by furin- and prostaticin-dependent release of an inhibitory peptide from the gamma-subunit. *J Biol Chem*, 282, 6153-60.
- BUENO, L. & FIORAMONTI, J. 2008. Protease-activated receptor 2 and gut permeability: a review. *Neurogastroenterol Motil*, 20, 580-7.

- BUGGE, T. H., ANTALIS, T. M. & WU, Q. 2009. Type II transmembrane serine proteases. *J Biol Chem*, 284, 23177-81.
- BUGGE, T. H., LIST, K. & SZABO, R. 2007. Matriptase-dependent cell surface proteolysis in epithelial development and pathogenesis. *Front Biosci*, 12, 5060-70.
- BUZZA, M. S., MARTIN, E. W., DRIESBAUGH, K. H., DESILETS, A., LEDUC, R. & ANTALIS, T. M. 2013. Prostasin Is Required for Matriptase Activation in Intestinal Epithelial Cells to Regulate Closure of the Paracellular Pathway. *Journal of Biological Chemistry*, 288, 10328-10337.
- BUZZA, M. S., NETZEL-ARNETT, S., SHEA-DONOHUE, T., ZHAO, A., LIN, C. Y., LIST, K., SZABO, R., FASANO, A., BUGGE, T. H. & ANTALIS, T. M. 2010. Membrane-anchored serine protease matriptase regulates epithelial barrier formation and permeability in the intestine. *Proc Natl Acad Sci U S A*, 107, 4200-5.
- CAMERER, E., BARKER, A., DUONG, D. N., GANESAN, R., KATAOKA, H., CORNELISSEN, I., DARRAGH, M. R., HUSSAIN, A., ZHENG, Y. W., SRINIVASAN, Y., BROWN, C., XU, S. M., REGARD, J. B., LIN, C. Y., CRAIK, C. S., KIRCHHOFER, D. & COUGHLIN, S. R. 2010. Local protease signaling contributes to neural tube closure in the mouse embryo. *Dev Cell*, 18, 25-38.
- CAO, J., CAI, X., ZHENG, L., GENG, L., SHI, Z., PAO, C. C. & ZHENG, S. 1997. Characterization of colorectal-cancer-related cDNA clones obtained by subtractive hybridization screening. *J Cancer Res Clin Oncol*, 123, 447-51.
- CARTER, P. & WELLS, J. A. 1988. Dissecting the catalytic triad of a serine protease. *Nature*, 332, 564-8.
- CEREIJIDO, M., ROBBINS, E. S., DOLAN, W. J., ROTUNNO, C. A. & SABATINI, D. D. 1978. Polarized monolayers formed by epithelial cells on a permeable and translucent support. *J Cell Biol*, 77, 853-80.
- CHARLES, R. P., GUITARD, M., LEYVRAZ, C., BREIDEN, B., HAFTEK, M., HAFTEK-TERREAU, Z., STEHLE, J. C., SANDHOFF, K. & HUMMLER, E. 2008. Postnatal requirement of the epithelial sodium channel for maintenance of epidermal barrier function. *J Biol Chem*, 283, 2622-30.
- CHEN, M., CHEN, L. M., LIN, C. Y. & CHAI, K. X. 2008. The epidermal growth factor receptor (EGFR) is proteolytically modified by the Matriptase-Prostasin serine protease cascade in cultured epithelial cells. *Biochim Biophys Acta*, 1783, 896-903.
- CHEN, M., CHEN, L. M., LIN, C. Y. & CHAI, K. X. 2010a. Hepsin activates prostaticin and cleaves the extracellular domain of the epidermal growth factor receptor. *Mol Cell Biochem*, 337, 259-66.
- CHEN, X., ZHU, H., LIU, X., LU, H., LI, Y., WANG, J., LIU, H., ZHANG, J., MA, Q. & ZHANG, Y. 2013. Characterization of two mammalian cortical collecting duct cell lines with hopping probe ion conductance microscopy. *J Membr Biol*, 246, 7-11.
- CHEN, Y. W., WANG, J. K., CHOU, F. P., CHEN, C. Y., RORKE, E. A., CHEN, L. M., CHAI, K. X., ECKERT, R. L., JOHNSON, M. D. & LIN, C. Y. 2010b. Regulation of the matriptase-prostasin cell surface proteolytic cascade by hepatocyte growth factor activator inhibitor-1 during epidermal differentiation. *J Biol Chem*, 285, 31755-62.
- CHO, E. G., KIM, M. G., KIM, C., KIM, S. R., SEONG, I. S., CHUNG, C., SCHWARTZ, R. H. & PARK, D. 2001. N-terminal processing is essential for release of epithin, a mouse type II membrane serine protease. *J Biol Chem*, 276, 44581-9.

- CHOKKI, M., YAMAMURA, S., EGUCHI, H., MASEGI, T., HORIUCHI, H., TANABE, H., KAMIMURA, T. & YASUOKA, S. 2004. Human airway trypsin-like protease increases mucin gene expression in airway epithelial cells. *Am J Respir Cell Mol Biol*, 30, 470-8.
- CLARK, E. B., JOVOV, B., ROOJ, A. K., FULLER, C. M. & BENOS, D. J. 2010. Proteolytic cleavage of human acid-sensing ion channel 1 by the serine protease matriptase. *J Biol Chem*, 285, 27130-43.
- COLLARES-BUZATO, C. B., JEPSON, M. A., MCEWAN, G. T., HIRST, B. H. & SIMMONS, N. L. 1998. Co-culture of two MDCK strains with distinct junctional protein expression: a model for intercellular junction rearrangement and cell sorting. *Cell Tissue Res*, 291, 267-76.
- COLOMBO, E., DESILETS, A., DUCHENE, D., CHAGNON, F., NAJMANOVICH, R., LEDUC, R. & MARSAULT, E. 2012. Design and Synthesis of Potent, Selective Inhibitors of Matriptase. *Acs Medicinal Chemistry Letters*, 3, 530-534.
- D'ANDREA, M. R., DERIAN, C. K., LETURCQ, D., BAKER, S. M., BRUNMARK, A., LING, P., DARROW, A. L., SANTULLI, R. J., BRASS, L. F. & ANDRADE-GORDON, P. 1998. Characterization of protease-activated receptor-2 immunoreactivity in normal human tissues. *J Histochem Cytochem*, 46, 157-64.
- DE FALCO, L., SANCHEZ, M., SILVESTRI, L., KANNENGIESSER, C., MUCKENTHALER, M. U., IOLASCON, A., GOUYA, L., CAMASCHELLA, C. & BEAUMONT, C. 2013. Iron refractory iron deficiency anemia. *Haematologica*, 98, 845-53.
- DENKER, B. M. & NIGAM, S. K. 1998. Molecular structure and assembly of the tight junction. *Am J Physiol*, 274, F1-9.
- DESILETS, A., BELIVEAU, F., VANDAL, G., MCDUFF, F. O., LAVIGNE, P. & LEDUC, R. 2008. Mutation G827R in matriptase causing autosomal recessive ichthyosis with hypotrichosis yields an inactive protease. *J Biol Chem*, 283, 10535-42.
- DIBONA, D. R. & CIVAN, M. M. 1973. Pathways for movement of ions and water across toad urinary bladder. I. Anatomic site of transepithelial shunt pathways. *J Membr Biol*, 12, 101-28.
- DIGNASS, A. U. & PODOLSKY, D. K. 1993. Cytokine modulation of intestinal epithelial cell restitution: central role of transforming growth factor beta. *Gastroenterology*, 105, 1323-32.
- DONATE, L. E., GHERARDI, E., SRINIVASAN, N., SOWDHAMINI, R., APARICIO, S. & BLUNDELL, T. L. 1994. Molecular evolution and domain structure of plasminogen-related growth factors (HGF/SF and HGF1/MSP). *Protein Sci*, 3, 2378-94.
- DONG, N., FANG, C., JIANG, Y., ZHOU, T., LIU, M., ZHOU, J., SHEN, J., FUKUDA, K., QIN, J. & WU, Q. 2013. Corin mutation R539C from hypertensive patients impairs zymogen activation and generates an inactive alternative ectodomain fragment. *J Biol Chem*, 288, 7867-74.
- DOUVILLE, N. J., TUNG, Y. C., LI, R., WANG, J. D., EL-SAYED, M. E. & TAKAYAMA, S. 2010. Fabrication of two-layered channel system with embedded electrodes to measure resistance across epithelial and endothelial barriers. *Anal Chem*, 82, 2505-11.
- DUDLEY, A. C., THOMAS, D., BEST, J. & JENKINS, A. 2004. The STATs in cell stress-type responses. *Cell Commun Signal*, 2, 8.
- DUKES, J. D., WHITLEY, P. & CHALMERS, A. D. 2011. The MDCK variety pack: choosing the right strain. *BMC Cell Biol*, 12, 43.

- ELLIS, V., BEHRENDT, N. & DANO, K. 1991. Plasminogen activation by receptor-bound urokinase. A kinetic study with both cell-associated and isolated receptor. *J Biol Chem*, 266, 12752-8.
- ELLIS, V. & DANO, K. 1993. Potentiation of plasminogen activation by an anti-urokinase monoclonal antibody due to ternary complex formation. A mechanistic model for receptor-mediated plasminogen activation. *J Biol Chem*, 268, 4806-13.
- ELLIS, V., SCULLY, M. F. & KAKKAR, V. V. 1987. Plasminogen activation by single-chain urokinase in functional isolation. A kinetic study. *J Biol Chem*, 262, 14998-5003.
- ELLIS, V., SCULLY, M. F. & KAKKAR, V. V. 1989. Plasminogen activation initiated by single-chain urokinase-type plasminogen activator. Potentiation by U937 monocytes. *J Biol Chem*, 264, 2185-8.
- ENCK, A. H., BERGER, U. V. & YU, A. S. L. 2001. Claudin-2 is selectively expressed in proximal nephron in mouse kidney. *American Journal of Physiology-Renal Physiology*, 281, F966-F974.
- ENJOJI, S., OHAMA, T. & SATO, K. 2014. Regulation of Epithelial Cell Tight Junctions by Protease-Activated Receptor 2. *J Vet Med Sci*.
- ERLIJ, D. & MARTINEZ-PALOMO, A. 1972. Opening of tight junctions in frog skin by hypertonic urea solutions. *J Membr Biol*, 9, 229-40.
- FAN, B., WU, T. D., LI, W. & KIRCHHOFER, D. 2005. Identification of hepatocyte growth factor activator inhibitor-1B as a potential physiological inhibitor of prostatic growth. *Journal of Biological Chemistry*, 280, 34513-34520.
- FANG, X., FUKUDA, N., BARBRY, P., SARTORI, C., VERKMAN, A. S. & MATTHAY, M. A. 2002. Novel role for CFTR in fluid absorption from the distal airspaces of the lung. *J Gen Physiol*, 119, 199-207.
- FARQUHAR, M. G. & PALADE, G. E. 1963. Junctional complexes in various epithelia. *J Cell Biol*, 17, 375-412.
- FORBS, D., THIEL, S., STELLA, M. C., STURZEBECKER, A., SCHWEINITZ, A., STEINMETZER, T., STURZEBECKER, J. & UHLAND, K. 2005. In vitro inhibition of matriptase prevents invasive growth of cell lines of prostate and colon carcinoma. *Int J Oncol*, 27, 1061-70.
- FRATESCHI, S., CAMERER, E., CRISANTE, G., RIESER, S., MEMBREZ, M., CHARLES, R. P., BEERMANN, F., STEHLE, J. C., BREIDEN, B., SANDHOFF, K., ROTMAN, S., HAFTEK, M., WILSON, A., RYSER, S., STEINHOFF, M., COUGHLIN, S. R. & HUMMLER, E. 2011. PAR2 absence completely rescues inflammation and ichthyosis caused by altered CAP1/Prss8 expression in mouse skin. *Nat Commun*, 2, 161.
- FRIIS, S., GODIKSEN, S., BORNHOLDT, J., SELZER-PLON, J., RASMUSSEN, H. B., BUGGE, T. H., LIN, C. Y. & VOGEL, L. K. 2011. Transport via the transcytotic pathway makes prostatic growth factor activator inhibitor-1B available as a substrate for matriptase. *J Biol Chem*, 286, 5793-802.
- FRIIS, S., SALES, K. U., GODIKSEN, S., PETERS, D. E., LIN, C. Y., VOGEL, L. K. & BUGGE, T. H. 2013. A Matriptase-Prostatic Growth Factor Activator Inhibitor-1B Reciprocal Zymogen Activation Complex with Unique Features. PROSTATIC GROWTH FACTOR ACTIVATOR INHIBITOR-1B AS A NON-ENZYMATIC CO-FACTOR FOR MATRIPTASE ACTIVATION. *Journal of Biological Chemistry*, 288, 19028-19039.

- FRIIS, S., SALES, K. U., SCHAFER, J. M., VOGEL, L. K., KATAOKA, H. & BUGGE, T. H. 2014. The protease inhibitor HAI-2, but not HAI-1, regulates matriptase activation and shedding through prostasin. *J Biol Chem*.
- FRIZELLE, F. A. 2006. When does a specialist assume the "duty of care" for a patient? The significance of Case 04HDC13909. *N Z Med J*, 119, U2072.
- FUCHS, E. & RAGHAVAN, S. 2002. Getting under the skin of epidermal morphogenesis. *Nat Rev Genet*, 3, 199-209.
- FURUSE, M., FURUSE, K., SASAKI, H. & TSUKITA, S. 2001. Conversion of zonulae occludentes from tight to leaky strand type by introducing claudin-2 into Madin-Darby canine kidney I cells. *J Cell Biol*, 153, 263-72.
- FURUSE, M., HATA, M., FURUSE, K., YOSHIDA, Y., HARATAKE, A., SUGITANI, Y., NODA, T., KUBO, A. & TSUKITA, S. 2002. Claudin-based tight junctions are crucial for the mammalian epidermal barrier: a lesson from claudin-1-deficient mice. *J Cell Biol*, 156, 1099-111.
- GAUSH, C. R., HARD, W. L. & SMITH, T. F. 1966. Characterization of an established line of canine kidney cells (MDCK). *Proc Soc Exp Biol Med*, 122, 931-5.
- GHERARDI, E., GRAY, J., STOKER, M., PERRYMAN, M. & FURLONG, R. 1989. Purification of scatter factor, a fibroblast-derived basic protein that modulates epithelial interactions and movement. *Proc Natl Acad Sci U S A*, 86, 5844-8.
- GODIKSEN, S., SELZER-PLON, J., PEDERSEN, E. D. K., ABELL, K., RASMUSSEN, H. B., SZABO, R., BUGGE, T. H. & VOGEL, L. K. 2008. Hepatocyte growth factor activator inhibitor-1 has a complex subcellular itinerary. *Biochemical Journal*, 413, 251-259.
- GRAY, K., ELGHADBAN, S., THONGYOO, P., OWEN, K. A., SZABO, R., BUGGE, T. H., TATE, E. W., LEATHERBARROW, R. J. & ELLIS, V. 2014. Potent and specific inhibition of the biological activity of the type-II transmembrane serine protease matriptase by the cyclic microprotein MCoTI-II. *Thromb Haemost*, 112.
- GUMBINER, B., LOWENKOPF, T. & APATIRA, D. 1991. Identification of a 160-kDa polypeptide that binds to the tight junction protein ZO-1. *Proc Natl Acad Sci U S A*, 88, 3460-4.
- GUNZEL, D. & YU, A. S. 2013. Claudins and the modulation of tight junction permeability. *Physiol Rev*, 93, 525-69.
- GUTTMAN, J. A. & FINLAY, B. B. 2009. Tight junctions as targets of infectious agents. *Biochim Biophys Acta*, 1788, 832-41.
- HARTSOCK, A. & NELSON, W. J. 2008. Adherens and tight junctions: structure, function and connections to the actin cytoskeleton. *Biochim Biophys Acta*, 1778, 660-9.
- HASKINS, J., GU, L., WITTCHEN, E. S., HIBBARD, J. & STEVENSON, B. R. 1998. ZO-3, a novel member of the MAGUK protein family found at the tight junction, interacts with ZO-1 and occludin. *J Cell Biol*, 141, 199-208.
- HEITZ, A., AVRUTINA, O., LE-NGUYEN, D., DIEDERICHSEN, U., HERNANDEZ, J. F., GRACY, J., KOLMAR, H. & CHICHE, L. 2008. Knottin cyclization: impact on structure and dynamics. *BMC Struct Biol*, 8, 54.
- HELLER, F., FLORIAN, P., BOJARSKI, C., RICHTER, J., CHRIST, M., HILLENBRAND, B., MANKERTZ, J., GITTER, A. H., BURGEL, N., FROMM, M., ZEITZ, M., FUSS, I., STROBER, W. & SCHULZKE, J. D. 2005. Interleukin-13 is the key effector Th2

- cytokine in ulcerative colitis that affects epithelial tight junctions, apoptosis, and cell restitution. *Gastroenterology*, 129, 550-64.
- HERNANDEZ-BARRANTES, S., TOTH, M., BERNARDO, M. M., YURKOVA, M., GERVASI, D. C., RAZ, Y., SANG, Q. X. A. & FRIDMAN, R. 2000. Binding of active (57 kDa) membrane type 1-matrix metalloproteinase (MT1-MMP) to tissue inhibitor of metalloproteinase (TIMP)-2 regulates MT1-MMP processing and pro-MMP-2 activation. *Journal of Biological Chemistry*, 275, 12080-12089.
- HERTER, S., PIPER, D. E., AARON, W., GABRIELE, T., CUTLER, G., CAO, P., BHATT, A. S., CHOE, Y., CRAIK, C. S., WALKER, N., MEININGER, D., HOEY, T. & AUSTIN, R. J. 2005. Hepatocyte growth factor is a preferred in vitro substrate for human hepsin, a membrane-anchored serine protease implicated in prostate and ovarian cancers. *Biochemical Journal*, 390, 125-136.
- HOFFMANN, A., BREDNO, J., WENDLAND, M., DERUGIN, N., OHARA, P. & WINTERMARK, M. 2011. High and Low Molecular Weight Fluorescein Isothiocyanate (FITC)-Dextrans to Assess Blood-Brain Barrier Disruption: Technical Considerations. *Transl Stroke Res*, 2, 106-11.
- HOOPER, J. D., CLEMENTS, J. A., QUIGLEY, J. P. & ANTALIS, T. M. 2001. Type II transmembrane serine proteases. Insights into an emerging class of cell surface proteolytic enzymes. *J Biol Chem*, 276, 857-60.
- HUH, C. G., FACTOR, V. M., SANCHEZ, A., UCHIDA, K., CONNER, E. A. & THORGEIRSSON, S. S. 2004. Hepatocyte growth factor/c-met signaling pathway is required for efficient liver regeneration and repair. *Proc Natl Acad Sci U S A*, 101, 4477-82.
- HUMBERT, F., GRANDCHAMP, A., PRICAM, C., PERRELET, A. & ORCI, L. 1976. Morphological changes in tight junctions of *Necturus maculosus* proximal tubules undergoing saline diuresis. *J Cell Biol*, 69, 90-6.
- HUMMLER, E., BARKER, P., GATZY, J., BEERMANN, F., VERDUMO, C., SCHMIDT, A., BOUCHER, R. & ROSSIER, B. C. 1996. Early death due to defective neonatal lung liquid clearance in alpha-ENaC-deficient mice. *Nat Genet*, 12, 325-8.
- IKARI, A., TAKIGUCHI, A., ATOMI, K., SATO, T. & SUGATANI, J. 2011. Decrease in claudin-2 expression enhances cell migration in renal epithelial Madin-Darby canine kidney cells. *J Cell Physiol*, 226, 1471-8.
- IKENOUCI, J., MATSUDA, M., FURUSE, M. & TSUKITA, S. 2003. Regulation of tight junctions during the epithelium-mesenchyme transition: direct repression of the gene expression of claudins/occludin by Snail. *J Cell Sci*, 116, 1959-67.
- ITOH, H., NAGANUMA, S., TAKEDA, N., MIYATA, S., UCHINOKURA, S., FUKUSHIMA, T., UCHIYAMA, S., TANAKA, H., NAGAIKE, K., SHIMOMURA, T., MIYAZAWA, K., YAMADA, G., KITAMURA, N., KOONO, M. & KATAOKA, H. 2004. Regeneration of injured intestinal mucosa is impaired in hepatocyte growth factor activator-deficient mice. *Gastroenterology*, 127, 1423-35.
- JACOBSON, B. A., ALTER, M. D., KRATZKE, M. G., FRIZELLE, S. P., ZHANG, Y., PETERSON, M. S., AVDULOV, S., MOHORN, R. P., WHITSON, B. A., BITTERMAN, P. B., POLUNOVSKY, V. A. & KRATZKE, R. A. 2006. Repression of cap-dependent translation attenuates the transformed phenotype in non-small cell lung cancer both in vitro and in vivo. *Cancer Res*, 66, 4256-62.
- JIANG, W. G., MARTIN, T. A., MATSUMOTO, K., NAKAMURA, T. & MANSEL, R. E. 1999. Hepatocyte growth factor/scatter factor decreases the expression of

- occludin and transendothelial resistance (TER) and increases paracellular permeability in human vascular endothelial cells. *J Cell Physiol*, 181, 319-29.
- KANG, J. Y., DOLLED-FILHART, M., OCAL, I. T., SINGH, B., LIN, C. Y., DICKSON, R. B., RIMM, D. L. & CAMP, R. L. 2003. Tissue microarray analysis of hepatocyte growth factor/Met pathway components reveals a role for Met, matriptase, and hepatocyte growth factor activator inhibitor 1 in the progression of node-negative breast cancer. *Cancer Res*, 63, 1101-5.
- KATAOKA, H., MIYATA, S., UCHINOKURA, S. & ITOH, H. 2003. Roles of hepatocyte growth factor (HGF) activator and HGF activator inhibitor in the pericellular activation of HGF/scatter factor. *Cancer Metastasis Rev*, 22, 223-36.
- KATAOKA, H., SUGANUMA, T., SHIMOMURA, T., ITOH, H., KITAMURA, N., NABESHIMA, K. & KOONO, M. 1999. Distribution of hepatocyte growth factor activator inhibitor type 1 (HAI-1) in human tissues. Cellular surface localization of HAI-1 in simple columnar epithelium and its modulated expression in injured and regenerative tissues. *J Histochem Cytochem*, 47, 673-82.
- KAWAGUCHI, M., TAKEDA, N., HOSHIKO, S., YORITA, K., BABA, T., SAWAGUCHI, A., NEZU, Y., YOSHIKAWA, T., FUKUSHIMA, T. & KATAOKA, H. 2011. Membrane-Bound Serine Protease Inhibitor HAI-1 Is Required for Maintenance of Intestinal Epithelial Integrity. *American Journal of Pathology*, 179, 1815-1826.
- KILPATRICK, L. M., HARRIS, R. L., OWEN, K. A., BASS, R., GHORAYEB, C., BAR-OR, A. & ELLIS, V. 2006. Initiation of plasminogen activation on the surface of monocytes expressing the type II transmembrane serine protease matriptase. *Blood*, 108, 2616-23.
- KIM, C., CHO, Y. C., KANG, C. H., KIM, M. G., LEE, H. S., CHO, E. G. & PARK, D. 2005. Filamin is essential for shedding of the transmembrane serine protease, epithin. *Embo Reports*, 6, 1045-1051.
- KIM, M. G., CHEN, C., LYU, M. S., CHO, E. G., PARK, D., KOZAK, C. & SCHWARTZ, R. H. 1999. Cloning and chromosomal mapping of a gene isolated from thymic stromal cells encoding a new mouse type II membrane serine protease, epithin, containing four LDL receptor modules and two CUB domains. *Immunogenetics*, 49, 420-8.
- KINOSHITA, T., SATO, H., OKADA, A., OHUCHI, E., IMAI, K., OKADA, Y. & SEIKI, M. 1998. TIMP-2 promotes activation of progelatinase A by membrane-type 1 matrix metalloproteinase immobilized on agarose beads. *J Biol Chem*, 273, 16098-103.
- KLEYMAN, T. R. & CRAGOE, E. J. 1988. Amiloride and Its Analogs as Tools in the Study of Ion-Transport. *Journal of Membrane Biology*, 105, 1-21.
- KLEZOVITCH, O., CHEVILLET, J., MIROSEVICH, J., ROBERTS, R. L., MATUSIK, R. J. & VASIOUKHIN, V. 2004. Hepsin promotes prostate cancer progression and metastasis. *Cancer Cell*, 6, 185-95.
- KOSA, P., SZABO, R., MOLINOLO, A. A. & BUGGE, T. H. 2012. Suppression of Tumorigenicity-14, encoding matriptase, is a critical suppressor of colitis and colitis-associated colon carcinogenesis. *Oncogene*, 31, 3679-3695.
- KOTTHAUS, J., STEINMETZER, T., KOTTHAUS, J., SCHADE, D., VAN DE LOCHT, A. & CLEMENT, B. 2010. Metabolism and distribution of two highly potent and selective peptidomimetic inhibitors of matriptase. *Xenobiotica*, 40, 93-101.

- KRAUSE, G., WINKLER, L., MUELLER, S. L., HASELOFF, R. F., PIONTEK, J. & BLASIG, I. E. 2008. Structure and function of claudins. *Biochim Biophys Acta*, 1778, 631-45.
- LAVELLE, J. P., NEGRETE, H. O., POLAND, P. A., KINLOUGH, C. L., MEYERS, S. D., HUGHEY, R. P. & ZEIDEL, M. L. 1997. Low permeabilities of MDCK cell monolayers: a model barrier epithelium. *Am J Physiol*, 273, F67-75.
- LEE, H., OVERALL, C. M., MCCULLOCH, C. A. & SODEK, J. 2006. A critical role for the membrane-type 1 matrix metalloproteinase in collagen phagocytosis. *Mol Biol Cell*, 17, 4812-26.
- LEE, M. S., TSENG, I. C., WANG, Y., KIYOMIYA, K., JOHNSON, M. D., DICKSON, R. B. & LIN, C. Y. 2007. Autoactivation of matriptase in vitro: requirement for biomembrane and LDL receptor domain. *Am J Physiol Cell Physiol*, 293, C95-105.
- LEE, S. L., DICKSON, R. B. & LIN, C. Y. 2000. Activation of hepatocyte growth factor and urokinase/plasminogen activator by matriptase, an epithelial membrane serine protease. *J Biol Chem*, 275, 36720-5.
- LEIGHTON, J., ESTES, L. W., MANSUKHANI, S. & BRADA, Z. 1970. A cell line derived from normal dog kidney (MDCK) exhibiting qualities of papillary adenocarcinoma and of renal tubular epithelium. *Cancer*, 26, 1022-8.
- LEYVRAZ, C., CHARLES, R. P., RUBERA, I., GUITARD, M., ROTMAN, S., BREIDEN, B., SANDHOFF, K. & HUMMLER, E. 2005. The epidermal barrier function is dependent on the serine protease CAP1/Prss8. *J Cell Biol*, 170, 487-96.
- LI, S., GUAN, J. L. & CHIEN, S. 2005. Biochemistry and biomechanics of cell motility. *Annu Rev Biomed Eng*, 7, 105-50.
- LIN, C. Y., ANDERS, J., JOHNSON, M. & DICKSON, R. B. 1999a. Purification and characterization of a complex containing matriptase and a Kunitz-type serine protease inhibitor from human milk. *J Biol Chem*, 274, 18237-42.
- LIN, C. Y., ANDERS, J., JOHNSON, M., SANG, Q. A. & DICKSON, R. B. 1999b. Molecular cloning of cDNA for matriptase, a matrix-degrading serine protease with trypsin-like activity. *J Biol Chem*, 274, 18231-6.
- LIPSCHUTZ, J. H., LI, S., ARISCO, A. & BALKOVETZ, D. F. 2005. Extracellular signal-regulated kinases 1/2 control claudin-2 expression in Madin-Darby canine kidney strain I and II cells. *J Biol Chem*, 280, 3780-8.
- LIST, K., BUGGE, T. H. & SZABO, R. 2006a. Matriptase: potent proteolysis on the cell surface. *Mol Med*, 12, 1-7.
- LIST, K., CURRIE, B., SCHARSCHMIDT, T. C., SZABO, R., SHIREMAN, J., MOLINOLO, A., CRAVATT, B. F., SEGRE, J. & BUGGE, T. H. 2007a. Autosomal ichthyosis with hypotrichosis syndrome displays low matriptase proteolytic activity and is phenocopied in ST14 hypomorphic mice. *J Biol Chem*, 282, 36714-23.
- LIST, K., HAUDENSCHILD, C. C., SZABO, R., CHEN, W., WAHL, S. M., SWAIM, W., ENGELHOLM, L. H., BEHRENDT, N. & BUGGE, T. H. 2002. Matriptase/MT-SP1 is required for postnatal survival, epidermal barrier function, hair follicle development, and thymic homeostasis. *Oncogene*, 21, 3765-79.
- LIST, K., HOBSON, J. P., MOLINOLO, A. & BUGGE, T. H. 2007b. Co-localization of the channel activating protease prostasin/(CAP1/PRSS8) with its candidate activator, matriptase. *J Cell Physiol*, 213, 237-45.
- LIST, K., KOSA, P., SZABO, R., BEY, A. L., WANG, C. B., MOLINOLO, A. & BUGGE, T. H. 2009. Epithelial integrity is maintained by a matriptase-dependent proteolytic pathway. *Am J Pathol*, 175, 1453-63.

- LIST, K., SZABO, R., MOLINOLO, A., NIELSEN, B. S. & BUGGE, T. H. 2006b. Delineation of matriptase protein expression by enzymatic gene trapping suggests diverging roles in barrier function, hair formation, and squamous cell carcinogenesis. *American Journal of Pathology*, 168, 1513-1525.
- LIST, K., SZABO, R., MOLINOLO, A., SRIURANPONG, V., REDEYE, V., MURDOCK, T., BURKE, B., NIELSEN, B. S., GUTKIND, J. S. & BUGGE, T. H. 2005. Deregulated matriptase causes ras-independent multistage carcinogenesis and promotes ras-mediated malignant transformation. *Genes Dev*, 19, 1934-50.
- LIST, K., SZABO, R., WERTZ, P. W., SEGRE, J., HAUDENSCHILD, C. C., KIM, S. Y. & BUGGE, T. H. 2003. Loss of proteolytically processed filaggrin caused by epidermal deletion of Matriptase/MT-SP1. *J Cell Biol*, 163, 901-10.
- MACAO, B., JOHANSSON, D. G., HANSSON, G. C. & HARD, T. 2006. Autoproteolysis coupled to protein folding in the SEA domain of the membrane-bound MUC1 mucin. *Nat Struct Mol Biol*, 13, 71-6.
- MADIN, S. H., ANDRIESE, P. C. & DARBY, N. B. 1957. The in vitro cultivation of tissues of domestic and laboratory animals. *Am J Vet Res*, 18, 932-41.
- MANDEL, L. J., BACALLAO, R. & ZAMPIGHI, G. 1993. Uncoupling of the molecular 'fence' and paracellular 'gate' functions in epithelial tight junctions. *Nature*, 361, 552-5.
- MARTIN, T. A. & JIANG, W. G. 2009. Loss of tight junction barrier function and its role in cancer metastasis. *Biochim Biophys Acta*, 1788, 872-91.
- MARTIN-BELMONTE, F. & PEREZ-MORENO, M. 2012. Epithelial cell polarity, stem cells and cancer. *Nat Rev Cancer*, 12, 23-38.
- MASSEY, A. P., HARLEY, W. R., PASUPULETI, N., GORIN, F. A. & NANTZ, M. H. 2012. 2-Amidino analogs of glycine-amiloride conjugates: inhibitors of urokinase-type plasminogen activator. *Bioorg Med Chem Lett*, 22, 2635-9.
- MAURO, T., GUITARD, M., BEHNE, M., ODA, Y., CRUMRINE, D., KOMUVES, L., RASSNER, U., ELIAS, P. M. & HUMMLER, E. 2002. The ENaC channel is required for normal epidermal differentiation. *J Invest Dermatol*, 118, 589-94.
- MCNEIL, E., CAPALDO, C. T. & MACARA, I. G. 2006. Zonula occludens-1 function in the assembly of tight junctions in Madin-Darby canine kidney epithelial cells. *Mol Biol Cell*, 17, 1922-32.
- MELNHORST, W. B., MULDER, G. M., XI, Q., HOENDEROP, J. G., KIMURA, K., EGUCHI, S. & VAN GOOR, H. 2008. Epidermal growth factor receptor signaling in the kidney: key roles in physiology and disease. *Hypertension*, 52, 987-93.
- MINOND, D., LAUER-FIELDS, J. L., CUDIC, M., OVERALL, C. M., PEI, D., BREW, K., VISSE, R., NAGASE, H. & FIELDS, G. B. 2006. The roles of substrate thermal stability and P2 and P1' subsite identity on matrix metalloproteinase triple-helical peptidase activity and collagen specificity. *J Biol Chem*, 281, 38302-13.
- MIYAKE, Y., TSUZUKI, S., FUSHIKI, T. & INOUE, K. 2010. Matriptase does not require hepatocyte growth factor activator inhibitor type-1 for activation in an epithelial cell expression model. *Biosci Biotechnol Biochem*, 74, 848-50.
- MOGENSEN, M. M. 1999. Microtubule release and capture in epithelial cells. *Biol Cell*, 91, 331-41.
- MOLL, S., SCHAEREN-WIEMERS, N., WOHLWEND, A., PASTORE, Y., FULPIUS, T., MONARD, D., SAPPINO, A. P., SCHIFFERLI, J. A., VASSALLI, J. D. & IZUI, S.

1996. Protease nexin 1 in the murine kidney: glomerular localization and up-regulation in glomerulopathies. *Kidney Int*, 50, 1936-45.
- MOMOSE, T., KRAUS, Y. & HOULISTON, E. 2012. A conserved function for Strabismus in establishing planar cell polarity in the ciliated ectoderm during cnidarian larval development. *Development*, 139, 4374-82.
- MULLER, D., KAUSALYA, P. J., CLAVERIE-MARTIN, F., MEIJ, I. C., EGGERT, P., GARCIA-NIETO, V. & HUNZIKER, W. 2003. A novel claudin 16 mutation associated with childhood hypercalciuria abolishes binding to ZO-1 and results in lysosomal mistargeting. *Am J Hum Genet*, 73, 1293-301.
- MUSCH, A. 2004. Microtubule organization and function in epithelial cells. *Traffic*, 5, 1-9.
- MUTO, S., HATA, M., TANIGUCHI, J., TSURUOKA, S., MORIWAKI, K., SAITOU, M., FURUSE, K., SASAKI, H., FUJIMURA, A., IMAI, M., KUSANO, E., TSUKITA, S. & FURUSE, M. 2010. Claudin-2-deficient mice are defective in the leaky and cation-selective paracellular permeability properties of renal proximal tubules. *Proc Natl Acad Sci U S A*, 107, 8011-6.
- NAGAIKE, K., KAWAGUCHI, M., TAKEDA, N., FUKUSHIMA, T., SAWAGUCHI, A., KOHAMA, K., SETOYAMA, M. & KATAOKA, H. 2008. Defect of hepatocyte growth factor activator inhibitor type 1/serine protease inhibitor, Kunitz type 1 (Hai-1/Spint1) leads to ichthyosis-like condition and abnormal hair development in mice. *Am J Pathol*, 173, 1464-75.
- NALDINI, L., TAMAGNONE, L., VIGNA, E., SACHS, M., HARTMANN, G., BIRCHMEIER, W., DAIKUHARA, Y., TSUBOUCHI, H., BLASI, F. & COMOGLIO, P. M. 1992. Extracellular Proteolytic Cleavage by Urokinase Is Required for Activation of Hepatocyte Growth-Factor Scatter Factor. *Embo Journal*, 11, 4825-4833.
- NELSON, W. J. 2003. Adaptation of core mechanisms to generate cell polarity. *Nature*, 422, 766-74.
- NETZEL-ARNETT, S., BUGGE, T. H., HESS, R. A., CARNES, K., STRINGER, B. W., SCARMAN, A. L., HOOPER, J. D., TONKS, I. D., KAY, G. F. & ANTALIS, T. M. 2009. The glycosylphosphatidylinositol-anchored serine protease PRSS21 (testisin) imparts murine epididymal sperm cell maturation and fertilizing ability. *Biol Reprod*, 81, 921-32.
- NETZEL-ARNETT, S., BUZZA, M. S., SHEA-DONOHUE, T., DESILETS, A., LEDUC, R., FASANO, A., BUGGE, T. H. & ANTALIS, T. M. 2012. Matriptase protects against experimental colitis and promotes intestinal barrier recovery. *Inflamm Bowel Dis*, 18, 1303-14.
- NETZEL-ARNETT, S., CURRIE, B. M., SZABO, R., LIN, C. Y., CHEN, L. M., CHAI, K. X., ANTALIS, T. M., BUGGE, T. H. & LIST, K. 2006. Evidence for a matriptase-prostasin proteolytic cascade regulating terminal epidermal differentiation. *J Biol Chem*, 281, 32941-5.
- NEURATH, H. 1985. Proteolytic enzymes, past and present. *Fed Proc*, 44, 2907-13.
- NEURATH, H. 1994. Proteolytic enzymes past and present: the second golden era. Recollections, special section in honor of Max Perutz. *Protein Sci*, 3, 1734-9.
- NIMISHAKAVI, S., BESPROZVANNAYA, M., RAYMOND, W. W., CRAIK, C. S., GRUENERT, D. C. & CAUGHEY, G. H. 2012. Activity and inhibition of prostatic and matriptase on apical and basolateral surfaces of human airway epithelial cells. *Am J Physiol Lung Cell Mol Physiol*, 303, L97-106.
- NUSRAT, A., PARKOS, C. A., BACCARRA, A. E., GODOWSKI, P. J., DELP-ARCHER, C., ROSEN, E. M. & MADARA, J. L. 1994. Hepatocyte growth factor/scatter factor

- effects on epithelia. Regulation of intercellular junctions in transformed and nontransformed cell lines, basolateral polarization of c-met receptor in transformed and natural intestinal epithelia, and induction of rapid wound repair in a transformed model epithelium. *J Clin Invest*, 93, 2056-65.
- OBERST, M. D., CHEN, L. Y., KIYOMIYA, K., WILLIAMS, C. A., LEE, M. S., JOHNSON, M. D., DICKSON, R. B. & LIN, C. Y. 2005. HAI-1 regulates activation and expression of matriptase, a membrane-bound serine protease. *Am J Physiol Cell Physiol*, 289, C462-70.
- OBERST, M. D., JOHNSON, M. D., DICKSON, R. B., LIN, C. Y., SINGH, B., STEWART, M., WILLIAMS, A., AL-NAFUSSI, A., SMYTH, J. F., GABRA, H. & SELLAR, G. C. 2002. Expression of the serine protease matriptase and its inhibitor HAI-1 in epithelial ovarian cancer: correlation with clinical outcome and tumor clinicopathological parameters. *Clin Cancer Res*, 8, 1101-7.
- OBERST, M. D., SINGH, B., OZDEMIRLI, M., DICKSON, R. B., JOHNSON, M. D. & LIN, C. Y. 2003a. Characterization of matriptase expression in normal human tissues. *Journal of Histochemistry & Cytochemistry*, 51, 1017-1025.
- OBERST, M. D., WILLIAMS, C. A., DICKSON, R. B., JOHNSON, M. D. & LIN, C. Y. 2003b. The activation of matriptase requires its noncatalytic domains, serine protease domain, and its cognate inhibitor. *J Biol Chem*, 278, 26773-9.
- OWEN, K. A., QIU, D., ALVES, J., SCHUMACHER, A. M., KILPATRICK, L. M., LI, J., HARRIS, J. L. & ELLIS, V. 2010. Pericellular activation of hepatocyte growth factor by the transmembrane serine proteases matriptase and hepsin, but not by the membrane-associated protease uPA. *Biochem J*, 426, 219-28.
- OZAWA, M., ENGEL, J. & KEMLER, R. 1990. Single amino acid substitutions in one Ca²⁺ binding site of uvomorulin abolish the adhesive function. *Cell*, 63, 1033-8.
- PALMER, L. G. 1992. Epithelial Na channels: function and diversity. *Annu Rev Physiol*, 54, 51-66.
- PARK, C. H., VALORE, E. V., WORING, A. J., GANZ, T. 2001. Hecparin, a urinary antimicrobial peptide synthesized in the liver. *J Biological Chemistry*, 16, 7806-10.
- PASTORELLI, L., DE SALVO, C., MERCADO, J. R., VECCHI, M. & PIZARRO, T. T. 2013. Central role of the gut epithelial barrier in the pathogenesis of chronic intestinal inflammation: lessons learned from animal models and human genetics. *Front Immunol*, 4, 280.
- PEARTON, D. J., DALE, B. A. & PRESLAND, R. B. 2002. Functional analysis of the profilaggrin N-terminal peptide: identification of domains that regulate nuclear and cytoplasmic distribution. *J Invest Dermatol*, 119, 661-9.
- PERUTZ, M. 1992. *Protein structure. New approaches to disease and therapy*, New York: W.H. Freeman and Co.
- PLANES, C., RANDRIANARISON, N. H., CHARLES, R. P., FRATESCHI, S., CLUZEAUD, F., VUAGNIAUX, G., SOLER, P., CLERICI, C., ROSSIER, B. C. & HUMMLER, E. 2010. ENaC-mediated alveolar fluid clearance and lung fluid balance depend on the channel-activating protease 1. *Embo Molecular Medicine*, 2, 26-37.
- POLLACK, A. L., APODACA, G. & MOSTOV, K. E. 2004. Hepatocyte growth factor induces MDCK cell morphogenesis without causing loss of tight junction functional integrity. *Am J Physiol Cell Physiol*, 286, C482-94.

- PRESLAND, R. B. & JUREVIC, R. J. 2002. Making sense of the epithelial barrier: what molecular biology and genetics tell us about the functions of oral mucosal and epidermal tissues. *J Dent Educ*, 66, 564-74.
- PUENTE, X. S., SANCHEZ, L. M., OVERALL, C. M. & LOPEZ-OTIN, C. 2003. Human and mouse proteases: A comparative genomic approach. *Nature Reviews Genetics*, 4, 544-558.
- QUIMBAR, P., MALIK, U., SOMMERHOFF, C. P., KAAS, Q., CHAN, L. Y., HUANG, Y. H., GRUNDHUBER, M., DUNSE, K., CRAIK, D. J., ANDERSON, M. A. & DALY, N. L. 2013. High-affinity Cyclic Peptide Matriptase Inhibitors. *Journal of Biological Chemistry*, 288, 13885-13896.
- RAMSAY, A. J., HOOPER, J. D., FOLGUERAS, A. R., VELASCO, G. & LOPEZ-OTIN, C. 2009. Matriptase-2 (TMPRSS6): a proteolytic regulator of iron homeostasis. *Haematologica*, 94, 840-9.
- RENARD, S., VOILLEY, N., BASSILANA, F., LAZDUNSKI, M. & BARBRY, P. 1995. Localization and regulation by steroids of the alpha, beta and gamma subunits of the amiloride-sensitive Na⁺ channel in colon, lung and kidney. *Pflugers Arch*, 430, 299-307.
- RICKERT, K. W., KELLEY, P., BYRNE, N. J., DIEHL, R. E., HALL, D. L., MONTALVO, A. M., REID, J. C., SHIPMAN, J. M., THOMAS, B. W., MUNSHI, S. K., DARKE, P. L. & SU, H. P. 2008. Structure of human prostaticin, a target for the regulation of hypertension. *J Biol Chem*, 283, 34864-72.
- RIDDICK, A. C., SHUKLA, C. J., PENNINGTON, C. J., BASS, R., NUTTALL, R. K., HOGAN, A., SETHIA, K. K., ELLIS, V., COLLINS, A. T., MAITLAND, N. J., BALL, R. Y. & EDWARDS, D. R. 2005. Identification of degradome components associated with prostate cancer progression by expression analysis of human prostatic tissues. *Br J Cancer*, 92, 2171-80.
- RODRIGUEZ-BOULAN, E. & MACARA, I. G. 2014. Organization and execution of the epithelial polarity programme. *Nat Rev Mol Cell Biol*, 15, 225-42.
- ROTHMEIER, A. S. & RUF, W. 2012. Protease-activated receptor 2 signaling in inflammation. *Semin Immunopathol*, 34, 133-49.
- ROTIN, D. & SCHILD, L. 2008. ENaC and its regulatory proteins as drug targets for blood pressure control. *Curr Drug Targets*, 9, 709-16.
- SAATIAN, B., REZAEE, F., DESANDO, S., EMO, J., CHAPMAN, T., KNOWLDEN, S. & GEORAS, S. N. 2013. Interleukin-4 and interleukin-13 cause barrier dysfunction in human airway epithelial cells. *Tissue Barriers*, 1, e24333.
- SALES, K. U., FRIIS, S., KONKEL, J. E., GODIKSEN, S., HATAKEYAMA, M., HANSEN, K. K., ROGATTO, S. R., SZABO, R., VOGEL, L. K., CHEN, W., GUTKIND, J. S. & BUGGE, T. H. 2014. Non-hematopoietic PAR-2 is essential for matriptase-driven pre-malignant progression and potentiation of ras-mediated squamous cell carcinogenesis. *Oncogene*.
- SANTULLI, R. J., DERIAN, C. K., DARROW, A. L., TOMKO, K. A., ECKARDT, A. J., SEIBERG, M., SCARBOROUGH, R. M. & ANDRADE-GORDON, P. 1995. Evidence for the presence of a protease-activated receptor distinct from the thrombin receptor in human keratinocytes. *Proc Natl Acad Sci U S A*, 92, 9151-5.
- SCHMASSMANN, A., STETTLER, C., POULSOM, R., TARASOVA, N., HIRSCHI, C., FLOGERZI, B., MATSUMOTO, K., NAKAMURA, T. & HALTER, F. 1997. Roles of hepatocyte growth factor and its receptor Met during gastric ulcer healing in rats. *Gastroenterology*, 113, 1858-72.

- SEGRE, J. 2003. Complex redundancy to build a simple epidermal permeability barrier. *Curr Opin Cell Biol*, 15, 776-82.
- SEITZ, I., HESS, S., SCHULZ, H., ECKL, R., BUSCH, G., MONTENS, H. P., BRANDL, R., SEIDL, S., SCHOMIG, A. & OTT, I. 2007. Membrane-type serine protease-1/matriptase induces interleukin-6 and-8 in endothelial cells by activation of protease-activated receptor-2 - Potential implications in atherosclerosis. *Arteriosclerosis Thrombosis and Vascular Biology*, 27, 769-775.
- SHALOM AVRAHAM, T.-S. L., HAVA KARSENTY AVRAHAM 2008. Blood-Brain Barrier. *Encyclopedia of Cancer*. Beth Israel Deaconess Medical Center, Harvard Institutes of Medicine.
- SHAN, J., OSHIMA, T., CHEN, X., FUKUI, H., WATARI, J. & MIWA, H. 2012. Trypsin impaired epithelial barrier function and induced IL-8 secretion through basolateral PAR-2: a lesson from a stratified squamous epithelial model. *Am J Physiol Gastrointest Liver Physiol*, 303, G1105-12.
- SHI, S. & KLEYMAN, T. R. 2013. Gamma subunit second transmembrane domain contributes to epithelial sodium channel gating and amiloride block. *Am J Physiol Renal Physiol*, 305, F1585-92.
- SHI, Y. E., TORRI, J., YIEH, L., WELLSTEIN, A., LIPPMAN, M. E. & DICKSON, R. B. 1993. Identification and characterization of a novel matrix-degrading protease from hormone-dependent human breast cancer cells. *Cancer Res*, 53, 1409-15.
- SHIMOMURA, T., DENDA, K., KITAMURA, A., KAWAGUCHI, T., KITO, M., KONDO, J., KAGAYA, S., QIN, L., TAKATA, H., MIYAZAWA, K. & KITAMURA, N. 1997. Hepatocyte growth factor activator inhibitor, a novel Kunitz-type serine protease inhibitor. *J Biol Chem*, 272, 6370-6.
- SHIN, K., FOGG, V. C. & MARGOLIS, B. 2006. Tight junctions and cell polarity. *Annu Rev Cell Dev Biol*, 22, 207-35.
- SHIPWAY, A., DANAHAY, H., WILLIAMS, J. A., TULLY, D. C., BACKES, B. J. & HARRIS, J. L. 2004. Biochemical characterization of prostasin, a channel activating protease. *Biochemical and Biophysical Research Communications*, 324, 953-963.
- SIEZEN, R. J. & LEUNISSEN, J. A. 1997. Subtilases: the superfamily of subtilisin-like serine proteases. *Protein Sci*, 6, 501-23.
- SILVESTRI, L., PAGANI, A., NAI, A., DE DOMENICO, I., KAPLAN, J. & CAMASCHELLA, C. 2008. The serine protease matriptase-2 (TMPRSS6) inhibits hepcidin activation by cleaving membrane hemojuvelin. *Cell Metab*, 8, 502-11.
- SINGH, A. B., SUGIMOTO, K., DHAWAN, P. & HARRIS, R. C. 2007. Juxtacrine activation of EGFR regulates claudin expression and increases transepithelial resistance. *Am J Physiol Cell Physiol*, 293, C1660-8.
- SINHA, A., NIGHTINGALE, J., WEST, K. P., BERLANGA-ACOSTA, J. & PLAYFORD, R. J. 2003. Epidermal growth factor enemas with oral mesalamine for mild-to-moderate left-sided ulcerative colitis or proctitis. *N Engl J Med*, 349, 350-7.
- STAEHELIN, L. A. 1973. Further observations on the fine structure of freeze-cleaved tight junctions. *J Cell Sci*, 13, 763-86.
- STAMOS, J., LAZARUS, R. A., YAO, X., KIRCHHOFER, D. & WIESMANN, C. 2004. Crystal structure of the HGF beta-chain in complex with the Sema domain of the Met receptor. *EMBO J*, 23, 2325-35.
- STEINMETZER, T., DONNECKE, D., KORSONEWSKI, M., NEUWIRTH, C., STEINMETZER, P., SCHULZE, A., SAUPE, S. M. & SCHWEINITZ, A. 2009.

- Modification of the N-terminal sulfonyl residue in 3-amidinophenylalanine-based matriptase inhibitors. *Bioorg Med Chem Lett*, 19, 67-73.
- STEINMETZER, T., SCHWEINITZ, A., STURZEBECKER, A., DONNECKE, D., UHLAND, K., SCHUSTER, O., STEINMETZER, P., MULLER, F., FRIEDRICH, R., THAN, M. E., BODE, W. & STURZEBECKER, J. 2006. Secondary amides of sulfonylated 3-amidinophenylalanine. New potent and selective inhibitors of matriptase. *J Med Chem*, 49, 4116-26.
- STEVEN, A. C. & STEINERT, P. M. 1994. Protein composition of cornified cell envelopes of epidermal keratinocytes. *J Cell Sci*, 107 (Pt 2), 693-700.
- STOKER, M., GHERARDI, E., PERRYMAN, M. & GRAY, J. 1987. Scatter factor is a fibroblast-derived modulator of epithelial cell mobility. *Nature*, 327, 239-42.
- SUZUKI, T., YOSHINAGA, N. & TANABE, S. 2011. Interleukin-6 (IL-6) regulates claudin-2 expression and tight junction permeability in intestinal epithelium. *J Biol Chem*, 286, 31263-71.
- SZABO, R., HOBSON, J. P., CHRISTOPH, K., KOSA, P., LIST, K. & BUGGE, T. H. 2009. Regulation of cell surface protease matriptase by HAI2 is essential for placental development, neural tube closure and embryonic survival in mice. *Development*, 136, 2653-63.
- SZABO, R., HOBSON, J. P., LIST, K., MOLINOLO, A., LIN, C. Y. & BUGGE, T. H. 2008. Potent inhibition and global co-localization implicate the transmembrane Kunitz-type serine protease inhibitor hepatocyte growth factor activator inhibitor-2 in the regulation of epithelial matriptase activity. *J Biol Chem*, 283, 29495-504.
- SZABO, R., MOLINOLO, A., LIST, K. & BUGGE, T. H. 2007. Matriptase inhibition by hepatocyte growth factor activator inhibitor-1 is essential for placental development. *Oncogene*, 26, 1546-56.
- SZABO, R., NETZEL-ARNETT, S., HOBSON, J. P., ANTALIS, T. M. & BUGGE, T. H. 2005. Matriptase-3 is a novel phylogenetically preserved membrane-anchored serine protease with broad serpin reactivity. *Biochem J*, 390, 231-42.
- SZABO, R., PETERS, D. E., KOSA, P., CAMERER, E. & BUGGE, T. H. 2014. Regulation of Feto-Maternal Barrier by Matriptase- and PAR-2-Mediated Signaling Is Required for Placental Morphogenesis and Mouse Embryonic Survival. *PLoS Genet*, 10, e1004470.
- SZABO, R., RASMUSSEN, A. L., MOYER, A. B., KOSA, P., SCHAFFER, J. M., MOLINOLO, A. A., GUTKIND, J. S. & BUGGE, T. H. 2011. c-Met-induced epithelial carcinogenesis is initiated by the serine protease matriptase. *Oncogene*, 30, 2003-2016.
- TAKEUCHI, T., HARRIS, J. L., HUANG, W., YAN, K. W., COUGHLIN, S. R. & CRAIK, C. S. 2000. Cellular localization of membrane-type serine protease 1 and identification of protease-activated receptor-2 and single-chain urokinase-type plasminogen activator as substrates. *J Biol Chem*, 275, 26333-42.
- TAKEUCHI, T., SHUMAN, M. A. & CRAIK, C. S. 1999. Reverse biochemistry: Use of macromolecular protease inhibitors to dissect complex biological processes and identify a membrane-type serine protease in epithelial cancer and normal tissue. *Proceedings of the National Academy of Sciences of the United States of America*, 96, 11054-11061.
- TANIMOTO, H., UNDERWOOD, L. J., WANG, Y., SHIGEMASA, K., PARMLEY, T. H. & O'BRIEN, T. J. 2001. Ovarian tumor cells express a transmembrane serine

- protease: a potential candidate for early diagnosis and therapeutic intervention. *Tumour Biol*, 22, 104-14.
- TANOS, B. & RODRIGUEZ-BOULAN, E. 2008. The epithelial polarity program: machineries involved and their hijacking by cancer. *Oncogene*, 27, 6939-57.
- THONGYOO, P., JAULENT, A. M., TATE, E. W. & LEATHERBARROW, R. J. 2007. Immobilized protease-assisted synthesis of engineered cysteine-knot microproteins. *Chembiochem*, 8, 1107-9.
- THONGYOO, P., ROQUE-ROSELL, N., LEATHERBARROW, R. J. & TATE, E. W. 2008. Chemical and biomimetic total syntheses of natural and engineered MCoTI cyclotides. *Org Biomol Chem*, 6, 1462-70.
- THONGYOO, P., TATE, E. W. & LEATHERBARROW, R. J. 2006. Total synthesis of the macrocyclic cysteine knot microprotein MCoTI-II. *Chem Commun (Camb)*, 2848-50.
- TONG, Z., ILLEK, B., BHAGWANDIN, V. J., VERGHESE, G. M. & CAUGHEY, G. H. 2004. Prostaticin, a membrane-anchored serine peptidase, regulates sodium currents in JME/CF15 cells, a cystic fibrosis airway epithelial cell line. *Am J Physiol Lung Cell Mol Physiol*, 287, L928-35.
- TSUZUKI, S., MURAI, N., MIYAKE, Y., INOUE, K., HIRAYASU, H., IWANAGA, T. & FUSHIKI, T. 2005. Evidence for the occurrence of membrane-type serine protease 1/matriptase on the basolateral sides of enterocytes. *Biochem J*, 388, 679-87.
- UHLAND, K. 2006. Matriptase and its putative role in cancer. *Cell Mol Life Sci*, 63, 2968-78.
- ULLUWISHEWA, D., ANDERSON, R. C., MCNABB, W. C., MOUGHAN, P. J., WELLS, J. M. & ROY, N. C. 2011. Regulation of tight junction permeability by intestinal bacteria and dietary components. *J Nutr*, 141, 769-76.
- USTACH, C. V., HUANG, W., CONLEY-LACOMB, M. K., LIN, C. Y., CHE, M., ABRAMS, J. & KIM, H. R. 2010. A novel signaling axis of matriptase/PDGF-D/ss-PDGFR in human prostate cancer. *Cancer Res*, 70, 9631-40.
- VAN DEURS, B. & KOEHLER, J. K. 1979. Tight junctions in the choroid plexus epithelium. A freeze-fracture study including complementary replicas. *J Cell Biol*, 80, 662-73.
- VAN ITALLIE, C. M. & ANDERSON, J. M. 2006. Claudins and epithelial paracellular transport. *Annu Rev Physiol*, 68, 403-29.
- VAN ITALLIE, C. M., HOLMES, J., BRIDGES, A., GOOKIN, J. L., COCCARO, M. R., PROCTOR, W., COLEGIO, O. R. & ANDERSON, J. M. 2008. The density of small tight junction pores varies among cell types and is increased by expression of claudin-2. *Journal of Cell Science*, 121, 298-305.
- VELASCO, G., CAL, S., QUESADA, V., SANCHEZ, L. M. & LOPEZ-OTIN, C. 2002. Matriptase-2, a membrane-bound mosaic serine proteinase predominantly expressed in human liver and showing degrading activity against extracellular matrix proteins. *J Biol Chem*, 277, 37637-46.
- VERGHESE, G. M., GUTKNECHT, M. F. & CAUGHEY, G. H. 2006. Prostaticin regulates epithelial monolayer function: cell-specific Gpld1-mediated secretion and functional role for GPI anchor. *Am J Physiol Cell Physiol*, 291, C1258-70.
- VESEY, D. A., SUEN, J. Y., SEOW, V., LOHMAN, R. J., LIU, L., GOBE, G. C., JOHNSON, D. W. & FAIRLIE, D. P. 2013. PAR2-induced inflammatory responses in human kidney tubular epithelial cells. *Am J Physiol Renal Physiol*, 304, F737-50.

- VINCENZA CARRIERO, M., FRANCO, P., VOCCA, I., ALFANO, D., LONGANESI-CATTANI, I., BIFULCO, K., MANCINI, A., CAPUTI, M. & STOPPELLI, M. P. 2009. Structure, function and antagonists of urokinase-type plasminogen activator. *Front Biosci*, 14, 3782-94.
- VOILLEY, N., LINGUEGLIA, E., CHAMPIGNY, G., MATTEI, M. G., WALDMANN, R., LAZDUNSKI, M. & BARBRY, P. 1994. The lung amiloride-sensitive Na⁺ channel: biophysical properties, pharmacology, ontogenesis, and molecular cloning. *Proc Natl Acad Sci U S A*, 91, 247-51.
- VUAGNIAUX, G., VALLET, V., JAEGER, N. F., HUMMLER, E. & ROSSIER, B. C. 2002. Synergistic activation of ENaC by three membrane-bound channel-activating serine proteases (mCAP1, mCAP2, and mCAP3) and serum- and glucocorticoid-regulated kinase (Sgk1) in *Xenopus* Oocytes. *J Gen Physiol*, 120, 191-201.
- WADHAWAN, V., KOLHE, Y. A., SANGITH, N., GAUTAM, A. K. & VENKATRAMAN, P. 2012. From prediction to experimental validation: desmoglein 2 is a functionally relevant substrate of matriptase in epithelial cells and their reciprocal relationship is important for cell adhesion. *Biochem J*, 447, 61-70.
- WALSH, K. A. & NEURATH, H. 1964. Trypsinogen and Chymotrypsinogen as Homologous Proteins. *Proc Natl Acad Sci U S A*, 52, 884-9.
- WANG, W., LIAO, X., FUKUDA, K., KNAPPE, S., WU, F., DRIES, D. L., QIN, J. & WU, Q. 2008. Corin variant associated with hypertension and cardiac hypertrophy exhibits impaired zymogen activation and natriuretic peptide processing activity. *Circ Res*, 103, 502-8.
- WATSON, A. J., SMITH, B. B., WHITEHEAD, M. R., SYKES, P. H. & FRIZELLE, F. A. 2006. Malignant progression of anal intra-epithelial neoplasia. *ANZ J Surg*, 76, 715-7.
- WEBB, C. P., LANE, K., DAWSON, A. P., VANDE WOUDE, G. F. & WARN, R. M. 1996. C-Met signalling in an HGF/SF-insensitive variant MDCK cell line with constitutive motile/invasive behaviour. *J Cell Sci*, 109 (Pt 9), 2371-81.
- WERLE, M., KAFEDJIISKI, K., KOLMAR, H. & BERNKOP-SCHNURCH, A. 2007. Evaluation and improvement of the properties of the novel cystine-knot microprotein McoEeTI for oral administration. *Int J Pharm*, 332, 72-9.
- WHITSON, B. A., JACOBSON, B. A., FRIZELLE, S., PATEL, M. R., YEE, D., MADDAUS, M. A. & KRATZKE, R. A. 2006. Effects of insulin-like growth factor-1 receptor inhibition in mesothelioma. Thoracic Surgery Directors Association Resident Research Award. *Ann Thorac Surg*, 82, 996-1001; discussion 1001-2.
- WILSON, S., GREER, B., HOOPER, J., ZIJLSTRA, A., WALKER, B., QUIGLEY, J. & HAWTHORNE, S. 2005. The membrane-anchored serine protease, TMPRSS2, activates PAR-2 in prostate cancer cells. *Biochem J*, 388, 967-72.
- WODARZ, A. 2002. Establishing cell polarity in development. *Nat Cell Biol*, 4, E39-44.
- YANO, T., MATSUI, T., TAMURA, A., UJI, M. & TSUKITA, S. 2013. The association of microtubules with tight junctions is promoted by cingulin phosphorylation by AMPK. *J Cell Biol*, 203, 605-14.
- YOSHIDA, N., TAKAGI, T., ISOZAKI, Y., SUZUKI, T., ICHIKAWA, H. & YOSHIKAWA, T. 2011. Proinflammatory role of protease-activated receptor-2 in intestinal ischemia/reperfusion injury in rats. *Mol Med Rep*, 4, 81-6.

- YU, A. S., CHENG, M. H., ANGELOW, S., GUNZEL, D., KANZAWA, S. A., SCHNEEBERGER, E. E., FROMM, M. & COALSON, R. D. 2009. Molecular basis for cation selectivity in claudin-2-based paracellular pores: identification of an electrostatic interaction site. *J Gen Physiol*, 133, 111-27.
- YU, H. C., HUANG, X. L., MA, Y. L., GAO, M., WANG, O., GAO, T., SHEN, Y. & LIU, X. H. 2013. Interleukin-8 Regulates Endothelial Permeability by Down-regulation of Tight Junction but not Dependent on Integrins Induced Focal Adhesions. *International Journal of Biological Sciences*, 9, 966-979.
- YU, J. X., CHAO, L. & CHAO, J. 1994. Prostaticin Is a Novel Human Serine Proteinase from Seminal Fluid - Purification, Tissue Distribution, and Localization in Prostate-Gland. *Journal of Biological Chemistry*, 269, 18843-18848.
- YU, J. X., CHAO, L. & CHAO, J. 1995. Molecular-Cloning, Tissue-Specific Expression, and Cellular-Localization of Human Prostaticin Messenger-Rna. *Journal of Biological Chemistry*, 270, 13483-13489.
- ZEUTHEN, T. 2002. General models for water transport across leaky epithelia. *Int Rev Cytol*, 215, 285-317.
- ZHANG, Y., CAI, X., SCHLEGELBERGER, B. & ZHENG, S. 1998. Assignment1 of human putative tumor suppressor genes ST13 (alias SNC6) and ST14 (alias SNC19) to human chromosome bands 22q13 and 11q24-->q25 by in situ hybridization. *Cytogenet Cell Genet*, 83, 56-7.

Appendices

Appendix- 1- Canine Matriptase sequence and shRNA cloning data and tools

1. Matriptase dog sequence:

Bold red and underlined= start codon

Yellow highlighted sequence= custom designed forward primer

Red highlighted sequence = custom designed reverse primer

Matriptase dog sequence, vectors and inserts

AGC**ATG**AGTGGCGTCGAGGAGGGCGTGGAGTTCCTGCCGGTCAACAACACCAGGAAGG
TGGAGAAGCGGGGCCCAAGCGCTGGGTGCTGCTGGTGACCGGGCTGGCCGGCCTGGTC
CTGCTTCCCTCGTGGCTTGCCTCCTGATGTGGCATTTCAGTACCAGAACATGCGGGT
TCAGAAGATCTTCAATGGCTACCTGAGGATCACCAACGAGAACTTCGTGGATGCCTATG
AGAACTCCAACCTCACGGAGTTTGC AAACCTGGCCAACAGGGTGAAGGAAGCGCTCAAG
CTGTTGTACAGTGGGGTGCCGTCCCTGGGCCCTACCACAAGAAGTCGATGGTGACCGC
CTTCAGCGAGGGCAGCGTCATCGCCTACTACTGGTCCGAGTTCAGCATCCCCCAGTACC
TGGTGGAGGATGCCGAGCGGTGATGGCCAGGAGCGGGCGGCCGTGCTGCCGCCCGA
GCCCCGCCCTCAACTCCTTCGTGCTCACCTCGGTGGTGGCCTTCCCCACTGACCCAGA
ACAGTACAGACCGCCAGGACAACAGCTGCAGCTTCGCCCTGCACGCCCGGAGCGGGGA
GCTGATGCGCTTACCACGCCCGGCTTCCCCGACAGCCGTACCCGGCCCGGGCCCGCTG
CCAGTGGACCCTGCGTGGGGATGCCGACTTCGTGCTGAGCCTCACCTTCCGCAGCTTTG
ACGTCGCGACCTGTGACGACCGGGCAGCGACCTGGTCATGGTGTATGACACCCTGAGC
CCCGTGGAAACCCGGGCCGTGGTGCAGCTGTGTGGCACCTACCCTCCCTCCTACAACCTG
ACCTTCCTCTCCTCCAGAACGTCTGCTCGTCAGCTGATCACCAACACGGAGCGGGCA
CACCTGGCTTTGAGGCCACGTTCTTCCAGCTGCCTAAGCTGAGCAGCTGTGGCGGCTC
CTTACGCGGCAGCCAGGGACCTTTAGCAGCCCCTACTATCCTGGCCACTACCCGCCCAA
CATGAACTGCACCTGGGACATTGAGGTGCCAGCCACCAGAACGTGAAGGTGCTCTTCA
AGGCCTTCTACATGCTGGAGCCCAACACCCCCCTGGGCACCTGCTCCAAGGACTACGTG
GAGGTCAACGGGGAGAAGTACTGCGGAGAGAGGCCCCAGTTTGTGGTCACCAGCAGGA
GCAACAAGATCACCGTTCGCTTCCACTCCGACCAGTCTACACCGACACGGGGTTCTTG
GCCGAGTACCTGTCATACGATTCCAGTGACCCGTGCCCGGGGAAGTTCATGTGTACAC
GGGAGATGCATCCGGAATGAGCTGCGCTGTGACGGCTGGGCTGACTGCACGGACTACA
GCGACGAGCTCAACTGCCAATGCAACGCCACCTACCAGTTCACATGCAAGAACAAGTTC
TGCAAGCCCCTCTTCTGGGTGTGCGACAGCGTGAACGACTGCGGAGACAACAGCGATGA
GCAGGAGTGCAGCTGCCCGGCTCAGACCTTCAAGTGTGGCAACGGGAAGTGCCTCCC**AC**
AGAACCAGCAGTGTGACGGGACGGACAACCTGCCGGGACGGATCCGATGAGGCCACGTG
TGACCTGGTGAGAAGTGTGGCCTGCACCAAACACACCTATCGCTGCCACAACGGGCTCT
GTTTGAGCAAGAGCAACCCGAGTGTGATGGGAAGAAGGACTGTAGCGACGGCTCGGA
TGAGAAGGATTGCCACTGTGgRGGCTGCGATCGTTCACCAGGCAGTCCCGGGTTCGTCGG
GGGCACGAATGCGGACGAAGGCGAGTGGCCCTGGCAGGTGAGCCTCCACGTGCTGGGCC

AGGGCCACGTGTGCGGGGCTTCCATCATCTCTCCAACTGGCTGGTGTGCGGCCGCTCAC
TGCTTCATCGACGACCGAGGATTACAGTACTCGGACCACATGGTGTGGACCGCCTTCCCT
GGGCCTGCATGACCAGAGCAAGCGCAGCGCCACTGGGGTGCAGGAGCTCGGCCTCAAGC
GCATCATCTCCACCCTTACTTCAACGACTTCACCTTCGACTATGACATTGCGCTGCTG
GAGCTGGAGCAGGCGGCCGAGTACAGCAGCACCGTGCGGCCATCTGCCTGCCCGAGAC
CTCGCACAGCTTCCCCGCGGCAAGGCCATCTGGGTCACCGGCTGGGGTCACACGCAGG
AAGGAGGCTCCGGCGCGCTGGTCCTGCAGAAGGGCGAGATCCGCGTCATCAACCAGACC
ACCTGGAGAACGGCTCCCGCAGCAGATCACGCCGCGCATGATGTTTCGTGGGCTACCTCA
GCGGCGGCGTGGACGCCTGCCATGGCGACTCCGGGGGCCCCCTGTCCAGCGTGGAGGCC
GACGGGCGGATCTTCCAGGCCGCGTGGTGGAGCTGGGGCGACGGCTGCGCTCAGAGGGA
CAAGCCGGGCGTGTACACGAGGCTCGCTGTATTTTCGGGACTGGATCAGAGAGGAGACGG
GGGTGTAGGTGCAGGGCCATCCGCGGCCACCCCGGCGTGCACACGTGCGGGCCAAGGAC
AGGACCGCTCACGGCACCCCTGACTTGGGCGCCCCGGAACCCAGACTGTGAACCCAATC
CCCAGGCCCTCCGGAGAGGGGCGCCCGGGCCTCCAGAGCAGCGCATGCAGGTGGGCGGAGG
ACGCTGGCCGCGCGGGGGCGCAGGCGTGAGGACTCAGCCTCCCGCCCGGAGACCTGCC
GCCCTGCCCCCCTGCCCGCCTGCCTGCCCGAGATCCCCCGGCGCAGGGGCCCTGCAGG
GCTGCCCCGGGATCCCTGCCGTGGGGCCGTGGCGCGGTCGGTTCCTAGGCCAGAGACCC
TGGAAGACACGCGGGCCTAAGATTGAATTTTACCAGCTCCTAGGGTGGGCTTCAGTGT
GTGTATTTGTGTGTATGAGTAAATTGTTTTTAGGTAAATTGTTTTCTCACTGGTCTTA
CTGCGGGCGCCCTTCCGCCTTCCCTCGTACCC

CACAGTCGCAATCCTTCTCA TGAGAAGGATTGCGACTGTG

Protein sequence:

Exons= Alternating exons

= Alternating exons

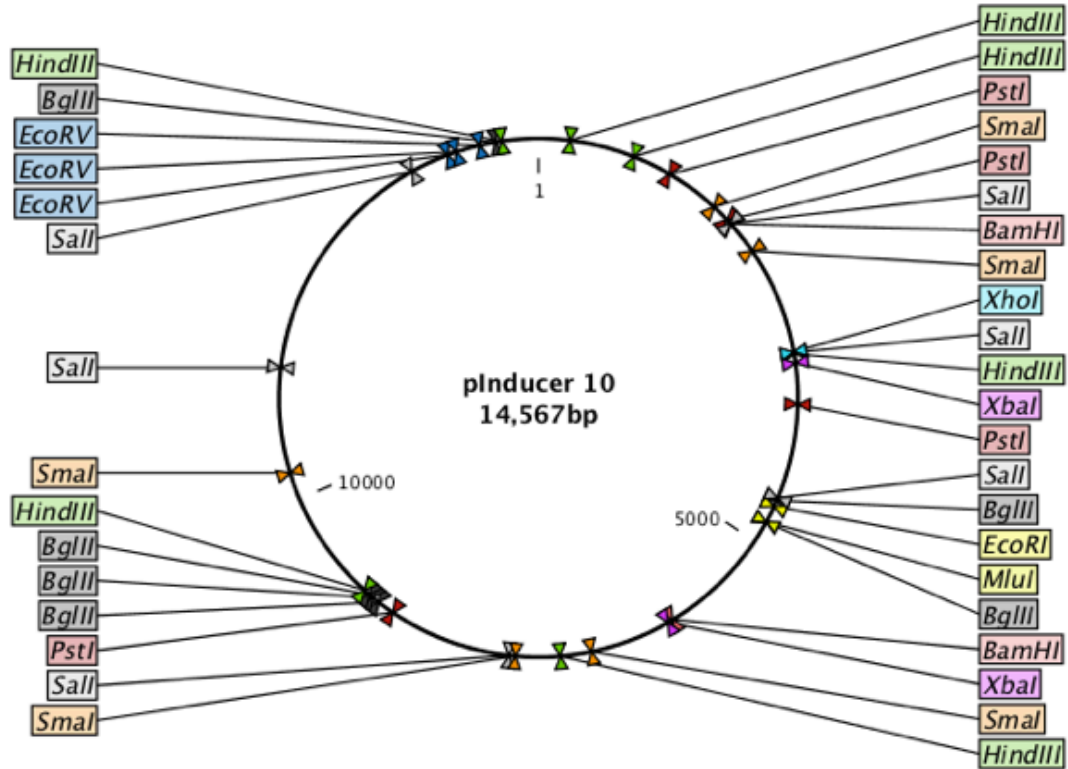
= Residue overlap splice site

MSGVEEGVEFLPVNNTRKVEKRGPKRWVLLVTGLAGLVLLSLVACLLMWHFQYQNM
VQKIFNGYLRITNENFVDAYENSSTEFANLANRVKEALKLLYSGVPSLGPYHKKSMVTA
FSEGSVIAYYWSEFSIPQYLVEDAERVMAQERAAVLPPRARALNSFVLTSVVAFPDPR
VQTAQDNSCSFALHARSGELMRFTTPGFPDSPYPARARCQWTLRGDADFVLSLTFRSF
VATCDDRGSIDLVMVYDTLSPVEPRAVQLCGTYPPSYNLTLSSQNVLLVTLITNTERRH
PGFEATFFQLPKLSSCGGSLRGSQGTFFSSPYYPGHYPPNMNCTWDIEVPSHQNVKVLFA
FYMLEPNTPLGTCSKDYVEVNGEKYCGERPQFVVTSRSNKITVRFHSDQSYTDTGFLA
EYLSYDSSDPCPGKFMCHTGR CIRNELRCDGWADCTDYSDELNCQCNATYQFTCKNFK
FKPLFWVCDVNDCGDNSDEQECSQAQTFRCGNGKCLPQNQQCDGTDNCGDGSDEATCD
LVRTVACTKHTYRCHNGLCLS KSNPECDGKKDCSDGSDEKDCDCGLRSFTRQSRVVG
GTNADEGEWPWQVSLHVLGQGHVCGASI SPNWLVSAAHCFIDDRGF RYSDHMVWTAFLG
LHDQSKRSATGVQELGLKRIISHPYFNDFTFDYDIALLELEQAAEYSSTVRPICLPETSH
SF PAGKAIWVTGWGHTQEGGSGALVLQKGEIRVINQTTWRTAPAADHAAHDVRGLPQR
RR RGLPWRLRGPVQRRGRRADLPGRRGELGRRRLRSEGQAGRVHEARCISGLDQRGDG
GVGAGPSAATPACARAGQQDRSRHP

2. ShRNA design, synthesis and cloning:

Cloning vectors:

Final Vector: pINDUCER 10 for inducible expression of mir30 shRNA



Green= Xho-I restriction site

Cyan= EcoRI restriction site

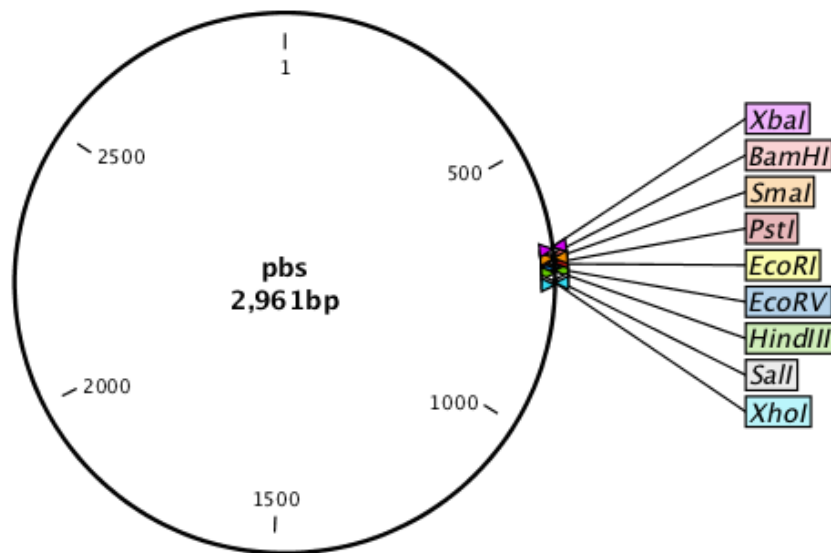
Purple= MluI restriction site

Yellow= Mir30a

agatgctgtaccccgtgacggcggcctgagaggccacagccagatggccctgaagctcgtgggcgggggctacctg
 cactgctcctcaagaccacatacagatccaagaaaccgctaagaacctcaagatgcccgcttccactcgtggacc
 acagactggaaagaatcaaggaggccgacaaagagacctagctcgagcagcagagatggctgtggccaagtactg
 cgacctccctagcaaaactggggcacagatgatgcgccgcaagccttgtaagtctcgcttcggcagcacatatacta
 tgttgaatgaggcttcagctactttacagaatcgttgctgcacatcttgaaacacttctgctgggattacttctcaggtta
 cccaacagaaggctcgaggctgacggtatcgataagcttgacgtccatctgctggtagctggtagctggtagctggaagttc
 tcttcaggggccgaaggagacgccaccatgggtctagatagggataacagggtaatggtagctggtagctggtagctggaagttc
 acttcaggcccgcattagtgattgattgaccagcgcacatcgctcaatcgccgggtcaccattcgctgaaccacagt
 tcaactgaattcataatctattcctgcctatttaaactgtttgaggaaacgcagatcgttttcgaagaatgaacgcaggtc
 ggtgacgccgtaacgcaacatagtcagacgctccatcccacccgaagccgaaaccagagtaaactccgggtcgat
 gccaacgttacgcaacacgttcggatgacccatcccgcagccagcacttcagccattaccggttttacccatgacgt
 ccacttctgcagaaggttcggttaaacgggaagtaggaaggacggaagcgaatctgcaaatcttctcaagaagttac
 gcaggaagtcgtgacgctgccttcagggttgtaaagctgatggttgatcaacaatcagaccttccatctgatggaac
 atcggcgtgtgagctggtcgtagctgttacgataaacacggccaggcgcgatgatacgaatcgggtgctgctgggctt
 tcatggtgcggatctgtacccagaggtctgggtacgcagcaggcgggtagtgtaaacagaaagtgcgtggtcag
 cgcgccgggtggtgaccaggaatgttcagagcatcgaagtattgataatcgtcttcgattccggcccgggtgaccag

```
gtaaagccaagctcaccgaagaaactttcgatacggtcgatggtagggtaaccggatgcagaccgctttcaatgc
gacgacctggcagagagacatcaatcgttccgcccagacgcgcattcagtcagcgcctttccagttccgctttacgc
gcattcagcgcctgctgaacctgctctttcgcttcggtgataaccgcaccagctgccggacgctctctggcgggcagctca
cgcagggtcgtcatctgaagggttaagtgcctttttacccaaatattcgacgcgcacattatctaacgcggcaacatct
gacgcctggctaatggccgccttcgactggcaaccagttctgcgagatgtgacatggtttctcattgtgtcagtggtg
acactggttcgttgacttagagcctatcccacaggctatcttacttgccatcttggtccccgataccgctgaccgcggat
tacctgttatccctagatctcacaattctgagaatttgatctttcagggatctccgtggatctattacgaattcaaggg
gctactttaggagcaattatctgtttactaaaactgaataccttgctatctctttgatacatTTTTTACAAAGCTGAATAAA
atggataaaattaaatcactTTTTTcaattggaagactaatgcgtttaaacacgcggcgacgcgtaagatctggcctccgc
gccgggtttggcgctcccgcgggcgccccctcctcacggcgagcgctgccacgtcagacgaagggcgcgagc
gagcgtcctgatccttccgc
```

pBluescript sequencing circular DNA map with multiple cloning site (MCS)- used as intermediate vector to check insert quality and ensure proper digestion:



Design of shRNA:

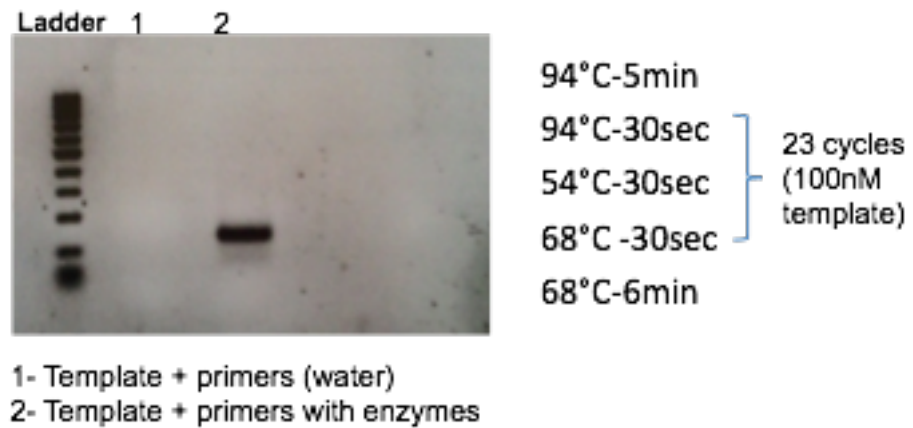
Table A: Online design of 96-mer insert sequence with matriptase shRNA:

XM_546396.2 Start position: 1400
TGCTGTTGACAGTGAGCGCTGCAAGAACAAGTTCTGCAAGTAGTGAAGCCACAGAT GTACTTGCAAGACTTGTTCTTGCATTGCCTACTGCCTCGGA

Table B: The hairpin oligonucleotides were amplified using PfuUltra (Stratagene) with pSM2C primers:

Forward primer
5'-GATGGCTGCTCGAGAAGGTATATTGCTGTTGACAGTGAGCG-3'
Reverse primer
5'-GTCTAGAGGAATTCCGAGGCAGTAGGCA-3'.

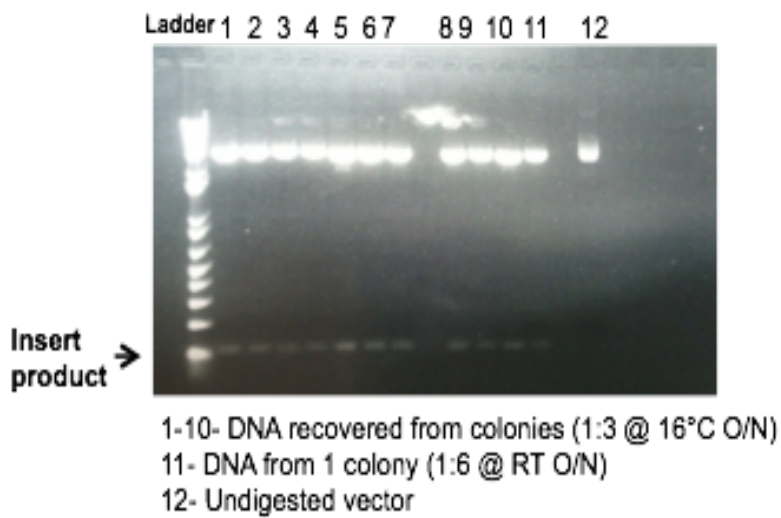
- 96-mer insert amplification using pSM2C primers with Xho-I and EcoR-I sequences:



Cloning of mer shRNA

Following insert digestion and purification this failed to clone directly into the pINDUCER 10 vector, so to check insert quality and proper digestion cloning into pBS was carried:

- Positive colonies were achieved as confirmed fragment from several colonies following digestion with Xho-I and EcoR-I



Clone 2:

pBluescript colony sample 2 (from gel 14-6-12 418.2ng/μl)

CTCGAGA- XhoI

NNNNNNNNNNNNNGNNNNNNN **NVCNNGA**AGGTATATTGCTGTTGACAGTGAGCGCTGC
AAGAACAAGTTCTGCAAGTAGTGAAGCCACAGATGTAAGTGCAGAACTTGTTCCTGCA
TTGCCTACTGCCTCG**GAATTC**CTGCAGCCCCGGGGATCCACTAGTTCCTAGAGCGGCCGC
CACCGCGGTGGAGCTCCAGCTTTTGTTCCTTTAGTGAGGGTTAATTGCGCGCTTGGCG
TAATCATGGTCATAGCTGTTTCCTGTGTGAAATTGTTATCCGCTCACAAATCCACACAA
CATACGAGCCGGAAGCATAAAGTGTAAGCCTGGGGTGCCTAATGAGTGAGCTAACTC
ACATTAATTGCGTTGCGCTCACTGCCCCGCTTTCCAGTCGGGAAACCTGTCGTGCCAGCT
GCATTAATGAATCGGCCAACGCGCGGGGAGAGGGCGTTTGCATATTGGGCGCTCTCCG
CTTCCTCGCTCACTGACTCGCTCGCTCGGTTCGGCTGCGGCGAGCGGTATCAGCTC
ACTCAAAGGCGGTAATACGGTTATCCACAGAATCAGGGGATAACGCAGGAAAGAACAT
GTGAGCAAAAGGCCAGCAAAAGGCCAGGAACCGTAAAAAGGCCGCGTTGCTGGCGTTT
TTCCATAGGCTCCGCCCCCTGACGAGCATCACAAAAATCGACGCTCAAGTCAGAGGTG
GCGAAACCCGACAGGACTATAAAGATACCAGGCGTTTCCCCCTGGAAGCTCCCTCGTGC
GCTCTCCTGTTCCGACCCTGCCGCTTACCGGATACCTGTCCGCCTTCTCCCTTCGGGAA
GCGTGGCGCTTCTCATAGCTCACGCTGTAGTATCTCAGTTCGGTGTAGGTCGTTCCGT
CCAAGCTGGGCTGTGTGCACGAACCCCCGTTTCAGCCCGACCGCTGCGCCTTATCCGGTA
ACTATCGTCTTGAGTCCAACCCGGTAAGACACGACTTATCGCCACTGGCAGCAGCNACT
GGTAACAGGATTAGCANANCGAGGTATGTAGCGGNGCTACAGANTTNTNAANTGGN
GGCCTAACTACGGCTNNNNCTANANAACAGTATTGGGNNNCTGCGCTCTGCTNANCC
NGTTNCCTTCGNAAAAGANTGNAGCTCTTGATCGNAANAANNCCGCGNGGNANNGN
NNNTTTTGTTCANANNNNATNNNCNCAAANNNNNNNNNAANATNNNNNTNTN
NNNNNNNNNNNNNNNCNANNNNNNNTNANNNTNNNNNNNGANATNNNNNNNNNG
NANTNTNNNNCN

KEY:

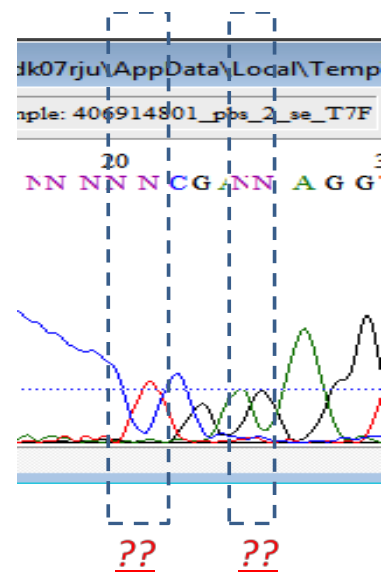
Matching sequenced insert

NN = UD

First NN = The peaks indicate a GA in this position

RED=Restriction sites

Blue= Insert sequence



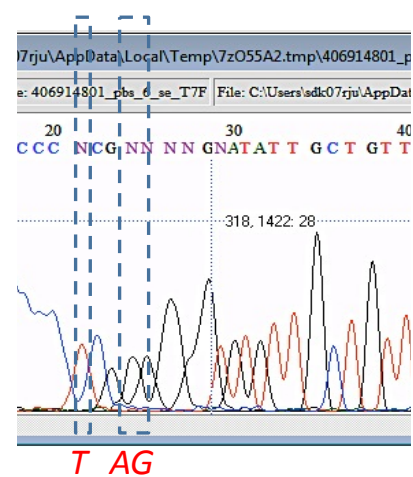
Clone 6:

pBluescript colony sample 3 (from gel 14-6-12 514.9ng/μl)

CTCGAG- XhoI

NNNNNNNNNNNNNGNCCCC**NCGMN**NNGNATATTGCTGTTGACAGTGAGCGCTGCA
AGAACAAGTTCTGCAAGTAGTGAAGCCACAGATGTACTTGCAGAATTGTTCTTGCAT
TGCCTACTGCCTCG**GAATTC**CTGCAGCCCGGGGATCCACTAGTTCTAGAGCGGCCGCC
ACCGCGGTGGAGCTCCAGCTTTTGTTCCTTTAGTGAGGGTTAATTGCGCGCTTGGCGT
AATCATGGTCATAGCTGTTTCCCTGTGTGAAATTGTTATCCGCTCACAATCCACACAAC
ATACGAGCCGGAAGCATAAAGTGTAAGCCTGGGGTGCCTAATGAGTGAGCTAACTCA
CATTAAATTGCGTTGCGCTCACTGCCCGCTTTCCAGTCGGGAAACCTGTCGTGCCAGCTG
CATTAAATGAATCGGCCAACGCGCGGGGAGAGGCGGTTTTCGTATTGGGCGCTCTTCCGC
TTCCTCGCTCACTGACTCGCTGCGCTCGGTCGTTTCGGCTGCGGCGAGCGGTATCAGCTC
ACTCAAAGGCGGTAATACGGTTATCCACAGAATCAGGGGATAACGCAGGAAAGAACAT
GTGAGCAAAGGCCAGCAAAGGCCAGGAACCGTAAAAAGGCCGCGTTGCTGGCGTTT
TTCCATAGGCTCCGCCCCCTGACGAGCATCACAAAAATCGACGCTCAAGTCAGAGGTG
GCGAAACCCGACAGGACTATAAAGATACCAGGCGTTTCCCCCTGGAAGCTCCCTCGTGC
GCTCTCCTGTTCCGACCCTGCCGCTTACCGGATACCTGTCCGCCTTCTCCCTTCGGGAA
GCGTGGCGCTTTCTCATAGCTCACGCTGTNNTATCTCAGTTCGGTGTAGGTCGTTTCGCT
CCNAGCTGGGCTGTGTGCACGAACCCCCGTTTCAGCCCGACCGCTGCGCCTTATCCGGT
AACTATCGTCTTGAGTCCAACCCGGTNAGACACGACTTATCGCCACTGGCAGCAGCCAC
TGGTAACAGGATTAGCAGAGCGAGGTATGTNCCGNGCTACNGAGTTCTTGAAGTGGT
GGNCTAACTACGGCTACNCTANANANAGTATTTGGTATCTGCGCTCTGCTGANCNNGTT
ACTNCGNAAAAGANTTTGGTAGNNCTTGATCCGCAANNAACNACNGCTGNAGCGGNTN
NTTTTTGNTTGCANNANCANNNTNNNCNNNNNAAAANNNNNNAGAANATCNNGNNN
NTTTTCNNNNNGNNNNNNNNNNNNNNNNNNNNNTCNCNNTANGGNTNNNNNNNGN
NNNNNNNNNGNNNNNNNTNNNNCNNNNNN

KEY:
Matching sequenced insert
NN = UD
*First **NN** = The peaks indicate an AG in this position*
RED=Restriction sites
Blue= Insert sequence



Clone 10:

pBluescript colony sample 8 (from gel 14-6-12 516.6ng/μl)

CTCGAG- XhoI

NNNNNNNNNNNGNNNNNNNNNN**NCNNNN**AAANGNATATTGCTGTTGACAGTGAGCGCT
GCAAGAACAAGTTCTGCAAGTAGTGANN**CCACAGATGTACTTGCAGAACTTGTTCTTG**
CATTGCCTACTGCCTCGGAATTCCTGCAGCCCGGGGATCCACTAGTTCTAGAGCGGCC
GCCACCGCGGTGGAGCTCCAGCTTTTGTTCCTTTAGTGAGGGTTAATTGCGCGCTTGG
CGTAATCATGGTCATAGCTGTTTCCTGTGTGAAATTGTTATCCGCTCACAATCCACAC
AACATACGAGCCGGAAGCATAAAGTGTAAGCCTGGGGTGCCTAATGAGTGAGCTAAC
TCACATTAATTGCGTTGCGCTCACTGCCCGCTTTCCAGTCGGGAAACCTGTCGTGCCAG
CTGCATTAATGAATCGGCCAACGCGCGGGGAGAGGCGGTTTGCATATTGGGCGCTCTTC
CGCTTCCTCGCTCACTGACTCGCTGCGCTCGGTCGTTCCGGCTGCGGCAGCGGTATCAGC
TCACTCAAAGGCGGTAATACGGTTATCCACAGAATCAGGGGATAACGCAGGAAAGAAC
ATGTGAGCAAAGGCCAGCAAAGGCCAGGAACCGTAAAAAGGCCGCGTTGCTGGCGT
TTTTCCATAGGCTCCGCCCCCTGACGAGCATCACAAAAATCGACGCTCAAGTCAGAGG
TGCGGAAACCCGACAGGACTATAAAGATACCAGGCGTTTCCCCCTGGAAGCTCCCTCGT
GCGCTCTCTGNTTCCGACCCTGCCGTTACCGGATACCTGTCCGCCTTCTCCCTTCGG
GAAGCGTGGCGCTTCTCATAGCTCACGCTGTAGTATCTCAGTTCGGTGTANGTCGTTT
GCTCCAAGCTGGGCTGTGTGCACGAACCCCCGTTACGCCNACCGCTGCGCCTTATCCG
GTAATATCGTCNTGAGTCCAACCCGNNAGANNCGACTTATCGCCACNGGCNCAGCCA
CTGGTAACAGGATTANCANANCGAGGTATGTAGGCGTGCTACNGANTTCNTGAANGG
NGGCCTAACTACCGCTACNCTANAANAACNNATTTGGTATCTGNNNTCNGCTGAANN
NGTTACCTTTNGNAAAANAANTGGTAGNNCTTGATCNNNNAANAACNACCGNNNG
TNNNG

KEY:

Matching sequenced insert

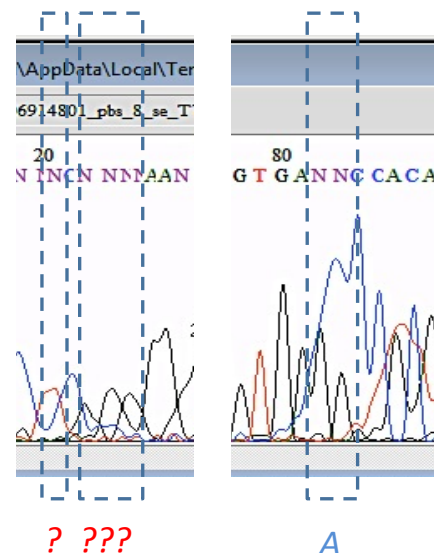
NN = UD

First **NN** = The peaks indicate an AG in this position

Second **NN** = The peaks indicate an AG in this position

RED=Restriction sites

Blue= Insert sequence



Appendix- 2-RT² Cytokine profiler array

384 Cytokine gene analysis array including all gene names and C_t values. Also included are several housekeeping genes and the melt curves for each

Table of C_t values for each gene and sample: (Undetermined = UD)

	gene name	1h control	1hr IN-1	2h control	2h IN-1	5h control	5hr IN-1	10h control	10h IN-1
1	AIMP1	23.30	23.73	23.35	22.96	23.48	23.61	23.77	23.25
2	BMP2	26.51	26.69	26.72	26.88	26.65	27.26	27.50	26.77
3	C5	29.98	30.90	30.26	31.15	30.27	31.80	30.44	29.88
4	CCL1	UD	UD	UD	UD	UD	UD	UD	UD
5	CCL11	38.10	UD	UD	UD	UD	35.84	38.13	UD
6	CCL13	33.82	UD	32.80	33.63	35.21	35.53	UD	UD
7	CCL15	20.57	20.91	20.66	20.53	20.33	20.75	20.57	20.10
8	CCL16	32.68	32.34	28.98	30.98	29.23	29.73	31.89	34.06
9	CCL17	UD	UD	UD	UD	UD	UD	UD	UD
10	CCL2	28.59	29.78	29.33	29.31	30.21	29.99	30.91	30.20
11	CCL20	27.91	29.37	29.99	28.44	31.27	32.63	31.67	28.20
12	CCL22	38.85	UD	UD	38.92	UD	UD	UD	UD
13	CCL23	UD	UD	UD	UD	UD	35.27	UD	UD
14	CCL24	30.65	30.20	30.15	30.88	30.67	30.42	30.73	30.38
15	CCL26	35.22	UD	35.12	UD	UD	36.01	35.11	UD
16	CCL3	35.56	UD	34.57	UD	UD	UD	UD	UD

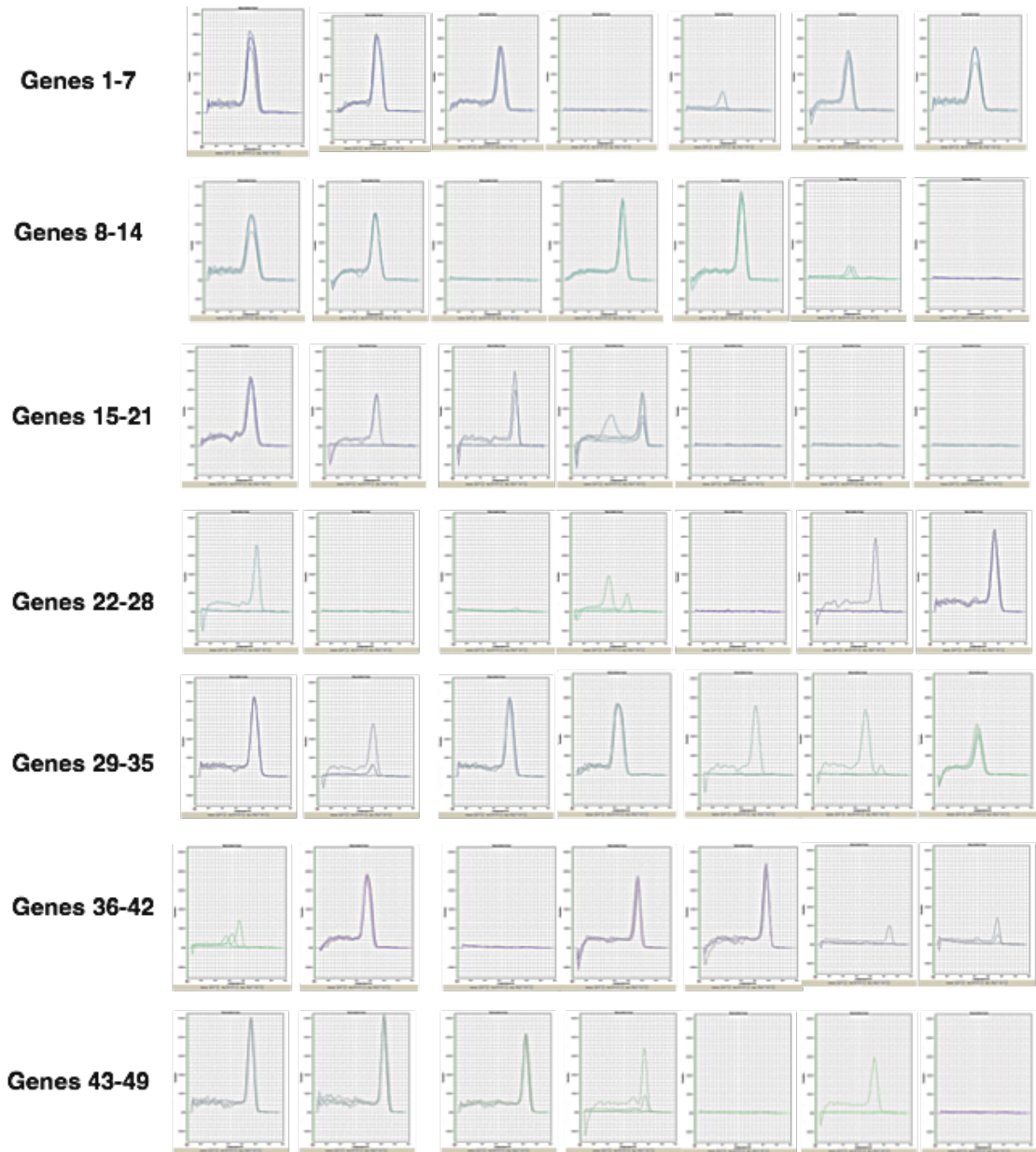
17	CCL4	UD							
18	CCL5	32.26	36.58	34.23	34.56	39.04	UD	35.00	32.88
19	CCL7	UD							
20	CCL8	UD							
21	CCR1	34.52	UD	UD	UD	UD	34.20	33.50	34.74
22	CCR2	UD							
23	CCR3	UD							
24	CCR4	UD	UD	35.89	38.30	UD	UD	UD	UD
25	CCR5	UD							
26	CCR6	UD	33.15	UD	UD	UD	UD	33.84	UD
27	CCR8	25.77	25.83	25.62	25.80	27.72	26.16	26.19	25.62
28	CD40LG	26.97	26.68	25.88	25.95	24.55	24.69	25.25	25.25
29	CSF1	35.40	38.56	38.67	UD	UD	UD	UD	39.33
30	CSF2	22.94	22.99	22.88	23.22	22.94	23.45	23.55	23.46
31	CSF3	UD	UD	34.26	UD	34.12	33.79	UD	UD
32	CCR3	29.92	29.55	28.89	30.45	29.24	29.28	26.57	28.33
33	CX3CL1	UD	UD	UD	34.11	UD	UD	UD	UD
34	CX3CR1	UD	UD	UD	34.62	UD	UD	UD	UD
35	CXCL1	36.47	33.96	36.55	35.88	36.55	37.40	35.96	36.32
36	CXCL10	38.59	UD	38.57	37.70	32.68	38.39	UD	UD

37	CXCL11	32.10	31.46	31.07	31.11	31.36	31.27	32.70	32.92
38	CXCL12	UD							
39	CXCL13	33.39	33.40	33.78	35.23	UD	UD	34.81	34.12
40	CXCL2	30.43	30.53	30.85	30.53	30.85	31.45	31.53	30.81
41	CXCL3	37.48	UD						
42	CXCL5	38.59	37.62	UD	UD	38.26	UD	UD	UD
43	CXCL6	24.40	24.46	24.15	24.72	23.41	25.21	24.19	25.63
44	CXCL9	22.45	22.48	22.28	22.59	22.55	22.77	22.49	23.08
45	CXCR1	26.60	26.77	25.84	26.26	26.45	26.64	26.69	26.98
46	CXCR2	UD	37.98	34.38	UD	UD	UD	37.71	37.06
47	FASLG	UD							
48	IFNA2	UD	UD	UD	34.74	UD	UD	UD	UD
49	IL10RA	UD							
50	IL10RB	33.24	33.63	32.43	34.74	UD	33.31	UD	UD
51	IL13	33.53	31.83	32.54	31.91	35.49	34.49	35.61	35.15
52	IL15	35.74	UD	34.66	UD	UD	38.01	33.56	UD
53	IL16	27.91	28.12	27.18	27.70	33.06	29.28	31.75	30.00
54	IL17A	UD	UD	38.48	UD	UD	UD	UD	UD
55	IL17C	27.17	28.28	26.34	26.88	33.98	32.12	33.04	30.22
56	IL17F	23.58	23.88	23.80	24.11	25.38	24.63	24.85	24.60
57	IL1A	UD							

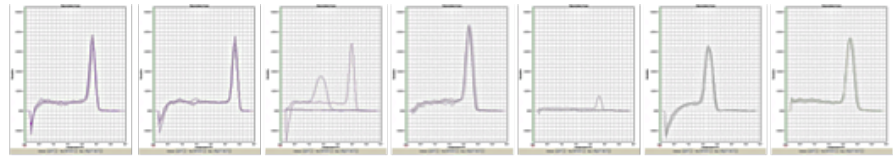
58	IL1B	31.98	33.18	31.10	32.86	31.03	34.08	32.38	32.46
59	IL1R1	UD	UD	UD	UD	UD	UD	35.06	UD
60	IL1RN	UD	UD	37.79	UD	UD	35.03	UD	UD
61	IL21	UD	UD	UD	35.17	UD	UD	36.56	39.70
62	IL27	UD	38.16						
63	IL3	21.25	33.48	32.67	34.50	36.13	34.24	UD	33.96
64	IL33	30.18	30.60	29.46	29.66	30.78	30.37	30.62	30.47
65	IL5	UD							
66	IL5RA	32.92	32.92	34.67	32.69	33.52	33.62	33.95	33.73
67	IL7	22.86	22.83	22.42	23.12	23.97	23.97	25.00	23.72
68	IL8	34.53	34.49	34.85	UD	UD	UD	UD	34.51
69	IL9	27.27	27.88	28.35	28.60	29.25	29.40	28.35	28.29
70	IL9R	UD							
71	LTA	UD	UD	38.01	UD	UD	UD	UD	UD
72	LTB	UD							
73	MIF	30.73	30.78	30.45	30.23	31.34	31.08	31.31	31.18
74	NAMPT	28.65	29.20	28.50	28.71	30.12	31.59	30.12	29.56
75	OSM	31.91	31.16	32.37	31.86	32.59	34.18	33.38	32.90
76	SPP1	19.14	19.36	18.73	18.66	21.74	21.09	19.96	19.13
77	TNF	33.65	UD	UD	38.30	39.52	UD	UD	34.45
78	TNFRSF11B	UD	UD	UD	35.15	UD	UD	UD	UD

7 9	TNFSF 10	23.47	26.03	22.44	23.60	32.08	31.36	27.48	25.48
8 0	TNFSF 11	24.71	25.10	24.05	24.11	26.40	24.40	25.93	25.16
8 1	TNFSF 13	33.21	34.50	32.82	32.95	33.22	32.86	34.79	33.83
8 2	TNFSF 13B	32.81	32.91	33.36	32.54	33.36	34.90	32.28	32.42
8 3	TNFSF 4	UD							
8 4	VEGFA	21.01	21.47	21.18	21.75	21.18	22.21	21.49	22.12
8 5	ACTB	16.81	16.83	16.94	17.53	17.01	17.59	17.59	17.46
8 6	B2M	20.25	20.51	20.33	19.75	20.00	20.48	20.40	20.13
8 7	GAPD H	16.14	15.98	15.98	16.28	16.00	16.16	16.19	15.89
8 8	RPLP0	22.56	22.72	22.39	22.48	22.35	22.56	22.83	22.34
8 9	HPRT1	20.89	20.89	20.69	20.18	20.49	20.85	20.33	20.42
9 0	HGDC	UD	27.61	UD	UD	UD	UD	UD	UD
9 1	RTC	UD							
9 2	RTC	UD							
9 3	RTC	UD							
9 4	PPC	21.19	23.29	21.50	22.16	27.42	34.70	23.12	27.88
9 5	PPC	21.85	23.38	25.26	21.39	25.44	22.70	23.06	28.41
9 6	PPC	20.37	23.78	21.97	21.41	26.59	33.34	21.79	24.72

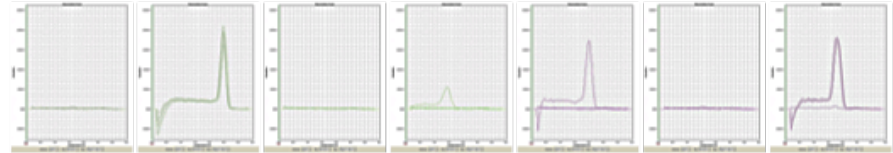
RT® profiler cytokine array- Gene melt curve:



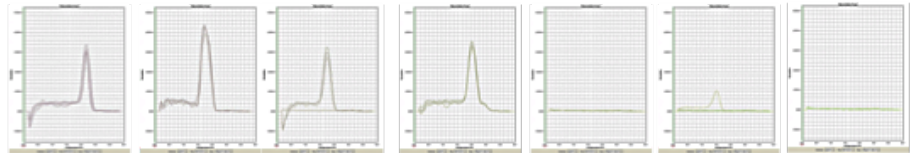
Genes 50-57



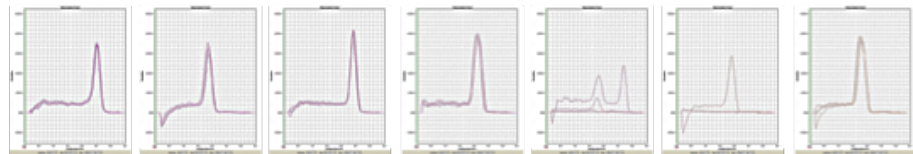
Genes 58-64



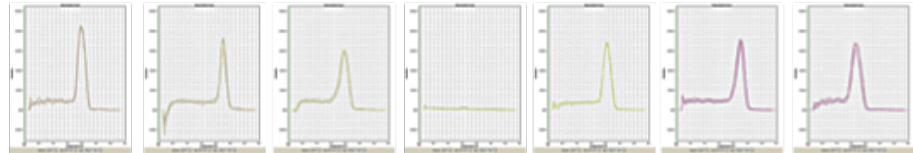
Genes 65-71



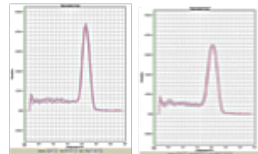
Genes 72-78



Genes 79-85



Genes 86-92



Appendix- 3-Details on Pathscan® RTK array

Target map of the Pathscan® RTK signaling array:

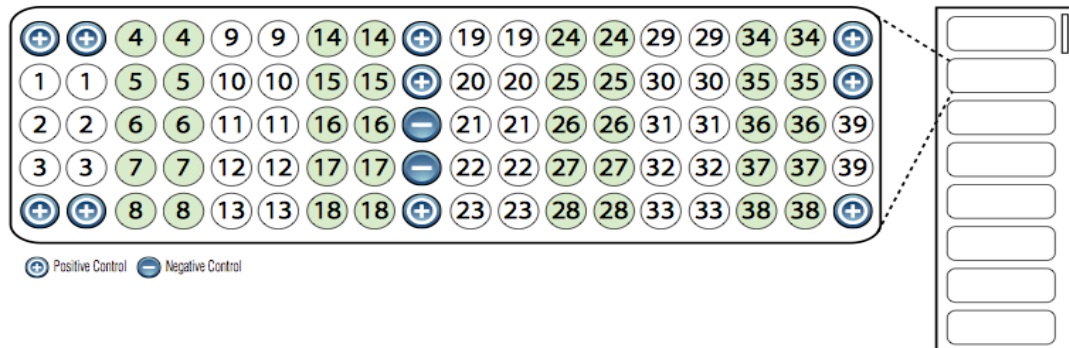


Table of target signaling RTK proteins corresponding to the array:

Receptor Tyrosine Kinases

Target	Phosphorylation Site	Family
1 EGFR/ErbB1	pan-Tyr	EGFR
2 HER2/ErbB2	pan-Tyr	EGFR
3 HER3/ErbB3	pan-Tyr	EGFR
4 FGFR1	pan-Tyr	FGFR
5 FGFR3	pan-Tyr	FGFR
6 FGFR4	pan-Tyr	FGFR
7 InsR	pan-Tyr	Insulin R
8 IGF-IR	pan-Tyr	Insulin R
9 TrkA/NTRK1	pan-Tyr	NGFR
10 TrkB/NTRK2	pan-Tyr	NGFR
11 Met/HGFR	pan-Tyr	HGFR
12 Ron/MST1R	pan-Tyr	HGFR
13 Ret	pan-Tyr	Ret
14 ALK	pan-Tyr	LTK
15 PDGFR	pan-Tyr	PDGFR
16 c-Kit/SCFR	pan-Tyr	PDGFR
17 FLT3/Fik2	pan-Tyr	PDGFR
18 M-CSFR/CSF-1R	pan-Tyr	PDGFR
19 EphA1	pan-Tyr	EphR
20 EphA2	pan-Tyr	EphR
21 EphA3	pan-Tyr	EphR
22 EphB1	pan-Tyr	EphR
23 EphB3	pan-Tyr	EphR
24 EphB4	pan-Tyr	EphR
25 Tyro3/Dtk	pan-Tyr	Axl
26 Axl	pan-Tyr	Axl
27 Tie2/TEK	pan-Tyr	Tie
28 VEGFR2/KDR	pan-Tyr	VEGFR

Table of target signaling nodes proteins corresponding to the array:

Signaling Nodes			
	Target	Phosphorylation Site	Family
29	Akt/PKB/Rac	Thr308	Akt
30	Akt/PKB/Rac	Ser473	Akt
31	p44/42 MAPK (ERK1/2)	Thr202/Tyr204	MAPK
32	S6 Ribosomal Protein	Ser235/236	RSK
33	c-Abl	pan-Tyr	Abl
34	IRS-1	pan-Tyr	IRS
35	Zap-70	pan-Tyr	Zap-70
36	Src	pan-Tyr	Src
37	Lck	pan-Tyr	Src
38	Stat1	Tyr701	Stat
39	Stat3	Tyr705	Stat

Appendix- 4- Published paper

Kelly Gray, Salma Elghadban, Panumart Thongyoo, Kate A. Owen, Roman Szabo, Thomas H. Bugge, Edward W. Tate, Robin J. Leatherbarrow, Vincent Ellis. **Potent and specific inhibition of the biological activity of the type-II transmembrane serine protease matriptase by the cyclic microprotein MCoTI-II. 2014.**

Potent and specific inhibition of the biological activity of the type-II transmembrane serine protease matriptase by the cyclic microprotein MCoTI-II

Kelly Gray¹; Salma Elghadban¹; Panumart Thongyoo²; Kate A. Owen¹; Roman Szabo³; Thomas H. Bugge³; Edward W. Tate²; Robin J. Leatherbarrow²; Vincent Ellis¹

¹School of Biological Sciences, University of East Anglia, Norwich Research Park, Norwich, UK; ²Biological and Biophysical Chemistry Section, Department of Chemistry, Imperial College London, UK; ³Oral and Pharyngeal Cancer Branch, National Institute of Dental and Craniofacial Research, NIH, Bethesda, Maryland, USA

Summary

Matriptase is a type-II transmembrane serine protease involved in epithelial homeostasis in both health and disease, and is implicated in the development and progression of a variety of cancers. Matriptase mediates its biological effects both via as yet undefined substrates and pathways, and also by proteolytic cleavage of a variety of well-defined protein substrates, several of which it shares with the closely-related protease hepsin. Development of targeted therapeutic strategies will require discrimination between these proteases. Here we have investigated cyclic microproteins of the squash *Momordica cochinchinensis* trypsin-inhibitor family (generated by total chemical synthesis) and found MCoTI-II to be a high-affinity (K_i 9 nM) and highly selective (> 1,000-fold) inhibitor of matriptase. MCoTI-II efficiently inhibited the proteolytic activation of pro-hepatocyte growth factor (HGF) by matriptase but not by hepsin, in both purified and cell-based systems, and inhibited HGF-dependent cell scattering. MCoTI-II also selectively

inhibited the invasion of matriptase-expressing prostate cancer cells. Using a model of epithelial cell tight junction assembly, we also found that MCoTI-II could effectively inhibit the re-establishment of tight junctions and epithelial barrier function in MDCK-I cells after disruption, consistent with the role of matriptase in regulating epithelial integrity. Surprisingly, MCoTI-II was unable to inhibit matriptase-dependent proteolytic activation of prostasin, a GPI-anchored serine protease also implicated in epithelial homeostasis. These observations suggest that the unusually high selectivity afforded by MCoTI-II and its biological effectiveness might represent a useful starting point for the development of therapeutic inhibitors, and further highlight the role of matriptase in epithelial maintenance.

Keywords

Serine protease, protease inhibitor, hepatocyte growth factor, epithelial cell, tight junctions, matriptase, cyclotide

Correspondence to:

Vincent Ellis, PhD
School of Biological Sciences, University of East Anglia
Norwich Research Park
Norwich, NR4 7TJ, UK
Tel.: +44 1603 592570
E-mail: v.ellis@uea.ac.uk

Financial support:

This study was supported by the Norfolk and Waveney Big C Cancer Charity, the John and Pamela Salter Charitable Trust and by European Union FP6 (Cancerdegradome) project.

Received: November 4, 2013

Accepted after major revision: March 10, 2014

Epub ahead of print: April 3, 2014

<http://dx.doi.org/10.1160/TH13-11-0895>

Thromb Haemost 2014; 112: 402-411

Introduction

Proteolytic enzymes play key regulatory roles in a wide variety of physiological and pathological process, ranging from fertility and development to cancer invasion and metastasis. The majority of these enzymes are soluble, extracellular proteins. However, a limited number are associated with the cell surface, restricting their activity to the pericellular environment and enabling them to affect cell function. This association can occur either through binding to membrane receptors or their expression as integral membrane proteins (1, 2). The latter includes matriptase, which is a member of the type-II transmembrane serine protease (TTSP) family (2, 3).

Matriptase is overexpressed in a wide range of human epithelial tumours, and often correlated with clinical outcome (4, 5). Experi-

mental evidence suggests that the proteolytic activity of matriptase may be causally associated with tumour development, as a low level of orthotopic expression of matriptase in mice leads to spontaneous tumours and increased carcinogen susceptibility (6, 7). Matriptase also has essential physiological functions in regulating the integrity of epithelial tissues. Mice with targeted deletion of matriptase have a severe epidermal barrier defect leading to neonatal mortality (8), and a mutation in matriptase that leads to reduced protease activity is associated with the human syndrome autosomal recessive ichthyosis with hypotrichosis (9). Conditional deletion of matriptase in mice demonstrates that it has a more wide-ranging postnatal effect on epithelial tissues leading to severe organ dysfunction (10), and intestinal barrier competence is lost in matriptase hypomorphic mice (11).

Matriptase, in common with the other TTSPs, has trypsin-like substrate specificity, hydrolysing the peptide bond C-terminal of the Lys or Arg side-chains that occupy the S1 primary substrate specificity pocket. The extended peptide substrate specificity of matriptase has been determined (12, 13) and several protein substrates have been identified *in vitro*. These include three proteins that can be considered to be serine protease zymogens, suggesting that matriptase is involved in zymogen activation cascades. These are the soluble serine protease uPA (12, 14, 15), the GPI-anchored serine protease prostaticin (16) and hepatocyte growth factor (HGF) (13, 14), a plasminogen-related growth factor also known as scatter factor. In addition to activating these substrates by limited proteolysis in purified systems, matriptase has also been shown to catalyse these reactions with high efficiency on the cell-surface. Endogenous matriptase on the surface of leukocytes has been demonstrated to proteolytically activate pro-uPA bound to its GPI-anchored cellular receptor uPAR and thereby facilitate pericellular plasmin generation (15), and endogenous matriptase mediates pro-HGF-dependent epithelial cell scattering (13). The proteolytic activation of each of these zymogens may potentially be involved in the pro-carcinogenic and other biological activities of matriptase (2, 7, 17). Interestingly, another TTSP, hepsin, appears to have protein substrate specificity that overlaps to a large extent with that of matriptase. Hepsin has been shown to activate pro-uPA, pro-HGF and pro-prostaticin (13, 18–20), despite having a dissimilar peptide substrate specificity to that of matriptase (13).

Proteolytic enzymes as a class are considered to be a major part of the drugable genome (21, 22), and inhibition of matriptase activity may therefore be an attractive target for therapeutic intervention in cancer. Although effective inhibition of protease activity is easily accomplished using synthetic small molecule inhibitors, selectivity of inhibition is much more difficult to achieve, particularly between closely related proteases. The well-publicised failure of clinical trials of matrix metalloprotease inhibitors in cancer is believed to be largely a consequence of such a lack of selectivity, i.e. inhibition of metalloproteases in addition to the target, with potentially differing biological activities (22, 23). Therefore, the ability to discriminate between matriptase and hepsin, with their overlapping substrate specificities, must be considered to be an important goal in the development of an effective inhibitory strategy targeted at matriptase activity.

To achieve this, and to overcome the possible limitations of small molecule inhibitors, we have investigated the unique class of macrocyclic cystine-knot microproteins known as cyclotides. These plant-derived cyclic proteins include *Momordica cochinchinensis* trypsin inhibitor-II (MCoTI-II), a 34-residue cyclotide originally isolated from the Vietnamese squash. These cyclotides have an exceptionally rigid structure, are highly resistant to thermal and enzymatic degradation, and have a high stability *in vivo* (24). We have developed an efficient strategy for the total chemical synthesis of MCoTI-II, which can be used as a scaffold for the introduction of sequence variations aimed at modulating the affinity and specificity of inhibition (25–27). In the present study we have found that it is a highly specific and selective inhibitor of the biochemical and biological activities of matriptase, and that it has no

detectable effect on the activity of hepsin. MCoTI-II effectively inhibits the activity of matriptase against both peptide and protein substrates, and potently inhibits the activity of matriptase in several complex cellular systems that reflect its *in vivo* functions. The inhibitory characteristics of MCoTI-II, and its wide-ranging biological effects, suggest that it may be a potential candidate for the development of matriptase-targeted therapeutic strategies.

Materials and methods

Proteins and reagents

MCoTI-II, MCoTI-II[K10R], MCoTI, MCoEeT-I and MCoEeT-I[K10R] were produced by total chemical synthesis as previously described (25, 27). Soluble matriptase, soluble hepsin and pro-HGF (with a C-terminal V5-His tag) were all expressed and purified as previously described (13). Recombinant human kallikrein-2 (KLK2) and kallikrein-3 (KLK3) were purchased from R&D Systems (Abingdon, UK). The fluorogenic peptide substrates H-D-Val-Leu-Lys-7-amino-4-methylcoumarin and H-Glu-Gly-Arg-7-amino-4-methylcoumarin were purchased from MP Biomedicals (Cambridge, UK). Mouse anti-V5 antibody was from Invitrogen (Paisley, UK), mouse anti-prostaticin from BD Biosciences (Oxford, UK), rabbit anti-claudin-1 and mouse anti-ZO-1 from Sigma-Aldrich (Poole, UK) and Alexa 488-labelled goat anti-mouse and Alexa 647-labelled goat anti-rabbit IgG from Abcam (Cambridge, UK).

Cell culture

Madine-Darby canine kidney cells (MDCK-I, MDCK-II) and HEK293 cells were routinely maintained in DMEM supplemented with 10% FCS and 2 mM L-glutamine. PC-3 cells were maintained in RPMI medium containing 10% FCS and 2 mM L-glutamine. All cell culture reagents were from Invitrogen.

Determination of K_i values for protease inhibition

Purified soluble matriptase (5 nM) or hepsin (2 nM) was incubated with varying concentrations of H-D-Val-Leu-Lys-7-amino-4-methylcoumarin (0 – 0.5 mM) in 50 mM Tris-HCl pH 7.6, 100 mM NaCl, 0.01% Tween 80. Varying concentrations of MCoTI-II or its derivatives were included in these incubations and substrate hydrolysis monitored continuously using a Spectramax Gemini fluorescence microplate reader (Molecular Devices, Berkshire, UK) using excitation and emission wavelengths of 360 nm and 440 nm, respectively. V_{max} and K_m values were determined from initial reaction rates at each substrate and inhibitor concentration and K_i values subsequently calculated from plots of K_m/V_{max} vs [inhibitor], as previously described (13). For each K_i determination, at least four substrate and four inhibitor concentrations were used, with each analysis performed in triplicate. K_i values for other proteases were determined as previously described (27). The K_i was also determined for the inhibition of pro-uPA activation using a range of pro-uPA concentrations (0.05 – 1 μ M). K_i

was calculated from plots of K_m/V_{max} vs [inhibitor], as previously described (13).

Inhibition of pro-HGF and pro-uPA activation

Purified pro-HGF or pro-uPA (both expressed in *Drosophila* S2 cells with a C-terminal V5-epitope tag) was incubated with either soluble matriptase or soluble hepsin in 50 mM Tris-HCl pH 7.6, 100 mM NaCl, 0.01% Tween 80, in the presence of varying concentrations of MCoTI-II. Aliquots of equal volume were taken from each reaction at timed intervals and the reaction terminated by addition of SDS-PAGE sample buffer containing dithiothreitol. Samples were analysed by SDS-PAGE and western blotting using anti-V5 primary antibody, as previously described (13).

Inhibition of cell-mediated pro-HGF activation

MDCK-II or PC-3 cells were seeded at a density of 1×10^4 cells per well in 96-well plates and allowed to adhere overnight. The cells were washed in serum-free medium prior to incubation with purified V5-tagged pro-HGF in the presence of MCoTI-II (100 nM or 500 nM). Medium was collected at timed intervals, the reaction terminated by addition of SDS-PAGE sample buffer containing dithiothreitol, and the samples analysed for pro-HGF activation by SDS-PAGE and western blotting for the V5 epitope.

Cell scatter assay

The biological activity of HGF was determined by its effect on the scattering of MDCK-II cells as previously described (13). Cells were seeded at a density of 1×10^3 cells per well and left to adhere overnight. Pro- or active HGF (10 ng/ml) was added in the presence of varying concentrations of MCoTI-II (0 - 500 nM) in serum-free medium. After 30 hours (h) the cells were washed twice with phosphate-buffered saline (PBS) and fixed with ice-cold methanol for 5 minutes, followed by a further PBS wash. Images were taken using a Zeiss CCD inverted microscope using x10 magnification. Treatments were performed in duplicate in three independent experiments.

Matrigel invasion assay

Precoated matrigel invasion chambers (BD Biosciences) were seeded with PC-3 cells at a density of 1×10^5 per well in 200 μ l serum-free medium. The lower chamber contained 2% FCS as a chemoattractant and the cells were allowed to invade the matrigel for 24 h in the presence of varying concentrations of MCoTI-II (0 - 500 nM). Non-invading cells and matrigel were removed and the cells on the underside of the membrane fixed with methanol, stained with haematoxylin-eosin and mounted in hydromount (National Diagnostics, Hull, UK). Invaded cells were counted using an inverted microscope, using three randomly chosen fields for each membrane. Each experimental condition was performed in duplicate and the experiment carried out on three separate occasions. Data were analysed using Student's t-test.

Transepithelial electrical resistance (TEER) measurements

MDCK-I cells (25,000/well) were seeded in triplicate into 6.5 mm Transwell chambers with 0.4 μ m pores (Costar, Corning Life Sciences, Tewksbury, MA, USA). The transepithelial ion permeability was determined every 24 h by measuring electric resistance across the monolayer using the EVOM Epithelial Voltohmmeter (World Precision Instruments, Sarasota, FL, USA). The medium in both internal and external compartments of each Transwell was changed every two days, and contained varying concentrations of MCoTI-II. In Ca^{2+} -switch experiments, cell monolayers with a stable level of TEER were incubated with Spinner's Ca^{++} -free medium for 16 h, followed by restoration of normal culture conditions.

Immunofluorescence microscopy

MDCK-I cells were grown on 6.5 mm polyester Transwell inserts with 0.4 μ m pores (Costar) for five days. Cells were fixed in methanol at -20° C, washed three times in PBS, three times with 1% goat serum/PBS and incubated with 10% goat serum/PBS at room temperature. Cells were incubated with primary antibodies against claudin-1 (1:100) and ZO-1 (1:50), washed and incubated with Alexa-labelled secondary antibodies (1:1,000). Cells were mounted in Pro-Long Gold antifade reagent (Invitrogen) and images obtained using x63 magnification on a Zeiss Axiovert 200M equipped with a Zeiss AxioCam and Axiovision software.

qRT-PCR

Matriptase expression in MDCK-I and MDCK-II cells was determined by qRT-PCR using SYBR-Green chemistry (Life Technologies, Warrington, UK). First-strand cDNA was synthesised from total RNA using random hexamer priming. qRT-PCR was performed on an ABI 7700 (Life Technologies) using primers for canine matriptase; forward 5'-ACAGAACCAGCAGTGTGACG-3', reverse 5'-ACTCTTCCTAACGCTGACAC-3'. Data are shown relative to the expression of 18S rRNA, which was used as an endogenous control.

Prostasin activation

HEK293 cells were transfected with full-length human prostasin cDNA in pIRES2-EGFP (16) and full-length matriptase cDNA in pcDNA3.1 (13) either alone or in combination using Fugene transfection reagent under serum free conditions according to manufacturer's guidelines (Promega, Southampton, UK). Cells were incubated for 24 h, washed and placed in serum-containing medium for a further 24 h. Cells were lysed, samples run on SDS-PAGE under reducing conditions and western blot performed with an anti-prostasin antibody. To determine the effect of matriptase inhibition, MCoTI-II was added at 6 h post-transfection, and added again at 24 h when the medium was changed.

Results

Selective inhibition of matrilysin by MCoTI-II

The ability of the squash trypsin inhibitor MCoTI-II and various derivatives, with sequence variations around the reactive centre residue, to inhibit matrilysin and hepsin was initially tested in solution using soluble forms of these proteases and a tripeptide fluorogenic peptide substrate. Analysis of K_i values revealed that MCoTI-II was the most effective inhibitor of matrilysin activity, with a K_i value of 9 nM (► Table 1). Replacement of the P1 residue (Lys-10) of MCoTI-II with Arg resulted in an 18-fold increase in K_i value, consistent with the slight preference for Lys over Arg at P1 displayed by matrilysin against peptide substrates (13). MCoEeTI, a hybrid with the related cystine-knot trypsin inhibitor from *Ecballium elaterium* (EETI-II), displayed a 60-fold increased K_i value for matrilysin, which in this case was slightly improved by Lys to Arg substitution at P1. The natural variant MCoTI-I, differing from MCoTI-II by two residues in a loop distal to the reactive centre loop, was also a less effective inhibitor of matrilysin.

In sharp contrast, none of the inhibitors had detectable activity against the closely related type-II transmembrane serine protease, hepsin, with at least a 1,000-fold difference in K_i value in the case of MCoTI-II. Notably, the two variants with Arg at P1, matching the very strong P1 preference of hepsin (13), also had no detectable inhibitory activity against hepsin.

A range of other serine proteases, mainly with trypsin-like activities, were also tested. Of these, only trypsin itself and β -trypsin were inhibited to any quantifiable extent.

Specific inhibition of matrilysin-catalysed activation of pro-HGF by MCoTI-II

Having established that MCoTI-II is an effective and selective inhibitor of the activity of matrilysin against a small peptide substrate, we aimed to determine whether MCoTI-II was also effective in inhibiting macromolecular substrate hydrolysis. Pro-HGF has been established as a key substrate for matrilysin in solution, at the cell-surface and *in vivo* (7, 13). Therefore, the effect of MCoTI-II on the activation of purified pro-HGF by soluble matrilysin was investigated, using western blotting for detection. MCoTI-II was observed to completely inhibit the activation of pro-HGF at increasing concentrations (► Figure 1A, left panel). Inhibition was detectable at concentrations above 10 nM, and was essentially complete at concentrations above 100 nM consistent with the determined K_i value of 9 nM. Also consistent with our initial observations, activation of pro-HGF by soluble hepsin was not inhibited by MCoTI-II at concentrations up to 500 nM (► Figure 1A, right panel).

The proteolytic activation of pro-uPA by matrilysin and hepsin was also affected by MCoTI-II in a manner consistent with these observations (► Figure 1B). The inhibition of matrilysin-catalysed pro-uPA activation by MCoTI-II was also analysed by enzyme kinetics (► Figure 1C, left panel). From these, and similar data at other concentrations of pro-uPA, a K_i value of 15 nM was determined, in close agreement with the K_i value determined directly by peptide substrate hydrolysis (► Table 1). No inhibition of

Table 1: Equilibrium dissociation constants (K_i) for MCoTI-II derivatives.

Protease	K_i value (nM)				
	MCoTI-II ^a	MCoTI-II [K10R]	MCoTI-I	MCoEeTI	MCoEeTI [K10R]
Matrilysin	9.0 ± 1 ^b	158 ± 46	155 ± 31	570 ± 85	370 ± 60
Hepsin ^c	> 10 ⁴	> 10 ⁴	> 10 ⁴	> 10 ⁴	> 10 ⁴
Trypsin	0.075 ± 0.005	0.085 ± 0.007	0.029 ± 0.002	48 ± 5	8.8 ± 0.3
Chymotrypsin	> 10 ⁴	> 10 ⁴	> 10 ⁴	ND ^e	ND
Thrombin	> 10 ⁵	> 10 ⁵	> 10 ⁵	ND	ND
uPA	> 10 ⁵	> 10 ⁵	ND	ND	ND
KLK2	> 10 ⁴	> 10 ⁴	ND	ND	ND
KLK3	> 10 ⁴	> 10 ⁴	ND	ND	ND
HLE ^d	> 10 ⁵	> 10 ⁵	> 10 ⁵	ND	ND
β -trypsin	600 ± 30	120 ± 50	1600 ± 140	33 ± 7	28 ± 2
Subtilisin	> 10 ⁵	> 10 ⁵	> 10 ⁵	ND	ND

(a) The amino acid sequences of these cyclic proteins, with P1 residue on bold and variations from the native MCoTI-II sequence underlined, are: MCoTI-II, SGSDGGVCPKILKKRRDSDCPGACIRGNGYCG; MCoTI-II[K10R], SGSDGGVCPRLKRRDSDCPGACIRGNGYCG; MCoTI-I, SGSDGGVCPKILQRRRDSDCPGACIRGNGYCG; MCoEeTI, SG----VCPKILKKRRDSDCLAGCVCGPNGYCG; MCoEeTI[K10R], SG----VCPRLKRRDSDCLAGCVCGPNGYCG. (b) Data are shown for soluble matrilysin catalytic domain (expressed in *E. coli*), but K_i values were essentially unchanged using full-length soluble matrilysin (expressed in *Drosophila* S2 cells). (c) The maximum concentration of each inhibitor used was at least 2 μ M, giving an estimated minimum K_i value of 10 μ M in the absence of detectable inhibition. (d) Human leukocyte elastase. (e) Not determined.

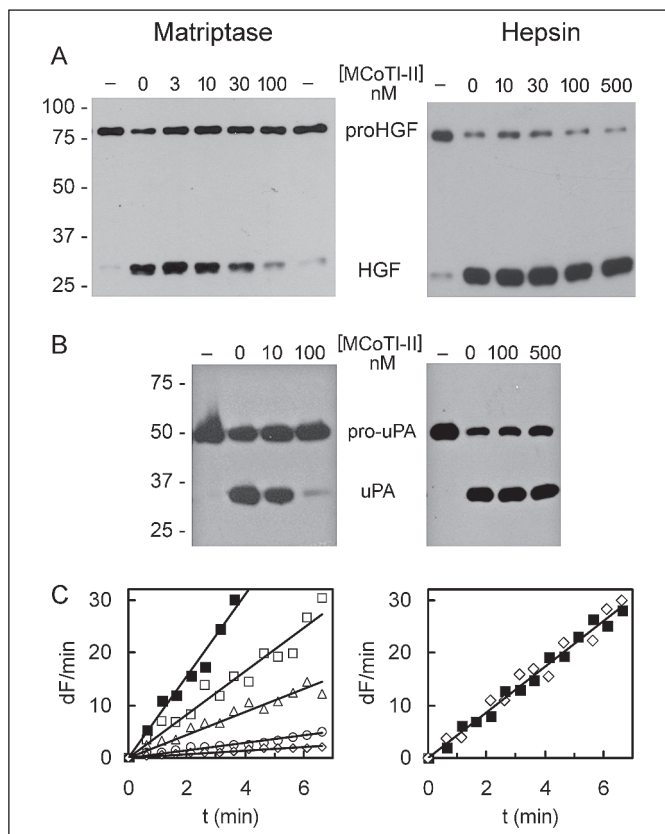


Figure 1: MCoTI-II specifically inhibits matriptase-catalysed activation of pro-HGF and pro-uPA. A) Varying concentrations of MCoTI-II were incubated with either soluble matriptase (1 nM, left panel) or soluble hepsin (10 nM, right panel) and pro-HGF for 2 h at 37°C. Activation of pro-HGF was determined by SDS-PAGE of reduced samples followed by western blotting for the C-terminal V5 epitope. B) Varying concentrations of MCoTI-II were incubated with either soluble matriptase (1 nM, left panel) or soluble hepsin (10 nM, right panel) and pro-uPA for 1 h at 37°C. Activation of pro-uPA was determined by SDS-PAGE of reduced samples followed by western blotting for the C-terminal V5 epitope. C) The generation of uPA activity by either soluble matriptase (1 nM, left panel) or soluble hepsin (1 nM, right panel) was determined in the presence of varying concentrations of MCoTI-II (■, 0, □, 30, △, 100, ○, 300, ◇, 1,000 nM) and expressed as change in fluorescence/min for the hydrolysis of the uPA-specific substrate H-Glu-Gly-Arg-7-amino-4-methylcoumarin.

hepsin-catalysed pro-uPA activation was observed (► Figure 1C, right panel), consistent with the high selectivity of MCoTI-II.

Inhibition of the cellular activation of pro-HGF by MCoTI-II

Having demonstrated the efficacy of MCoTI-II at inhibiting the proteolytic activity of matriptase in solution, its activity against endogenous, membrane-associated matriptase was investigated. We have previously demonstrated that pro-HGF is efficiently activated by the prostate cancer cell line PC-3, and that this activation can be abolished by matriptase-targeting siRNA (13). Therefore, the ability of MCoTI-II to inhibit the cellular activation of pro-HGF

was determined using this system. The data in ► Figure 2 show that using 100 nM MCoTI-II, partial and variable inhibition of pro-HGF activation was observed at two different time points, and that inhibition was essentially complete at 500 nM of the cyclotide inhibitor. These concentrations are less than five-fold higher than those giving comparable inhibition in the purified system, and therefore it appears that endogenous, transmembrane matriptase is completely accessible to the macromolecular inhibitor MCoTI-II.

The dog cell-line MDCK is a well-established model system used to study many aspects of epithelial biology, and may represent a useful model for the study of matriptase function. Therefore the ability of MCoTI-II to inhibit matriptase-dependent pro-HGF activation on these cells was also determined, employing the widely-used MDCK-II strain (28). The results were similar to those observed with PC-3 cells, with complete inhibition of pro-HGF activation between 100-500 nM MCoTI-II (► Figure 2). Therefore the potency of MCoTI-II is retained for the inhibition of dog matriptase, and MDCK cells can be used to further study the role of matriptase in epithelial cell function.

Effect of inhibition of matriptase activity on HGF-induced cell scatter

Binding of activated HGF to its singular cell-surface receptor c-Met causes a well-described dissolution of cell-cell junctions and scattering of MDCK-II cells, the initial stages of epithelial-mesenchymal transition (EMT). Pro-HGF cannot signal through c-Met, but cell scattering can be promoted by the pericellular proteolytic activation of pro-HGF (13). Therefore, the ability of MCoTI-II to inhibit cell scattering in the presence of pro-HGF was determined. MDCK-II cells at low density grow as tightly packed colonies (► Figure 3A), which disperse upon treatment with either active HGF (► Figure 3B) or pro-HGF (► Figure 3D) over a 24-h period. Cells treated with pro-HGF and 100 nM MCoTI-II displayed markedly less scattering (► Figure 3E), and scattering was completely abolished at 500 nM MCoTI-II (► Figure 3F). By contrast, MCoTI-II had no effect on cell scattering induced by active HGF (► Figure 3C). Therefore, inhibition of matriptase by MCoTI-II on the surface of these cells restricts the bioavailability of active HGF and its downstream effects on cell scattering.

MCoTI-II can inhibit matriptase activity in complex cellular processes: invasive cell migration

In common with a variety of other proteolytic enzymes, matriptase is implicated in invasive cell migration (29), a process occurring subsequent to EMT in epithelial carcinogenesis. To determine whether MCoTI-II could inhibit this activity, we made use of two invasive prostate cancer cell lines that differ in their levels of matriptase expression. PC-3 cells display robust expression of matriptase, but it is essentially undetectable in DU-145 cells, as determined by qRT-PCR (13). Both cell lines were found to have similar rates of invasion through the basement membrane preparation, matrigel (► Figure 4). MCoTI-II inhibited the invasion of matriptase

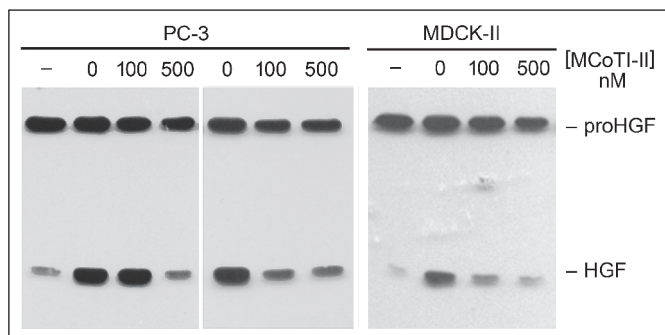


Figure 2: MCoTI-II inhibits the cellular activation of pro-HGF. MDCK-II or PC-3 cells were incubated with pro-HGF in the presence and absence of MCoTI-II (100 and 500 nM). Medium was removed at timed intervals, samples resolved by SDS-PAGE under reducing conditions and activation of pro-HGF determined by western blotting for the C-terminal V5 epitope. Data shown are at 2 h (left) and 4 h (right) for PC-3 cells, and 4 h incubation for MDCK-II cells. Control lanes are pro-HGF incubated in medium alone, and display a low-molecular-weight band due to traces of active, two-chain HGF as a minor contaminant in the purified protein preparation (13).

tase-expressing PC-3 cells by greater than 40%. However, MCoTI-II had no effect on the invasion of DU-145 cells, consistent with the lack of matriptase expression in these cells.

MCoTI-II can inhibit matriptase activity in complex cellular processes: epithelial barrier formation

Matriptase is known to play a role in epithelial barrier integrity in various tissues, and this can be recapitulated in cell culture (11). As we showed that MCoTI-II could inhibit matriptase activity in

MDCK cells, we used these cells to study the role of matriptase in epithelial barrier formation and stability.

MDCK cells grown on semi-permeable membranes develop functional tight junctions, which display trans-epithelial electrical resistance (TEER), a functional measure of tight junction integrity. MDCK-I cells develop high TEER over time (► Figure 5A), and this is reflected by the distribution of the canonical tight junction proteins ZO-1 and claudin-1 (► Figure 5C). MCoTI-II was found to have only a minor effect on the acquisition of TEER in these cells. Concentrations up to 1 μ M had no dose-dependent effect on the development of TEER up to a level of approximately 4,000 Ω .cm². Above this level, the TEER became slightly unstable and the presence of MCoTI-II had a minor effect on its further development. Therefore, these observations suggest that in MDCK-I cells matriptase has only a minor role in the development of a functional epithelial barrier, or is poorly inhibited by MCoTI-II.

Tight junctions are dynamic structures and can be readily disrupted by alteration of [Ca²⁺] in the medium, the so-called “calcium-switch” model (30). Removal of Ca²⁺ from the medium rapidly disrupts tight junction structure and function, assessed by loss of membrane localisation of ZO-1 and claudin-1 (► Figure 5D) and abolition of TEER (► Figure 5B), respectively. Repletion with Ca²⁺ leads to a slow reestablishment of TEER (► Figure 5B) and ZO-1 and claudin-1 localisation (► Figure 5E). In contrast to the lack of effect of MCoTI-II on the initial establishment of functional tight junctions, the data in ► Figure 5B show that MCoTI-II had a dramatic effect on the reestablishment of TEER. At a concentration of 250 nM, MCoTI-II caused at least a five-fold prolongation of the rate of TEER development (determined as the time taken to reach the same level of TEER), rising to 10-fold at the highest concentration used. Therefore, in MDCK-I cells, matriptase

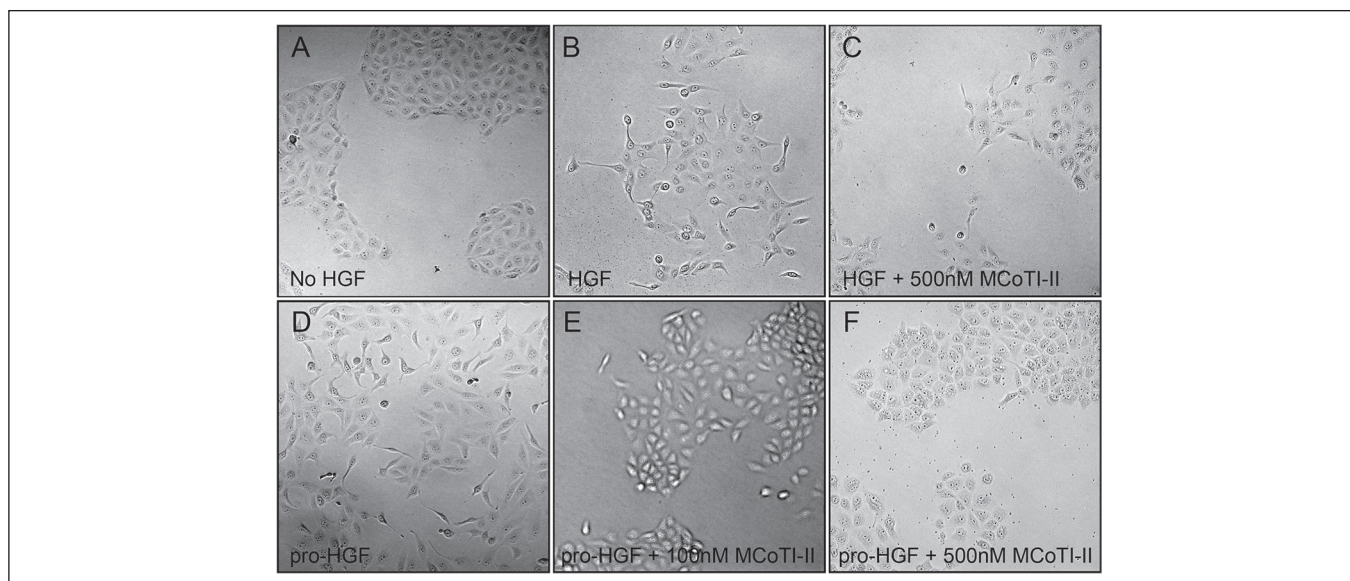


Figure 3: Effect of inhibition of matriptase activity on HGF-induced cell scattering. MDCK cells were seeded at a density of 10³ cells per well. Cells were treated with pro-HGF (10 ng/ml) in serum-free medium in the presence of 100 nM or 500 nM MCoTI-II for 24 h at 37°C. Cells treated with active HGF (10 ng/ml) and cells without HGF treatment served as positive

and negative controls respectively. Cells were fixed with ice cold methanol for 5 min and images taken using the Zeiss CCD inverted microscope using a x10 magnification. Data are representative of three separate experiments performed in duplicate.

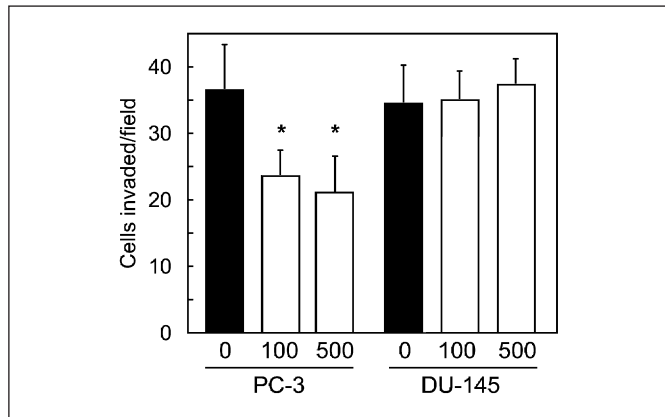


Figure 4: Effect of MCoTI-II on cell invasion. Invasion of PC-3 and DU-145 cells through matrigel-coated semi-permeable membranes, in response to 2% FCS, was determined in the absence (solid bars) and presence of 100 and 500 nM MCoTI-II (open bars, concentrations indicated below) over a 24-h time period. Data are shown as cell number invaded per microscopic field (mean ± SEM). Statistical differences between inhibitor-treated and untreated cells were assessed by Student's t-test (* $p < 0.05$).

tase activity is involved in the dynamic behaviour of tight junction and can be effectively inhibited by MCoTI-II.

MCoTI-II does not inhibit matriptase-catalysed prostatic activation

In addition to pro-HGF, the only other substrate for matriptase that has been demonstrated *in vivo* is the zymogen of the GPI-anchored serine protease prostatic (16). To determine whether MCoTI-II could inhibit this process, HEK293 cells which express neither of these proteases endogenously were transfected with both matriptase and prostatic. Cells transfected with prostatic alone displayed a single band of approximately 41 kDa on western blot corresponding to the inactive zymogen form of prostatic (▶ Figure 6). Co-transfection with matriptase led to complete activation of prostatic, with a single band observed at 38 kDa representing the C-terminal part of the protein after proteolytic activation at Arg-18. In contrast to the activation of pro-HGF, inclusion of MCoTI-II was unable to inhibit the matriptase-catalysed activation of pro-prostatic. In these experiments MCoTI-II was initially added 24 h after transfection and incubated for a further

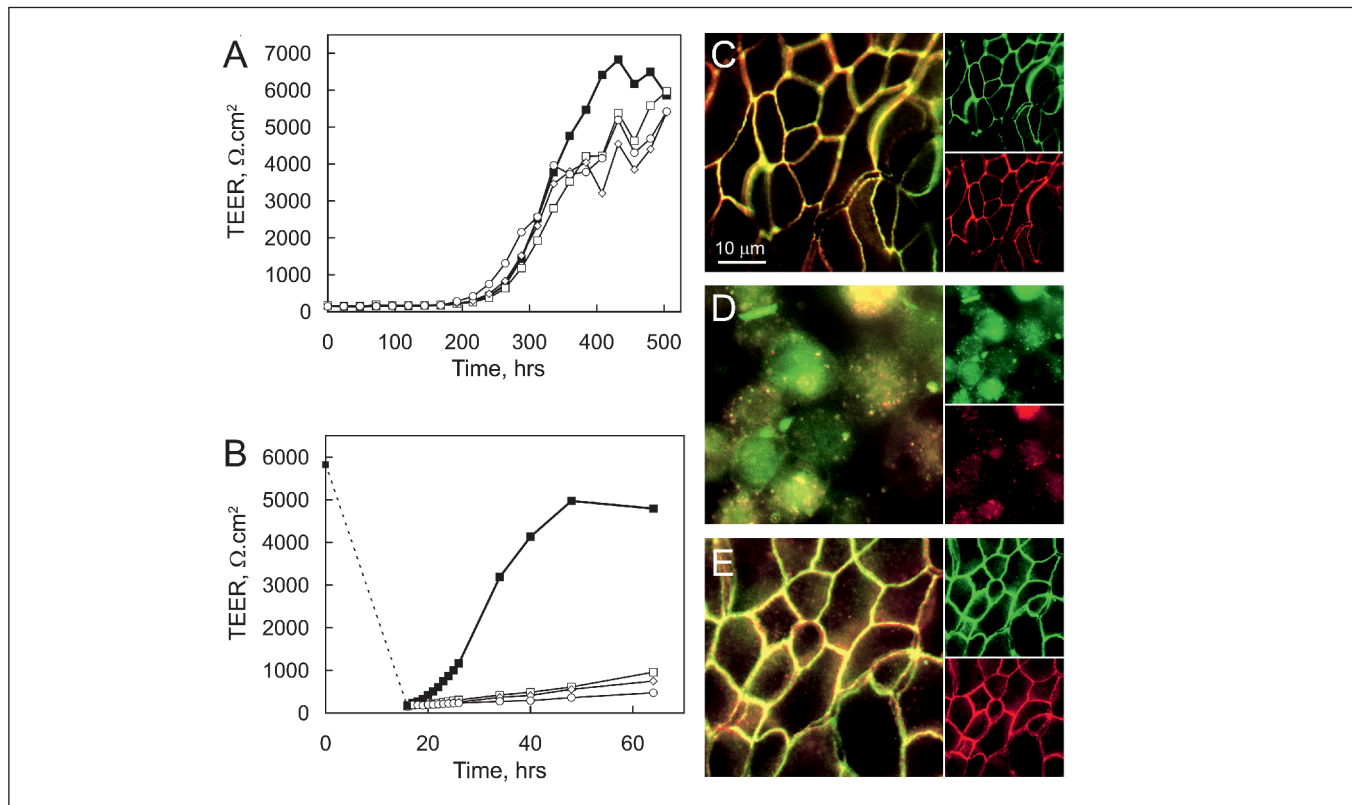


Figure 5: MCoTI-II abolishes the reestablishment of tight junctions in MDCK-I cells. A) MDCK-I cells were grown on Transwell filters in the absence (●) or presence of varying concentrations of MCoTI-II (□ 250 nM, ◇ 500 nM, ○ 1,000 nM) and transepithelial electrical resistance (TEER) measured. B) MDCK-I cells with high TEER were disrupted by removal of Ca²⁺ for 16 h (dashed line) prior to repletion with Ca²⁺. MCoTI-II concentrations as in panel A. In all experiments MCoTI-II was included at each change of culture medium. All TEER data shown are means of triplicate determinations. C-E) In-

direct immunofluorescence staining for tight junction proteins in MDCK-I cells grown on Transwell filters as for the TEER experiments. C) Prior to Ca²⁺-switch, D) after Ca²⁺-depletion, E) after Ca²⁺-repletion for 24 h. Each panel shows claudin-1 staining (green), ZO-1 staining (red) and co-localisation (yellow). Loss of claudin-1 (green) and ZO-1 (red) localisation is apparent during the Ca²⁺-switch due to disruption of tight junctions, correlating with the changes in TEER shown in panel B.

24 h, without effect. Subsequently MCoTI-II was included directly after transfection of the cells, but inhibition of prostatic activation was still not observed (► Figure 6).

Discussion

In the present study we have found that the cyclic cystine-knot microprotein MCoTI-II is an effective and specific inhibitor of the catalytic activity of the type-II transmembrane serine protease matriptase, influencing several biological functions that mirror the role of matriptase *in vivo*. Using a combination of biochemical and cell biological approaches we show that MCoTI-II efficiently inhibits the proteolytic activation of pro-HGF at the surface of matriptase-expressing cells, reducing the bioavailability of HGF and the induction of c-Met-dependent cell-scattering. MCoTI-II was also found to inhibit the invasive migration of PC-3 prostate carcinoma cells. In addition to these activities of matriptase that may underpin its involvement in cancer, MCoTI-II was also found to affect epithelial tight junction dynamics, potentially giving insights into the poorly understood role of matriptase in this process. Despite its efficacy, MCoTI-II was unable to inhibit the cellular activation of prostatic, a serine protease regarded as another major substrate for matriptase *in vivo*.

Achieving specificity of inhibition and selectivity between enzymes with similar activities is one of the main challenges in the therapeutic use of inhibitors, and this is particularly true for proteolytic enzymes (31). In the case of matriptase, hepsin is a closely related protease that shares overlapping protein substrate specificity: it can activate pro-HGF at the cell surface (13), and also activate both pro-uPA and pro-prostatic (19, 20). Therefore, the ability of MCoTI-II to discriminate between matriptase and hepsin, with a greater than 1,000-fold differential in K_i values is an important feature of its inhibitory activity. The reason for this exceptional level of discrimination is not immediately clear, but matriptase and hepsin have significant differences in the loop regions surrounding the active site that are often responsible for modulating substrate accessibility (32). Matriptase has a large 60s insertion loop, which has been shown to engage in favourable electrostatic interactions with the Kunitz-type inhibitor BPTI, (33), and is modelled in proximity to Arg16-Arg17 of MCoTI-II (34). The equivalent loop in hepsin is four residues shorter and has a higher net positive charge, possibly disfavouring such interactions with MCoTI-II. The 90s-loop is also unusually large in hepsin which, based on the previous modelling with matriptase, may restrict access of MCoTI-II by sterically hindering the loop delimited by Cys21 and Cys25 of the inhibitor. Interestingly, although the inhibitory characteristics of MCoTI-II were determined using human matriptase, the experiments with MDCK cells demonstrate that it has a similar inhibitory potency against canine matriptase. This apparent lack of species specificity may prove to be useful, for example, in inhibiting matriptase activity in various animal models.

Our study confirms and extends the findings of a recent report demonstrating that MCoTI-II is more potent than sunflower trypsin inhibitor (SFTI) as an inhibitor of matriptase in purified sys-

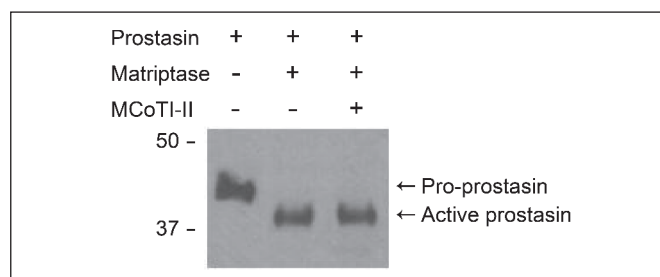


Figure 6: Effect of MCoTI-II on activation of prostatic zymogen. HEK-293 cells were transfected with either prostatic alone or cotransfected with both prostatic and matriptase. MCoTI-II (500 nM) was incubated with the cells 6 h after transfection. Cell lysates were collected at 48 h post-transfection and subjected to SDS-PAGE and western blot for prostatic. Prostatic zymogen is detected at 41 kDa in the cells transfected with prostatic alone, and the N-terminally truncated activated form is detected at 38 kDa in the cells cotransfected with matriptase.

tems (34). This study also identified the variant MCoTI-II [V3R] (V7R in the numbering system used here) as having a 10-fold lower K_i value than the wild-type sequence. Several other macromolecular inhibitors have been shown to inhibit matriptase activity in purified systems, including variants of the natural protease inhibitors ecotin, eglin C and SFTI (35-38), although neither their efficacy in cellular systems nor their inhibitory activity towards hepsin have been reported. Irrespective of their affinity for matriptase, all of these inhibitors retain substantial inhibitory activity towards pancreatic trypsin, as also observed here for MCoTI-II. Whether this might contribute to potential biological effects of MCoTI-II (or other inhibitors of matriptase) via inhibition of non-pancreatic trypsin (mesotrypsin, PRSS3), which plays a role in several malignancies including prostate cancer, is not known, although this form of trypsin has been shown to be poorly inhibited by canonical trypsin inhibitors (39).

Several small molecule inhibitors of matriptase have been developed, and some shown to be effective *in vivo* using xenograft models of tumour growth, albeit at high concentrations (40, 41). However, the inhibitory activity of these compounds against hepsin has not been reported, and our own data with the 3-amidinophenylalanine-based inhibitor CJ-730 (41) demonstrated a less than five-fold selectivity between matriptase and hepsin (13). Another disadvantage apparent with small molecule inhibitors is their efficacy in complex cellular systems is far lower than suggested by K_i values determined in solution. For example, an approximately 100-fold differential has been observed between the K_i values and the estimated IC_{50} values for the cellular activation of pro-HGF (13, 29), and 300-fold for the autoactivation of matriptase (42). This is in marked contrast to the efficacy of MCoTI-II in cellular systems, which demonstrates essentially complete inhibition of the cellular activities of matriptase at concentrations 10-20-fold above the K_i value; entirely consistent with full bioavailability of the inhibitor in these complex systems.

Matriptase inhibition by MCoTI-II was found to inhibit the formation of functional tight junctions in MDCK-I cells, using the Ca^{2+} -switch model. This is in contrast to previous observations

with overexpression of HAI-2, which was observed to increase the rate of acquisition of TEER in these cells (43). Although HAI-2 is clearly a major inhibitor of matriptase *in vivo* (43), it lacks selectivity, inhibiting a wide range of serine proteases *in vitro* (44), and, unlike MCoTI-II, inhibiting matriptase and hepsin equally well (18). Therefore, HAI-2 potentially inhibits a trypsin-like protease that acts to increase epithelial permeability, for example, by the degradation of junctional proteins (45, 46). Consistent with our observations, siRNA silencing of matriptase in human Caco-2 epithelial cells has been shown to delay the reestablishment of TEER, as well as its initial acquisition (11, 47). The mechanism by which matriptase influences the behaviour of epithelial tight junctions is poorly understood, but appears to be independent of its established protein substrates (11).

Despite the poor understanding of the role of matriptase in regulating epithelial barrier function, there is compelling evidence for two authentic substrates *in vivo*, both of which have important roles in epithelial cell function. A mouse model of matriptase-initiated squamous cell carcinoma has been shown to be absolutely dependent on the presence of c-Met, directly implicating pro-HGF as a key substrate for matriptase (7). We demonstrate here that MCoTI-II can effectively inhibit the activation of pro-HGF, both in MDCK and PC-3 cells, and that it was also able to inhibit the cell-scattering that is a central to the biological activity of HGF. The observation that MCoTI-II was able to inhibit the invasion of PC-3 cells suggests that matriptase can also promote carcinogenesis in an HGF-independent manner, possibly by direct effect on extracellular matrix proteins or by activation of the plasminogen

activation system (15, 48). Members of the kallikrein-related family of serine proteases are thought to play significant roles in several of these process, but MCoTI-II was found to have no inhibitory activity towards either KLK2 (glandular kallikrein) or KLK3 (prostate-specific antigen), although neither of these proteases is highly expressed in PC-3 cells.

The second substrate for matriptase demonstrated *in vivo* is the zymogen of the GPI-anchored serine protease, prostasin (16). However, despite the efficacy of MCoTI-II, the activation of prostasin by matriptase was unaffected by MCoTI-II. This is potentially related to several unusual characteristics reported for this reaction. It has been suggested that prostasin activation is temporally coupled to matriptase activation (49) and that the latter can occur intracellularly (50) and, intriguingly, that prostasin can be activated by the zymogen form of matriptase (51). In either of these situations, the activation of prostasin might be expected to be refractory to inhibition by MCoTI-II. However, it cannot be completely excluded that our observation is related to limitations imposed by the extraordinary efficiency of prostasin activation, as we observe its complete activation when coexpressed with matriptase. However, inclusion of MCoTI-II for the duration of the experiment failed to affect prostasin activation; conditions where a steady-state level of the zymogen might be expected to accumulate.

The specific and selective inhibition of matriptase activity by the macrocyclic cystine-knot microprotein MCoTI-II observed here in complex cellular systems demonstrates the potential usefulness of this type of inhibitor in the development of protease-targeted therapies. MCoTI-II has the ability to efficiently inhibit the activation of pro-HGF and HGF-dependent cell scattering, and invasive cell migration; processes closely linked to pathological events, particularly in cancer. Intriguingly, the lack of effect of MCoTI-II on prostasin activation may also be therapeutically beneficial, as the roles of matriptase in normal physiology are largely prostasin-dependent; highlighted by the similarity in the phenotypes of the respective null mice (16). In addition to its pro-carcinogenic roles, matriptase has been shown to have tumour-suppressive effects in colon carcinogenesis (52), consistent with its role in the maintenance of the epithelial barrier, as recapitulated here in MDCK-I cells. These opposing roles of matriptase in the initiation and progression of cancer highlight the importance of gaining a deeper understanding of the functions of matriptase in regulating epithelial cell behaviour for the development of potential therapeutic strategies. Highly specific matriptase inhibitors such as MCoTI-II and the MDCK cell model system described here may help contribute to this understanding.

Conflicts of interest

None declared.

References

1. Ellis V, Murphy G. Cellular strategies for proteolytic targeting during migration and invasion. *FEBS Lett* 2001; 506: 1-5.
2. Qiu D, Owen K, Gray K, et al. Roles and regulation of membrane-associated serine proteases. *Biochem Soc Trans* 2007; 35: 583-587.

What is known about this topic?

- Matriptase is involved in a range of biological processes and these may be mediated by a range of protein substrates for this protease.
- The closely related protease hepsin shares several different protein substrates with matriptase, yet has distinct biological functions.
- Efforts to inhibit the proteolytic activity of matriptase are hampered by lack of specificity/selectivity of small molecule inhibitors.

What does this paper add?

- The cyclic microprotein MCoTI-II is identified as a high affinity inhibitor of matriptase that is highly selective with respect to inhibition of hepsin.
- MCoTI-II efficiently inhibits the activity of matriptase against several of its known protein substrates in both purified and complex cellular systems.
- MCoTI-II also inhibits the activity of matriptase that is required to maintain epithelial barrier function via an as yet unknown substrate.
- The class of protease inhibitors exemplified by MCoTI-II have potential as highly selective inhibitors of matriptase in biological systems.

3. Szabo R, Wu Q, Dickson RB, et al. Type II transmembrane serine proteases. *Thromb Haemostasis* 2003; 90: 185-193.
4. Kang JY, Dolled-Filhart M, Ocal IT, et al. Tissue Microarray Analysis of Hepatocyte Growth Factor/Met Pathway Components Reveals a Role for Met, Matrilysin, and Hepatocyte Growth Factor Activator Inhibitor 1 in the Progression of Node-negative Breast Cancer. *Cancer Res* 2003; 63: 1101-1105.
5. Riddick AC, Shukla CJ, Pennington CJ, et al. Identification of degradome components associated with prostate cancer progression by expression analysis of human prostatic tissues. *Br J Cancer* 2005; 92: 2171-2180.
6. List K, Szabo R, Molinolo A, et al. Deregulated matrilysin causes ras-independent multistage carcinogenesis and promotes ras-mediated malignant transformation. *Genes Dev* 2005; 19: 1934-1950.
7. Szabo R, Rasmussen AL, Moyer AB, et al. c-Met-induced epithelial carcinogenesis is initiated by the serine protease matrilysin. *Oncogene* 2011; 30: 2003-2016.
8. List K, Haudenschild CC, Szabo R, et al. Matrilysin/MT-SP1 is required for postnatal survival, epidermal barrier function, hair follicle development, and thymic homeostasis. *Oncogene* 2002; 21: 3765-3779.
9. Basel-Vanagaite L, Attia R, Ishida-Yamamoto A, et al. Autosomal recessive ichthyosis with hypotrichosis caused by a mutation in ST14, encoding type II transmembrane serine protease matrilysin. *Am J Hum Genet* 2007; 80: 467-477.
10. List K, Kosa P, Szabo R, et al. Epithelial integrity is maintained by a matrilysin-dependent proteolytic pathway. *Am J Pathol* 2009; 175: 1453-1463.
11. Buzza MS, Netzel-Arnett S, Shea-Donohue T, et al. Membrane-anchored serine protease matrilysin regulates epithelial barrier formation and permeability in the intestine. *Proc Natl Acad Sci USA* 2010; 107: 4200-4205.
12. Takeuchi T, Harris JL, Huang W, et al. Cellular localization of membrane-type serine protease 1 and identification of protease-activated receptor-2 and single-chain urokinase-type plasminogen activator as substrates. *J Biol Chem* 2000; 275: 26333-26342.
13. Owen KA, Qiu D, Alves J, et al. Pericellular activation of hepatocyte growth factor by the transmembrane serine proteases matrilysin and hepsin, but not by the membrane-associated protease uPA. *Biochem J* 2010; 426: 219-228.
14. Lee SL, Dickson RB, Lin CY. Activation of hepatocyte growth factor and Urokinase/Plasminogen activator by matrilysin, an epithelial membrane serine protease. *J Biol Chem* 2000; 275: 36720-36725.
15. Kilpatrick LM, Harris RL, Owen KA, et al. Initiation of plasminogen activation on the surface of monocytes expressing the type II transmembrane serine protease matrilysin. *Blood* 2006; 108: 2616-2623.
16. Netzel-Arnett S, Currie BM, Szabo R, et al. Evidence for a matrilysin-prostasin proteolytic cascade regulating terminal epidermal differentiation. *J Biol Chem* 2006; 281: 32941-32945.
17. Bugge TH, Antalis TM, Wu Q. Type II transmembrane serine proteases. *J Biol Chem* 2009; 284: 23177-23181.
18. Kirchhofer D, Peek M, Lipari MT, et al. Hepsin activates pro-hepatocyte growth factor and is inhibited by hepatocyte growth factor activator inhibitor-1B (HAI-1B) and HAI-2. *FEBS Lett* 2005; 579: 1945-1950.
19. Moran P, Li W, Fan B, et al. Pro-urokinase-type plasminogen activator is a substrate for hepsin. *J Biol Chem* 2006; 281: 30439-30446.
20. Chen MQ, Chen LM, Lin CY, et al. Hepsin activates pro-stasin and cleaves the extracellular domain of the epidermal growth factor receptor. *Mol Cell Biochem* 2010; 337: 259-266.
21. Hopkins AL, Groom CR. The druggable genome. *Nat Rev Drug Discov* 2002; 1: 727-730.
22. Overall CM, Lopez-Otin C. Strategies for MMP inhibition in cancer: innovations for the post-trial era. *Nat Rev Cancer* 2002; 2: 657-672.
23. Coussens LM, Fingleton B, Matrisian LM. Matrix metalloproteinase inhibitors and cancer: trials and tribulations. *Science* 2002; 295: 2387-2392.
24. Werle M, Kafedjijski K, Kolmar H, et al. Evaluation and improvement of the properties of the novel cystine-knot microprotein MCoTI-II for oral administration. *Intern J Pharmaceut* 2007; 332: 72-79.
25. Thongyoo P, Tate EW, Leatherbarrow RJ. Total synthesis of the macrocyclic cysteine knot microprotein MCoTI-II. *Chem Commun* 2006; 2848-2850.
26. Thongyoo P, Jaulent AM, Tate EW, et al. Immobilized protease-assisted synthesis of engineered cysteine-knot microproteins. *Chembiochem* 2007; 8: 1107-1109.
27. Thongyoo P, Bonomelli C, Leatherbarrow RJ, et al. Potent inhibitors of beta-trypsin and human leukocyte elastase based on the MCoTI-II scaffold. *J Med Chem* 2009; 52: 6197-6200.
28. Dukes JD, Whitley P, Chalmers AD. The MDCK variety pack: choosing the right strain. *BMC Cell Biology* 2011; 12: 43.
29. Förbs D, Thiel S, Stella MC, et al. In vitro inhibition of matrilysin prevents invasive growth of cell lines of prostate and colon carcinoma. *Int J Oncol* 2005; 27: 1061-1070.
30. Nigam SK, Rodriguez-Boulan E, Silver RB. Changes in intracellular calcium during the development of epithelial polarity and junctions. *PNAS* 1992; 89: 6162-6166.
31. Deu E, Verdoes M, Bogoy M. New approaches for dissecting protease functions to improve probe development and drug discovery. *Nat Struct Mol Biol* 2012; 19: 9-16.
32. Bode W, Turk D, Karshikov A. The refined 1.9-Å X-ray crystal structure of d-Phe-Pro-Arg chloromethylketone-inhibited human α -thrombin: Structure analysis, overall structure, electrostatic properties, detailed active-site geometry, and structure-function relationships. *Protein Sci* 1992; 1: 426-471.
33. Friedrich R, Fuentes-Prior P, Ong E, et al. Catalytic domain structures of MT-SP1/matrilysin, a matrix-degrading transmembrane serine proteinase. *J Biol Chem* 2002; 277: 2160-2168.
34. Quimbar P, Malik U, Sommerhoff CP, et al. High-affinity cyclic peptide matrilysin inhibitors. *J Biol Chem* 2013; 288: 13885-13896.
35. Stoop AA, Craik CS. Engineering of a macromolecular scaffold to develop specific protease inhibitors. *Nat Biotechnol* 2003; 21: 1063-1068.
36. Desilets A, Longpre JM, Beaulieu ME, et al. Inhibition of human matrilysin by eglin c variants. *FEBS Lett* 2006; 580: 2227-2232.
37. Li P, Jiang S, Lee SL, et al. Design and synthesis of novel and potent inhibitors of the type II transmembrane serine protease, matrilysin, based upon the sunflower trypsin inhibitor-1. *J Med Chem* 2007; 50: 5976-5983.
38. Fittler H, Avrutina O, Glotzbach B, et al. Combinatorial tuning of peptidic drug candidates: high-affinity matrilysin inhibitors through incremental structure-guided optimization. *Orga Biomol Chem* 2013; 11: 1848-1857.
39. Salameh MA, Soares AS, Navaneetham D, et al. Determinants of Affinity and Proteolytic Stability in Interactions of Kunitz Family Protease Inhibitors with Mesotrypsin. *J Biol Chem* 2010; 285: 36884-36896.
40. Galkin AV, Mullen L, Fox WD, et al. CVS-3983, a selective matrilysin inhibitor, suppresses the growth of androgen independent prostate tumor xenografts. *Prostate* 2004; 61: 228-235.
41. Steinmetzer T, Schweinitz A, Sturzebecher A, et al. Secondary amides of sulfonlated 3-aminophenylalanine. New potent and selective inhibitors of matrilysin. *J Med Chem* 2006; 49: 4116-4126.
42. Xu ZH, Chen YW, Battu A, et al. Targeting zymogen activation to control the matrilysin-prostasin proteolytic cascade. *J Med Chem* 2011; 54: 7567-7578.
43. Szabo R, Hobson JP, Christoph K, et al. Regulation of cell surface protease matrilysin by HAI2 is essential for placental development, neural tube closure and embryonic survival in mice. *Development* 2009; 136: 2653-2663.
44. Delaria KA, Muller DK, Marlor CW, et al. Characterization of placental bikunin, a novel human serine protease inhibitor. *J Biol Chem* 1997; 272: 12209-12214.
45. Scudamore CL, Jepson MA, Hirst BH, et al. The rat mucosal mast cell chymase, RMCPII, alters epithelial cell monolayer permeability in association with altered distribution of the tight junction proteins ZO-1 and occludin. *Eur J Cell Biol* 1998; 75: 321-330.
46. Willemsen LEM, Hoetjes JP, Van Deventer SJH, et al. Abrogation of IFN-gamma mediated epithelial barrier disruption by serine protease inhibition. *Clin Exp Immunol* 2005; 142: 275-284.
47. Buzza MS, Martin EW, Driesbaugh KH, et al. Prostasin Is Required for Matrilysin Activation in Intestinal Epithelial Cells to Regulate Closure of the Paracellular Pathway. *J Biol Chem* 2013; 288: 10328-10337.
48. Tripathi M, Potdar AA, Yamashita H, et al. Laminin-332 cleavage by matrilysin alters motility parameters of prostate cancer cells. *Prostate* 2011; 71: 184-196.
49. Chen YW, Wang JK, Chou FP, et al. Regulation of the matrilysin-prostasin cell surface proteolytic cascade by hepatocyte growth factor activator inhibitor-1 during epidermal differentiation. *J Biol Chem* 2010; 285: 31755-31762.
50. Tseng IC, Xu H, Chou FP, et al. Matrilysin activation, an early cellular response to acidosis. *J Biol Chem* 2010; 285: 3261-3270.
51. Friis S, Uzzun Sales K, Godiksen S, et al. A matrilysin-prostasin reciprocal zymogen activation complex with unique features: Prostasin as a non-enzymatic co-factor for matrilysin activation. *J Biol Chem* 2013; 288: 19028-19039.
52. Kosa P, Szabo R, Molinolo AA, et al. Suppression of Tumorigenicity-14, encoding matrilysin, is a critical suppressor of colitis and colitis-associated colon carcinogenesis. *Oncogene* 2012; 31: 3679-3695.